CompCytogen 15(4): 329–338 (2021)
doi: 10.3897/compcytogen.v15.i4.64350
https://compcytogen.pensoft.net

RESEARCH ARTICLE

COMPARATIVE Cytogenetics
A peer-reviewed open-access journal
International Journal of Plant & Animal Cytogenetics, Karyosystematics, and Molecular Systematics

Study of chromatin diminution in *Cyclops kolensis* (Copepoda, Crustacea) by radiobiological methods

Andrey Grishanin[1,2], Oksana Chinyakova[2]

1 *Papanin Institute for Biology of Inland Waters Russian Academy of Sciences 152742, Borok Nekouzskii Raion, Yaroslavl Oblast, Russia* **2** *Dubna State University, 19, Universitetskaya str,141980, Dubna, Moscow Oblast, Russia*

Corresponding author: Andrey Grishanin (andreygrishanin@mail.ru)

Academic editor: S. Salvadori | Received 12 February 2021 | Accepted 6 May 2021 | Published 28 September 2021

http://zoobank.org/AE77A7EE-AB9E-4443-8548-426745847FED

Citation: Grishanin A, Chinyakova O (2021) Study of chromatin diminution in *Cyclops kolensis* (Copepoda, Crustacea) by radiobiological methods. CompCytogen 15(4): 329–338. https://doi.org/10.3897/compcytogen.v15.i4.64350

Abstract

The experimental results show that at doses of 20 Gy and 100 Gy, the development of *Cyclops kolensis* Lilljeborg, 1901 (Copepoda, Cyclopoida) embryos ceases at the 16-cell stage, without affecting the course of chromatin diminution. A dose of 200 Gy terminated the process of chromatin diminution in some of the embryos. These results support the hypothesis that cytoplasmic factors in the egg play an important role in the process of chromatin diminution.

Keywords

Copepoda, embryogenesis, radiation

Introduction

The presence of chromatin diminution was carried out on the zooplanctonic crustacean *Cyclops kolensis* Lilljeborg, 1901 (Copepoda, Cyclopoida), in which the diminution process occurs at the stage of an 8-cell embryo (Grishanin et al. 1996). Chromatin diminution in Cyclopoida is the removal of a portion of the chromatin from chromosomes of the embryonic presomatic cells in one or two sequential cleavage divisions, while germ-line cells retain their nuclear DNA unchanged throughout ontogeny (Beermann 1977). The interphase of diminution divisions is significantly lengthened.

Chromatin diminution in *C. kolensis* is a process of programmed removal of 90% of DNA from the nuclear genome of somatic line cells during the 4th cleavage division, while the germ cell genome of these organisms remains unchanged (Zagoskin et al. 2010; Semeshin et al. 2011; Wyngaard et al. 2011). Chromatin diminution marks the timing of germline-soma differentiation: embryos prior to diminution possess a presomatic genome equal to that of the germline genome. After diminution the embyros possess what is referred to as a post somatic genome.

According to modern concepts of developmental biology, maternal genes of the egg determine the pattern of embryonic formation before fertilization and during initial cleavage divisions, after which the genes localized in the nuclei of embryonic cells play a role in the developmental process (Pomar and Jackle 1996; Jaeger 2018). The history of the study of factors controlling the chromatin diminution goes back to the beginning of the 20th century, when the discoverer of chromatin diminution, Theodore Boveri, conducted an experiment to determine these factors. Boveri (1910) showed in *Ascaris* (Nematoda) Karl Linney, 1758 that there are two types of cytoplasmic factors: one initiates chromatin diminution, and the other inhibits it. This result was later confirmed by Moritz (1967) for *Parascaris equorum* (Nematoda) Goeze, 1782 and Geyer-Dushinskaya (1959) for the cecidomyiid *Wachtiella* Rübsaamen, 1916. Amma (1911) found in the cytoplasm of embryonic cells of 16 copepod species the presence of ectosomes, which are associated with the differentiation of germ line cells. Although chromatin diminution is not found in most of these species, Beermann (1977) suggests that mechanisms of diminution in the presomatic cells in *Cyclops* involves the synthesis and activation of a series of enzymes, which in copepods probably are set in action only during the long interphase preceeding the diminution division.

The goal of the present study is to determine whether a dose of radiation that blocks the action of the nuclear genome of *C. kolensis* embryos is capable of terminating the chromatin diminution processes. The results obtained will help us to understand when the factors of initiation of chromatin diminution processes appear or are activated: either in the cytoplasm of an unfertilized egg, or as a result of gene expression in the presomatic cells of *C. kolensis* embryos. To distinguish between these two alternative mechanisms, we chose the method of radiation inactivation of nuclei (Neyfakh 1961). This method is based on the fact that radiation doses of the order of 10–20 Gy destroy chromosomes, causing numerous aberrations, but allow the cytoplasm of embryonic cells to continue performing its functions. Such methods have not yet been used to study chromatin diminution.

Materials and methods

Individuals of *C. kolensis* were collected from the small Andreevsky pond in Vorobievy Gory, Moscow, Russia (55°42'35.40"N, 37°34'6.61"E). This oligotrophic pond is located in a park area that prevents pollutants from entering into it, with the exception of pollutants that arise from atmospheric precipitation. Thus the impact of any significant exposure to chemicals that can affect the results of experiments on the individual's

body is practically eliminated. A necessary condition for the experiment was a method that allowed us to determine the stage of chromosomal fragmentation in developing *C. kolensis* embryos that could be assayed with a light microscope *in vivo*. The number of blastomeres in the embryos of *C. kolensis* corresponds to the number of spherical formations, which are sections of the cytoplasm with a nucleus that possess an optical density different from that of the surrounding yolk. Similarly, it is possible to reliably determine the stage of development of the embryo until the end of the 6th cleavage division (Grishanin and Zagoskin 2019).

Irradiation of *C. kolensis* embryos was performed at the 4 cell stage with gamma (γ)-radiation. The amount of absorbed dose of ionizing radiation in the experiment varied from 5 to 200 Gray (Gy). The irradiation experiment was carried out in the Laboratory of Nuclear Problems of the Joint Institute for Nuclear Research at the Rokus-M facility. The absorbed dose rate was 1.37 G/min, delivered from the distance is 0.75 m. The irradiated embryos were examined for number of cells and any chromosomal irregularities 24 hours following irradiation. Fixation was performed with a mixture of ethanol and acetic acid in a ratio of 3:1 for one hour. The preparations were further stained with acetoorcein according to the method described earlier (Grishanin et al. 1996). Embryos were examined for presence of micronuclei at the interphase stage, indicative of chromosomal abnormalities. Statistical processing of the data was performed using the '*t*-test.'

Results

We initiated the experiment with a dose of 5 Gy, based on previous studies that showed a high level of chromosome aberrations in pre-diminution cleavage divisions under irradiation with this level of radiation (Grishanin and Akifiev 2005). We assumed that this dose could be considered as a starting point for studying the process of suppression of nuclear functions in *C. kolensis*. At 5 Gy dosage approximately half of the embryos reached the stage of 128–256 cells; the second half ceased their development at the stage of 32 cells (Table 1). Taking into account that chromatin diminution in *C. kolensis* occurs at the 4th cleavage division, and visually observing granules of eliminated chromatin in cells at the 32-cell stage, we can state that chromatin diminution occurs in all embryos irradiated with a dose of 5 Gy. In the few anaphases that could be observed, we found numerous bridges, fragments, and fused chromosomes (Fig. 1). After irradiation of *C. kolensis* embryos with a dose of 20 Gy at the 4-cell stage, about 40% of embryos underwent only one-cell division, reaching the 8-cell stage of development, while the remainder of the embryos ceased their development at the 16-cell stage, having passed the chromatin diminution stage (Table 1).

C. kolensis embryos irradiated at the 4 cell stage with a dose of 100 Gy also comprised two similar groups: 65% of embryos ceased development at the 8-cell stage and, 35% of embryos ceased development at 16-cell stage, having passed the stage of chromatin diminution. Of those few anaphases that could be observed, we found numerous bridges, fragments and chromosomes adhering to each other (Fig. 2).

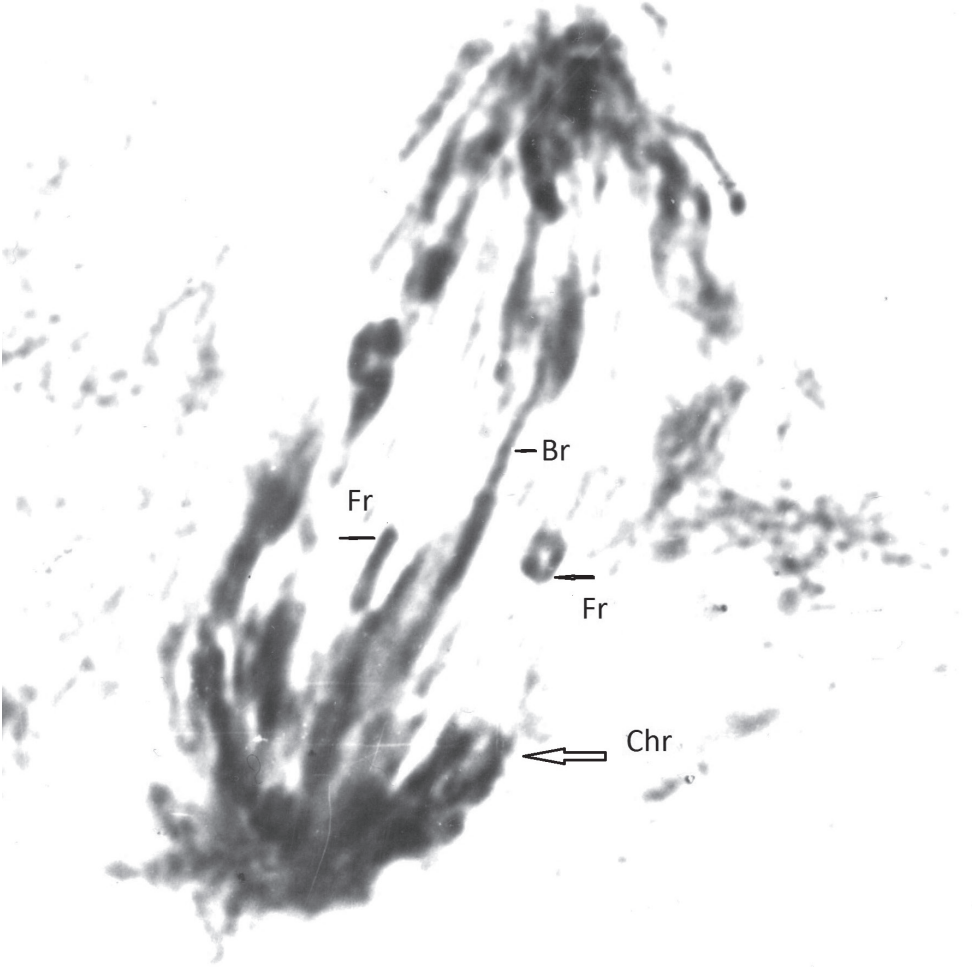

Figure 1. Anaphase of 3rd cleavage division of *C. kolensis* embryo at 5 Gy (dose of ionizing radiation). Designations: Chr- chromosome, Br- bridge, Fr- fragment.

Irradiation with a dose of 200 Gy at the 2-cell stage apparently caused several disturbances in 34% of the embryos not only in the nucleus, but also in the cytoplasmic structures, as a result of which the development of the embryos stopped at the 2-cell stage. Nevertheless, more than half of the embryos reached the stage of the 8-cell embryo, and 25% of the embryos reached the stage of 16 cells, while in 14 out of 36 embryos chromatin diminution did not occur. We concluded that chromatin diminution did not occur in 14 embryos because we did not observe the usual pattern for embryos after chromatin diminution: an abundance of granules and sharp differences in size between cells of the somatic line before and after chromatin diminution. Damage to nuclear structures at a dose of 200 Gy was so

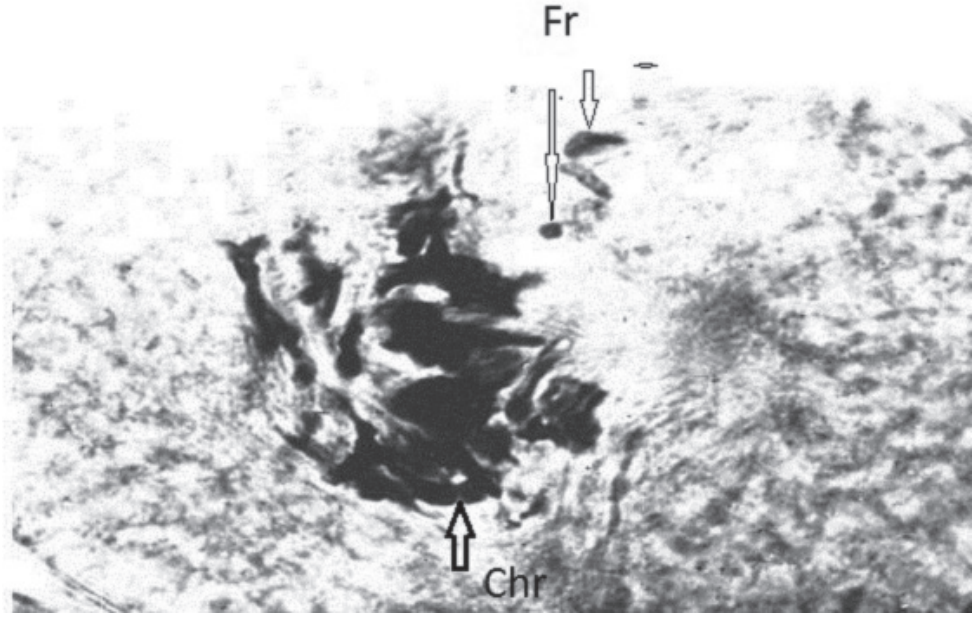

Figure 2. Metaphase of a *C. kolensis* embryo cell after irradiation at a dose of 100 Gy. Chr- chromosome, Fr- fragment.

Table 1. Cell stage and number of cells before and after exposure to gamma radiation in Gray (Gy) units.

Dose (Gy)	Initial cell stage of exposure	Cell stage after 24 hrs exposure	n	% of Embryos at cell stage after 24 hrs	Number of interphase figures	Average number of micronuclei ± SEM
5	1	128–256	86	52.4	n.a.	
		32	82	48.8	n.a.	
20	4	8	126	41.0	80	1.14 ± 0.35
		16	181	58.9	n.a.	
100	4	8	228	64.5	94	4.5 ± 0.6
		16	125	35.4	n.a.	
200	2	2	50	34.2	n.a.	
		8	60	41.0	n.a.	6.3 ± 0.8
		16	36(14)**	24.6 (9.5)	n.a.	
Control	1	238	>1000		202	

Number of embryos at a particular cell stage 24 hours after exposure is noted by n. Chromosomal abnormalities (micronuclei) are reported for cells at the interphase stage in which the granules did not obscure their presence; Standard deviation of the mean is denoted by SEM. n.a. – denotes data are not available. ** partial suppression of chromatin diminution.

significant that adhered chromosomes at the meta- and anaphase stages formed conglomerates and were not capable of segregation during cell division. No chromosomal aberrations were observed in the control embryos (Fig. 3). Numerous micronuclei were observed in 8-cell embryos at the interphase stage. With an increase in the dose from 20 to 200 Gy, an increase in the number of micronuclei per cell is observed (Table 1).

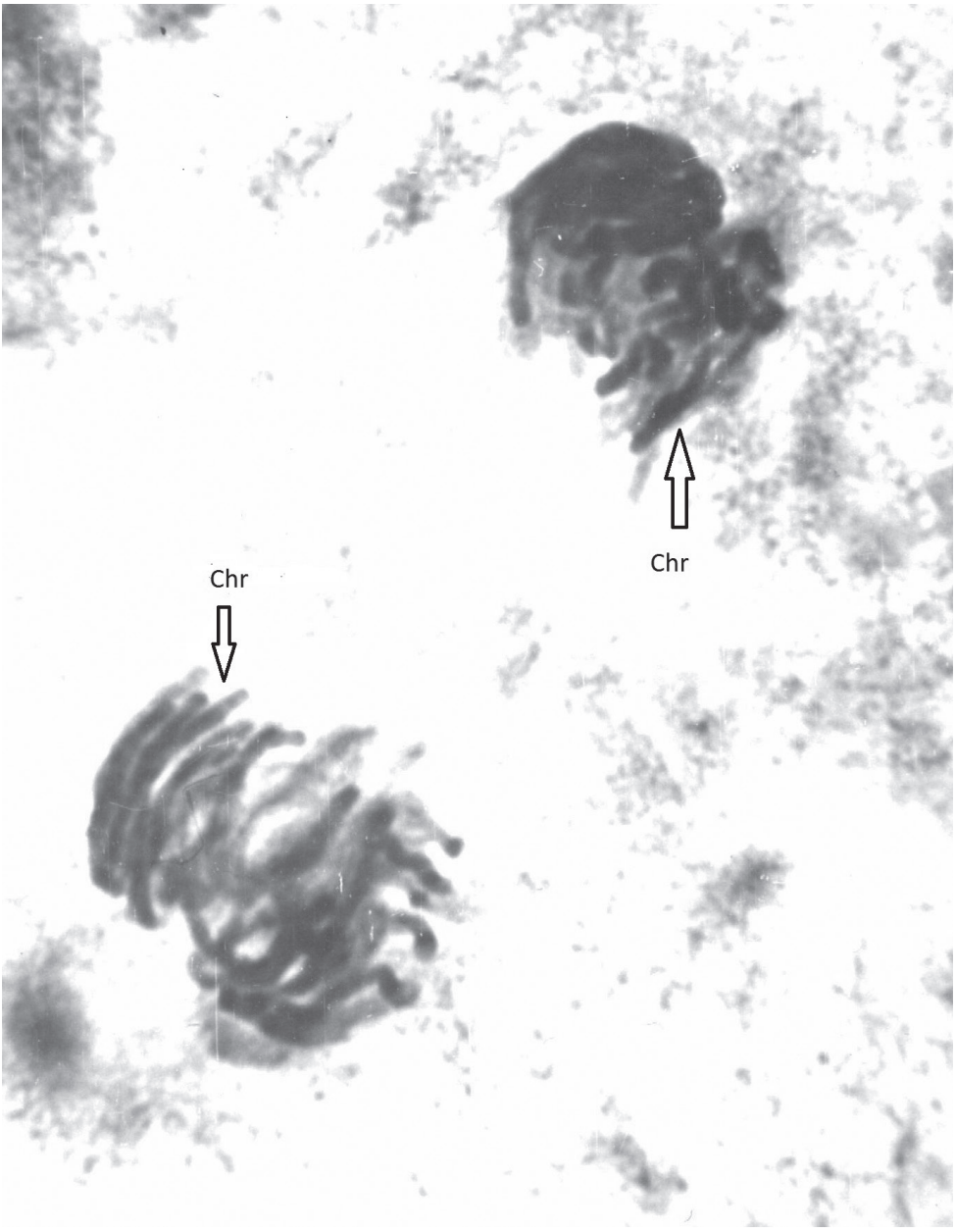

Figure 3. Anaphase of 3-d cleavage division of *C. kolensis* embryo in the control experiment. Chr- chromosome.

Discussion

The results of experiments with embryos of *C. kolensis* at doses from 20 to 200 Gy have almost identical results: the development of embryos did not progress beyond the 16-cell stage (Fig. 4). The fact that some of the embryos ceased developing at the stage of

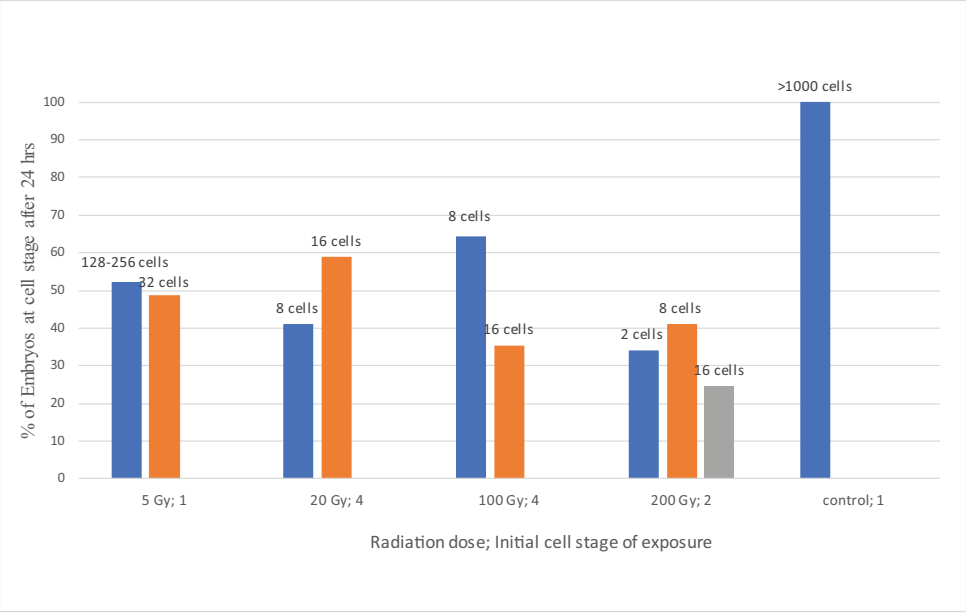

Figure 4. The percentage of *Cyclops kolensis* embryos that reached a particular cell stage of embryonic development in embryos exposed to different levels of radiation for 24 hours.

8-cell stage can be explained by damage to the cytoplasmic structures that ensure progression to 4th cleavage division. In more than 30% of embryos irradiated with doses of 100 and 200 Gy, and in more than 50% of embryos irradiated with a dose of 20 Gy, development stopped at the stage of 16-cell stage and while the mechanism of chromatin diminution processes was realized. It can therefore be concluded that the development of embryos of *C. kolensis* with radiation inactivated nuclei up to the stage of 16 cells is determined by a development program and is regulated by the determinants in the egg cytoplasm. Having lost its potential, the embryo ceases its development. Numerous chromosomal aberrations may block the function of the nuclear genome of presomatic cells, and hence the morphogenetic function of nuclei. A similar trend in the dynamics of developmental processes during early embryogenesis was observed in the nematode *Ascaris suum* (Nematoda) Goeze, 1782. Irradiation of *A. suum* embryos at the 4-cell stage prevented them from developing past the 16-cell stage (Neyfakh 1961). Neyfakh's intention was not to study the effect of γ-radiation on the chromatin diminution process in *A. suum. A. suum* undergoes chromatin diminution at the 3rd, 4th, and 5th cleavage divisions (Niedermayer and Moritz 2000). Radiation blocked the function of the nuclear genome of *A. suum*, but did not suppress the chromatin diminution process.

We conclude that in the *C. kolensis* zygote, transcription factors and signaling molecules are expressed in precise patterns that determine the fate of somatic and germ line cells, and consequently the diminution processes in somatic line cells. High doses of gamma- radiation inactivate the hereditary information contained in the cell nuclei

of *C. kolensis* embryos at doses up to 200 Gy, but do not affect the components of the cytoplasm that are important for patterning the chromatin diminution, which control the development up to the stage of 16-cells stage. But still, a dose of 200 Gy in some embryos was capable of disrupting the structure or dynamics of cytoplasmic factors that determine the possibility of chromatin diminution.

Thus, the results of the experiment confirm the assumptions of Boveri (1910), Geyer-Dushinskaya (1959) and Beermann (1977) in the cytoplasm of the embryos of the *Ascaris* Linnaeus, 1758, Cecidomyiidae and *Cyclops* Müller, 1785, species, in which the phenomenon of chromatin diminution is observed in early embryogenesis, there are factors that determine this process.

We did not attempt to compare the frequency of chromosomal aberrations at different doses of radiation using the methods of analysis of anaphases and counting micronuclei in the interphase stage. The relatively low frequency of chromosome aberrations, which we observed in this experiment, should be noted in comparison with earlier experiments on irradiation of *C. kolensis* embryos with the same dose but with a time interval of 60–180 min before embryo fixation (Grishanin and Akifiev 2005). Unfortunately, we could not observe the numbers of micronuclei present after irradiation of *C. kolensis* embryos at the 16- and 32-cell stages that were irradiated with doses of 20 and 100 Gy, since at these stages of development there were always a large number of granules of eliminated chromatin obscuring micronuclei. The tendency of an increase in the number of micronuclei per cell seems to occur naturally with an increase in the dose of γ-radiation.

The present study supports the following conclusions with regard to γ-radiation of *C. kolensis* embryos irradiated with a doses over 20Gy:

1. Development of *C. kolensis* embryos ceases at the 8–16 cell stage,
2. Initiation of the chromatin diminution program is not suppressed, except at the irradiation level of 200 Gy

Acknowledgements

The author is grateful to Alexander Molokanov (Laboratory of Nuclear Problems of the Joint Institute for Nuclear Research) for help in conducting an experiment on the irradiation of *C. kolensis* embryos.

References

Amma K (1911) Uber die differenzeirung der Keimbahnzellen bei den Copepoden. Archive Experimental Zellforschung 6: 497–576.

Beermann S (1977) The diminution of heterochromatic chromosomal segments in *Cyclops* (Crustacea, Copepoda). Chromosoma 60: 297–344. https://doi.org/10.1007/BF00292858

Boveri Th (1910) Die Potenzen der Ascaris-Blastomeren bei abgeanderter Furchung Zugleich ein Beitrag zur Frage quilitatve ungleicher Chromosomenteilung. Festschrift für R. Hertwig, Jena 3: 131–214.

Geyer-Dushinskaya I (1959) Experimental research on chromosome elimination in Cecidomyiidae (Diptera). Journal of Experimental Zoology 141: 391–441. https://doi.org/10.1002/jez.1401410302

Grishanin AK (1995) Comparative electron microscopic study of chromosomes and interphase nuclei in cells of *Cyclops kolensis* (Copepoda, Crustacea) before and after chromatin diminution. Russian Journal of Developmental Biology 26(3): 153–158.

Grishanin AK, Khudolii GA, Shaikhaaev GO, Brodskii VYa, Makarov VB, Akif'ev AP (1996) Chromatin diminution in *Cyclops kolensis* (Copepoda, Crustacea) is a unique example of genetic engineering in nature. Russian Journal of Genetics 32(4): 424–430.

Grishanin AK, Akifyev AP (2005) The Peculiarities of the Radiation Mutagenesis of *Cyclops kolensis* and *Cyclops insignis* (Crustacea, Copepoda). Radiation biology. Radioecology 45: 294–298. [In Russian]

Grishanin AK, Zagoskin MV (2019) Chromatin Diminution in *Cyclops kolensis* Lill. (Copepoda, Crustacea) as a Radical Way to Inactivate Redundant Genome in Somatic Cells. Cytogenetic and Genome Research 156(3): 165–172. https://doi.org/10.1159/000494157

Jaeger J (2018) Shift happens: The developmental and evolutionary dynamics of gap gene system. Current Opinion in Systems Biology 11: 65–73. https://doi.org/10.1016/j.coisb.2018.08.004

Moritz KB (1967) Die Blastomerendifferenzierung fur Soma and Keimbahn bei *Parascaris equorum*. II. Untersuchungen mittels UV-Bestrahlung und Zentrrifugierung. Wilhelm Roux' Archiv für Entwicklugsmechanik der Organismen 159: 203–266. https://doi.org/10.1007/BF00573440

Neyfakh AA (1961) Comparative study with the use of radiation of developmental function of nuclei in the development of animals. Ontogenez 22(1): 42–57. [In Russian]

Niedermeier J, Moritz KB (2000) Organisation and dynamics of satellite and telomere DNAs in *Ascaris*: implications for formation and programmed breakdown of compound chromosomes. Chromosoma 109: 439–452. https://doi.org/10.1007/s004120000104

Rivera-Pomar R, Lu X, Perrimon N, Taubert H, Jackle H (1995) Activation of posterior gap gene expression in the Drosophila blastoderm. Nature 376: 253–256. https://doi.org/10.1038/376253a0

Semeshin VF, Omelianchuk LV, Alekseeva AA, Ivankina EA, Sheveleva NG, Zhimulev IF (2011) DNA Content in Nuclei of *Cyclops kolensis* and *Cyclops insignis* (Crustacea, Copepoda). Cell and Tissue Biology 5(3): 300–310. https://doi.org/10.1134/S1990519X11030102

Wyngaard GA, Rash EM, Connelly BA (2011) Unusual augmentation of germline genome size in *Cyclops kolensis* (Crustacea, Copepoda): further evidence in support of a revised model of chromatin diminution. Chromosome Research 19(7): 911–923. https://doi.org/10.1007/s10577-011-9234-3

Zagoskin MV, Marshak TL, Mukha DV, Grishanin AK (2010) Chromatin diminution process regulates rRNA gene copy number in freshwater copepods. Acta Naturae 2(4): 52–57. https://doi.org/10.32607/20758251-2010-2-4-52-57

CompCytogen 15(4): 339–343 (2021)
doi: 10.3897/compcytogen.v15.i4.68309
https://compcytogen.pensoft.net

RESEARCH ARTICLE

COMPARATIVE Cytogenetics
A peer-reviewed open-access journal
International Journal of Plant & Animal Cytogenetics, Karyosystematics, and Molecular Systematics

The chiasmata systems of Scottish *Chysolina latecincta* (Demaison, 1896) (Coleoptera, Chrysomelidae)

Eduard Petitpierre[1]

1 *Dept. of Biology, University of Balearic Islands, 07122, Palma de Mallorca, Spain*

Corresponding author: Eduard Petitpierre (eduard.petitpierre @uib.es)

Academic editor: Dorota Lachowska | Received 7 May 2021 | Accepted 4 June 2021 | Published 28 September 2021

http://zoobank.org/21330929-BEA7-4F34-8661-E7A5B98D4E15

Citation: Petitpierre E (2021) The chiasmata systems of Scottish *Chysolina latecincta* (Demaison, 1896) (Coleoptera, Chrysomelidae). CompCytogen 15(4): 339–343. https://doi.org/10.3897/compcytogen.v15.i4.68309

Abstract

The meiotic systems of some Scottish individuals of the rare *Chrysolina latecincta* ssp. *intermedia* (Franz, 1938) have been analyzed from meiotic cells at diakinesis to study the types of chromosomal bivalents and the number and locations of their chiasmata. The mean number of unichiasmate was about two-thirds and that of bichiasmate bivalents about one-third. Most chiasmata were at distal positions and there were no pairwise statistically significant differences in the mean number of chiasmata and those of unichiasmate and bichiasmate bivalents between the three surveyed geographic sources of these Scottish individuals. However, pairwise significant differences were found in the mean number of proximal + interstitial chiasmata between Loch Etive (Argyllshire) and both Orkney and Shetland Islands individuals. The presumed higher values of genetic recombination due to the proximal + interstitial chiasmata with regard to the prevailing distal ones, might provide a slight selective advantage to the insular individuals against the more extreme climates of both islands compared with the Loch Etive site.

Keywords

Coleoptera, chiasmata, Chrysomelidae, *Chrysolina latecincta intermedia*, meiosis

Introduction

Chrysolina latecincta (Demaison, 1896) is a species distributed in western and central Europe from southern Norway to Spain and from Scotland to the Alps and Apennines (Kippenberg 2010). There are ten described subspecies that include the rare *Ch. l.* ssp.

intermedia (Franz, 1938), which is found in a few cliff Scottish localities (Hubble 2017; Bienkowski 2019). A cytogenetic analysis of three male individuals of *Ch. latecincta* ssp. *latecincta* from southern France has shown 2n = 24 chromosomes, with four large and seven small autosome pairs, plus a medium size X and a very small Y sex-chromosomes (Petitpierre 2000). In agreement with this size asymmetric karyotype the meiotic metaphases I display a male meioformula of 11 + Xy_p, with four large and seven small autosome bivalents and the achiasmate "parachute-like" Xy_p sex-chromosome (Petitpierre 1999). The aim of this paper is to get an insight on the chiasmate systems of the Scottish *Ch. l.* ssp. *intermedia* from three distinct geographic sources to compare them with data previously published from the above French typical *Ch. latecincta* subspecies and with further others closely related species in the same subgenus *Stichoptera* (Motschulsky, 1860). Moreover, the possible differences in chiasmate systems between these Scottish individuals will be also studied.

Materials and methods

One male individual from Orkney Islands, another one from Shetland Islands and two from Loch Etive, Argyllshire, in mainland Scotland, were chromosomally surveyed. The four samples of preserved testes in ethanol: glacial acetic acid (3:1) were sent to our laboratory at the University of Balearic Islands, in Palma de Mallorca, for their chromosomal analyses. We used a simple technique reported by Petitpierre et al. (1998) to obtain slides that were later stained in 4% diluted Giemsa in tap water before their final checking under a ZEISS AXIOSKOP microscope.

Results

The observations and scoring of chiasmata were performed on cells at meiotic diakinesis in order to know the number of unichiasmate and bichiasmate bivalents and their locations as proximal, interstitial or distal, in each type of meiotic configurations, according with the drawings by John and Lewis (1975, p. 50). Results are given in Table 1. From the total number of our 1264 scored bivalents, 68.2% were unichiasmate, mostly rod-shaped and much less often cross-shaped, and 31.8% bichiasmate, mostly ring-shaped. The percentage of distal chiasmata was clearly exceeding, from 87.7% to 96.3%, to those of proximal + interstitial ones. The mean total number of chiasmata per cell was very similar in all individuals because the four large autosome pairs were responsible for at least two and mostly three or four bichiasmate bivalents in all cells scored. The analysis of statistically significant differences between individuals from the three sites (Table 2, *t*-Student test), showed that the number of proximal + interstitial chiasmata varied significantly (**$P < 0.01$) between the Loch Etive individuals and those of Shetland and Orkney Islands individuals; a less significantly difference was found (*$P < 0.05$) in the mean number of distal chiasmata between Loch Etive and Orkney Islands individuals.

Discussion and conclusions

From the total number of our 1265 studied bivalents in *Ch. latecincta intermedia* 68.2% were unichiasmate, mostly rod-shaped, and 31.8% bichiasmate, mostly ring-shaped (Table 1).

The mean number of chiasmata per cell in Scottish *Ch. latecincta* were very similar in all studied individuals from the three sites, 14.4 to 14.8, due to the regular formation of a single chiasma in the seven smaller pairs of autosomes, and a varying number of one or two chiasmata in each of the four larger pairs (Table 1). The small differences in mean total number of chiasmata and in both bichiasmate and unichiasmate bivalent numbers between Scottish individuals were not statistically significant (Table 2). These results are in agreement with those obtained in other *Ch. latecincta* individuals from Southern France, whose four larger autosomes correspond to 57.44% of the total complement length and are responsible for all the bichiasmate bivalents scored (Petitpierre 2000). Another closely related species, *Ch. oceanoripensis* Bourdonné, Doguet & Petitpierre, 2013 (*Ch. ripoceanensis*; Petitpierre 2000), from Southwestern France, and belonging to the same subgenus *Stichoptera* Motschulsky, 1860, has 2n = 24 (Xy_p) too, and displays equally 14 chiasmata per cell, but a bit lower average of 27.3% of bichiasmate bivalents than those shown in Scottish individuals, from 30.8% to 34.7%. The finding of a clear prevalence of distal chiasmata in Scottish individuals (Table 1), agrees with the results found in other species of the subgenus *Stichoptera*, *Ch. oceanoripensis* and *Ch. gypsophilae* (Petitpierre 2000). A similar distal localization has been reported in *Pleocoma* Le Conte, 1856 (Scarabaeidae), *Pissodes* Germar, 1817 (Curculionidae) and even in almost all the New World Oedionychina subtribe of chrysomelids (Smith and Virkki 1978). In two hispini Chrysomelidae the same prevalence of distal localisations of chiasmata was found, namely, more than 85% of them in *Dicladispa testacea* (Linnaeus, 1767) and 75% in *Polyconia caroli* (Leprieur, 1883), were distally positioned (Alegre and Petitpierre 1990).

The significant difference in the mean number of proximal + interstitial chiasmata between Loch Etive and both Shetland and Orkney Islands (Table 2), might be re-

Table 1. Number of each class of chiasma and mean values per cell in Scottish individuals of *Chrysolina latecincta* ssp. *intermedia*. pro. = proximal, int. = interstitial, nr. = number.

Islands	Loch Etive	Orkney Islands	Shetland Islands
Cells scored	75	11	29
bivalents scored	825	121	319
bichiasmate bivalents	254 (30.8%)	42 (34.7%)	106 (33.2%)
unichiasmate bivalents	570 (69.2%)	79 (65.3%)	213 (66.8%)
total nr. of chiasmata	1078	163	425
mean nr. of chiasmata	14.373±0.117	14.818±0.157	14.60±0.162
nr. of distal chiasmata	1038 (96.3%)	143 (87.7%)	392 (92.2%)
mean nr. of distal chiasmata	x = 13.84±0.122	x = 13.00±0.374	x = 13.517±0.297
pro. + int. nr. of chiasmata	40 (3.7%)	20 (12.3%)	33 (7.76%)
mean pro.+ int. nr. of chiasmata	x = 0.533±0.089	x=1.818±0.395	x = 1.138±0.207

Table 2. Pairwise comparisons for chiasma mean numbers between individuals from the three Scottish sites of *Chrysolina latecincta* ssp. *intermedia*. pro. = proximal, int. = interstitial.

Islands	Bichiasmate	Unichiasmate	Pro. + Int.	Distal	Total
Loch Etive & Orkney Isl.	0.872	1.398	**3.000 *2.228	*2.228	1.422
Loch Etive & Shetland Isl.	0.845	1.321	**3.563 1.022	1.022	1.433
Orkney Islands & Shetland Isl.	0.370	0.506	1.453 1.122	1.022	0.492

**P < 0.01 *P < 0.05

lated to environmental differences between these sites. The recombination level derived from these proximal + interstitial chiasmata is presumably higher than that derived from distal chiasmata, due to the much larger size of chromatids exchanged. However, it should be noted that although extreme environments, such as low temperatures, may have some influence on chiasma formation, their effects on chiasma frequency are ambiguous (Wilson 1959). The 7.1 °C mean year temperature in Shetland Islands is lower than that of 7.8 °C in Orkney Islands, and both are lower to that of 8.1 °C in Loch Etive. Whether these temperature differences among the three Scottish sites have any effect on the frequency of proximal + interstitial chiasmata, is a question that needs to be answered in a much deeper analysis, with a much larger sample of individuals and a more insightful kind of experiment.

Acknowledgements

I would like thank to Dr. Michael Cox (Sussex, United Kingdom) who has sent me the preserved samples of Scottish *Chrysolina latecincta intermedia* and has given the mean year temperatures of the three surveyed sites. Drs. José Serrano (Murcia, Spain) and Dorota Lachowska-Cierlik (Kraków, Poland) have done a critical review in a first draft of this paper.

References

Alegre MC, Petitpierre E (1990) The chiasmatic systems in populations of two spiny leaf beetles (Coleoptera, Chrysomelidae). Genetica 80: 81–86. https://doi.org/10.1007/BF00127127

Bienkowski AO (2019) *Chrysolina* of the World. Taxonomic Review. Livny: G.V. Mukhametov Publ., 920 pp.

Hubble D (2017) Leaf beetles. Naturalist' Handbooks 34. Exeter: Pelagic Publishing, 149 pp.

John B, Lewis KR (1975) Chromosome Hierarchy. An Introduction to the Biology of the Chromosome. Clarendon Press, Oxford, 171 pp.

Kippenberg H (2010) Chrysomelinae. In: Löbl I, Smetana A (Eds) Catalogue of Palaearctic Coleoptera (Vol. 6). Chrysomeloidea. Apollo Books, Stenstrup, Denmark, 390–443.

Petitpierre E (1999) The cytogenetics and cytotaxonomy of *Chrysolina* Mots. and *Oreina* Chevr. (Coleoptera, Chrysomelidae, Chrysomelinae). Hereditas 131: 55–62. https://doi.org/10.1111/j.1601-5223.1999.00055.x

Petitpierre E (2000) The cytogenetics and cytotaxonomy of the subgenus *Stichoptera* of *Chrysolina* (Coleoptera, Chrysomelidae). In: Sobti RC, Yadav JS (Eds) Some Aspects on the Insight on the Insect Biology. Delhi: Narendra Publishing House, 181–187.

Petitpierre E, Carreras I, Gómez-Zurita J (1998) Cytogenetic analysis of European *Cassida* (Coleoptera, Chrysomelidae). Hereditas 128: 1–8. https://doi.org/10.1111/j.1601-5223.1998.00001.x

Smith SG, Virkki N (1978) Coleoptera. In: John B (Ed.) Animal Cytogenetics (Vol. 3): Insecta 5. Berlin-Stuttgart: Gebrüder Borntraeger, 366 pp.

Wilson JY (1959) Chiasma frequency in relation to temperature. Genetica 29: 290–303. https://doi.org/10.1007/BF01535715

CompCytogen 15(4): 345–354 (2021)
doi: 10.3897/compcytogen.v15.i4.67681
https://compcytogen.pensoft.net

RESEARCH ARTICLE

COMPARATIVE Cytogenetics
A peer-reviewed open-access journal
International Journal of Plant & Animal Cytogenetics, Karyosystematics, and Molecular Systematics

Derived karyotypes in two elephantfish genera (*Hyperopisus* and *Pollimyrus*): lowest chromosome number in the family Mormyridae (Osteoglossiformes)

Sergey Simanovsky[1], Dmitry Medvedev[1], Fekadu Tefera[2], Alexander Golubtsov[1]

1 *Severtsov Institute of Ecology and Evolution, Russian Academy of Sciences, 33 Leninskij prosp., Moscow, 119071 Russia* **2** *National Fishery and Aquatic Life Research Center, Ethiopian Institute of Agricultural Research, Sebeta, P.O. Box 64, Ethiopia*

Corresponding author: Sergey Simanovsky (sergey.a.simanovsky@gmail.com)

Academic editor: Patrícia Parise-Maltempi | Received 21 April 2021 | Accepted 25 August 2021 | Published 8 October 2021

http://zoobank.org/D02706AB-ACEF-43EE-9BD6-137DB62BA683

Citation: Simanovsky S, Medvedev D, Tefera F, Golubtsov A (2021) Derived karyotypes in two elephantfish genera (*Hyperopisus* and *Pollimyrus*): lowest chromosome number in the family Mormyridae (Osteoglossiformes). CompCytogen 15(4): 345–354. https://doi.org/10.3897/compcytogen.v15.i4.67681

Abstract

The African weakly electric elephantfish family Mormyridae comprises 22 genera and almost 230 species. Up-to-date cytogenetic information was available for 17 species representing 14 genera. Here we report chromosome number and morphology in *Hyperopisus bebe* (Lacepède, 1803) and *Pollimyrus isidori* (Valenciennes, 1847) collected from the White Nile system in southwestern Ethiopia. Both taxa displayed the diploid chromosome number 2n = 40, but they differed in fundamental numbers: FN = 66 in *H. bebe* and FN = 72 in *P. isidori*; previously the same diploid chromosome number 2n = 40 was reported in an undescribed species of *Pollimyrus* Taverne, 1971 (FN = 42) from the same region. Our results demonstrate that not only pericentric inversions, but fusions also played a substantial role in the evolution of the mormyrid karyotype structure. If the hypothesis that the karyotype structure with 2n = 50–52 and prevalence of the uni-armed chromosomes close to the ancestral condition for the family Mormyridae is correct, the most derived karyotype structures are found in the *Mormyrus* Linnaeus, 1758 species with 2n = 50 and the highest number of bi-armed elements in their compliments compared to all other mormyrids and in *Pollimyrus isidori* with the highest number of bi-armed elements among the mormyrids with 2n = 40.

Keywords

Africa, chromosomes, karyotype evolution, chromosome fusions, *Hyperopisus*, *Pollimyrus*

Introduction

The African weakly electric elephantfishes comprise the family Mormyridae including 22 genera and almost 230 species (Eschmeyer et al. 2021; Froese and Pauly 2021). To date, the representatives of 14 mormyrid genera have been studied cytogenetically (Uyeno 1973; Krysanov and Golubtsov 2014; Ozouf-Costaz et al. 2015; Canitz et al. 2016; Simanovsky et al. 2020, 2021). The diploid chromosome numbers in most elephantfishes vary between 48 and 52 with the mode 50 (Simanovsky et al. 2020). While a single studied species of the genus *Pollimyrus* Taverne, 1971 exhibited 2n = 40 (Krysanov and Golubtsov 2014).

A problem of the ancestral karyotype for the family Mormyridae was discussed by Canitz et al. (2016) and Simanovsky et al. (2020). In the first study, the most likely ancestral chromosome number for the family was identified as n = 24 or n = 25. In the latter study, three most parsimonious scenarios of the early karyotype evolution within the family were considered and the karyotype structure with 2n = 50–52 and prevalence of the uni-armed elements was suggested for a hypothetical ancestor. This suggestion was based on the following points. First, the family Mormyridae belongs to one of the most primitive groups of teleostean fishes, the cohort Osteoglossomorpha (Nelson et al. 2016), while the recent genomic data give evidence for the ancestral Euteleostomi karyotype of 50 chromosomes with domination by acrocentric elements (Nakatani et al. 2007; Sacerdot et al. 2018; de Oliveira et al. 2019). Second, for the family Notopteridae, the osteoglossomorph group closely related to mormyrids (Lavoué and Sullivan 2004, Nelson et al. 2016), the ancestral karyotype structure with 2n = 50 composed exclusively of uni-armed elements was suggested (Barby at al. 2018). Third, the karyotype structure with 2n = 50–52 and prevalence of the uni-armed elements is rather infrequent among mormyrids but appears in the genera displaying primitive morphology (mainly, dentition and electrocyte structure) and mainly basal phylogenetic positions (Taverne 1972; Alves-Gomes and Hopkins 1997; Sullivan et al. 2000).

Indeed, such karyotype structure is found in the two genera (*Petrocephalus* Marcusen, 1854 and *Mormyrops* Müller, 1843) appearing among the basal groups in molecular phylogenies of the family Mormyridae (Alves-Gomes and Hopkins 1997; Sullivan et al. 2000; Lavoué et al. 2003). The third basal genus (*Myomyrus* Boulenger, 1898) is not yet studied cytogenetically, while one more group with the seemingly primitive karyotype – *Stomatorhinus walkeri* (Günther, 1867) (2n = 50, FN = 52) – does not display a basal position in the phylogenetic trees but its stemming is varying and poorly supported (Lavoué et al. 2003; Sullivan et al. 2016; Levin and Golubtsov 2018).

The karyotype structure with chromosome number unusually low for mormyrids was reported by Krysanov and Golubtsov (2014) for a representative of the genus *Pollimyrus*. This genus is among the most species-rich of mormyrid genera, and includes 19 species widely distributed throughout sub-Saharian Africa (Eschmeyer et al. 2021; Froese and Pauly 2021). Variation of the karyotype structure among the different *Pollimyrus* species has not been studied. The genus *Hyperopisus* Gill, 1862 not yet studied cytogenetically includes the only species *H. bebe* distributed in the Sahelo-

Sudanese river basins (Eschmeyer et al. 2021; Froese and Pauly 2021). Both *Pollimyrus* and *Hyperopisus* never appeared among basal groups in the mormyrid molecular based phylogenies (Alves-Gomes and Hopkins 1997; Sullivan et al. 2000; Lavoué et al. 2003). Moreover, both genera exhibit some apparently derived morphological features related to the peculiarities of electrogeneration in *Pollimyrus* (Sullivan et al. 2000) and molluscivory in *Hyperopisus* (Taverne 1972; Bailye 1994).

In the present study, we address the uniqueness of the low chromosome numbers in mormyrids; *H. bebe* and the second species of the genus *Pollimyrus* were cytogenetically analyzed (for chromosome number and morphology). Based on the obtained and previous results, the two types of karyotype structure most derived from a hypothetical ancestral condition within the family Mormyridae were defined.

Material and methods

Fishes were collected in Ethiopia within the framework of the Joint Ethiopian-Russian Biological Expedition (**JERBE**) with permission from the National Fishery and Aquatic Life Research Center under the Ethiopian Institute of Agricultural Research and the Ethiopian Ministry of Innovation and Technology. The experiments were carried out in accordance with the rules of the Severtsov Institute of Ecology and Evolution, Russian Academy of Sciences.

Three individuals (two females and a male) of each of the two species – *Hyperopisus bebe* (Lacepède, 1803) (standard length, SL 131–356 mm) and *Pollimyrus isidori* (Valenciennes, 1847) (SL 54–60 mm) – were karyotyped; total numbers of complete metaphase plates studied for each species were 30 and 33, respectively. Fish were sampled in the Gambela Peoples' Region, a regional state in western Ethiopia at two sites in November of 2017: *P. isidori* from the Baro River downstream of the City of Itang (8°10'47"N, 34°15'2"E) and *H. bebe* from the Alvero River downstream of the Abobo Dam (7°52'23"N, 34°29'48"E). Both rivers belong to the Sobat River drainage discharging into the White Nile in South Sudan. Fish were caught with gill (*H. bebe*) and cast (*P. isidori*) nets, delivered in 80-l plastic containers into the field laboratory, where they were kept in permamently aerated water for several hours before treatment.

Before preparation fish were treated intraperitoneally with 0.1% colchicine for 3–4 hours. Then fish were euthanized with an overdose of tricaine methanesulfonate (MS-222), identified based on morphological key characters, measured to an accuracy of 1 mm, dissected for gonad examination and tissue sampling, and preserved in 10% formaldehyde. Vouchers are deposited at the Severtsov Institute of Ecology and Evolution (Moscow) under provisional labels of JERBE.

Chromosome preparations were obtained from anterior kidney according to Kligerman and Bloom (1977), procedures were described by Simanovsky and coauthors (2020, 2021). Giemsa-stained chromosome spreads were analysed under an "Axioplan 2 Imaging" microscope (Carl Zeiss, Germany) equipped with a "CV-M4+CL" camera (JAI, Japan) and "Ikaros" software (MetaSystems, Germany). Karyotypes were established according to

the centromere position following the nomenclature of Levan et al. (1964). Chromosomes were classified as metacentric (m), submetacentric (sm) and acrocentric (a), including subtelocentric and telocentric chromosomes, and grouped according to their morphology in order of decreasing size. To determine the fundamental number (FN), metacentrics and submetacentrics were considered bi-armed and acrocentrics as uni-armed.

Results and discussion

Hyperopisus bebe has karyotype with 2n = 40 (Fig. 1) consisting of 24 metacentrics, 2 submetacentrics and 14 acrocentrics, the fundamental number FN = 66. *Pollimyrus isidori* has karyotype with 2n = 40 consisting of 26 metacentrics, 6 submetacentrics and

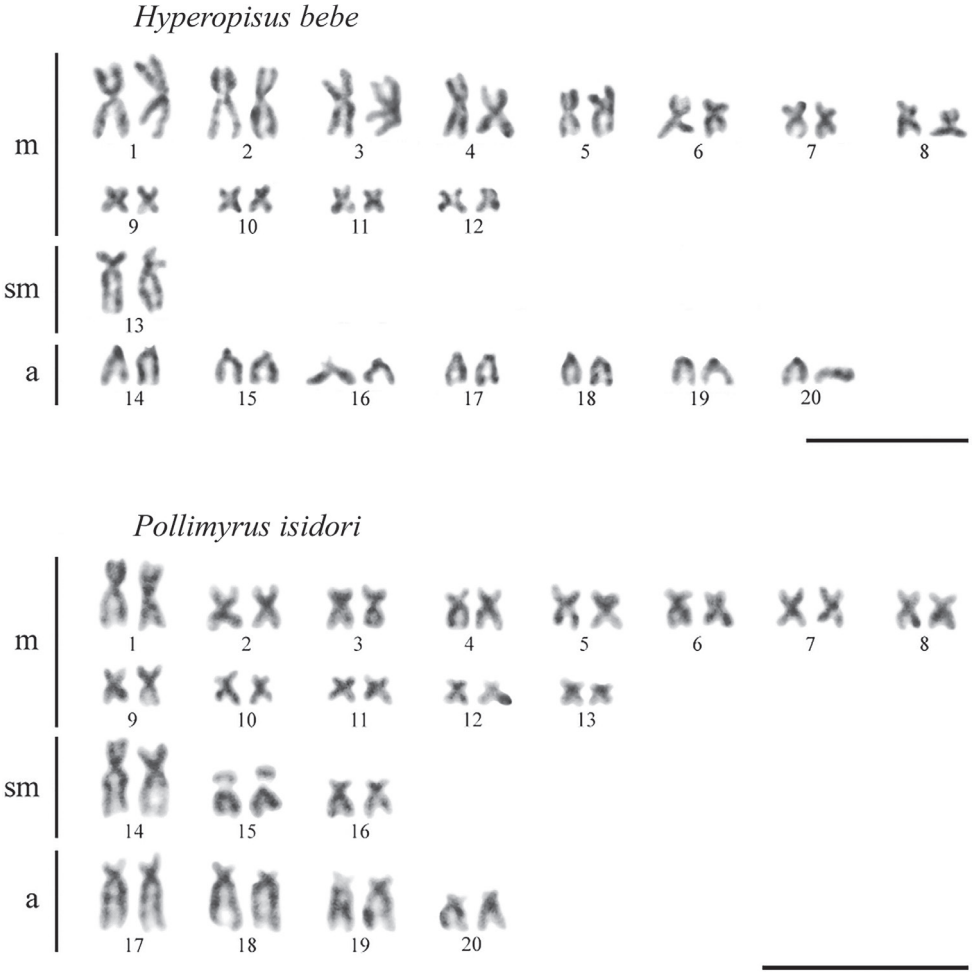

Figure 1. Karyotypes of *Hyperopisus bebe* and *Pollimyrus isidori* after conventional Giemsa staining. Scale bars: 10 μm.

Table 1. Cytogenetically studied elephantfishes of the family Mormyridae arranged in accordance with increasing (1) diploid chromosome number – 2n and (2) fundamental number – FN; karyotypic formulas most close to that in a hypothetic ancestor of the family are highlighted with bold.

Taxon	2n	Karyotypic formula	FN	Origin	References
2n = 40					
Pollimyrus prope *nigricans* (Boulenger, 1906)	40	2m + 38a	42	White Nile and Omo-Turkana Basins, Ethiopia	Krysanov and Golubtsov 2014
Hyperopisus bebe (Lacepède, 1803)	40	24m + 2sm + 14a	66	White Nile Basin, Ethiopia	This study
Pollimyrus isidori (Valenciennes, 1847)	40	26m + 6sm + 8a	74	White Nile Basin, Ethiopia	This study
2n = 48					
Brienomyrus brachyistius (Gill, 1862)	48	1m + 4sm + 2st + 41a	53	Unknown (fish store)	Uyeno 1973
Brevimyrus niger (Günther, 1866)	48	4m + 2sm + 42a	54	White Nile Basin, Ethiopia	Simanovsky et al. 2020
Gnathonemus petersii (Günther, 1862)	48	10m + 6sm + 32a	64	Unknown (fish store)	Uyeno 1973
	48	18m + 2sm + 28a	68	Unknown (fish store)	Ozouf-Costaz et al. 2015
Campylomormyrus rhynchophorus (Boulenger, 1898)	48	26m + 4sm + 18a	78	Unknown (laboratory stock)	Canitz et al. 2016
2n = 50					
Petrocephalus microphthalmus Pellegrin, 1909	50	**2sm + 48a**	52	Ogooué Basin, Gabon	Ozouf-Costaz et al. 2015
Stomatorhinus walkeri (Günther, 1867)	50	**2sm + 48a**	52	Ogooué Basin, Gabon	Ozouf-Costaz et al. 2015
Marcusenius moorii (Günther, 1867)	50	4sm + 46a	54	Ntem River, Gabon	Ozouf-Costaz et al. 2015
Paramormyrops sp.7	50	2m + 6sm + 42a	58	Woleu River, Gabon	Ozouf-Costaz et al. 2015
Ivindomyrus opdenboschi Taverne et Géry, 1975	50	10m + 2sm + 38a	62	Ntem River, Gabon	Ozouf-Costaz et al. 2015
Cyphomyrus petherici (Boulenger, 1898)	50	18m + 4sm + 28a	72	White Nile Basin, Ethiopia	Simanovsky et al. 2020
Marcusenius cyprinoides (Linnaeus, 1758)	50	22m + 4sm + 24a	76	White Nile Basin, Ethiopia	Simanovsky et al. 2020
Hippopotamyrus pictus (Marcusen, 1864)	50	24m + 4sm + 22a	78	White Nile Basin, Ethiopia	Simanovsky et al. 2020
Mormyrus caschive Linnaeus, 1758	50	20m + 14sm + 16a	84	White Nile Basin, Ethiopia	Simanovsky et al. 2021
Mormyrus hasselquistii Valenciennes, 1847	50	20m + 14sm + 16a	84	White Nile Basin, Ethiopia	Simanovsky et al. 2021
Mormyrus kannume Fabricius, 1775	50	20m + 14sm + 16a	84	Omo-Turkana Basin, Ethiopia	Simanovsky et al. 2021
2n = 52					
Mormyrops anguilloides (Linnaeus, 1758)	52	**52a**	52	White Nile Basin, Ethiopia	Simanovsky et al. 2020

8 acrocentrics, FN = 72. In agreement with the lack of reports on sex chromosomes in other mormyrids, no distinguishable sex chromosomes were observed in complements of the two species.

For comparative purposes, all the currently available data on the karyotype structure in mormyrids are given in Table 1. Usage of the name *Pollimyrus* prope *nigricans* (Boulenger, 1906) has been substantited by Krysanov and Golubtsov (2014). Division of the family Mormyridae into two subfamilies Petrocephalinae (including the single genus *Petrocephalus*) and Mormyrinae (including all other mormyrid genera), as well as usage of the names *Brienomyrus brachyistius* (Gill, 1862), *Campylomormyrus rhynchophorus* (Boulenger, 1898) and *Paramormyrops* sp.7, have been discussed by Simanovsky et al. (2020). The karyotypes most similar to a hypothetical ancestral condition within the family based on arguments considered above are highlighted with bold in the Table 1.

The chromosome set of the undescribed species reported by Krysanov and Golubtsov (2014) as *Pollimyrus* prope *nigricans* possessing 2n = 40 includes 2 small metacentric and 38 acrocentric chromosomes (FN = 42). Thus, despite the same diploid number of chromosomes (2n = 40), three taxa – *H. bebe* and two *Pollimyrus* species studied –

display the substantially diverged structure of their karyotypes. Interestingly, two *Pollimyrus* species differ from each other in karyotype structure – mostly in the number of uni-armed elements – more than both from *H. bebe*. Judging from the molecular phylogenies (Lavoué et al. 2003; Sullivan et al. 2016; Levin and Golubtsov 2018), there is a possibility of independent reduction of the chromosome numbers in *Hyperopisus* and *Pollimyrus*. Eight studied species of the latter genus form a well supported monophyletic clade within the mormyrid tree, while the two *Pollimyrus* species analyzed cytogenetically are closely related (Levin and Golubtsov 2018). *Stomatorhinus* in some analyses appears as a sister group to the *Pollimyrus* clade, but the clade *Pollimyrus* + *Stomatorhinus* is poorly supported (Lavoué et al. 2003; Sullivan et al. 2016; Levin and Golubtsov 2018). The phylogenetic position of *Hyperopisus* is not resolved in any molecular phylogenetic studies. The unusually low number of chromosomes for mormyrids in this genus makes the question of its phylogenetic position even more intriguing.

Pollimyrus appears the third mormyrid genus for which the data on intrageneric variation of the karyotype structure are available (Table 1). In this genus the pronounced divergence between species is similar to the situation in *Marcusenius* Gill, 1862, where two species studied have the same diploid chromosome number, but different karyotypic formula – *M. moorii* (Günther, 1867) has 4sm + 46a, *M. cyprinoides* (Linnaeus, 1758) has 22m + 4sm + 24a (2n = 50 for both) (Ozouf-Costaz et al. 2015; Simanovsky et al. 2020). On the contrary, among three species of the genus *Mormyrus* Linnaeus, 1758 no difference in their karyotype structure was found (Simanovsky et al. 2021). Thus, a search for interspecific differences in the non-monotypic mormyrid genera looks quite informative.

Pericentric inversions are considered as the main type of chromosomal rearrangements in mormyrid karyotype evolution by Ozouf-Costaz et al. (2015). Finding of the three species with substantially reduced chromosome numbers (Table 1) indicates that fusions also played a substantial role in the evolution of the mormyrid karyotype structure. Along with the family Mormyridae, a substantial reduction of chromosome numbers seems to occur in the related lineages of the cohort Osteoglossomorpha. Very interesting data on *Gymnarchus niloticus* Cuvier, 1829, the only representative of the family Gymnarchidae and a sister group of Mormyridae, reveal unexpectedly different karyotype structures – 2n = 34 (26m + 8sm) and 2n = 54 (26m + 14sm + 14sta) – in the two Nigerian populations separated by a distance of less than 200 km (Hatanaka et al. 2018; Jegede et al. 2018). Notopteridae is a sister group of Mormyridae + Gymnarchidae (Lavoué, Sullivan 2004; Nelson et al. 2016). Concerning the only notopterid *Papyrocranus afer* (Günther, 1868) exhibiting karyotype with 2n = 50 (2m + 2sm + 46a), it was suggested that its diploid number remains unchanged compared to a hypothetical common ancestor of notopterids but the karyotype structure in *P. afer* is formed by intrachromosomal rearrangement of two chromosome pairs, resulting in bi-armed elements (Barby at al. 2018). The other notopterids possess exclusively uni-armed elements in their karyotype with 2n ranging from 38 to 46. For this group of taxa Barby at al. (2018) suggest the reduction of 2n via tandem fusions.

One may suggest that just tandem fusions played an important role in reduction of chromosome number to 2n = 40 at least in *Pollimyrus* prope *nigricans* with FN = 42 (Table 1). Based on hypotheses about the dominating role of pericentric inversions in karyotype evolution in most other mormyrids (Ozouf-Costaz et al. 2015) and the ancestral karyotype structure with 2n = 50–52 and prevalence of the uni-armed chromosomes (Simanovsky et al. 2020), it is possible to consider the most parsimonious scenarios of an emergence of the karyotype diversity in the family. It is noteworthy that the karyotypes of all species with 2n = 50 could evolve from the ancestral karyotype with 2n = 50 and FN = 50 via pericentric inversions exclusively: from rearrangement of a single chromosome pair in *Petrocephalus* and *Stomatorhinus* to rearrangements of 17 chromosome pairs in *Mormyrus* Linnaeus, 1758 (Table 1). In our view, the karyotypes characterized by the lowest numbers of uni-armed elements may be considered as the most derived condition of the karyotype structure within the family. Particularly, based on the most parsimonious scenarios, the *Mormyrus* karyotype may be recognized as most derived among the mormyrids with 2n = 48–52, while the karyotype of *Pollimyrus isidori* seems to be most derived among the mormyrids with 2n = 40. Further studies with the use of more advanced cytogenetic techniques could verify the presented suggestions on the karyotype evolution within the family Mormyridae.

Acknowledgements

We gratefully acknowledge the JERBE coordinator Andrey Darkov (IEE RAS, Moscow) for logistic support, Sergey Cherenkov (IEE) for sharing field operations and assistance in collecting material, Eugeny Krysanov (IEE) for precious help at different stages of our work. This work is financially supported by the Russian Foundation for Basic Research Project no. 18-34-00638 for SS and benefits also (at the stage of manuscript preparation) from the Russian Science Foundation Project no. 19-14-00218 for AG.

References

Alves-Gomes J, Hopkins CD (1997) Molecular insights into the phylogeny of mormyriform fishes and the evolution of their electric organs. Brain, Behavior and Evolution 49: 324–350. https://doi.org/10.1159/000113001

Bailye RG (1994) Guide to the fishes of the River Nile in the Republic of the Sudan. Journal of Natural History 28: 937–970. https://doi.org/10.1080/00222939400770501

Barby FF, Ráb P, Lavoué S, Ezaz T, Bertollo LAC, Kilian A, Maruyama SR, de Oliveira EA, Artoni RF, Santos MH, Jegede OI, Hatanaka T, Tanomtong A, Liehr T, Cioffi MB (2018) From chromosomes to genome: insights into the evolutionary relationships and biogeography of Old World knifefishes (Notopteridae; Osteoglossiformes). Genes 96(6): e306. https://doi.org/10.3390/genes9060306

Canitz J, Kirschbaum F, Tiedemann R (2016) Karyotype description of the African weakly electric fish *Campylomormyrus compressirostris* in the context of chromosome evolution in Osteoglossiformes. Journal of Physiology-Paris 110: 273–280. https://doi.org/10.1016/j.jphysparis.2017.01.002

de Oliveira EA, Bertollo LAC, Rab P, Ezaz T, Yano CF, Hatanaka T, Jegede OI, Tanomtong A, Liehr T, Sember A, Maruyama SR, Feldberg E, Viana PF, Cioffi MB (2019) Cytogenetics, genomics and biodiversity of the South American and African Arapaimidae fish family (Teleostei, Osteoglossiformes). PLoS ONE 14(3): e0214225. https://doi.org/10.1371/journal.pone.0214225

Eschmeyer WN, Fricke R, van der Laan R [Eds] (2021) Catalog of Fishes: Genera, Species, References. http://researcharchive.calacademy.org/research/ichthyology/catalog/fishcatmain.asp [Accesed 20.04.2021]

Froese R, Pauly D [Eds] (2021) FishBase. http://www.fishbase.org [accessed 20.04.2021]

Hatanaka T, de Oliveira EA, Ráb P, Yano CF, Bertollo LAC, Ezaz T, Jegede OOI, Liehr T, Olaleye VF, Cioffi MB (2018) First chromosomal analysis in *Gymnarchus niloticus* (Gymnarchidae: Osteoglossiformes): insights into the karyotype evolution of this ancient fish order. Biological Journal of the Linnean Society 125: 83–92. https://doi.org/10.1093/biolinnean/bly098

Jegede O, Akintoye MA, Awopetu JI (2018) Karyotype of the African weakly electric fish, *Gymnarchus niloticus* (Osteoglossiformes: Gymnarchidae) from Oluwa River, Nigeria. Ife Journal of Science 20(3): 539–545. https://doi.org/10.4314/ijs.v20i3.8

Kligerman AD, Bloom SE (1977) Rapid chromosome preparations from solid tissues of fishes. Journal of the Fisheries Research Board of Canada 34(2): 266–269. https://doi.org/10.1139/f77-039

Krysanov EYu, Golubtsov AS (2014) Karyotypes of four fish species from the Nile and Omo-Turkana basins in Ethiopia. Journal of Ichthyology 54: 889–892. https://doi.org/10.1134/S0032945214100087

Lavoué S, Sullivan JP, Hopkins CD (2003) Phylogenetic utility of the first two introns of the S7 ribosomal protein gene in African electric fishes (Mormyroidea: Teleostei) and congruence with other molecular markers. Biological Journal of the Linnean Society 78: 273–292. https://doi.org/10.1046/j.1095-8312.2003.00170.x

Lavoué S, Sullivan JP (2004) Simultaneous analysis of five molecular markers provides a well-supported phylogenetic hypothesis for the living bony-tongue fishes (Osteoglossomorpha: Teleostei). Molecular Phylogenetics and Evolution 33: 171–185. https://doi.org/10.1016/j.ympev.2004.04.021

Levan A, Fredga K, Sandberg A (1964) Nomenclature for centromeric position on chromosomes. Hereditas 52: 201–220. https://doi.org/10.1111/j.1601-5223.1964.tb01953.x

Levin BA, Golubtsov AS (2018) New insights into the molecular phylogeny and taxonomy of mormyrids (Osteoglossiformes, Actinopterygii) in northern East Africa. Journal of Zoological Systematics and Evolutionary Research 56(1): 61–76. https://doi.org/10.1111/jzs.12186

Nakatani Y, Takeda H, Kohara Y, Morishita S (2007) Reconstruction of the vertebrate ancestral genome reveals dynamic genome reorganization in early vertebrates. Genome Research 17: 1254–1265. https://doi.org/10.1101/gr.6316407

Nelson JS, Grande T, Wilson MVH (2016) Fishes of the World, Fifth Edition, John Wiley & Sons, Inc., Hoboken, New Jersey, [xli +] 707 pp. https://doi.org/10.1002/9781119174844

Ozouf-Costaz C, Coutanceau J-P, Bonillo C, Belkadi L, Fermon Y, Agnèse J-F, Guidi-Rontani C, Paugy D (2015) First insights into karyotype evolution within the family Mormyridae. Cybium 39: 227–236. https://doi.org/10.26028/cybium/2015-393-006

Sacerdot C, Louis A, Bon C, Berthelot C, Crollius HR (2018) Chromosome evolution at the origin of the ancestral vertebrate genome. Genome Biology 19: 1–166. https://doi.org/10.1186/s13059-018-1559-1

Simanovsky S, Medvedev D, Tefera F, Golubtsov A (2020) First cytogenetic information for five Nilotic elephantfishes and a problem of ancestral karyotype of the family Mormyridae (Osteoglossiformes). Comparative Cytogenetics 14(3): 387–397. https://doi.org/10.3897/CompCytogen.14i3.52727

Simanovsky S, Medvedev D, Tefera F, Golubtsov A (2021) Similarity of karyotype structure in three *Mormyrus* species (Mormyridae) from the White Nile and Omo River tributaries (Ethiopia). Journal of Ichthyology 61(2): 323–326. https://doi.org/10.1134/S003294522102017X

Sullivan JP, Lavoué S, Hopkins CD (2000) Molecular systematics of the African electric fishes (Mormyroidea: Teleostei) and a model for the evolution of their electric organs. Journal of Experimental Biology 203: 665–683. https://doi.org/10.1242/jeb.203.4.665

Sullivan JP, Lavoué S, Hopkins CD (2016) *Cryptomyrus*: A new genus of Mormyridae (Teleostei, Osteoglossomorpha) with two new species from Gabon, West-Central Africa. ZooKeys 561: 117–150. https://doi.org/10.3897/zookeys.561.7137

Taverne L (1972) Ostéologie des genres *Mormyrus* Linné, *Mormyrops* Müller, *Hyperopisus* Gill, *Myomyrus* Boulenger, *Stomatorhinus* Boulenger et *Gymnarchus* Cuvier. Considérations générales sur la systématique des Poissons de l'ordre des Mormyriformes. Annales du Musée Royal de l'Afrique Centrale, Sciences Zoologiques 200: 1–194.

Uyeno T (1973) A comparative study of chromosomes in the teleostean fish order Osteoglossiformes. Japanese Journal of Ichthyology 20: 211–217.

ORCID

Sergey Simanovsky https://orcid.org/0000-0002-0830-7977
Dmitry Medvedev https://orcid.org/0000-0001-8560-8186
Alexander Golubtsov https://orcid.org/0000-0002-8317-7527

CompCytogen 15(4): 355–374 (2021)
doi: 10.3897/compcytogen.v15.i4.68761
https://compcytogen.pensoft.net

RESEARCH ARTICLE

COMPARATIVE Cytogenetics
A peer-reviewed open-access journal
International Journal of Plant & Animal Cytogenetics, Karyosystematics, and Molecular Systematics

High karyotypic variation in *Orthemis* Hagen, 1861 species, with insights about the neo-XY in *Orthemis ambinigra* Calvert, 1909 (Libellulidae, Odonata)

Liliana M. Mola[1], María Florencia Fourastié[2], Silvia Susana Agopian[3]

1 *Laboratorio de Citogenética y Evolución - Departamento de Ecología, Genética y Evolución, Instituto de Ecología, Genética y Evolución (CONICET-UBA), Facultad de Ciencias Exactas y Naturales, Universidad de Buenos Aires, Buenos Aires, Argentina* **2** *Instituto de Ecología, Genética y Evolución (CONICET-UBA), Facultad de Ciencias Exactas y Naturales, Universidad de Buenos Aires, Buenos Aires, Argentina* **3** *Scientist working privately, CABA, Argentina*

Corresponding author: Liliana María Mola (lilimola@yahoo.com.ar)

Academic editor: Natalia Golub | Received 17 May 2021 | Accepted 14 September 2021 | Published 3 November 2021

http://zoobank.org/4EAAA922-7CB6-43E3-9740-7C65645A5F69

Citation: Mola LM, Fourastié MF, Agopian SS (2021) High karyotypic variation in *Orthemis* Hagen, 1861 species, with insights about the neo-XY in *Orthemis ambinigra* Calvert, 1909 (Libellulidae, Odonata). CompCytogen 15(4): 355–374. https://doi.org/10.3897/compcytogen.v15.i4.68761

Abstract

The American dragonfly genus *Orthemis* Hagen, 1861 is mainly found in the Neotropical region**.** Seven of 28 taxonomically described species have been reported from Argentina. Chromosome studies performed on this genus showed a wide variation in chromosome number and a high frequency of the neoXY chromosomal sex-determination system, although the sexual pair was not observed in all cases. This work analyzes the spermatogenesis of *Orthemis discolor* (Burmeister, 1839), *O. nodiplaga* Karsch, 1891 and *O. ambinigra* Calvert, 1909 in individuals from the provinces of Misiones and Buenos Aires, Argentina. *Orthemis discolor* has 2n=23, n=11+X and one larger bivalent. *Orthemis nodiplaga* exhibits the largest chromosome number of the order, 2n=41, n=20+X and small chromosomes. *Orthemis ambinigra* shows a reduced complement, 2n=12, n=5+neo-XY, large-sized chromosomes, and a homomorphic sex bivalent. Fusions and fragmentations are the main evolutionary mechanisms in Odonata, as well as in other organisms with holokinetic chromosomes. *Orthemis nodiplaga* would have originated by nine autosomal fragmentations from the ancestral karyotype of the genus (2n=22A+X in males). We argue that the diploid number 23 in *Orthemis* has a secondary origin from the ancestral karyotype of family Libellulidae (2n=25). The complement of *O. ambinigra* would have arisen from five autosomal fusions and the insertion of the X chromosome into a fused autosome. C-banding and DAPI/CMA_3 staining allowed the identification of the sexual bivalent, which revealed the presence of constitutive heterochromatin. We propose that the chromosome with intermediate C-staining intensity and three medial heterochromatic

regions corresponds to the neo-Y and that the neo-system of this species has an ancient evolutionary origin. Moreover, we discuss on the mechanisms involved in the karyotypic evolution of this genus, the characteristics of the neo sex-determining systems and the patterns of heterochromatin distribution, quantity and base pair richness.

Keywords
Chromosomal evolution, holokinetic chromosomes, heterochromatin characterization, sex-determination system

Introduction

Family Libellulidae is characterized by having a modal number 2n=25 (n=12+X) in males, an XX/X0 chromosomal sex-determination system and chromosomes that decrease gradually in size, with the X chromosome being one of the smaller in the complement (Mola et al. 1999; Mola 2007; Kuznetsova and Golub 2020). *Orthemis* Hagen, 1861 is a common genus of American dragonflies mainly located in the Neotropical region. Seven of the 28 taxonomically described species have been reported from Argentina (*Orthemis aequilibris* Calvert, 1909, *Orthemis ambinigra* Calvert, 1909, *Orthemis ambirufa* Calvert, 1909, *Orthemis cultriformis* Calvert, 1899, *Orthemis discolor* (Burmeister, 1839), *Orthemis nodiplaga* Karsch, 1891 and *Orthemis phillipi* von Ellenrieder, 2009) (von Ellenrieder 2012; Mauffray and Tennessen 2019; Lozano et al. 2020).

Chromosome studies performed on this genus have revealed two particular characteristics: first, a wide variation in chromosome number, ranging from 2n=7 with two bivalents and a trivalent in meiosis (n=2II+1III) in *Orthemis levis* Calvert, 1906 to 2n=41 (n=20+X0) in *O. nodiplaga*, with no species having the characteristic modal number 25 of Libellulidae; and, second, a high frequency of neoXYsex-determining systems (Cumming 1964; Cruden 1968; Kiauta and Boyes 1972; Ferreira et al. 1979; Kiauta 1979; Souza Bueno 1982; Agopian and Mola 1984a). Taking into account the small size of the X chromosome in Odonata, the recognition of a heteromorphic sex bivalent at the different meiotic stages is difficult, as it depends on both the size of the autosome with which it was fused, and the degree of contraction of the bivalents. About half of the species in the order with this neoXY system have a homomorphic sex bivalent in males, including the species of *Orthemis* (Oksala 1943; Cumming 1964; Kiauta 1971, 1972, 1979; Ferreira et al. 1979; Souza Bueno 1982; Mola 1996; Perepelov et al. 1998; Perepelov and Bugrov 2002).

In Odonata, as in most organisms with holokinetic chromosomes, karyotype evolution might have occurred through fusions and fragmentations. Both types of rearrangements are favored because no limitations are imposed by the centromere (Kiauta 1969b; Mola and Papeschi 2006; Mola 2007; Kuznetsova and Golub 2020).

The heterochromatin is one of the key components of the genome and its biology is based on both the repetitive DNA sequences and the proteins specifically bound to this DNA. Although many of the structural and functional characteristics

of heterochromatin remain to be elucidated, there is evidence that its content and distribution affect DNA replication, modulate chromosome structure, and play a role in karyotypic evolution, gene expression and differentiation, and in genome organization and evolution (Hennig 1999; Redi et al. 2001; Straub 2003). The C-banding staining technique is frequently used to detect heterochromatin, allowing the visualization of most of the constitutive heterochromatin segments. The use of base-specific fluorochromes improves the characterization of heterochromatic regions with regard to their relative enrichment with AT or GC base pairs. The most widely used fluorochromes are CMA_3 and DAPI, which preferentially stain GC- and AT-rich DNA zones, respectively.

The heterochromatin in monocentric chromosomes is mainly located in centromeric and nucleolar organizer regions (NORs), while in holokinetic chromosomes it is predominantly located in the telomeric regions, with variations in base pair richness and distribution among different holokinetic systems (Mola and Papeschi 2006). Almost 80 species of Odonata have been studied with C-banding, of which 75% belong to seven families of Anisoptera and the rest to six families of Zygoptera. Libellulidae includes the greatest number of species analyzed (about 33% of the total).

C-banding revealed that, in general, autosomes present heterochromatic blocks in both telomeric regions. These blocks are small or large, symmetric or asymmetric. The free sex chromosome of males is entirely C-positive, shows intermediate staining, or has C-positive bands only located in terminal or interstitial regions (Suzuki and Saitoh 1988; Perepelov et al. 1998, 2001; Nokkala et al. 2002; Perepelov and Bugrov 2002; Walia and Chahal 2014; Kuznetsova et al. 2018; Walia and Devi 2018). In about half of the species so far analyzed, the X chromosome is entirely C-positive, which is consistent with its allocycly (facultative heterochromatinization) during male meiosis and reflects a different degree of condensation rather than the presence of constitutive chromatin.

In terms of base pair richness, it may be AT-rich or GC-rich, with variations between species, chromosomes of the same species and even within the same chromosome (Grozeva and Marinov 2007; De Gennaro et al. 2008; Walia and Katnoria 2017; Walia and Chahal 2018, 2019, 2020; Walia et al. 2018a, 2018b; Walia and Somal 2019; Walia and Devi 2020).

Taking into account the broad karyotypic variation observed within *Orthemis* and aiming to elucidate the mechanisms involved in the karyotypic evolution of this genus, our study analyzes the meiotic development, karyotype and patterns of heterochromatin distribution, quantity and base pair richness in *Orthemis discolor*, *O. ambinigra* and *O. nodiplaga*. In addition, we identify the homomorphic neo-XY sex pair of *O. ambinigra* with C-banding and fluorescent staining and propose a hypothesis of its origin.

Methods

The present study was performed on nine adult males of *Orthemis discolor*: three males from Santo Pipó (27°08'28"S, 55°24'32"W), five males from Parque Nacional Iguazú (25°41'35"S, 54°26'12"W) and one male from María Magdalena (26°14'15"S,

54°36'13"W) (Misiones Province), three adult males of *O. nodiplaga* from Parque Pereyra Iraola (34°50'38"S, 58°08'56"W) (Buenos Aires Province) and 19 adult males of *O. ambinigra*: 14 males from Delta del Paraná (34°25'15"S, 58°32'31"W) (Buenos Aires Province) and five males from Parque Nacional Iguazú (25°41'35"S, 54°26'12"W) (Misiones Province), Argentina. Administración de Parques Nacionales, Argentina, issued the permit for collection and transport of material from the Parque Nacional Iguazú.

The specimens were etherized in the field, a dorsal longitudinal cut in the abdomen was made and they were whole fixed in 3:1 (absolute ethanol: glacial acetic acid). Later, the gonads were dissected out and placed in fresh fixative for one day and stored in 70% ethanol at 4 °C. For meiotic studies a piece of gonad was placed in 45% acetic acid for 2 or 3 min to facilitate cell spreading and slides were made by the squash method in iron propionic hematoxylin.

C-Banding, fluorescent staining with CMA_3 (chromomycin A_3) and DAPI (4'-6-diamidino-2-phenylindole) and Feulgen staining were carried out on unstained slides. A piece of gonad was squashed in 45% acetic acid, the coverslip was removed by the dry-ice method and the slide was air-dried. For C-banding, slides were first dehydrated in absolute ethanol, followed by hydrolysis with 0.2N HCL at 60 °C for 30–60 sec., then, they were treated with a saturated solution of $Ba(OH)_2$ at room temperature for 15–20 min., incubated in 2XSSC at 60 °C for 1 h, stained with 2% Giemsa in Phosphate Buffer at pH 6.8, washed in tap water, air-dried and mounted (Giraldez et al. 1979). The sequential DAPI-CMA_3 banding was performed using the technique described by Rebagliati et al. (2003). For Feulgen staining, slides were washed twice in distilled water for 10 min each, and then air-dried and hydrolyzed in 5 N HCl at 25 °C for 60 min. This was followed by washing twice in distilled water for 10 min each, air-drying, staining with Schiff's reagent for 2 h in the dark, washing twice in SO_2 water for 10 min each, air-drying, washing twice in distilled water for 5 min each, air-drying and mounting.

Results

Orthemis discolor presents 2n=23, n=11+X, with no chromosomal differences between locations. At spermatogonial prometaphase the X chromosome, a pair of small chromosomes (*m* chromosomes), and one larger pair are distinguished (Fig. 1A). At both spermatogonial prometaphase and metaphase, the chromosomes always show thin associations between some telomeric regions.

At early prophase I, the X chromosome is isopycnotic or slightly negatively heteropycnotic and is separated from the chromatin mass formed by the autosomes (Fig. 1B). At pachytene, the X chromosome is isopycnotic or slightly positively heteropycnotic and is located near to the nuclear periphery, associated with the telomeric regions of some autosomes (Fig. 1C). At diakinesis and prometaphase I, bivalents present one subterminal chiasma. At this stage, a large bivalent and the *m* bivalent – of similar size to that of the X chromosome – are distinguished, while the rest of the bivalents

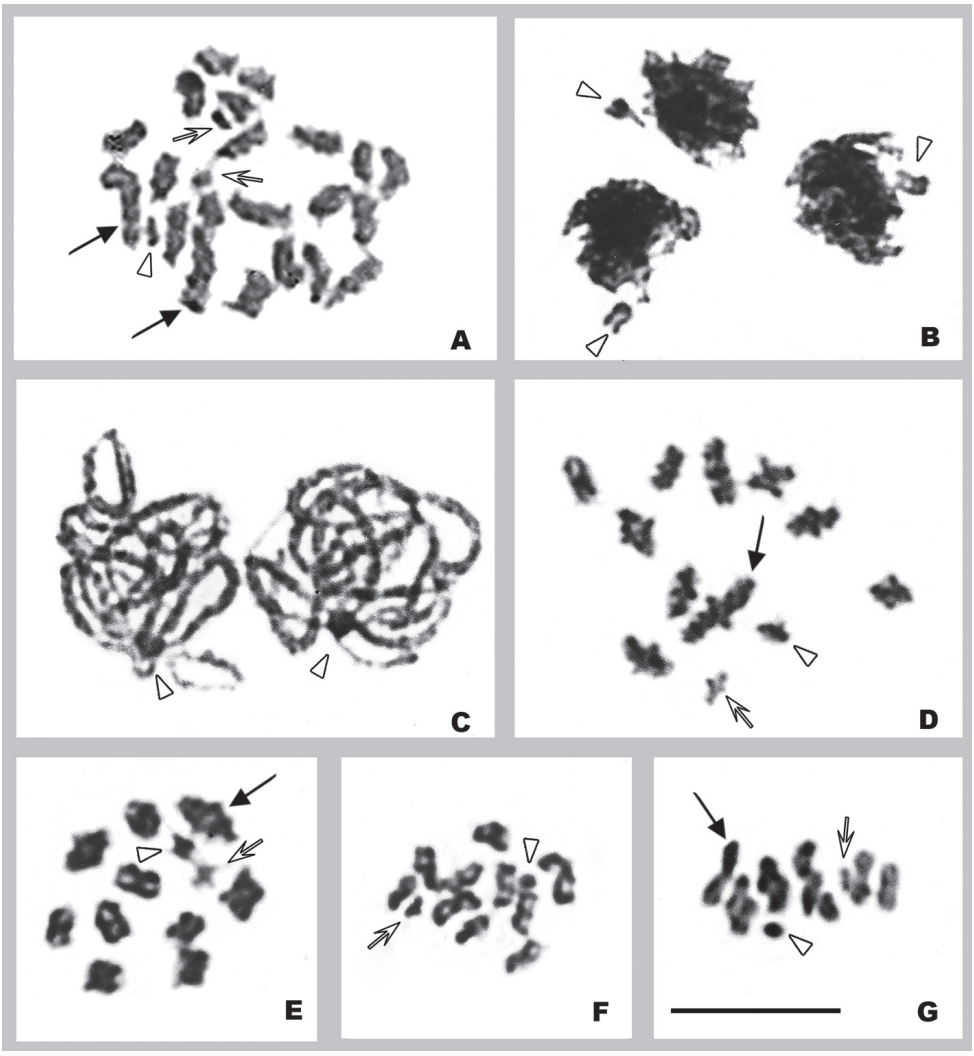

Figure 1. *Orthemis discolor* **A** spermatogonial prometaphase **B** zygotene **C** pachytene **D** diakinesis **E** prometaphase I **F** prophase II **G** metaphase II. Arrowheads point X chromosome. White arrows point *m* chromosomes. Black arrows point larger pair. Scale bar: 10 μm.

decrease gradually in size (Fig. 1D, E). The X chromosome divides equationally at anaphase I and there are 12 chromosomes in all cells during the second division. At prophase II, the autosomes adopt a ε shape (Fig. 1F) and at metaphase II, the X chromosome is somewhat separated from the autosomes on the equatorial plate (Fig. 1G).

Orthemis nodiplaga presents 2n=41, n=20+X (Agopian and Mola 1984a). The study of new specimens allowed us to confirm previous results and describe the meiotic stages. At spermatogonial metaphase the chromosomes vary in size, and the X chromosome is distinguished because it is the largest of the complement (See Fig. 2 in Agopian and Mola 1984a).

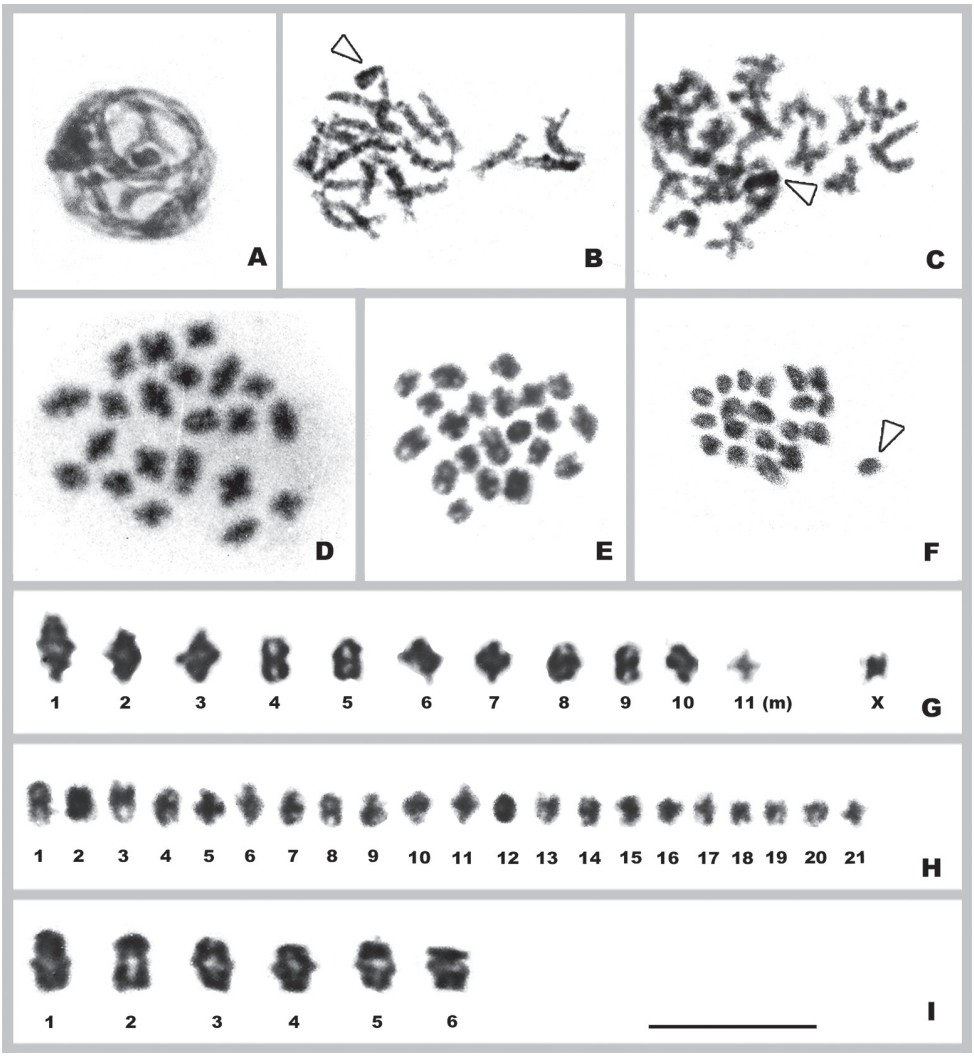

Figure 2. *Orthemis nodiplaga* (**A–F**) and meiotic karyotypes of *Orthemis* species (**G–I**) **A** pachytene **B** late pachytene **C** diplotene **D** diakinesis **E** prometaphase I **F** metaphase II **G** *O. discolor* (from Fig. 1E) **H** *O. nodiplaga* (from Fig. 2E) **I** *O. ambinigra* (from Fig. 3H). Arrowheads point X chromosomes. Scale bar: 10 μm.

At pachytene, the X chromosome is isopycnotic or slightly positively heteropycnotic and at late pachytene, the bivalents show separate telomeric zones (Fig. 2A, B). From diplotene onward, the bivalents exhibit one subterminal chiasma, and less often, one medial chiasma (Fig. 2C). At diakinesis and prometaphase I, the bivalents decrease slightly in size, no *m* bivalent is distinguished and the X chromosome is of similar size to that of medium bivalents (Fig. 2D, E). All the metaphases II exhibit 21 chromosomes and the X chromosome is separated from the autosomes (Fig. 2F). The bivalents of this species are smaller than those of *O. discolor* (Fig. 2G, H).

Orthemis ambinigra presents 2n=12 and n=5+neo-XY, with no chromosomal differences between individuals from distinct geographical locations. At spermatogonial prometaphase, the chromosomes are of similar size (Fig. 3A).

At early pachytene, no positive heteropycnotic bodies are observed and bivalents are often arranged in a *bouquet* (Fig. 3B). At mid and late pachytene, one bivalent shows a small interstitial loop (Fig. 3C, D). At diplotene and diakinesis, the six bivalents are homomorphic and present one subterminal chiasma, and one or unusually two bivalents seldom show two terminal chiasmata (Fig. 3E–G). At prometaphase I, two slightly larger bivalents are identified, and none of the six bivalents are heteromorphic (Fig. 3H). The bivalents of this species are comparable to the largest bivalent of *O. discolor* (Fig. 2G, I). The low number of bivalents and long duration of anaphase I (as indicated by the large number of cells at this stage) allowed us to perform a detailed analysis. At early anaphase, chromatids that migrate to the same pole lie approximately parallel to the equatorial plane, with the two medial telomeric regions held together and moving a little ahead. The two outer telomeric regions are connected by thin chromatin threads to the outer telomeric regions that migrate to the other pole, and exceptionally, there may be thin chromatin threads between the medial telomeric regions (Fig. 3I). The DNA presence in the threads was confirmed with Feulgen staining (Fig. 3J). These chromatin threads remain until late telophase (Fig. 3K). There is no true interkinesis because chromosomes do not undergo complete despiralization. At prophase II, the chromatids remain joined by the same telomeric regions as at anaphase I and adopt the characteristic ε shape (Fig. 3L). At prometaphase II, the free telomeres of the chromatids with ε shape get close to the central ones, which remain associated with each other and adopt an 8 shape (Fig. 3M). Later chromatids rotate so that U-shaped chromosomes face the poles at metaphase II and persist in this arrangement in anaphase II, where thin chromatin threads attached to chromosome ends moving poleward are observed again (Fig. 3N, O).

Heterochromatin characterization

Orthemis discolor exhibits C-positive bands in the telomeric region of all bivalents, either symmetric or asymmetric, in the scarce pachytenes and diakinesis able to be analyzed (data not shown).

Orthemis nodiplaga has small DAPI bright bands in the telomeric region of all the chromosomes except in the telomeric region of a pair of chromosomes that shows one DAPI dull/CMA_3 bright band at zygotene-pachytene (DAPI dull band not shown) (Fig. 4A, B).

In *O. ambinigra* the fluorescent banding indicates that from pachytene onward, the telomeric regions of all bivalents present DAPI bright/CMA_3 bright bands (Fig. 4C–F). At diakinesis, a heteromorphic bivalent is observed; one of the homologues shows a DAPI bright/CMA_3 bright staining, which is slightly less intense than that in the telomeric region (Fig. 4E, F).

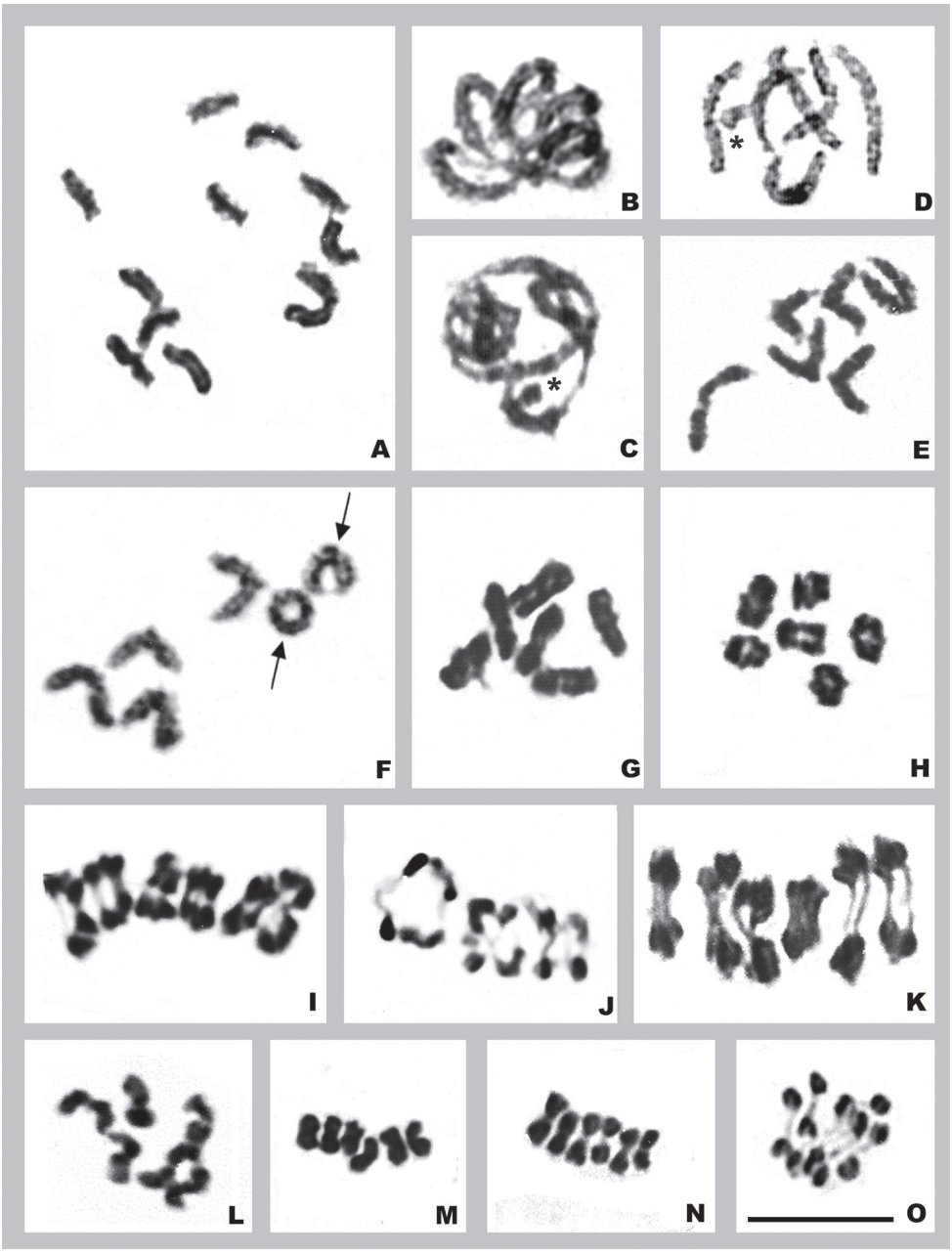

Figure 3. *Orthemis ambinigra* **A** spermatogonial prometaphase **B** bouquet stage **C** pachytene **D** late pachytene **E** diplotene **F** early diakinesis with one bivalent with two terminal chiasmata **G** diakinesise **H** prometaphase I **I** early anaphase I **J** early anaphase I (Feulgen staining) **K** medium anaphase I **L** prophase II **M** prometaphase II **N** early anaphase II **O** anaphase II. Asterisks point interstitial loop. Black arrows point bivalent with two chiasmata. Scale bar: 10 μm.

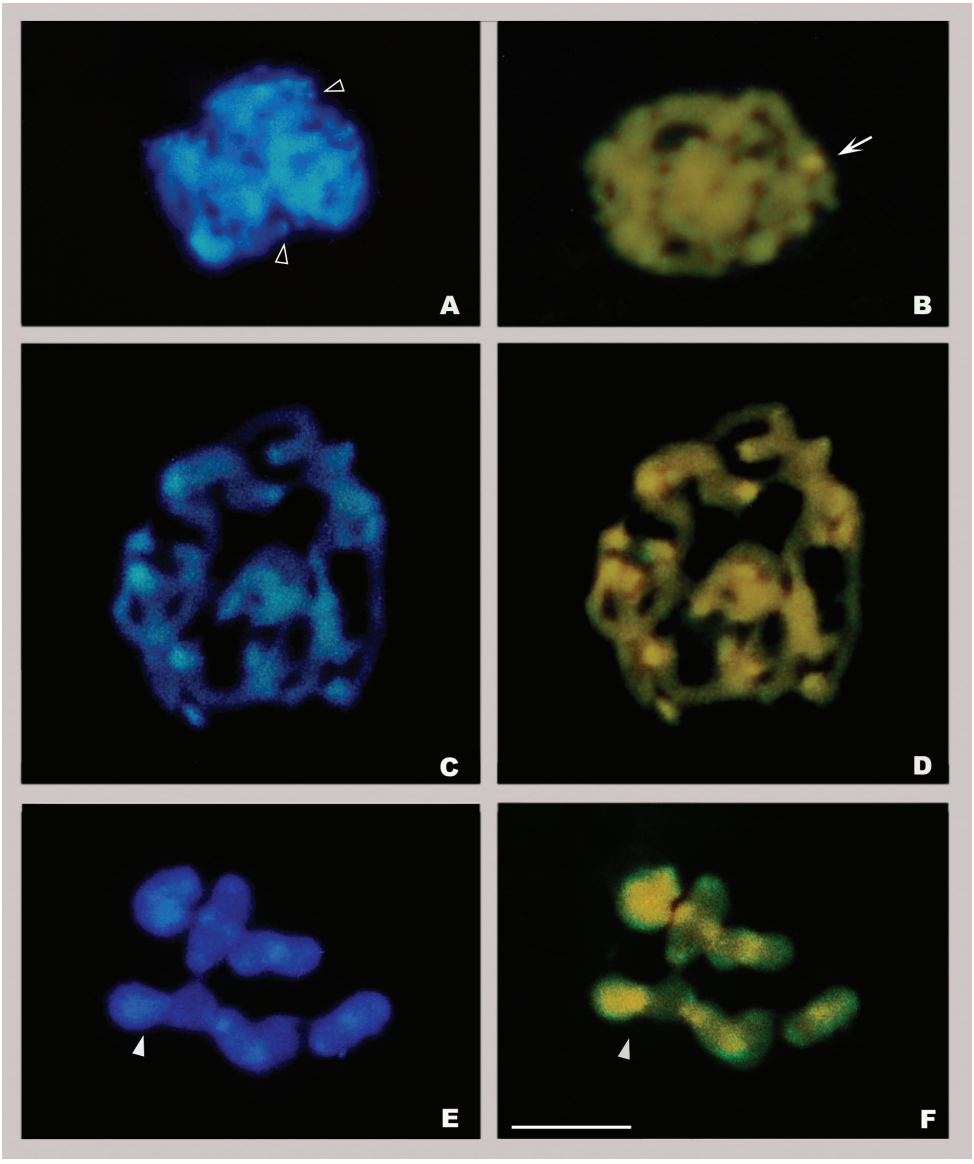

Figure 4. DAPI/CMA_3 staining of *Orthemis nodiplaga* (**A, B**) and *Orthemis ambinigra* (**C–F**) **A, B** zygotene **C, D** pachytene **E, F** diakinesis. Arrow points to DAPI dull/CMA_3 bright band. Empty arrowheads point to small DAPI bright bands. White arrowheads point to neo-XY bivalent. Scale bar: 10 μm.

In *Orthemis ambinigra*, all chromosomes at spermatogonial prometaphase show C-positive bands in the telomeric region and a few chromosomes have a C-positive band adjacent to this region; some chromosomes also exhibit a C-positive bands in their interstitial region, which are less stained than those in the telomeric region, and one chromosome exhibit two interstitial bands slightly separated. In addition, one chro-

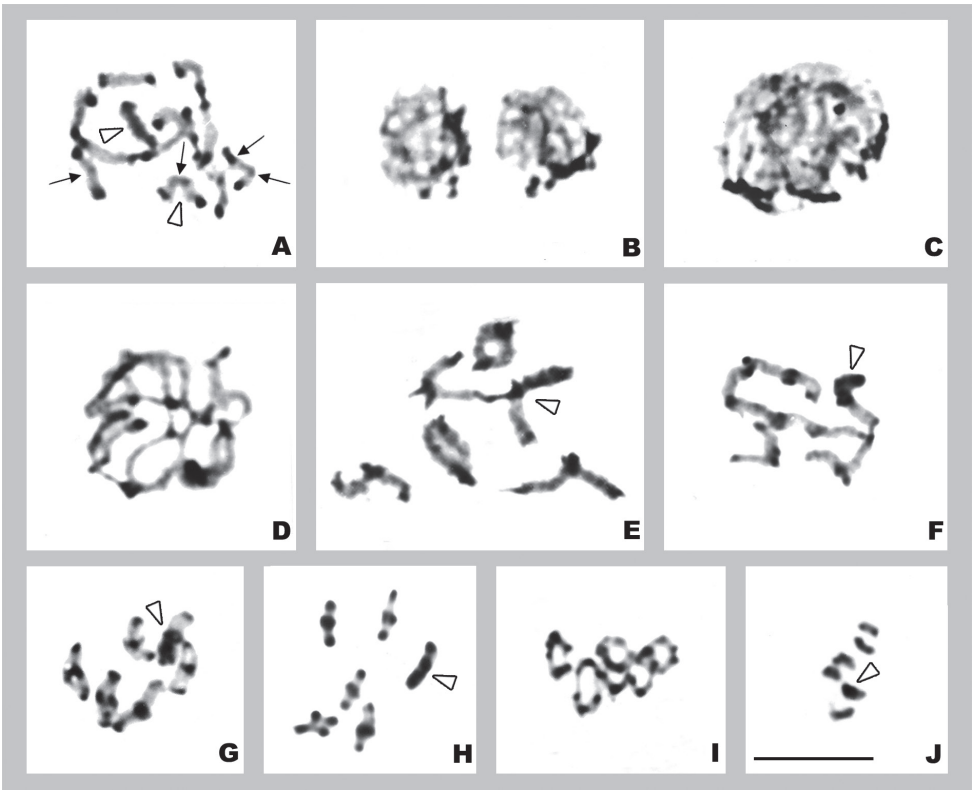

Figure 5. C-Banding of *Orthemis ambinigra* **A** spermatogonial prometaphase **B** zygotene **C** pachytene **D** early diplotene **E, F** diplotene **G** diakinesis **H** prometaphase I **I** early anaphase I **J** metaphase II. Arrowheads point to neo-XY bivalent/chromosomes. Black arrows point subterminal and interstitial bands. Scale bar: 10 μm.

mosome shows intermediate C-staining intensity along its length, where two or three darker regions can be distinguished (Fig. 5A). Also at this stage, several chromosomes show nonspecific associations between telomeric C bands. At zygotene, the C-positive regions show polarization at the nuclear periphery and this bouquet arrangement persists through pachytene (Fig. 5B, C). During diplotene, bivalents show a single C-band in the telomeric region and there are associations between the bands of different chromosomes (Fig. 5D–F). From mid-diplotene onward, one of the larger bivalents is heteromorphic, one homologue has C-positive bands in the telomeric region and the other one is almost completely C-positive. In the latter, at this stage, staining allows visualizing three large interstitial and closely located C-bands, besides the telomeric bands (Fig. 5E, F). From diakinesis onward, these three bands are unified into one band due to chromosome condensation (Fig. 5G, H). At anaphase I each chromosome presents four C-bands; the central ones are very close to each other and the outer ones are connected to those of the chromosome moving to the opposite pole by thin chromatin threads (Fig. 5I). At metaphase II, the chromosomes present terminal C-bands and the chromatid of one chromosome is entirely C-positive (Fig. 5J).

Discussion

Karyotype evolution in the genus *Orthemis*

None of the species studied showed the modal chromosome number of the family Libellulidae (2n=25, n=12+X in males), while the complement 2n=23/24, n=11+X0/11+XX (male/female) is present in 50% of the species (Table 1). Kiauta and Boyes (1972) assumed that the typical number of the genus would be of primary origin, as opposed of being derived from the modal number of the family. However, the presence of a larger bivalent in some species (see below) suggests that this complement derived from the typical complement of the family and originated in the common ancestor of the genus by an autosomal fusion.

In the genus *Orthemis* there is a tendency towards reduction in chromosome number through fusions. *Orthemis nodiplaga* seems to be the exception, in which the karyo-

Table 1. Chromosomal data of *Orthemis* species.

Specie	2n	n	N	Locality	References
Orthemis levis Calvert, 1906	7	2 II+1III	2	Arround Buena Vista, Santa Cruz Department, Bolivia	Cumming 1964
Orthemis sp.†	10	4+neo-XY	4	Near Buena Vista, Santa Cruz Department, Bolivia	Cumming 1964 as *O. ferruginea*
O. aequilibris Calvert, 1909	12	5+neo-XY	1	Borro-Borro, Paramaaribo District, Surinam	Kiauta 1979
O. ambinigra Calvert, 1909	12	5+neo-XY	14	Delta del Paraná, Buenos Aires Province, Argentina	Agopian and Mola 1984b,
			5	Parque Nacional Iguazú, Misiones Province, Argentina	Mola 2007, this work
O. biolleyi Calvert, 1906	23	11+X0	–	Eastern Bolivia	Cumming 1964
O. cultriformis Calvert, 1899	23	11+X0	–	Eastern Bolivia	Cumming 1964
			3	Cruzeiro do Sul, Acre State, Brazil	Ferreira et al 1979
O. discolor (Burmeister, 1839)		11+X0	1	Zanderij, Para District, Surinam	Kiauta 1979 as *O. ferruginea*
	23	11+X0†	4	Zanderij, Para District, Surinam	
	(25)	(11+neo-XY)† (10+neo-XY)†			
	23	11+X0	1	Cieneguilla, Lima Province, Perú	Kiauta and Boyes 1972 as *O. ferruginea*
	24 F	–	1		
		11+X0	2	Rio Claro, São Paulo State, Brazil	Ferreira et al. 1979 as *O. ferruginea*
		11+X0	2	Borecéia, São Paulo State, Brazil	Souza Bueno 1982 as *O. ferruginea*
		11+X0	1	Florianopolis, Santa Catarina State, Brazil	
	23	11+X0	3	Santo Pipó, Misiones Province, Argentina	Mola 2007, this work,
	23	11+X0	5	Parque Nacional Iguazú, Misiones Province, Argentina	This work
	23	11+X0	1	María Magdalena, Misiones Province, Argentina	This work
O. ferruginea (Fabricius, 1775)	23	11+X0	–	Central Texas State, US	Cumming 1964
			–	Marshall Co., Oklahoma State, US	Cruden 1968
O. ferruginea or *O. discolor*‡	23	11+X0	–	Tikal, Peten Department, Guatemala	Cruden 1968
Unnamed Antillean form sp.‡	23	11+X0	–	Commonwealth Dominica	Cruden 1968
O. nodiplaga Karsch, 1891	41	20+X0	2	Parque Peryra Iraola, Buenos Aires Province, Argentina	Agopian and Mola 1988
			1	Buenos Aires City, Argentina	
			3	Parque Peryra Iraola, Buenos Aires Province, Argentina	This work

Notes: N: Number of individuals analyzed; F: female; † See Discussion; ‡ According to Donnelly (1995) and Paulson (1998).

type derived from nine autosomal fragmentations within the ancestral karyotype of the genus that became fixed, while two pairs of autosomes were not fragmented. It is worthwhile to mention that the X chromosome remained intact despite the high number of fragmentations, and turned out to be the largest chromosome of the complement of this species (Agopian and Mola 1984a; this work).

The modal chromosome number is present in five species (Table 1). *Orthemis discolor* and *O. ferruginea* (Fabricius, 1775) represent an extremely similar, closely related sibling species pair occurring in sympatry from southern US to Costa Rica (Donnelly 1995; Paulson 1998). This raises questions about the identity of the species from Guatemala analyzed by Cruden (1968) and also if the species described by Cumming (1964) from Central Texas is *O. ferruginea* (Table 1).

Orthemis discolor is the most cytogenetically studied species. Kiauta (1979) reported two morphs from Surinam, one with the modal complement and the other with variations in the chromosome number and in the sex-determining system (Table 1). In the latter, the neo-XY found in 25% of the cells is indistinguishable. The fact that the author expressed the results as a percentage of cells from all four specimens prevents us from knowing if some individuals had neo-XY and others X0 or if both types of sex chromosomes were present in all the individuals, though the latter assumption seems much less likely.

Orthemis discolor and *O. cultriformis* exhibit a distinguishable largest pair (Cumming 1964; Kiauta and Boyes 1972; Ferreira et al. 1979; Kiauta 1979; Souza Bueno 1982; this work). Cumming (1964) and Cruden (1968) do not provide a detailed analysis of the autosomal karyotype for *O. ferruginea*, *O. biolleyi* Calvert, 1906 and the unnamed Antillean form species.

The four remaining species show a markedly reduced complement, 2n=7 in *Orthemis levis*, 2n=10 in *Orthemis* sp. and 2n=12 in *O. aequilibris* and *O. ambinigra*, originated by fusions between autosomes or an autosome and the X chromosome (Table 1). The individuals from Bolivia with 2n=10 described by Cumming (1964) as *O. ferruginea* do not correspond to this species. *Orthemis ferruginea* is found in North America and occur in Central America as far as to Costa Rica (Donnelly 1995; Paulson 1998).

We propose that the complement of *O. ambinigra* originated from the ancestral karyotype of the genus (2n=22+X) by five fusions of non-homologous autosomes in pairs, which eventually became fixed in the population, and by the interstitial insertion of the X chromosome in one of them leading to the neo-XY system (see below). The autosomal fusions occurred between chromosomes of different size, giving rise to a karyotype with chromosomes of similar size, where the largest autosomal pair of the ancestral karyotype remained unchanged. All or a large proportion of the telomeric heterochromatin would have been lost in the course of the multiple fusions that originated this complement. This is reflected in the current karyotype by the absence of interstitial heterochromatin in the chromosomes; in the few cases where the interstitial heterochromatin is present, it is less conspicuous than that in the telomeric regions.

Heterochromatin distribution, quantity and base pair richness

In Odonata, heterochromatin characterization has been mainly carried out using C-banding and in a less extent with DAPI/CMA_3 staining. Most species present heterochromatic blocks in both telomeric regions of the autosomes (Frankovič and Jurečič 1989; Prasad and Thomas 1992; Perepelov et al. 1998, 2001; Perepelov and Bugrov 2001, 2002; Nokkala et al. 2002; Grozeva and Marinov 2007; Mola 2007; Walia et al. 2011, 2016a, 2018a, 2018b; Walia and Chahal 2014, 2018, 2019, 2020; Walia and Katnoria 2017, 2018; Kuznetsova et al. 2018, 2020; Walia and Devi 2018, 2020; Walia and Somal 2019; this work). There are exceptions, where some or all the chromosomes of the complement show blocks in only one telomeric region or some chromosomes lack heterochromatin (Prasad and Thomas 1992; Perepelov et al. 2001; Walia et al. 2016b; Walia and Katnoria 2017; Kuznetsova et al. 2018, 2020; Walia and Devi 2018). The amount quantity of heterochromatin may vary from large blocks to tiny ones. In turn, these blocks may be symmetric (of equal size in both telomeric regions) or asymmetric (Perepelov et al. 1998). Species having a large amount quantity of heterochromatin show natural banding similar to C-banding in telomeric heterochromatin zones, as is the case of *Brachymesia furcata* (Hagen, 1861) (Agopian and Mola 1988). The presence of distinct heterochromatic blocks in all autosomes is the most common feature, which is also observed in the three especies of *Orthemis* studied herein.

A few species possess interstitial or subtelomeric blocks. The subtelomeric blocks, distinguished at pachytene or spermatogonial prometaphase, are usually small and are seen in some or all of the bivalents. As chromosome condensation proceeds, these blocks fuse with those in the telomeric region into a single block (Perepelov et al. 1998, 2001; Nokkala et al. 2002; Kuznetsova et al. 2018, 2020). The interstitial blocks are found in one or a few chromosomes and are detected until late prophase I (Perepelov et al. 1998; Walia et al 2016a, 2016b; Kuznetsova et al. 2018; Walia and Katnoria 2018). *Orthemis ambinigra* has both subtelomeric and interstitial blocks, the latter would be remnants of the multiple fusions that originated its reduced chromosome complement.

In Odonata, base-specific fluorochromes (DAPI/CMA_3) have been scarcely used for heterochromatin characterization. *Somatochlora borisi* Marinov, 2001 presents bright bands in the telomeric region of most bivalents with variable base pair richness, each one being AT- or GC-rich even in the same chromosome (Grozeva and Marinov 2007). In some Anisoptera and Zygoptera species collected from India, the heterochromatin in the terminal bands show variation in base pair richness. They are mainly AT- and GC-rich or only AT-rich (Walia and Katnoria 2017; Walia and Chahal 2018, 2019, 2020; Walia et al. 2018a, 2018b; Walia and Somal 2019; Walia and Devi 2020). *Orthemis ambinigra*, herein studied, also shows large bands of telomeric heterochromatin with interspersed AT- and GC-rich blocks (equally localized DAPI and CMA_3 bright bands). *Orthemis nodiplaga*, as well as *Erythrodiplax nigricans* (Rambur, 1842), has small heterochromatic AT-rich bands in the telomeric region of all chromosomes, except for one GC-rich band in a telomeric region of one pair of chromosomes (De Gennaro et al. 2008; this work). *Coryphaeschna perrensi* (McLachlan, 1887) shows only

one GC-rich band in the telomeric region of the largest pair, in this pair a correlation was established between the nucleolar organiser region (NOR) and the GC-rich band (De Gennaro et al. 2008). The association between GC-rich bands and NORs is frequent in insects with holokinetic chromosomes (Mola 2007; De Gennaro et al. 2008). The GC-rich telomeric band of *O. nodiplaga* and *E. nigricans* might correspond to the nucleolus organizer region as well.

Despite the small number of studies using fluorescent staining, our results support the hypothesis that the telomeric heterochromatin of Odonata has a heterogeneous base pair richness (Mola 2007).

Characterization and origin of the neo-XY in Orthemis ambinigra

In Odonata, the recognition of a heteromorphic sex bivalent in all meiotic stages is difficult, and about half of the species with this neo sex chromosomes system have a homomorphic sex bivalent in males. Its presence is inferred by the even number of chromosomes in the spermatogonial cells, the absence of a univalent in the first meiotic division and the absence of a chromosome that migrates ahead in the second meiotic division, which is a characteristic behavior of the free X chromosome in most of the species studied. In *Aeshna grandis* (Linnaeus, 1758), for instance, the sex bivalent is heteromorphic in both the first and second meiotic divisions, but in *Erythrodiplax media* Borror, 1942 the heteromorphism of the sex bivalent is recognized only at diplotene and diakinesis because it is masked by strong chromosome contraction at metaphase I (Oksala 1943; Kiauta 1969a; Mola 1996; Perepelov and Bugrov 2002).

The heterochromatin characterization of the neoXY has only been performed in three species of *Aeschna* Fabricius, 1775 (Perepelov et al. 1998; Perepelov and Bugrov 2002). Perepelov and Bugrov (2002) conclude that the formation of the neo-XY/neo-XX system in three *Aeschna* species was accompanied by the heterochromatinization of the autosomal regions of the neo-X and neo-Y, though these chromosomes are partially heterochromatic.

Several authors hypothesized that the evolution of the sex chromosomes of different insect orders such as orthopterans, lepidopterans and dipterans included total or partial loss of recombination, inactivation or loss of genes and progressive accumulation of repetitive DNAs and heterochromatinization of the Y (or W) or neo-Y chromosomes (Fuková et al. 2005; Vitková et al. 2007; Kaiser and Bachtrog 2010; Castillo et al. 2010a, 2010b, 2014; Bidau et al. 2011; Sahara et al. 2012; Zhou et al 2013; Palacios-Gimenez et al. 2015, 2018; Jetybayev et al. 2017; Buleu et al. 2020). The first step in Y chromosome degeneration is determined by the accumulation of transposable elements and their enrichment along a degenerating Y chromosome could explain the shift from euchromatic to heterochromatic chromatin structure (Steinemann and Steinemann 1998; Charlesworth et al. 2005).

Taking this into account, we propose that in *O. ambinigra* the chromosome mostly C-positive, with three large interstitial regions and two telomeric C-bands should correspond to the neo-Y chromosome. Besides, we propose that the bivalent that at pachytene presents a submedial loop should be the neo-XY. This loop may correspond

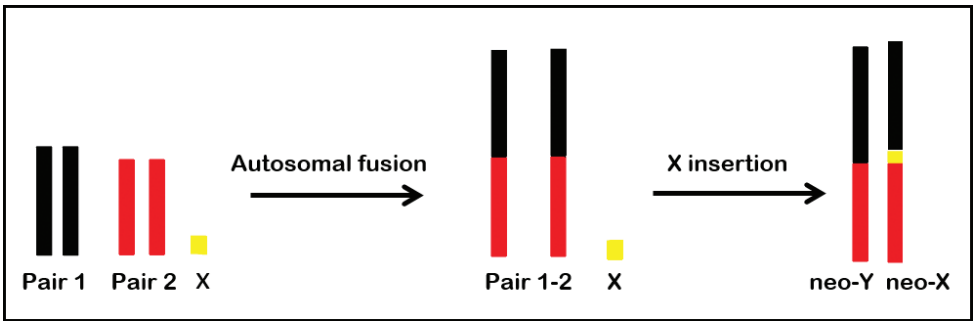

Figure 6. Diagram of the chromosome rearrangements that could give rise to the neo-X and neo-Y chromosomes of *Orthemis ambinigra*.

to the original X chromosome of the neo-X, with no homology in the neo-Y. Likewise, the chromosome at mitosis with two interstitial C-positive bands slightly separated and telomeric C-bands should also correspond to the neo-X. These submedial bands could delimit the site of insertion of the original X into one of the fused autosomes, thus indicating that the X telomeric heterochromatin was not completely lost due to insertion (Fig. 6). We propose that the sex chromosomes should correspond to a fused pair due to its large size. An alternative hypothesis of the origin of this neo-system could be that the fusion of the X chromosome with an autosome (forming a neo-X chromosome) occurred first, and this was followed by the fusion of both members of another autosomal pair to the neo-X and neo-Y. The first hypothesis appears to be the most plausible, providing the most parsimonious explanation for the origin of the neo-system. Since the fusion of the two homologous with other two chromosomes (neo-X, neo-Y) in the same orientation is less evolutionary probable than the insertion of the X chromosome in a fused chromosome, which had previously become structural homozygous by crossing. In contrast to the results reported by Perepelov and Bugrov (2002) for the species of *Aeschna*, in our study *O. ambinigra* showed no evidence of heterochromatinization of the autosomal region of the neo-X.

Given that in *O. ambinigra* the bivalents present a single subterminal chiasma, the differentiation of the neo-Y from the homologous autosomal region of the neo-X would be facilitated by the accumulation of repetitive DNA sequences, which can modify chromatin structure leading to its heterochromatinization. On this basis, the presence of three interstitial blocks of heterochromatin in the neo-Y may indicate an advanced evolutionary stage of a neo-XX/neo-XY sex determination system in this species.

Acknowledgements

This work was supported by grants from the National Council of Scientific and Technological Research (CONICET, PIP 112-201201-00107) and University of Buenos Aires (UBA, 20020130100694BA) to L. Mola and L. Poggio. Our sincere gratitude to

Dr. J. Muzón for his invaluable collaboration in the tentative identification of *Orthemis* species analyzed in the bibliography according to their geographical distribution. We wish to thank Drs. A. Rodrigues Capítulo and Javier Muzón for his advice in the taxonomy of the specimens included in the study.

References

Agopian SS, Mola LM (1984a) An exceptionally high chromosome number in *Orthemis nodiplaga* Kersch (Anisoptera, Libellulidae). Notulae Odonatologicae 2(3): 45.

Agopian SS, Mola LM (1984b) Bandeo C en Odonata. Abstracts of papers of the XV Congreso de la Sociedad Argentina de Genética. Corrientes, September 10–14, 1984, 17.

Agopian SS, Mola LM (1988) Intra and interspecific karyotype variability in five species of Libellulidae (Odonata, Anisoptera). Caryologia 41(1): 69–78. https://doi.org/10.1080/00087114.1988.10797849

Bidau CJ, Marti DA, Castillo ER (2011) Inexorable spread: inexorable death? The fate of neo-XY chromosomes of grasshoppers. Journal of Genetics 90: 397–400. https://doi.org/10.1007/s12041-011-0108-4

Buleu O, Jetybayev I, Mofidi-Neyestanak M, Bugrov A (2020) Karyotypes diversity in some Iranian Pamphagidae grasshoppers (Orthoptera, Acridoidea, Pamphagidae): new insights on the evolution of the neo-XY sex chromosomes. Comparative Cytogenetics 14(4): 549–566. https://doi.org/10.3897/compcytogen.v14.i4.53688

Castillo ER, Bidau CJ, Martí DA (2010a) Neo-sex chromosome diversity in Neotropical melanopline in grasshoppers (Melanoplinae, Acrididae). Genetica 138: 775–786. https://doi.org/10.1007/s10709-010-9458-8

Castillo ER, Martí DA, Bidau CJ (2010b) Sex and neo-sex chromosomes in Orthoptera: a review. Journal of Orthopteran Research 19: 213–231. https://doi.org/10.1665/034.019.0207

Castillo ER, Tafarel A, Martí DA (2014) The early evolutionary history of neo-sex chromosomes in Neotropical grasshoppers, *Boliviacris noroestensis* (Orthoptera: Acrididae: Melanoplinae). European Journal of Entomology 111: 321–327. https://doi.org/10.14411/eje.2014.047

Charlesworth D, Charlesworth B, Marais G (2005) Steps in the evolution of heteromorphic sex chromosomes. Heredity 95: 118–128. https://doi.org/10.1038/sj.hdy.6800697

Cruden RW (1968) Chromosome numbers of some North American dragonflies (Odonata). Canadian Journal of Genetics and Cytology 10: 200–214. https://doi.org/10.1139/g68-029

Cumming RB (1964) Cytogenetic studies in the order Odonata. PhD thesis, University of Texas, Austin, 93 pp.

De Gennaro D, Rebagliati PJ, Mola LM (2008) Fluorescent banding and meiotic behaviour in *Erythrodiplax nigricans* (Libellulidae) and *Coryphaeschna perrensi* (Aeschnidae) (Anisoptera, Odonata). Caryologia 61: 60–67. https://doi.org/10.1080/00087114.2008.10589610

Donnelly N (1995) *Orthemis ferruginea* – An adventure in Caribbean biogeography. Argia 7(4): 9–12.

Ferreira A, Kiauta B, Zaha A (1979) Male germ cell chromosomes of thirty-two Brazilian dragonflies. Odonatologica 8: 5–22.

Francovič M, Jurečič R (1989) Comparative cytogenetic analysis of karyotype morphology and organization in males of species *Libellula depressa* L. and *L. fulva* Müll. (Insecta: Odonata). Periodicum Biologorum 91(1): 32–33.

Fuková I, Nguyen P, Marec F (2005) Codling moth cytogenetics: Karyotype, chromosomal location of rDNA, and molecular differentiation of sex chromosomes. Genome 48(6): 1083–1092. https://doi.org/10.1139/g05-063

Giraldez R, Cermeno MC, Orellana J (1979) Comparison of C-banding pattern in the chromosomes of inbred lines and open pollinated varieties of rye. Zeitschrift fur Pflanzenzüchtung 83: 40–48.

Grozeva SM, Marinov MG (2007) Cytogenetic study of *Somatochlora borisi* Marinov, 2001 (Odonata: Corduliidae), and three relative species. Acta Zoologica Bulgarica 59(1): 53–58.

Hennig W (1999) Heterochromatin. Chromosoma 108: 1–9. https://doi.org/10.1007/s004120050346

Jetybayev IY, Bugrov AG, Ünal M, Buleu OG, Rubtsov NB (2017) Molecular cytogenetic analysis reveals the existence of two independent neo-XY sex chromosome systems in Anatolian Pamphagidae grasshoppers. BMC Evolutionary Biology 17(Suppl. 1): e20. https://doi.org/10.1186/s12862-016-0868-9

Kaiser VB, Bachtrog D (2010) Evolution of Sex Chromosomes in Insects. Annual Review of Genetics 44: 91–112. https://doi.org/10.1146/annurev-genet-102209-163600

Kiauta B (1969a) Sex chromosomes and sex determining mechanisms in Odonata, with a review of the cytological conditions in the family Gomphidae, and reference to the karyotypic evolution in the order. Genetica 40(2): 127–157. https://doi.org/10.1007/BF01787346

Kiauta B (1969b) Autosomal fragmentations and fusions in Odonata and their evolutionary implications. Genetica 40(2): 158–180. https://doi.org/10.1007/BF01787347

Kiauta B (1971) Studies on the germ cell chromosome cytology of some cytotaxonomically interesting or hitherto not studied Odonata from the autonomous region Friuli-Venezia Giulia (northern Italy). Atti del Museo civico di Storia naturale di Trieste 27: 65–127.

Kiauta B (1972) Notes on new or little known dragonfly karyotypes, 2. Male germ cell chromosomes of four East Mediterranean species: *Lestes barbarus* (Fabricius), *Calopteryx splendens amasina* Bartenev (Zygoptera: Lestidae, Calopterygidae), *Caliaeschna microstigma* (Schneider) and *Orthetrum taeniolatum* (Schneider) (Anisoptera: Aeshnidae, Libellulidae). Genen en Phaenen 15: 95–98.

Kiauta B (1979) The karyotypes of some Anisoptera from Surinam. Odonatologica 2: 267–283.

Kiauta B, Boyes JW (1972) Cytology of ten South American Libellulidae, with cytophylogenetic consideration of the genera *Orthemis* Hagen and *Erythrodipax* Brauer (Odonata, Anisoptera). Genetica 43(3): 407–421. https://doi.org/10.1007/BF00156136

Kuznetsova VG, Golub NV (2020) A checklist of chromosome numbers and a review of karyotype variation in Odonata of the world. Comparative Cytogenetics 14(4): 501–540. https://doi.org/10.3897/CompCytogen.v14.i4.57062

Kuznetsova VG, Maryańska-Nadachowska A, Shapoval NA, Anokhin BA, Shapoval AP (2018) Cytogenetic characterization of eight Odonata species originating from the Curonian Spit (the Baltic Sea, Russia) using C-banding and FISH with 18S rDNA and telomeric $(TTAGG)_n$ probes. Cytogenetic and Genome Research 153: 147–157. https://doi.org/10.1159/000486088

Kuznetsova VG, Maryańska-Nadachowska A, Anokhin BA, Shapoval NA, Shapoval AP (2020) Chromosomal analysis of eight species of dragonflies (Anisoptera) and damselflies (Zygoptera) using conventional cytogenetics and FISH: insights into the karyotype evolution of the ancient insect order Odonata. Journal of Zoological Systematics and Evolutionary Research 58: 1–13. https://doi.org/10.1111/jzs.12429

Lozano F, del Palacio A, Ramos L, Muzón J (2020) The Odonata of Argentina: state of knowledge and updated checklist. International Journal of Odonatology 23(2): 113–153. https://doi.org/10.1080/13887890.2020.1737585

Mauffray WF, Tennessen KJ (2019) A catalogue and historical study of the Odonata of Ecuador. Zootaxa 4628 (1): 1–265. https://doi.org/10.11646/zootaxa.4628.1.1

Mola LM (1996) Meiotic studies in nine species of *Erythrodiplax* (Libellulidae, Odonata). Neo-XY sex chromosome system in *Erythrodiplax media*. Cytologia 61: 349–357. https://doi.org/10.1508/cytologia.61.349

Mola LM (2007) Cytogenetics of American Odonata. In: Tyagi BK (Ed.) Odonata: Biology of Dragonflies. Scientific Publishers, India, 153–173.

Mola LM, Papeschi AG (2006) Holokinetic chromosomes at a glance. Journal of Basic & Applied Genetics 17(1): 17–33.

Mola LM, Papeschi AG, Carrillo ET (1999) Cytogenetics of seven species of dragonflies. Hereditas 131: 147–153. https://doi.org/10.1111/j.1601-5223.1999.00147.x

Nokkala S, Laukkanen A, Nokkala C (2002) Mitotic and meiotic chromosomes in *Somatochlora metallica* (Corduliidae, Odonata). The absence of localized centromeres and inverted meiosis. Hereditas 136: 7–12. https://doi.org/10.1034/j.1601-5223.2002.1360102.x

Oksala T (1943) Zytologische Studien an Odonaten I. Chromosomenverhältnisse bei der Gattung *Aeschna* mit besonderer Berücksichtigung der postreduktionellen Teilung der Bivalente. Annales Academiae Scientiarum Fennicae (A) IV, Biologica (4): 1–64.

Palacios-Gimenez OM, Marti DA, Cabral-de-Mello DC (2015) Neo-sex chromosomes of *Ronderosia bergii*: insight into the evolution of sex chromosomes in grasshoppers. Chromosoma 124(3): 353–365. https://doi.org/10.1007/s00412-015-0505-1

Palacios-Gimenez OM, Milani D, Lemos B, Castillo ER, Martí DA, Ramos E, Martins C, Cabral-de-Mello DC (2018) Uncovering the evolutionary history of neo-XY sex chromosomes in the grasshopper *Ronderosia bergii* (Orthoptera, Melanoplinae) through satellite DNA analysis. BMC Evolutionary Biology 18(2): 1–10. https://doi.org/10.1186/s12862-017-1113-x

Paulson DR (1998) The distribution and relative abundance of the sibling species *Orthemis ferruginea* (Fabricius, 1775) and *O. discolor* (Burmeister, 1839) in North and Middle America (Anisoptera: Libellulidae). International Journal of Odonatology 1(1): 89–93. https://doi.org/10.1080/13887890.1998.9748094

Perepelov E, Bugrov AG (2001) C-heterochromatin in chromosomes of *Ophiogomphus cecilia cecilia* (Four.) (Anisoptera: Gomphidae) with notes on the sex chromosome origin in the species. Caryologia 54(2): 169–172. https://doi.org/10.1080/00087114.2001.10589224

Perepelov E, Bugrov AG (2002) Constitutive heterochromatin in chromosomes of some Aeshnidae, with notes on the formation of the neo-XY/neo-XX mode of sex determination in *Aeshna* (Anisoptera). Odonatologica 31(1): 77–83.

Perepelov EA, Bugrov AG, Warchałowska-Śliwa E (1998) C-banded karyotypes of some dragonfly species from Russia. Folia biologica (Kraków) 46(3): 137–142.

Perepelov EA, Bugrov AG, Warchałowska-Śliwa E (2001) C-banded karyotypes of some dragonfly species from Russia. II. The families Cordulegasteridae, Corduliidae and Gomphidae. Folia biologica (Kraków) 49(3–4): 175–178.

Prasad K, Thomas KI (1992) C-band pattern homogeneity in dragonflies (Odonata). Caryologia 45: 57–68. https://doi.org/10.1080/00087114.1992.10797211

Rebagliati PJ, Papeschi AG, Mola LM (2003) Meiosis and fluorescent banding in *Edessa meditabunda* and *Edessa rufomarginata* (Heteroptera: Pentatomidae: Edessinae). European Journal of Entomology 100: 11–18. https://doi.org/10.14411/eje.2003.002

Redi CA, Garagna S, Zacharias H, Zuccotti M, Capanna E (2001) The other chromatin. Chromosoma 110: 136–147. https://doi.org/10.1007/s004120000114

Sahara K, Yoshido A, Traut W (2012) Sex chromosome evolution in moths and butterflies. Chromosome Research 20: 83–94. https://doi.org/10.1007/s10577-011-9262-z

Souza Bueno AM (1982) Estudos cromossomicos na ordem Odonata. M. Sc. Thesis, Universidad Estatal Paulista, 140 pp.

Steinemann M, Steinemann S (1998) Enigma of Y chromosome degeneration: neo-Y and neo-X chromosomes of *Drosophila miranda* a model for sex chromosome evolution. Genetica 102-103: 409–420. https://doi.org/10.1023/A:1017058119760

Straub T (2003) Heterochromatin Dynamics. PLoS Biology 1(1): e14. https://doi.org/10.1371/journal.pbio.0000014

Suzuki KJ, Saitoh K (1988) Germ-line chromosomes of two species of *Dadivíus* with special reference to the sex chromosomes (Anisoptera, Gomphidae). Odonatologia 17(3): 275–280.

Vítková M, Fuková I, Kubícková S, Marec F (2007) Molecular divergence of the W chromosomes in pyralid moths (Lepidoptera). Chromosome Research 15: 917–930. https://doi.org/10.1007/s10577-007-1173-7

von Ellenrieder N (2012) The levis group of Orthemis revisited: a sinopsis including a synonymy and description of six new species of *Orthemis* from South America (Odonata: Libellulidae). International Journal of Odonatology 15(3): 115–207. https://doi.org/10.1080/13887890.2012.688186

Walia GK, Chahal SS (2014) Distribution of constitutive heterochromatin and nucleolar organizer regions in two species of family Gomphidae (Odonata: Anisoptera). Nucleus 57: 223–227. https://doi.org/10.1007/s13237-014-0122-z

Walia GK, Chahal SS (2018) Cytogenetic characterization of *Macromia moorei* Selys, 1874 of family Macromiidae (Odonata: Anisoptera) from India by C-banding, silver nitrate staining and sequence specific staining. International Journal of Life Sciences Research 6(2): 64–68.

Walia GK, Chahal SS (2019) Cytogenetic report on *Cordulegaster brevistigma* and *Watanabeopetalia atkinsoni* (Odonata: Cordulegastridae, Chlorogomphidae). Odonatologica 48(1–2): 101–113.

Walia GK, Chahal SS (2020) Linear differentiation of chromosomes of *Anisogomphus bivittatus* Selys, 1854 from India (Odonata: Anisoptera: Gomphidae). International Journal of Entomology 5(2): 120–122.

Walia GK, Devi M (2018) Distribution of constitutive heterochromatin in four species of genus *Copera* of family Platycnemididae (Odonata: Zygoptera) from India. International Journal of Life Sciences 6(2): 457–461.

Walia GK, Devi M (2020) Cytogenetic data of subfamily Disparoneurinae (Odonata: Zygoptera: Platycnemididae) based on localization of C-heterochromatin, AgNOR's and AT-GC regions. International Journal of Entomology Research 5(2): 70–73.

Walia GK, Katnoria N (2017) Linear characterization of chromosomes in two species of family Euphaeidae (Odonata: Zygoptera). International Journal of Entomology Research 2(4): 75–78.

Walia GK, Katnoria N (2018) Morphological variation in the chromosome complement of *Neurobasis chinensis chinensis* of family Calopterygidae (Odonata: Zygoptera). International Journal of Life Sciences Research 6(4): 260–266.

Walia GK, Somal DS (2019) Cytogenetic report on *Gynacantha subinterrupta* Rambur, 1842 of family Aeshnidae (Odonata: Anisoptera) from Himachal Pradesh, India. Journal of Advanced Zoology 40(2): 128–135.

Walia GK, Chahal SS, Babu R (2016a) Cytogenetic report on *Gynacanthaeschna sikkima* from India (Odonata: Aeshnidae). Odonatologica 45: 87–94.

Walia GK, Kaur H, Kaur J (2016b) C-Banding and Ag-NOR staining on *Neurobasis chinensis chinensis* (Linnaeus) of family Clopterygidae from Himachaln Pradesh, India (Odonata: Zygoptera). Cytologia 81(2): 175–178. https://doi.org/10.1508/cytologia.81.175

Walia GK, Chahal SS, Somal DS (2018a) Chromosome observations based on C-banding, Ag-NOR and sequence-specific staining in two *Anax* species from India (Odonata: Aeshnidae). Odonatologica 47(1–2) 2018: 145–160.

Walia GK, Katnoria N, Gill JK (2018b) Chromosomes of *Libellago lineata lineata* (Chlorocyphidae: Odonata). Indian Journal of Entomology 80(3): 737–740. https://doi.org/10.5958/0974-8172.2018.00118.9

Walia GK, Kaur H, Kaur J (2011) Karyotypic variations in the chromosome complement of *Pantala flavescens* (Fabricius) of the family Libellulidae (Anisoptera: Odonata). Cytologia 76(3): 301–307. https://doi.org/10.1508/cytologia.76.301

Zhou Q, Ellison CE, Kaiser VB, Alekseyenko AA, Gorchakov AA, Bachtorg D (2013) The epigenome of evolving Drosophila Neo-Sex Chromosomes: Dosage compensation and heterochromatin formation. PLoS Biology 11(11): e1001711. https://doi.org/10.1371/journal.pbio.1001711

ORCID

Liliana M. Mola https://orcid.org/0000-0003-2511-8067
María Florencia Fourastié https://orcid.org/0000-0002-4039-5858
Silvia Susana Agopian https://orcid.org/0000-0003-1947-4049

CompCytogen 15(4): 375–392 (2021)
doi: 10.3897/compcytogen.v15.i4.71525
https://compcytogen.pensoft.net

RESEARCH ARTICLE

COMPARATIVE Cytogenetics
A peer-reviewed open-access journal
International Journal of Plant & Animal Cytogenetics, Karyosystematics, and Molecular Systematics

The *Kengyilia hirsuta* karyotype polymorphisms as revealed by FISH with tandem repeats and single-gene probes

Xiaoyan Tao[1,3*], Bo Liu[1,3*], Quanwen Dou[1,2]

1 *Key Laboratory of Adaptation and Evolution of Plateau Biota, Northwest Institute of Plateau Biology, Chinese Academy of Sciences, Xining, China* **2** *Key Laboratory of Crop Molecular Breeding, Qinghai Province, Northwest Institute of Plateau Biology, Chinese Academy of Sciences, Xining, China* **3** *University of Chinese Academy of Sciences, Beijing, China*

Corresponding author: Quanwen Dou (douqw@nwipb.cas.cn)

Academic editor: Gennady Karlov | Received 13 July 2021 | Accepted 23 September 2021 | Published 3 November 2021

http://zoobank.org/3B669F9C-B977-4777-97F3-F5FE96865156

Citation: Tao X, Liu B, Dou Q (2021) The *Kengyilia hirsuta* karyotype polymorphisms as revealed by FISH with tandem repeats and single-gene probes. CompCytogen 15(4): 375–392. https://doi.org/10.3897/compcytogen.v15.i4.71525

Abstract

Kengyilia hirsuta (Keng, 1959) J. L. Yang, C. Yen et B. R. Baum, 1992, a perennial hexaploidy species, is a wild relative species to wheat with great potential for wheat improvement and domestication. The genome structure and cross-species homoeology of *K. hirsuta* chromosomes with wheat were assayed using 14 single-gene probes covering all seven homoeologous groups, and four repetitive sequence probes 45S rDNA, 5S rDNA, pAs1, and $(AAG)_{10}$ by FISH. Each chromosome of *K. hirsuta* was well characterized by homoeological determination and repeats distribution patterns. The synteny of chromosomes was strongly conserved in the St genome, whereas synteny of the Y and P genomes was more distorted. The collinearity of 1Y, 2Y, 3Y and 7Y might be interrupted in the Y genome. A new 5S rDNA site on 2Y might be translocated from 1Y. The short arm of 3Y might involve translocated segments from 7Y. The 7 Y was identified as involving a pericentric inversion. A reciprocal translocation between 2P and 4P, and tentative structural aberrations in the subtelomeric region of 1PL and 4PL, were observed in the P genome. Chromosome polymorphisms, which were mostly characterized by repeats amplification and deletion, varied between chromosomes, genomes, and different populations. However, two translocations involving a P genome segmental in 3YL and a non-Robertsonial reciprocal translocation between 4Y and 3P were identified in two independent populations. Moreover, the proportion of heterozygous karyotypes reached almost 35% in all materials, and almost 80% in the specific population. These results provide new insights into the genome organization of *K. hirsuta* and will facilitate genome dissection and germplasm utilization of this species.

* These authors contribute equally to this work.

Keywords
Homoeology, karyotype, *Kengyilia hirsuta*, single-gene FISH

Introduction

Kengyilia Yen, Yang, C. Yen et J. L. Yang, 1990, is a perennial genus belonging to the tribe Triticeae (family Poaceae), species of which are commonly distributed in central Asia and the Qinghai–Tibetan plateau (Yen and Yang 1990). *Kengyilia* grows in meadows, steppes, the fringes of forests, and also semi deserts or extremely dry deserts at altitudes from 1100 to 4750 m (Yang et al. 1992). Approximately 32 species and subspecies have been documented in this genus (Cai 1999). *Kengyilia hirsuta* (Keng, 1959) J. L. Yang, C. Yen et B. R. Baum, 1992, is a species of *Kengyilia*, which is distributed in Qinghai and Gansu in China. *K. hirsuta* can be found around sandy areas in high altitude regions, owing to its high tolerance to cold hardness and drought, as well as its distinct perennial characteristics. As a grain grass, *K. hirsuta* has potential genetic resources for utilization in cereal crop development.

Many desired genes, such as disease resistance and stress tolerant genes, were introduced to the wheat background using specific cytology techniques involving hybridization with the tertiary gene pool species (Jiang et al. 1994). The transfer of apomixis into wheat was attempted by crossing wheat and *Elymus rectisetus* (Nees, 1846) Á. Löve et Connor, 1982, which is apomictic (Wang et al. 1993; Liu et al. 1994). Perennial crops are thought to have great potential for truly sustainable production systems (Glover et al. 2010). The perennial habit has been transferred into annual wheat by introducing alien chromosomes from related perennial species (Lammer 2004; Abbasi et al. 2020). However, no widely used perennial cultivars were produced following these attempts (Dehaan et al. 2020). Direct domestication of wild perennial grass relatives of wheat, such as *Thinopyrum intermedium* (Host, 1805) Barkworth et Dewey, 1985, is an alternative approach (Dehaan et al. 2020). *K. hirsuta*, which is a close perennial relative of wheat, is charaterized by tall stalks, high seed setting rates, and mild seed shattering in the growing regions, and is a promising perennial grain candidate for domestication in the alpine or wider regions.

Kengyilia species were identified by cytological methods as allopolyploids with the genome constitution StPY (Jensen 1990, 1996). The St and P genomes are derived from *Pseudoroegneria* (Nevski, 1934) Á. Löve, 1980, and *Agropyron* Gaertner, 1770, respectively, although the origin of the Y genome is still unknown (Wang et al. 1994). The molecular karyotype of *K. hirsuta* was first characterized by using chromosome identification under florescence *in situ* hybridization (FISH), with probes of 5S rDNA, 45S rDNA, pAs1, and $(AAG)_{10}$ (Dou et al. 2013). However, the cross-species homoeology of the identified chromosomes have not yet been ascertained. Moreover, inter-genomic arrangements significantly affected by the environmental factors were reported in *K. thoroldiana* (Oliver, 1893) J. L. Yang, C. Yen et B. R. Baum, 1992

(Wang et al. 2012) and *Elymus dahuricus* Turcz. ex Griseb. complex (Yang et al. 2017), whereas chromosomal variations between different populations in *K. hirsuta* remain unknown. Determination of chromosomal homoeology is very useful for the discovery and utilization of important genes and alleles in wild relatives. Alien gene transfer by interspecific hybridization is strongly affected by chromosome collinearity (Friebe et al. 1996; Qi et al. 2007). Targeted gene cloning may be facilitated by capturing the syntenic chromosomes of the wild relatives, which include complex genomes, by flow sorting (Tiwari et al. 2015; Said et al. 2018) or even by micro dissection (Sheng et al. 2020; Soares et al. 2020).

In the present study, the homoeology of the *K. hirsuta* chromosomes with those of wheat were determined using single-genes FISH. Further, the polymorphisms of the chromosomes between different populations were investigated. The results will be helpful for exploring genes from *K. hirsuta* by comparison of genomics in the chromosomal levels, and could accelerate the domestication of *K. hirsuta* as a new perennial crop.

Material and methods

Plant material

The seeds of *K. hirsuta* were collected individually from 7 different locations in Qinghai, China. Three to five individuals were randomly selected for cytological investigation in each population. Detailed information on collection sites is listed in Table 1 and Fig. 1.

Preparation of cDNA sequences

Fourteen cDNA clones were selected for single-gene probes, which were previously mapped to the short and long arms of the seven homoeologous chromosomes in common wheat, respectively, by Danilova et al. (2014) (Table 2). The cDNA clones were developed and kindly supplied by the National BioResource Project-Wheat, Japan. cDNA sequences were amplified with PrimeSTAR Max DNA Polymerase (Takara Bio Inc., Kusatsu, Shiga, Japan Cat. # R001B) and standard primers T3/T7 by polymerase amplification reactions (PCR). The amplification products were purified with an Omega MicroElute Cycle-Pure Kit (Omega Bio-tek, Inc., Norcross, Georgia, USA Cat. # D6293-02).

Probes labeling

All cDNA probes were labeled by nick translation as described previously, with minor modifications (Kato et al. 2004, 2006). Briefly, all cDNA amplifications were labeled with tetramethyl-rhodamine-5-dUTP (Roche Diagnostics GmbH, Mannheim, Germany Cat. # 11534378910). After the addition of EDTA (500 mM, pH 8.0) to terminate

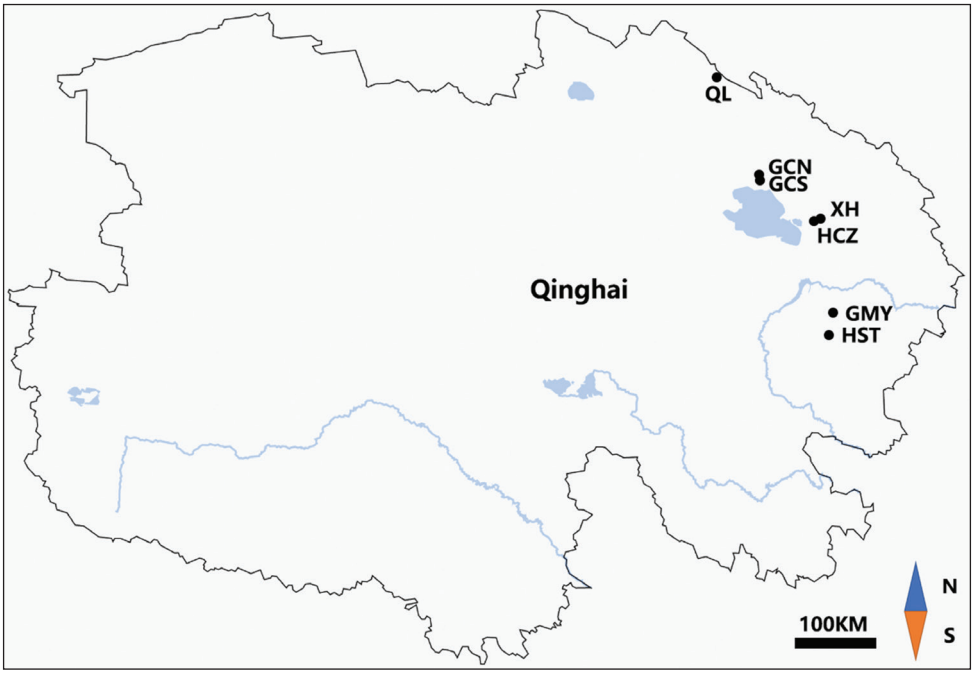

Figure 1. Map of sample collection sites.

Table 1. Plant materials used in this study.

Identification ID	Location	Latitude (N), Longitude (E)	Altitude (m)
HST	Guinan, Qinghai	35°31'21"N, 101°6'9.8"E	3370
GMY	Guinan, Qinghai	35°47'28"N, 101°8'51"E	3200
HCZ	Haiyan, Qinghai	36°50'44"N, 100°56'0.9"E	3500
XH	Haiyan, Qinghai	36°58'43"N, 100°54'24"E	3130
GCN	Gangcha, Qinghai	37°21'33"N, 100°8'0.4"E	3350
GCS	Gangcha, Qinghai	37°19'19"N, 100°10'7.6"E	3350
QL	Qilian, Qinghai	38°29'18"N, 99°34'22"E	3450

the nick translation reaction, the probes were purified using the Omega DNA Probe Purification Kit (Cat. # D6538-02) following the manufacturer's recommendations.

The oligonucleotide probes were used for 5S rDNA, 45S rDNA, pAs1, and $(AAG)_{10}$. The designated oligonucleotides pAs1-1 plus pAs1-2, 5Sg, Oligo-pTa71-2 representing pAs1, 5S and 45S rDNA respectively (Danilova et al. 2012; Tang et al. 2014). All oligonucleotides were end-labeled using either fluorescein amidite (FAM; green) or carboxy tetramethyl rhodamine (TAMRA; red) (Sangon Biotech Co., Ltd., Shanghai, China).

Genomic DNAs of *Pseudoroegneria stipifolia* (Nevski, 1934) Á. Löve, 1984 ($2n = 2x = 14$; St genome) and *Aropyron cristatum* Gaertner, 1770, ($2n = 4x = 28$; P genome) were fragmented by autoclaving following the procedures of Dou et al. (2009). The treated genomic DNAs were labeled with tetramethyl-rhodamine-5-dUTP (red) or fluorescein-12-dUTP (green) (Roche Diagnostics, Germany) by a random primer labeling method.

Table 2. Localization of full length cDNA probes by FISH on chromosomes of *K. hirsuta*.

Wheat FISH probe name	FISH probe order on *Kengilia hirsuta*	Average distance from the centromere (μm) ± SE	FLcDNA, KOMUGI database	cDNA length, (bp, KOMUGI database)
1S-1	1St-S	0.36 ± 0.03	tplb0048d21	3487
	1Y-S	0.24 ± 0.01		
	1P-S	0.26 ± 0.01		
1L-1	1St-L	0.77 ± 0.02	tplb0013a02	5094
	1Y-L	0.61 ± 0.01		
	1P-L-1	0.92 ± 0.02		
2S-1	2St-S	0.42 ± 0.02	tplb0006k18	3777
	2Y-S	1.51 ± 0.01		
	4P-S	1.33 ± 0.03		
2L-1	2St-L	0.76 ± 0.01	tplb0007l09	3184
	2Y-L	0.83 ± 0.03		
	2P-L	1.54 ± 0.04		
3S-1	3St-S	0.71 ± 0.02	tplb0014n06	3256
	3Y-S-1	1.10 ± 0.01		
	3P-S	2.52 ± 0.05		
3L-1	3St-L	0.54 ± 0.02	AK336104	3860
	3Y-L	0.32 ± 0.02		
	3P-L	0.46 ± 0.03		
4S-6	4St-S	2.23 ± 0.03	plb0017g02	3191
	4Y-S	2.08 ± 0.02		
	4P-L	2.85 ± 0.07		
4L-4	4St-L	2.08 ± 0.03	AK335609	4790
	4Y-L	2.29 ± 0.03		
	2P-S-2	5.46 ± 0.02		
5S-1	5St-S	0.22 ± 0.01	tplb0016k09	3057
	5Y-S	0.26 ± 0.01		
	5P-S	0.90 ± 0.03		
5L-2	5St-L	2.20 ± 0.06	AK331808	4827
	5Y-L	2.60 ± 0.03		
	5P-L	3.72 ± 0.08		
6S-2	6St-S	0.79 ± 0.01	tplb0006a09	3703
	6Y-S	1.26 ± 0.01		
	6P-S	1.37 ± 0.03		
6L-1	6St-L	0.52 ± 0.01	tplb0009a09	3298
	6Y-L	0.70 ± 0.03		
	1P-L-2	6.18 ± 0.07		
	6P-L	1.69 ± 0.05		
7S-1	7St-S	1.00 ± 0.03	AK334430	4424
	3Y-S-2	1.45 ± 0.01		
	7Y-L	2.26 ± 0.03		
	2P-S-1	5.29 ± 0.04		
	7P-S	2.47 ± 0.04		
7L-4	7St-L	3.60 ± 0.06	tplb0007o14	3982
	7Y-L	3.56 ± 0.03		
	7P-L	6.55 ± 0.06		

Chromosome preparation

The seeds were germinated on moist filter paper in Petri dishes at room temperature. Root tips with a length of 1–2 cm were collected and pretreated with nitrous oxide at a pressure of 7–8 atm for 2 h at room temperature following the method of Kato (1999). The pretreated root tips were fixed in ethanol-glacial acetic acid (3:1, v/v) for at least 30 min at room temperature, subsequently; each root tip was

squashed in a drop of 45% acetic acid and observed with a phase contrast microscope (Olympus BX43). The slides with good chromosome spread were selected for further FISH.

FISH and microphotometry

The chromosome preparations were denatured in 0.2M NaOH and 70% ethanol for 10 minutes at room temperature; subsequently, they were rinsed in cold 70% ethanol for 1 hour and quickly air dried. The hybridization mixture per slide (total volume = 10 μl) contained 100 ng labeled probe DNA, 50% v/v formamide, 2 × SSC, 10% w/v dextran sulfate, and 0.1 μg salmon sperm DNA. The hybridization mixture with single-gene probes or labeled genomic DNAs was denatured in the boiled water for 5 minutes, and immersed in ice-water for at least 10 minutes. The hybridization with oligo-based probes was conducted directly without denaturation. The hybridization was carried out overnight at 37 °C. A sequential FISH technique with multiple rounds of hybridization on the same chromosome preparation was adopted in this study. The first hybridization was conducted with single-gene probes. The slide was washed in 2 × SSC at 42 °C three times in this round, and at least 10 cells with distinct signals were captured. Subsequently, the slide was washed by tap water. The second and third round hybridizations were carried out using the probe combination 45S rDNA and 5S rDNA, and the combination of pAs1 and $(AAG)_{10}$, respectively. After each of the second and third rounds of hybridization, the hybridization signals were removed by heating at 55 °C for 10 minutes on hot plate, followed by washing in tap water. The last round was genomic hybridization *in situ* hybridization (GISH) with genomic DNA probes of *P. stipifolia* and *A. cristatum*. Images were captured with a cooled CCD camera (DP80) under a fluorescence microscope (Olympus BX63). Finally, images were adjusted with Adobe Photoshop 6.0 for contrast and background optimization.

Results

Karyotype with homoeology determination

Fourteen selected single-gene probes are evenly distributed on the chromosomes of the seven homoeologous groups in wheat, two of which were mapped on the short arm and the long arm on each chromosome, respectively. Thus, two single-gene probes on each chromosome were used in the present study to identify the corresponding species-crossed homoeologous chromosomes in *K. hirsuta*. The individuals of the population HCZ (Table 1) were randomly selected for single-gene mapping. The first round of hybridization using single-gene probes showed that most of the single-gene probes produced the expected six hybridization signals in *K. hirsuta*, each genome of which had two hybridization signals on the pair of the homologous chromosomes (Fig. 2a). Exceptionally, the single-gene probe 6L-1 produced eight signals (Fig. 2 a5), whereas the single-gene probe 7S-1 yielded 10 signals in the chromosomes (Fig. 2 a6). Further,

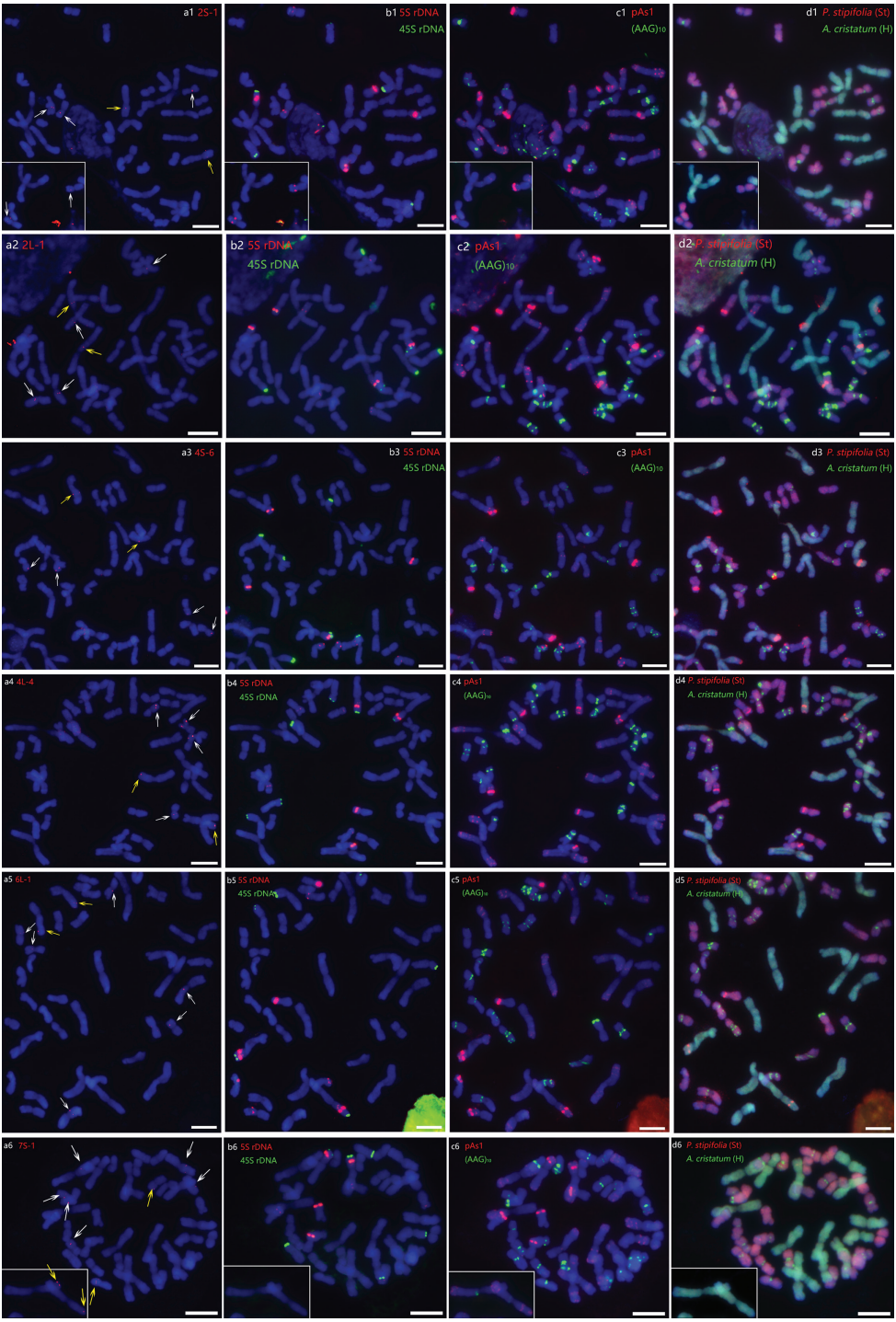

Figure 2. Sequential FISH-GISH on mitotic chromosomes of *K. hirsuta* with single-gene and repetitive sequence probes **a** single-gene probes (arrowed) **b** 45S rDNA (green) and 5S rDNA (red) **c** pAs1 (red) and $(AAG)_{10}$ (green) **d** genomic DNA probes of *P. stipifolia* (red) and *A. cristatum* (green). Scale bars: 10 μm.

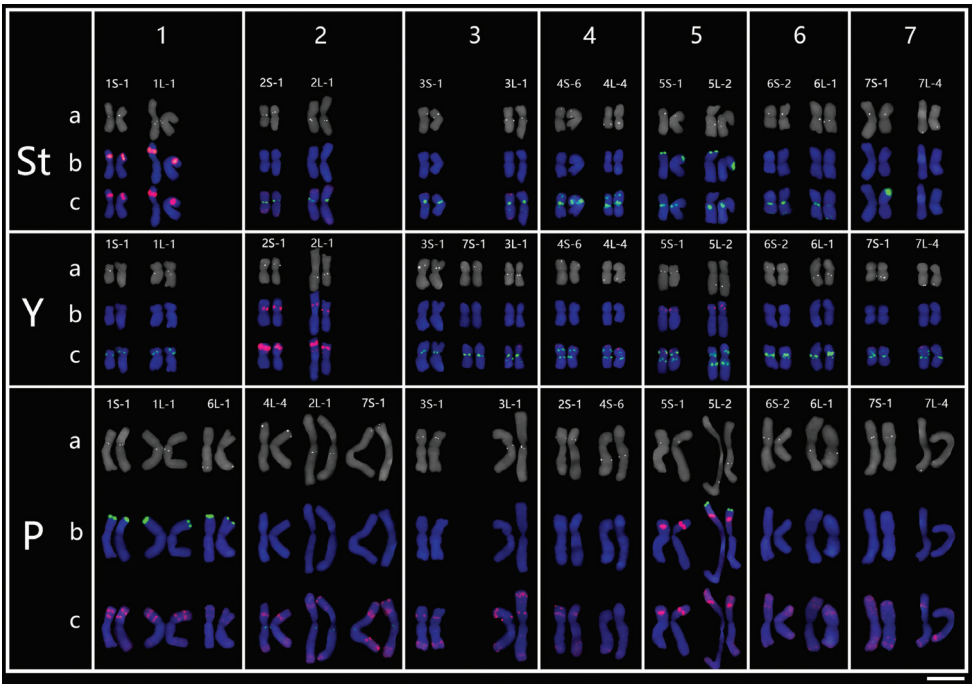

Figure 3. Molecular karyotype of *K. hirsuta* with 14 single-gene probes and repetitive sequences probes **a** single-gene probe **b** 45S rDNA (green) and 5S rDNA (red) **c** pAs1 (red) and $(AAG)_{10}$ (green). Scale bar: 10 μm.

the single-gene mapped chromosomes were clearly identified by hybridizations with 5S rDNA, 45S rDNA, pAs1, and $(AAG)_{10}$ after the second and third rounds of hybridization (Fig. 2b and 2c). Lastly, the characterized target chromosomes were allocated to the different genomes as St, Y and P by GISH (Fig. 2d).

After multiple hybridizations with 14 single-gene probes, each of the *K. hirsuta* chromosomes was not only characterized with distinct chromosomal markers, but also its homoeology was determined (Fig. 3; Table 3). The St genome chromosome sizes ranged from 6.60 to 8.76 μm with an average of 7.68 μm; the Y genome chromosome sizes ranged from 5.54 to 7.56 μm with an average of 6.55 μm; and the P genome chromosome sizes ranged from 11.70 to 14.21 μm with an average of 12.96 μm. The relative chromosome arm ratio (long arm to short arm) ranged from 2.13 for the largest chromosome, 5St, to 1.07 for the smallest, 7St, in the St genome; the corresponding ratios ranged from the 2.08 for the largest chromosome, 5Y, to 1.09 for the smallest, 6Y in the Y genome; and from 1.90 for the largest chromosome, 4P, to 1.12 for the smallest, 7P in the P genome (Table 3). A referenced karyotype idiogram of *K. hirsuta* was suggested with the designated chromosome number from 1–7 corresponding to those in common wheat (Fig. 4). The features of chromosomes in *K. hirsuta* are as follows.

Table 3. Chromosome measurements of *K. hirsuta*.

Chromosome	Long arm (L) ± SE μm	Short arm (S) ± SE μm	Total Length (T=L+S) ± SE μm	Arm ratio (L/S)	Centromeric index (S/T) × 100
1St	4.40 ± 0.96	3.14 ± 0.75	7.54 ± 1.60	1.40	41.67
2St	4.68 ± 0.62	4.08 ± 0.69	8.76 ± 1.25	1.15	46.62
3St	4.73 ± 0.43	3.09 ± 0.47	7.82 ± 0.87	1.53	39.52
4St	3.68 ± 0.40	2.98 ± 0.41	6.66 ± 0.80	1.23	44.78
5St	5.69 ± 0.78	2.67 ± 0.22	8.36 ± 0.98	2.13	31.95
6St	3.49 ± 0.54	3.11 ± 0.42	6.60 ± 0.90	1.12	47.08
7St	4.17 ± 0.70	3.88 ± 0.44	8.05 ± 1.14	1.07	48.24
1Y	3.47 ± 0.30	2.07 ± 0.16	5.54 ± 0.36	1.68	37.34
2Y	4.13 ± 0.34	3.43 ± 0.52	7.56 ± 0.83	1.20	45.40
3Y	3.83 ± 0.48	3.25 ± 0.32	7.08 ± 0.76	1.18	45.91
4Y	3.26 ± 0.21	2.46 ± 0.28	5.72 ± 0.47	1.33	42.96
5Y	4.60 ± 0.58	2.21 ± 0.33	6.81 ± 0.88	2.08	32.44
6Y	3.19 ± 0.25	2.92 ± 0.24	6.11 ± 0.46	1.09	47.77
7Y	3.97 ± 0.35	3.06 ± 0.50	7.03 ± 0.77	1.30	43.47
1P	7.16 ± 0.98	4.72 ± 0.80	11.88 ± 1.73	1.52	39.74
2P	7.90 ± 0.97	5.90 ± 1.18	13.80 ± 2.13	1.34	42.76
3P	7.67 ± 0.67	5.77 ± 0.73	13.44 ± 1.39	1.33	42.94
4P	7.60 ± 0.52	4.40 ± 0.40	12.00 ± 0.79	1.90	34.45
5P	8.80 ± 1.07	4.88 ± 0.56	13.68 ± 1.58	1.80	35.66
6P	6.30 ± 0.49	5.40 ± 0.71	11.70 ± 1.06	1.17	46.18
7P	7.51 ± 0.82	6.70 ± 0.67	14.21 ± 1.47	1.12	47.15

Chromosomes 1St and 5St were distinguished by 5S rDNA and 45S rDNA sites on the short arm, respectively. Both 2St and 6St have one major $(AAG)_{10}$ hybridization site, differing from 3St and 4St which both included two discrete $(AAG)_{10}$ hybridization sites. However, 2St was associated with $(AAG)_{10}$ on the short arm near the centromere, distinct from 6St with $(AAG)_{10}$ around the centromere, while 3St showed an additional $(AAG)_{10}$ minor signals in the long arm rather than 4St showed an additional major signal in the short arm. 7St showed none or one major $(AAG)_{10}$ hybridization site in the telomeric region of the short arm, and thus differed from the others (Fig. 4).

Chromosome 1Y was the smallest, with one major or minor $(AAG)_{10}$ site on the short arm. Chromosomes 2Y and 5Y harbored a 5S rDNA site in the intercalary and subtelomeric regions on the short arm, respectively. Both 3Y and 6Y had one distinct major $(AAG)_{10}$ site around the centromere, but 6Y showed stronger hybridization intensity than 3Y. Chromosome 4Y showed the two $(AAG)_{10}$ sites similar to 5Y, but 5Y was with the 5S sites. Chromosome 7Y exhibited one major $(AAG)_{10}$ site near the centromere on the long arm and one or two minor $(AAG)_{10}$ sites in the intercalary region on the short arm (Fig. 4).

Chromosome 1P was distinct with one major 45S rDNA in the telomeric region of the short arm. Chromosome 2P was identified as a metacentric chromosome with a distinct pAs1 hybridization on the intercalary part of the short arm, and a weak $(AAG)_{10}$ around the centromere. The single gene probe 4L-4 and 2L-1 produced hybridizations on the short and the long arms, respectively, in this chromosome. Chromosome 4P

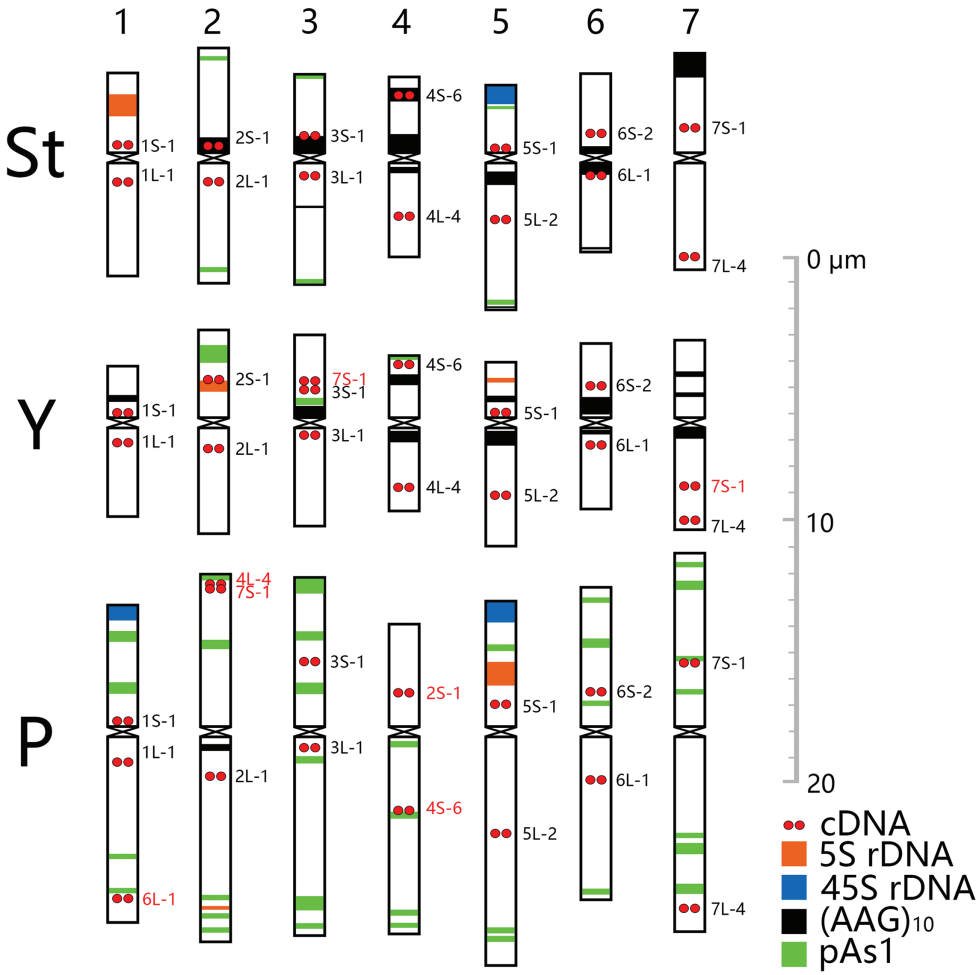

Figure 4. Idiogram for chromosomes of *K. hirsuta* showing the distribution of 45S rDNA, 5S rDNA, pAs1, $(AAG)_{10}$ and single-genes. The names of single-gene probes that hybridized to more than one chromosome, and to non-homoeologous chromosome are highlighted in red. The color scheme (bottom right) shows the color of each probe as represented in this idiogram.

was characterized as a sub-metacentric chromosome with more pAs1 hybridizations on the long arm than on the short arm. The single gene probes 2S-1 and 4S-6 produced hybridizations on the respective short and long arms in this chromosome. Therefore, 2P and 4P could be reciprocal translocation chromosomes. Tentatively, 2P and 4P were respectively designated as 4PL/2PL and 2PS/4PS. Chromosome 3P was identified as a metacentric chromosome with opulent pAs1 hybridizations on the short arm. Chromosome 5P was characterized by the segregated 5S rDNA and 45S rDNA sites on the short arm. Chromosome 6P was characterized by weakly dispersed pAs1 hybridizations mostly distributed in the half of the short arm near the telomere, whereas 7P was identified as including dispersed pAs1 hybridizations on both arms (Fig. 4).

Synteny between chromosomes of *K. hirsuta* and those of common wheat and *Agropyron cristatum*

Comparison between the single-gene probes on *K. hirsuta* and the homoeologous groups of common wheat showed that most of the probes hybridized to the corresponding homoeologous chromosome arms of *K. hirsuta*, generally in their corresponding positions (Danilova et al. 2014). This indicates the chromosomal synteny across species. However, the degree of synteny varied between the genomes and between the chromosomes. The St genome chromosomes were revealed to be most strongly conserved, with each of the 14 single-gene probes in the corresponding positions as described in the wheat chromosomes. Most of the Y genome chromosomes maintained the same synteny as the St chromosomes, except that 3Y was detected as having an additional hybridization site at 7S-1 in the interstitial regions of the short arm. Both 7S-1 and 7L-4 mapped on the long arm of 7Y, suggesting the pericentric inversion in this chromosome. The collinearity of the P genome chromosomes was more distorted. Besides the translocation between 2P and 4P, additional hybridization of 6L-1 in the subtelomeric region of the 1PL and additional site of 7S-1 in the telomeric regions of 2PS were revealed in P genome (Figs 3 and 4; Table 2).

The same original cDNA probes were used for karyotype and chromosome structural analysis in *Agropyron cristatum* Gaertner, 1770, ($2n$ = 14; P genome) (Said et al. 2018). Though fewer single-gene probes were used in *K. hirsuta* than in *A. cristatum*, chromosomal collinearity of the P genome across species was compared by shared common single-probes. Well-conserved single-probe hybridization positions were revealed in 3P, 5P and 7P across both species. Chromosome 1P in both *K. hirsuta* and *A. cristatum* showed conserved 1S-1 and 1L-1 hybridizations, but 1P in *A. hirsuta* included an additional hybridization 6L-1 in the subtelomeric region of the long arm. Chromosome 1P in *A. cristatum* was characterized as metacentric, whereas 1P in *K. hirsuta* was submentacentic. This indicates that 1P in *A. hirsuta* was structurally different from that in *A. cristatum*. Coincidentally, the reciprocal translocations between 2P and 4P were identified in both *K. hirsuta* and *A. cristatum*. The hybridization positions of single-gene probes 4L-4 and 2L-1 in 2P of *K. hirsuta* were corresponding to those in 2P of *A. cristatum*. Physical mapping more single-genes on 4P of *A. cristatum* revealed more complicated structural variations such as inversion. Though the limited single-gene probes were mapped in 4P of *K. hirsuta*, the single-gene probe 4S-6 in the long arm on 4P of *K. hirsuta* was accordant to those 4S-1, 4S-2, 4S-3, and 4S-4 in the long arm on 4P of *A. cristatum*. This observation indicates that although chromosomes 2P and 4P in *K. hirsuta* may be modified from those in *A. cristatum*, they are still considered to include an ancient common rearrangement. A paracentric inversion on the long arm of 6P was identified in *A. cristatum* (Said et al. 2018). However, the 6L-1 hybridization position in 6P of *K. hirsuta* was equivalent to the position of the homoeologous wheat chromosome This indicates no major chromosome arrangements in 6PL in *K. hirsuta*.

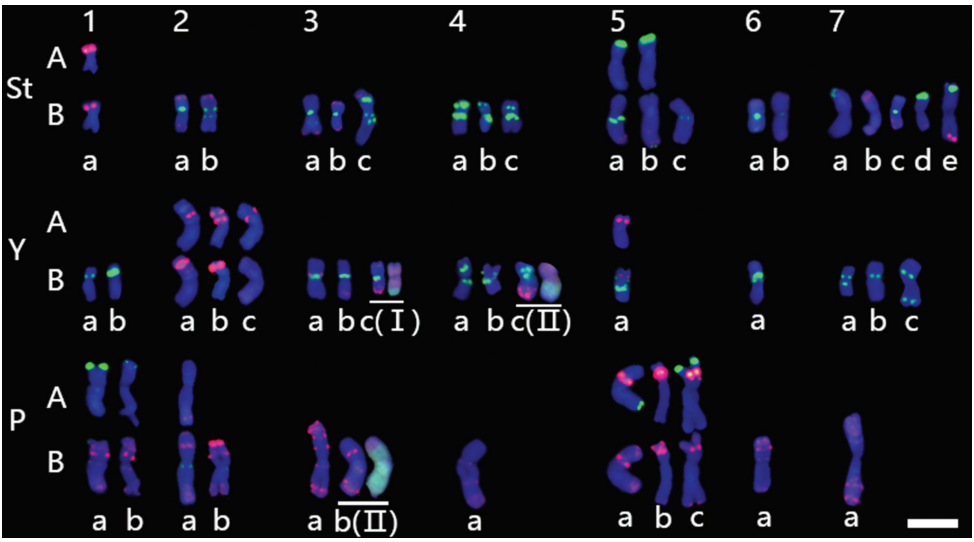

Figure 5. Molecular karyotypes of 29 *K. hirsuta* samples. The patterns of chromosomes were characterized by probe combinations A: 45S rDNA (green) and 5S rDNA (red); and B: pAs1 (red) and $(AAG)_{10}$ (green). Different variants are annotated by different letters. The translocated chromosomes are underlined, and indicated by Roman numerals I–II. Scale bar: 10 μm.

Chromosome polymorphisms between different populations

Karyotyping was conducted on 29 individuals of *K. hirsuta* from 7 different populations, by using repetitive sequences as chromosomal landmarkers. Chromosomal homoeology were detenmined referring the above reference karyotype derived from HCZ population. The polymorphisms of each chromosome and the karyotype of each individual were well described (Fig. 5; Table 4). The results identified a total of 47 chromosomal variants in the 29 individuals (Table 4). The St genome showed the highest number of chromosome variants (19), whereas the Y genome had 16 and the P genome had 12. Chromosomes 1St, 5Y, 6Y, 4P, 6P, and 7P were the most stable, with identical variants across populations, while 7St was the most variable with more than 3 variants. The majority of individuals showed FISH patterns in the homozygous state, although some were in the heterozygous state (34.48%, ten of 29 plants; Table 4).

Most of the variants were characterized by the absence or presence of additional hybridization signals due to duplications, or deletions of repeats of pAs1 and $(AAG)_{10}$, as well as the absence or presence of hybridizations of 45S rDNA (Fig. 5 5St c, 5P b). Moreover, translocations involved in 3Y, 4Y, and 3P were detected in a few individuals. A tentative pericentric inversion was identified in 5P (Fig. 5 5P a) in different populations.

Chromosomal structural variations were detected in 3Y, 7Y, 1P, 2P, and 4P by using single-gene probes in the individuals of the population HCZ. Furthermore, the chromosomal polymorphisms were revealed in above chromosomes across different populations. The polymorphisms of 1P were detected as the hybridization intensity

Table 4. Chromosome variants in *K. hirsuta*.

Population	Samples	St genome							Y genome							H genome							heterozygosis
		1	2	3	4	5	6	7	1	2	3	4	5	6	7	1	2	3	4	5	6	7	
GCN	2	a	a	a	a	a	a	a	a	a	a	a	a	a	a	b	a	a	a	a	a		-
	4	a	a	a	ab	a	a	b	a	a	cT	a	a	a	a	a	a	a	a	b	a	a	+
	10	a	a	ab	a	b	a	c	a	a	cT	a	a	a	a	b	b	a	a	b	a	a	+
	12	a	a	a	a	a	a	b	a	b	cT	a	a	a	a	a	b	a	a	b	a	a	-
GCS	7	a	a	a	a	a	a	b	a	a	b	a	a	a	a	a	a	a	a	c	a	a	-
	10	a	a	a	a	a	a	b	b	a	b	b	a	a	a	a	a	a	a	c	a	a	-
	16	a	a	a	b	a	a	b	b	c	b	b	a	a	b	a	a	a	a	c	a	a	-
GMY	1	a	a	a	b	c	b	b	a	a	a	a	a	a	b	a	a	a	a	c	a	a	-
	3	a	a	a	b	a	a	a	a	a	a	b	a	a	b	a	a	a	a	c	a	a	-
	4	a	a	ab	b	a	b	a	a	a	a	a	a	a	b	a	a	a	a	c	a	a	+
	5	a	a	a	c	a	a	b	a	a	a	a	a	a	b	b	a	a	a	c	a	a	-
QL	1	a	a	a	c	a	b	a	ab	ac	a	a	a	a	b	b	a	a	a	c	a	a	+
	2	a	a	a	b	a	b	b	a	a	a	b	a	a	c	a	a	a	a	c	a	a	-
	3	a	a	ac	a	bc	a	b	a	a	a	a	a	a	ab	a	b	a	a	a	a	a	+
	9	a	a	a	a	ac	a	bd	a	ac	a	a	a	a	ab	ab	b	a	a	c	a	a	+
	6	a	a	a	a	c	ab	de	a	ac	a	a	a	a	b	b	a	a	a	c	a	a	+
HST	1	a	a	a	b	b	ab	b	a	a	a	a	a	a	b	a	a	a	a	c	a	a	+
	2	a	a	a	b	b	b	b	a	a	a	b	a	a	b	a	a	a	a	c	a	a	-
	8	a	a	a	a	a	b	b	a	a	a	a	a	a	b	a	a	a	a	c	a	a	-
XH	3	a	a	a	a	a	b	d	a	a	a	b	a	a	b	a	b	a	a	c	a	a	-
	5	a	a	a	a	a	b	d	a	a	a	b	a	a	b	a	b	a	a	c	a	a	-
	11	a	a	a	b	a	a	b	a	a	a	b	a	a	b	a	b	a	a	c	a	a	-
	10	a	a	a	a	b	a	d	a	a	a	b	a	a	b	a	a	a	a	c	a	a	-
	8	a	a	ab	a	b	a	d	a	a	a	b	a	a	b	ab	b	a	a	c	a	a	+
HCZ	1	a	a	a	a	a	b	b	a	a	b	cT	a	a	b	a	a	bT	a	b	a	a	-
	3	a	a	a	a	b	a	b	a	a	b	b	a	a	b	a	a	a	a	c	a	a	-
	4	a	b	a	a	a	a	a	a	a	b	b	a	a	b	a	a	a	a	c	a	a	-
	7	a	a	a	ac	b	a	b	a	a	b	b	a	a	b	a	a	a	a	c	a	a	+
	lb	a	a	a	a	a	b	b	a	a	b	cT	a	a	b	a	b	bT	a	b	a	a	-
No. of variants		1	2	3	3	3	2	5	2	3	3	3	1	1	3	2	2	2	1	3	1	1	
Total								19							16							12	10

Note: plus sign represents heterozygous karyotypes, minus sign represents homozygous karyotypes.

variation of 45S rDNA in the terminal part of the short arm (Fig. 5 1P a and b), whereas those of 2P were detecet as an additional 5S hybridization in the intrcalary region of the long arm (Fig. 5 2P a and b). However, the structural variation detected by single-gene FISH was in the distal part of the long arm of 1P and the distal part of the short arm of 2P, respectively. No polymorphisms of 4P were detected between populations. It suggests that the chromosomal structural variation in 1P, 2P, and 4P might be species-specific. Since the polymorphism sites on the short arm of 3Y and those on the long arm of 7Y were corresponding to the arms involving structural variation detected by single-gene probes, it indicates the structural variations in 3Y and 7Y might be population-specific.

Although the number of samples was not the same in the different populations, the results indicate that the populations QL, HCZ, and GCN included more variants than the others (Table 4). In particular, one specific inter-genomic translocation variant (3Y c) with the P genome segment was identified in the population GCN; one specific reciprocal translocation (4Y c and 3P b) was identified in the population HCZ (Fig. 5); and the individuals of QL showed a high heterozygous state of 80% (Table 4).

Discussion

The 45S rDNA products join with the 5S rDNA and the ribosomal proteins to make the ribosomes. The major sites of the 45s rDNA correspond to the NOR. The 45S rDNA sites of wheat were physically mapped in four different homoeologous groups, as noted in the short arms of 1A, 1B, 6B and 5D, and 7DL (Mukai et al. 1991). In *K. hirsuta*, 45S rDNA sites were mapped in the short arms of 5St, 1P, and 5P. The 45S rDNA sites in 1P and 5P detected in the present study were consistent with those in the P genome of *A. cristatum* (Said et al. 2018). 5S rDNA sites were physically mapped on chromosomes homoeologous group 1 (1AS, 1BS, 1DS) and group 5 (5AS, 5BS, and 5DS) (Mukai et al. 1990). In *K. hirsuta*, 5S rDNA sites were mapped in the short arms of 1St, 2Y, 5Y, and 5P. The detected 5S rDNA in the homoeologous group 2 in the Y genome was notably exceptional. Since the 5S rDNA site was absent in 1Y, the 5S site in 2Y might have been transferred from 1Yto 2Y by chromosomal rearrangements. The 45S rDNA, or 5S rDNA, or both detected in the short arms of homoeologous 5 of each genome suggests these are highly conservable across species. Moreover, the chromosomes of the homoeologous 5 group in each genome in *K. hirsuta* mostly showed the highest long arm to short arm ratio, consistent with the morphological characteristics of those in each genome in common wheat (Gill et al. 1991). This indicates that the chromosomal morphology of the homoeologous 5 across distant species in Triticeae is strongly conserved.

Four 45 rDNA sites were reported in accessions of the diploid species in *Agrypyron cristatum* and *Agrypyron mongolicum* (Keng, 1938) (Zhao et al. 2017). However, two 45S rDNA sites on 1P and 5P were mostly identified in this study. We also note the variability of the 45S rDNA in *K. hirsuta* in different populations. They were mostly identified as the presence and absence of the hybridization signals in the origins. The instability and copy number variation of rDNA were regarded to be particularly sensitive to genomic stresses, and acted as a source of adaptive response (Salim and Gerton 2019). Whether the detected intra population variations of 45S rDNA are associated with intra population differentiation needs further investigation.

Species in the tribe Triticeae are characterized by large genomes, the majority of which are repetitive DNA sequences (Flavell et al. 1974, 1986; Bennett et al. 1982). *K. hirsuta* has a large and complex genome as an allopolyploid species with three different genomes. Despite the high through-put sequencing techniques that are now available, exploring targeted genes from such large and complex genomes is still highly challenging. Since a few of crops in Triticeae are wholly sequenced, comparing genomics will be a shortcut for cloning targeted genes from wild relatives. For example, seed shattering is a key character for wild species domestication. The genes *Btr-1* and *Btr-2* controlling seed shattering were conservatively located in the short arms of homeologue 3 chromosomes in barley and wheat (Pourkheirandish et al. 2015; Zhao et al. 2019). In this study, the conserved synteny of chromosome 3St and 3P, and possible structural aberrations in the short arm of 3Y, were identified in *K. hirsuta*. This implies that the *Btr-1* and *Btr-2* might be more strongly conserved in the 3St and 3P chromosomes. Moreover, gene cloning may be facilitated by genome dissection during flow sorting or micro dissection (Tiwari et al. 2015; Said et al. 2018; Sheng et al. 2020; Soares et

al. 2020). In this study, the chromosomes belong to the homoeologous group 3 were clearly identified. Furthermore, the target chromosomes can be labeled using more specific chromosomal markers, and tentatively isolated for gene cloning.

High karyotype variation was observed in the sympatric distributed Triticeae species *Elymus nutans* Griseb., 1868 (Dou et al. 2017). Though chromosomal polymorphisms were found in different individuals in *K. hirsuta* (47 in 29 individuals), there were far fewer variants than in *E. nutans* (100 in 27 individuals). In addition, in the related species *K. thoroldiana*, inter-genomic rearrangements affected by environmental factors were reported (Wang et al. 2012). However, only limited inter-genomic translocations were uncovered in the specific populations, suggesting that the karyotype of *K. hirsuta* is more stable than those of the related species. Nearly 40% of the individuals had heterozygous karyotypes in *K. hirsuta*, the frequency of which is higher than those in *E. nutans* (22.2%) (Dou et al. 2017). In the population of QL, the highest karyotype heterozygosis of 90% was detected in the present study. The higher heterozygosis indicates the frequencies of out-crossing in the populations in *K. hirsuta*. The origin of *Kengyilia* was suggested to be from natural amphiploids between the tetraploid *Roegneria* C. Koch, 1848 (StY genome) and diploid *A. cristatum* (P genome) (Yang et al. 1992). The StY species are highly self-crossing, but the P genome species are self-compatible as well as facultative allogamous (Dewey 1983). Whether or not the facultative allogamous system of P genome is functioning in *K. hirsuta* needs further investigation.

Acknowledgements

This research was supported by the Chinese Academy of Sciences strategic leading science and technology project (XDA24030502) and the Second Tibet Plateau Scientific Expedition and Research (STEP) Program (Grant No. 2019QZKK0303).

The authors declare that the research was conducted in the absence of any commercial or financial relationships that could be construed as a potential conflict of interest.

Karyotype polymorphism analysis, X.-Y.T.; Chromosome homoeology analysis, B.L.; Designed the experiment and analyzed the data, Q.-W.D.

References

Abbasi J, Xu J, Dehghani H, Luo MC, Deal KR, McGuire PE, Dvorak J (2020) Introgression of perennial growth habit from *Lophopyrum elongatum* into wheat. Theoretical and Applied Genetics 133: 2545–2554. https://doi.org/10.1007/s00122-020-03616-x

Bennett MD, Smith JB, Heslop-Harrison JS, Riley R (1982) Nuclear DNA amounts in angiosperms. Proceedings of the Royal Society of London Series B Biological Sciences 216: 179–199. https://doi.org/10.1098/rspb.1982.0069

Cai L (1999) A taxonomical study on the genus *Kengyilia* Yen et J. L. Yang. Acta Phytotaxonomica Sinica 37: 451–467. http://ir.nwipb.ac.cn/handle/363003/871

Danilova TV, Friebe B, Gill BS (2012) Single-copy gene fluorescence in situ hybridization and genome analysis: *Acc-2* loci mark evolutionary chromosomal rearrangements in wheat. Chromosoma 121: 597–611. https://doi.org/10.1007/s00412-012-0384-7

Danilova TV, Friebe B, Gill BS (2014) Development of a wheat single gene FISH map for analyzing homoeologous relationship and chromosomal rearrangements within the Triticeae. Theoretical and Applied Genetics 127: 715–730. https://doi.org/10.1007/s00122-013-2253-z

Dehaan L, Larson S, López-Marqués RL, Wenkel S, Gao C, Palmgren M (2020) Roadmap for accelerated domestication of an emerging perennial grain Crop. Trends in Plant Science 25: 525–537. https://doi.org/10.1016/j.tplants.2020.02.004

Dewey DR (1983) Historical and Current Taxonomic Perspectives of *Agropyron*, *Elymus*, and Related Genera 1. Crop Science 23: 637–642. https://doi.org/10.2135/cropsci1983.0011183X002300040009x

Dou QW, Chen ZG, Liu YA, Tsujimoto H (2009) High frequency of karyotype variation revealed by sequential FISH and GISH in plateau perennial grass forage *Elymus nutans*. Breeding Science 59: 651–656. https://doi.org/10.1270/jsbbs.59.651

Dou QW, Wang RRC, Lei YT, Yu F, Li Y, Wang HQ, Chen ZG (2013) Genome analysis of seven species of *Kengyilia* (Triticeae: Poaceae) with FISH and GISH. Genome 56: 641–649. https://doi.org/10.1139/gen-2013-0113

Dou QW, Yu F, Li Y, Zhao YY, Liu RJ (2017) High molecular karyotype variation revealed in indigenous *Elymus nutans* in the Qinghai Plateau. Plant Diversity 39: 117–122. https://doi.org/10.1016/j.pld.2017.05.003

Flavell RB, Bennett MD, Smith JB, Smith DB (1974) Genome size and the proportion of repeated nucleotide sequence DNA in plants. Biochemical Genetics 12: 257–269. https://doi.org/10.1007/BF00485947

Flavell RB, Clarke BC, Robertson A, Jeffreys AJ (1986) Repetitive DNA and chromosome evolution in plants. Philosophical Transactions of the Royal Society of London B, Biological Sciences 312: 227–242. https://doi.org/10.1098/rstb.1986.0004

Friebe B, Jiang J, Raupp WJ, McIntosh RA, Gill BS (1996) Characterization of wheat-alien translocations conferring resistance to diseases and pests: current status. Euphytica 91: 59–87. https://doi.org/10.1007/BF00035277

Gill BS, Friebe B, Endo TR (1991) Standard karyotype and nomenclature system for description of chromosome bands and structural-aberrations in wheat (*Triticum aestivum*). Genome 34: 830–839. https://doi.org/10.1139/g91-128

Glover JD, Reganold JP, Bell LW, Borevitz J, Brummer EC, Buckler ES, Cox CM, Cox TS, Crews TE, Culman SW, Dehaan LR, Eriksson D, Gill BS, Holland J, Hu F, Hulke BS, Ibrahim AMH, Jackson W, Jones SS, Murray SC, Paterson AH, Ploschuk E, Sacks EJ, Snapp S, Tao D, Van Tassel DL, Wade LJ, Wyse DL, Xu Y (2010) Increased food and ecosystem security via perennial grains. Science 328: 1638–1639. https://doi.org/10.1126/science.1188761

Jensen KB (1990) Cytology and taxonomy of *Elymus kengii*, *E. grandiglumis*, *E. alatavicus*, and *E. batalinii* (Poaceae: Triticeae). Genome 33: 668–673. https://doi.org/10.1139/g90-099

Jensen KB (1996) Genome analysis of Eurasian *Elymus thoroldianus*, *E. melantherus*, and *E. kokonoricus* (Triticeae: Poaceae). International Journal of Plant Sciences 157: 136–141. https://doi.org/10.1086/297330

Jiang J, Friebe B, Gill BS (1994) Recent advances in alien gene transfer in wheat. Euphytica 73: 199–212. https://doi.org/10.1007/BF00036700

Kato A (1999) Air drying method using nitrous oxide for chromosome counting in maize. Biotechnic & Histochemistry 74: 160–166. https://doi.org/10.3109/10520299909047968

Kato A, Albert PS, Vega JM, Birchler JA (2006) Sensitive fluorescence in situ hybridization signal detection in maize using directly labeled probes produced by high concentration DNA polymerase nick translation. Biotechnic & Histochemistry 81: 71–78. https://doi.org/10.1080/10520290600643677

Kato A, Lamb JC, Birchler JA (2004) Chromosome painting using repetitive DNA sequences as probes for somatic chromosome identification in maize. Proceedings of the National Academy of Sciences 101: 13554–13559. https://doi.org/10.1073/pnas.0403659101

Lammer D (2004) A single chromosome addition from *Thinopyrum elongatum* confers a polycarpic, perennial habit to annual wheat. Journal of Experimental Botany 55: 1715–1720. https://doi.org/10.1093/jxb/erh209

Liu ZW, Wang RRC, Carman JG (1994) Hybrids and backcross progenies between wheat (*Triticum aestivum* L.) and apomictic Australian wheatgrass [*Elymus rectisetus* (Nees in Lehm.) A. Löve & Connor]: karyotypic and genomic analyses. Theoretical and Applied Genetics 89: 599–605. https://doi.org/10.1007/BF00222454

Mukai Y, Endo TR, Gill BS (1990) Physical mapping of the 5S rRNA multigene family in common wheat. Journal of Heredity 81: 290–295. https://doi.org/10.1093/oxfordjournals.jhered.a110991

Mukai Y, Endo TR, Gill BS (1991) Physical mapping of the 18S.26S rRNA multigene family in common wheat: Identification of a new locus. Chromosoma 100: 71–78. https://doi.org/10.1007/BF00418239

Pourkheirandish M, Hensel G, Kilian B, Senthil N, Chen G, Sameri M, Azhaguvel P, Sakuma S, Dhanagond S, Sharma R, Mascher M, Himmelbach A, Gottwald S, Nair SK, Tagiri A, Yukuhiro F, Nagamura Y, Kanamori H, Matsumoto T, Willcox G, Middleton CP, Wicker T, Walther A, Waugh R, Fincher GB, Stein N, Kumlehn J, Sato K, Komatsuda T (2015) Evolution of the grain dispersal system in Barley. Cell 162: 527–539. https://doi.org/10.1016/j.cell.2015.07.002

Qi L, Friebe B, Zhang P, Gill BS (2007) Homoeologous recombination, chromosome engineering and crop improvement. Chromosome Research 15: 3–19. https://doi.org/10.1007/s10577-006-1108-8

Said M, Hřibová E, Danilova TV, Karafiátová M, Čížková J, Friebe B, Doležel J, Gill BS, Vrána J (2018) The *Agropyron cristatum* karyotype, chromosome structure and cross-genome homoeology as revealed by fluorescence in situ hybridization with tandem repeats and wheat single-gene probes. Theoretical and Applied Genetics 131: 2213–2227. https://doi.org/10.1007/s00122-018-3148-9

Salim D, Gerton JL (2019) Ribosomal DNA instability and genome adaptability. Chromosome Research 27: 73–87. https://doi.org/10.1007/s10577-018-9599-7

Sheng M, Gao M, Wang L, Ren X (2020) Chromosome microdissection and microcloning: technique and application in the plant Sciences. Cytologia 85: 93–100. https://doi.org/10.1508/cytologia.85.93

Soares FAF, Carvalho CR, Sattler MC, Silva JC, Pinto DEE, Passamani PZ, Silva AJ, Clarindo WR (2020) Plant chromosome-specific probes by microdissection of a single chromosome: Is that a Reality? Frontiers in Plant Science 11: e334. https://doi.org/10.3389/fpls.2020.00334

Tang ZX, Yang ZJ, Fu SL (2014) Oligonucleotides replacing the roles of repetitive sequences pAs1, pSc119.2, pTa-535, pTa71, CCS1, and pAWRC.1 for FISH analysis. Journal of Applied Genetics 55: 313–318. https://doi.org/10.1007/s13353-014-0215-z

Tiwari VK, Wang S, Danilova T, Koo DH, Vrána J, Kubaláková M, Hribova E, Rawat N, Kalia B, Singh N, Friebe B, Doležel J, Akhunov E, Poland J, Sabir JSM, Gill BS (2015) Exploring the tertiary gene pool of bread wheat: sequence assembly and analysis of chromosome 5M g of *Aegilops geniculata*. The Plant Journal 84: 733–746. https://doi.org/10.1111/tpj.13036

Wang Q, Liu H, Gao A, Yang X, Liu W, Li X, Li L (2012) Intergenomic rearrangements after polyploidization of *Kengyilia thoroldiana* (Poaceae: Triticeae) affected by environmental factors. PLoS ONE 7: e31033. https://doi.org/10.1371/journal.pone.0031033

Wang RRC, Liu ZW, Carman JG (1993) The introduction and expression of apomixis in hybrids of wheat and *Elymus rectisetus*. In: Li ZS, Xin ZY (Eds) Proceedings of 8th International Wheat Genetics Symposium, Beijing (China), 20–25 July 1993. China AgriScientech, Beijing, 317–319.

Wang RRC, von Bothmer R, Dvorak J, Fedak G, Linde-Laursen I, Muramatsu M (1994) Genome Symbols in the Triticeae (Poaceae). In: Wang RRC, Jensen KB, Jaussi (Eds) Proceedings of the 2nd International Triticeae symposium, Logan, Utah, USA, 29–34. Herbarium Publications: e20. https://digitalcommons.usu.edu/herbarium_pubs/20

Yang JL, Yen C, Baum BR (1992) *Kengyilia*: synopsis and key to species. Hereditas 116: 25–28. https://doi.org/10.1111/j.1601-5223.1992.tb00200.x

Yang CR, Zhang HQ, Chen WH, Kang HY, Wang Y, Sha LN, Fan X, Zeng J, Zhou YH (2017) Genomic constitution and intergenomic translocation in the *Elymus dahuricus* complex revealed by multicolor GISH. Genome 60: 510–517. https://doi.org/10.1139/gen-2016-0199

Yen C, Yang JL (1990) Kengyilia gobicola, a new taxon from west China. Canadian Journal of Botany 68: 1894–1897. https://doi.org/10.1139/b90-248

Zhao Y, Xie JH, Dou QW, Wang JJ, Zhang Z (2017) Diversification of the P genome among *Agropyron* Gaertn.(Poaceae) species detected by FISH. Comparative cytogenetics 11(3): 495–509. https://doi.org/10.3897/CompCytogen.v11i3.13124

Zhao Y, Xie P, Guan PF, Wang YF, Li YH, Yu KH, Xin MM, Hu ZR, Yao YY, Ni ZF, Sun QX, Xie CJ, Peng HR (2019) *Btr1-A* Induces Grain Shattering and Affects Spike Morphology and Yield-Related Traits in Wheat. Plant and Cell Physiology 60: 1342–1353. https://doi.org/10.1093/pcp/pcz050

ORCID

Xiaoyan Tao https://orcid.org/0000-0002-9414-3461
Bo Liu https://orcid.org/0000-0002-3694-2716
Quanwen Dou https://orcid.org/0000-0001-5910-6270

CompCytogen 15(4): 393–411 (2021)
doi: 10.3897/compcytogen.v15.i4.67112
https://compcytogen.pensoft.net

RESEARCH ARTICLE

COMPARATIVE Cytogenetics
A peer-reviewed open-access journal
International Journal of Plant & Animal Cytogenetics, Karyosystematics, and Molecular Systematics

Intraspecies multiple chromosomal variations including rare tandem fusion in the Russian Far Eastern endemic evoron vole *Alexandromys evoronensis* (Rodentia, Arvicolinae)

Irina V. Kartavtseva[1], Irina N. Sheremetyeva[1], Marina V. Pavlenko[1]

1 *Federal Scientific Center of the East Asia Terrestrial Biodiversity Far Eastern Branch of Russian Academy of Sciences, Vladivostok 690022, Russia*

Corresponding author: Irina V. Kartavtseva (Kartavtseva@biosoil.ru)

Academic editor: Irina Bakloushinskaya | Received 12 April 2021 | Accepted 23 September 2021 | Published 22 November 2021

http://zoobank.org/2DDE9369-3DF3-4B02-9DC8-AAF63196ED67

Citation: Kartavtseva IV, Sheremetyeva IN, Pavlenko MV (2021) Intraspecies multiple chromosomal variations including rare tandem fusion in the Russian Far Eastern endemic evoron vole *Alexandromys evoronensis* (Rodentia, Arvicolinae). CompCytogen 15(4): 393–411. https://doi.org/10.3897/compcytogen.v15.i4.67112

Abstract

The vole *Alexandromys evoronensis* (Kovalskaya et Sokolov, 1980) with its two chromosomal races, "Evoron" (2n = 38–41, NF = 54–59) and "Argi" (2n = 34, 36, 37, NF = 51–56) is the endemic vole found in the Russian Far East. For the "Argi" chromosomal race, individuals from two isolated populations in mountain regions were investigated here for the first time using GTG-, GTC-, NOR methods. In the area under study, 8 new karyotype variants have been registered. The karyotype with 2n = 34 has a rare tandem fusion of three autosomes: two biarmed (Mev6 and Mev7) and one acrocentric (Mev14) to form a large biarmed chromosome (Mev6/7/14), all of which reveal a heterozygous state.

For *A. evoronensis*, the variation in the number of chromosomes exceeded the known estimate of 2n = 34, 36 and amounted to 2n = 34, 36, 38–41. The combination of all the variations of chromosomes for the species made it possible to describe 20 variants of the *A. evoronensis* karyotype, with 11 chromosomes being involved in multiple structural rearrangements. In the "Evoron" chromosomal race 4 chromosomes (Mev1, Mev4, Mev17, and Mev18) and in the "Argi" chromosomal race 9 chromosomes (Mev6, Mev7, Mev14, Mev13, Mev11, Mev15, Mev17, Mev18, and Mev19) were observed. Tandem and Robertsonian rearrangements (Mev17/18 and Mev17.18) were revealed in both chromosomal races "Evoron" and "Argi".

Keywords

Chromosomal races, chromosomal rearrangements, polymorphism, Robertsonian translocation, tandem fusion

Introduction

With evolutionary processes underway, structural chromosomal rearrangements (fusion) could be of great importance (White 1973; King 1993; Ferguson-Smith and Trifonov 2007; Bakloushinskaya 2016; Dobigny et al. 2017). Studies of the tandem rearrangements in animal speciation are of great interest (Huang et al. 2006; Kulemzina et al. 2009; Swier et al. 2009; Bulatova et al. 2020), since it has been shown that translocations and tandem fusions cause transformation of karyotypes in many groups of mammals (White 1973; Elder 1980; Huang et al.1980; Elder and Hsu 1988; King 1993).

Voles of the genus *Microtus* (Schrank, 1798) sensu lato represent one of the groups in which speciation processes are accompanied by intense chromosomal rearrangements (Modi 1987; Meyer et al. 1996; Mazurok et al. 2001; Sitnikova et al. 2007; Lemskaya et al. 2010, 2015; Romanenko et al. 2018). Some species of the genus *Microtus* have karyotypic polymorphism with structural rearrangements (Zagorodnyuk 1990). Numerous observations described nine chromosomal races of vole endemic to the Balkan region in *M.* (*Terricola*) *thomasi* (Barrett-Hamilton, 1903), and two in *M.* (*T.*) *atticus* (Miller, 1910) (Giagia-Athanasopoulou et al. 1995; Giagia-Athanasopoulou and Stamatopoulos 1997; Rovatsos et al. 2021). The variation in the number of chromosomes (2n = 38, 40–44) among the chromosomal races of *M.* (*Terricola*) *thomasi* can probably be attributed to the Robertsonian translocations and tandem fusions (Rovatsos et al. 2011, 2017). Eleven karyomorphs with different chromosomal numbers (2n = 54–52, 46–43, 42 "A", 42 "B", 40, 38) and with a stable number of chromosomal arms (NF = 58) have been described for the endemic cryptic vole species in the Caucasian Region *M.* (*T.*) *daghestanicus* (Schidlovskii, 1919) (the Robertsonian fan) (Lyapunova et al. 1988; Akhverdyan et al. 1992). For two species of the related genus *Alexandromys* Ognev, 1914, inhabiting northeastern Asia – *Alexandromys maximowiczii* (Schrank, 1859) and *A. evoronensis* (Kovalskaya et Sokolov, 1980) a polymorphism has emerged due to structural rearrangements of chromosomes, including Robertsonian translocations and tandem fusions (Meyer et al. 1996; Kartavtseva et al. 2008, 2021). The *A. maximowiczii* has four chromosomal polymorphic forms (2n = 36–42) in Transbaikalia, the Russian Far East, and Mongolia (Kartavtseva et al. 2008, 2013). *A. evoronensis* has two chromosomal races in isolated populations in the mountainous regions of the Russian Far East (Kartavtseva et al. 2018).

The Evoron vole *A. evoronensis* is the endemic vole species found in the intermountain landscape of the southern Russian Far East (Fig. 1). It inhabits the Evoron-Chukchagir lowland, the Upper Zeya Plain (Sheremetyeva et al. 2017a), and the Upper Bureya Depression (Sheremetyeva et al. 2017b). Their description was based on the mtDNA data. The Evoron voles of the Evoron-Chukchagir lowland, with the maximum number of chromosomes for the species (2n = 38–41) (Kartavtseva et al. 2021), belong to the "Evoron" chromosomal race, as they were the first to be found on the shores of Lake Evoron (Kovalskaya and Sokolov 1980). Voles with the minimum number of chromosomes for the species (36 and 37) were assigned to the "Argi"

chromosomal race to be later named after the Argi River, the Zeya River tributary (Kartavtseva et al. 2018).

We have confirmed the chromosomal polymorphism of *A. evoronensis* (Kartavtseva et al. 2021) which had been previously discovered (2n = 38–40) and described by Rajabli and Sablina (Meyer et al. 1996). Analysis of differentially stained chromosomes (GTG-, C-, NOR) of voles of the "Evoron" chromosomal race (Kartavtseva et al. 2021) allowed us for the first time to describe 2n = 41 and twelve karyotype variants: two with 2n = 41, six with 2n = 40, three with 2n = 39, and one with 2n = 38. The most impressive was the tandem telomere-telomere fusion (TTel) of two metacentric No 1 and No 4 of autosomes (named Mev1 and Mev4, accordingly; see Kartavtseva et al. 2021), as a result of inactivation of the centromere in one of the metacentric forms a large biarmed element (Mev1/4).

Three variants of acrocentric chromosomes fusions and one variant of metacentric chromosomes fusion were first suggested using the G-banding of the chromosomes of voles from Lake Evoron shores without numbers for all pairs (Meyer et al. 1996). We have confirmed the data by studying the voles of Chukchagir and Evoron lakes using GTG-, C- and NOR methods. We also assigned numbers to these chromosomes (Mev17 and Mev18) and indicated that Mev17 and Mev20 carry NORs (Kartavtseva et al. 2021). The tandem fusion of telomere-centromere (TCen) of two acrocentrics (Mev17 and Mev18) were shown to form chromosomes with distinct morphology, acrocentric (Mev17/18 A) by TCen and metacentric (Mev17/18 M) by TCen. The metacentric variant of the Mev17.18 (Rb translocation) also emerged after the centric fusion of the Mev17 and Mev18.

The variability in the number of chromosome arms may be related to the centromere positions in two pairs of autosomes (Mev8 and Mev13). All the detected chromosomal rearrangements of the Evoron vole karyotype of the "Evoron" chromosomal race were found in both homozygous and heterozygous states. The tandem fusion (Mev1/4) of two metacentric autosomes Mev1 and Mev4 was taken as a marker for the vole karyotype of the Evoron – Chukchagir lowland population (Kartavtseva et al. 2021). Voles of laboratory breeding carrying such rearrangement did not reveal any effect on the fertility and viability of the offspring. The kind of rearrangements which created new karyotype variants of the "Argi" chromosomal race in two isolated populations from the Upper Zeya Plain and the Upper Bureya Depression remains unclear.

This work focuses on studying structural rearrangements in two isolated populations of the "Argi" chromosomal race. A comparative analysis of chromosomal rearrangements in the "Argi" and "Evoron" chromosomal races using GTG-, GTC-, NOR methods was done, which revealed the similarity and difference of the two chromosomal races.

Material and methods

A total of 17 individuals of *A. evoronensis* (chromosomal race "Argi") from two populations of the Russian Far East and 26 laboratory-bred voles were studied. Since the

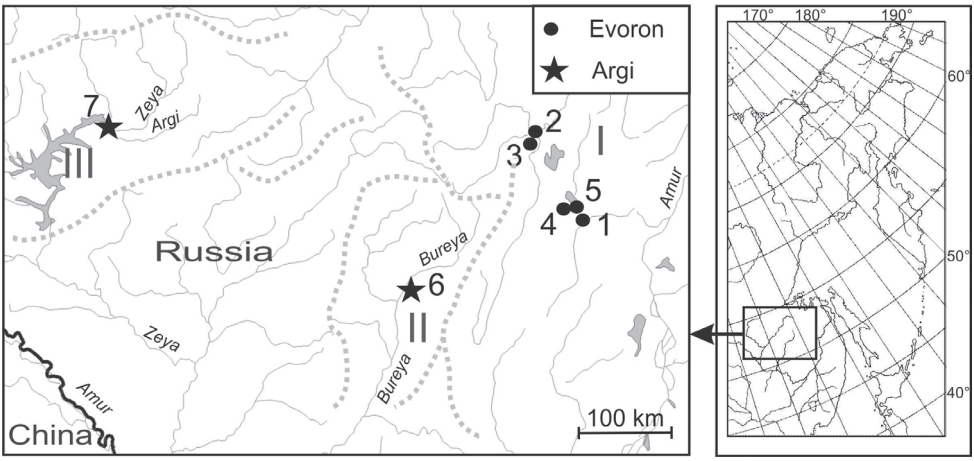

Figure 1. The map showing the collection localities of the *Alexandromys evoronensis* specimens was used in this study with the following legend: black circles stand for "Evoron" chromosomal race Nos. 1–5 according to Kartavtseva et al. 2021; black stars – for "Argi" chromosomal race Nos. 6–7 that are discussed in the material. Intermountain regions of the South of the Russian Far East: I – Evoron-Chukchagirskaya Lowland; II – Verkhnebureinskaya Depression; III – Verkhnezeiskaya Plain. Rows of dotted lines indicate mountain ranges.

voles from five local populations (Nos. 1–5) of the "Evoron" chromosomal race have been studied before (Sheremetyeva et al. 2017a, b), this work continues numbering populations as Nos. 6–7, see Fig. 1. When using animals in research, all applicable international, national and institutional ethical standards have been met.

The voles studied were assigned a double number: zoological number/tissue sample number of mt DNA. The numbers were provided to link the present study with the previously published mt DNA data (Sheremetyeva et al. 2017a, b). From population No. 6 in the Urgal River valley in the Verkhnebureinskaya depression of the Khabarovsk Territory, eight individuals were captured in August 2019, about 40 km south-west of the Chegdomyn village (51°05'54.49"N, 132°33'04.79"E) and near the village, located on the eastern bank of the Bureya River (51°07'34.15"N, 132°31'11.55"E). Females received the following identifying numbers: 4549 / 101–19, 4550 / 102–19, 4553 / 105–19, 4556 / 107–19, 4557 / 108–19 and 4567 / 121–19; respectively, male numbers were 4548 / 100–19 and 4554 / 106–19. The karyotypes of four laboratory animals from one pair of voles (without karyotyping) were also examined.

From population No. 7 in the Argi River valley of the Upper Zeya Plain in the Amur Region (54°40'10.62"N, 129°06'39.73"E), 9 individuals were caught in July 2015; females received the following identifying numbers: 3992 / 22–15 and 3997 / 27–15; male numbers were 3950 / 4–15, 3991 / 21–15, 3993 / 23–15, 3994 / 24–15, 3995 / 25–15, 3996 / 26–15, 3999 / 29–15. The karyotypes of 22 laboratory-bred individuals from parental individuals – female 3992 and males 3995, 3996 with 2n = 36 were also studied.

Chromosome suspensions were prepared from femoral bone marrow cells using the standard method (Ford and Hamerton 1956). The homology of chromosome pairs

was detected using the GTG method (Seabright 1971). The Sumner method (1972) with a slight modification, i.e., without the preparation's pretreatment in hydrochloric acid, was used to reveal C-heterochromatic blocks. Nucleolar organizer staining (NOR) was performed according to the Miinke and Schmiady (1979) method, with a modification that eliminates the pretreatment with formic acid. We inferred the fundamental number (chromosome arm number, NF) for females based on the absence of the acrocentric Y and the presence of two metacentric X chromosomes (Table 1).

We used the karyotype of the race "Evoron" (GTG method) with the highest 2n (42) number, including 26 acrocentric (A) and 14 biarmed (M) autosomes (Kartavtseva et al. 2021) as a reference for rating and numbering chromosomes in other forms. Pairs of chromosomes were ranked not by size, but by the similarity of differential staining with those of the "Evoron" chromosomal race. The size of the Mev3 of some voles of the "Argi" race was smaller than that of the "Evoron" race; the upper arm is likely to be divided and part of the chromosome to be translocated to another chromosome, which we cannot determine at the present time.

For the tandem (TTel and TCen) and Robertsonian (Rb) fusions, two different markings of the chromosomes were used. The first marking corresponds to the tandem fusion, forming acrocentrics pairs (Mev11/19; Mev17/18 and Mev 13/15), while the second one corresponds to the Robertsonian fusion (Rb), forming metacentrics (Mev17.18 and 13.15). The different morphology possibly was the result of a centromere shift (or centromere reposition).

At least 20 chromosome plates per individual were performed to determine the number of chromosomes. The Axio Imager 1 microscope with the digital camera (AxioCamHR) and the software (Axiovision 4.7, Germany) as part of the equipment of the Joint Use Center "Biotechnology and Genetic Engineering" of the Federal Scientific Center for Terrestrial Biodiversity of East Asia, the Far East, Department of the Russian Academy of Sciences (Vladivostok, Russia) were used.

Results

We studied two wild populations of voles (n = 17, see the Table 1) and laboratory-bred (n = 22) belonging to the Evoron vole of the chromosomal race "Argi". We described 8 karyotypic variants which were revealed: two variants with 2n = 34, four with 2n = 36 and two with 2n = 37. Two chromosomal variants of the karyotype with 2n = 36 were found in laboratory-bred (Lb) animals (see the Table 1).

The Karyotype variants with 2n = 36

Variant 2n = 36a, NF = 54

Variant 2n = 36a, NF = 54 (Fig. 3a) includes 16 biarmed and 18 acrocentric autosomes. The Mev13/15 chromosome was defined as acrocentric, while the Mev17.18

was described as a metacentric one. This chromosome is similar in size and morphology to chromosomes Mev1 and Mev2, and therefore it cannot be detected without differential staining. Mev6 and Mev 7 are always the smallest metacentric ones in this set. This variant was found in the voles from two localities; individuals from wild population No. 7 and a laboratory lineage (population No. 6).

Variant 2n = 36b, NF = 56

Variant 2n = 36b, NF = 56 contains 18 biarmed and 16 acrocentric autosomes. The Mev13.15 and Mev17.18 were defined as metacentric. This variant was found in voles of population No. 6 and laboratory lineage of population No. 7 (Fig. 2b).

Variant 2n = 36c, NF = 55

Variant 2n = 36c, NF = 55 (Fig. 3c) consists of 17 biarmed and 17 acrocentric autosomes. The Mev13/15 and Mev13.15 was defined as a heteromorphic pair (A, M), and Mev17.18 was defined as a metacentric one. This variant was found in voles of both populations and in the laboratory lines.

Variant 2n = 36d, NF = 55

Variant 2n = 36d, NF = 55 (Fig. 3d) includes 15 biarmed and 19 acrocentric autosomes. The Mev13.15 was defined as acrocentric, and the Mev17/18 and Mev17.18 was heteromorphic (A, M). Among the majority of acrocentric, the Mev9 had clearly visible short arms (they were not accounted for when calculating the number of chromosome arms).

Most of the voles (76.5%) of the two wild populations studied had the karyotype 2n = 36, which we defined as the main karyotype for the "Argi" chromosomal race (Table 1). The differential chromosome staining performed for selected individuals made it possible to identify the chromosomes: Mev11/19; Mev13/15 and 13.15; Mev17/18 (Fig. 2) which most likely were formed due to the fusion (Rb or tandem) of six acrocentric of the ancestral karyotype for *A. evoronensis*. Heterochromatin blocks were revealed in the pericentromeric regions of all autosomes. In addition to these, the X chromosome had a centromeric block. The Y chromosome was entirely heterochromatic (Fig. 2b). The X chromosome is a medium-sized submetacentric, Y is a small acrocentric that is slightly larger than the last pair of acrocentric autosomes.

The NORs localized in the pericentromeric regions of the Mev17/18 and Mev20 of the "Argi" chromosomal race (Fig. 2c) correspond to the Mev17 and Mev20 acrocentrics of voles of the "Evoron" chromosomal race (Kartavtseva et al. 2021).

We have also found morphological variability of the chromosomes in Mev9, Mev12, and Mev16 (Fig. 3b, d). When stained for structural heterochromatin, the short arms failed to have brightly colored blocks. The variability nature of these chromosomes was not investigated due to a different spiralization.

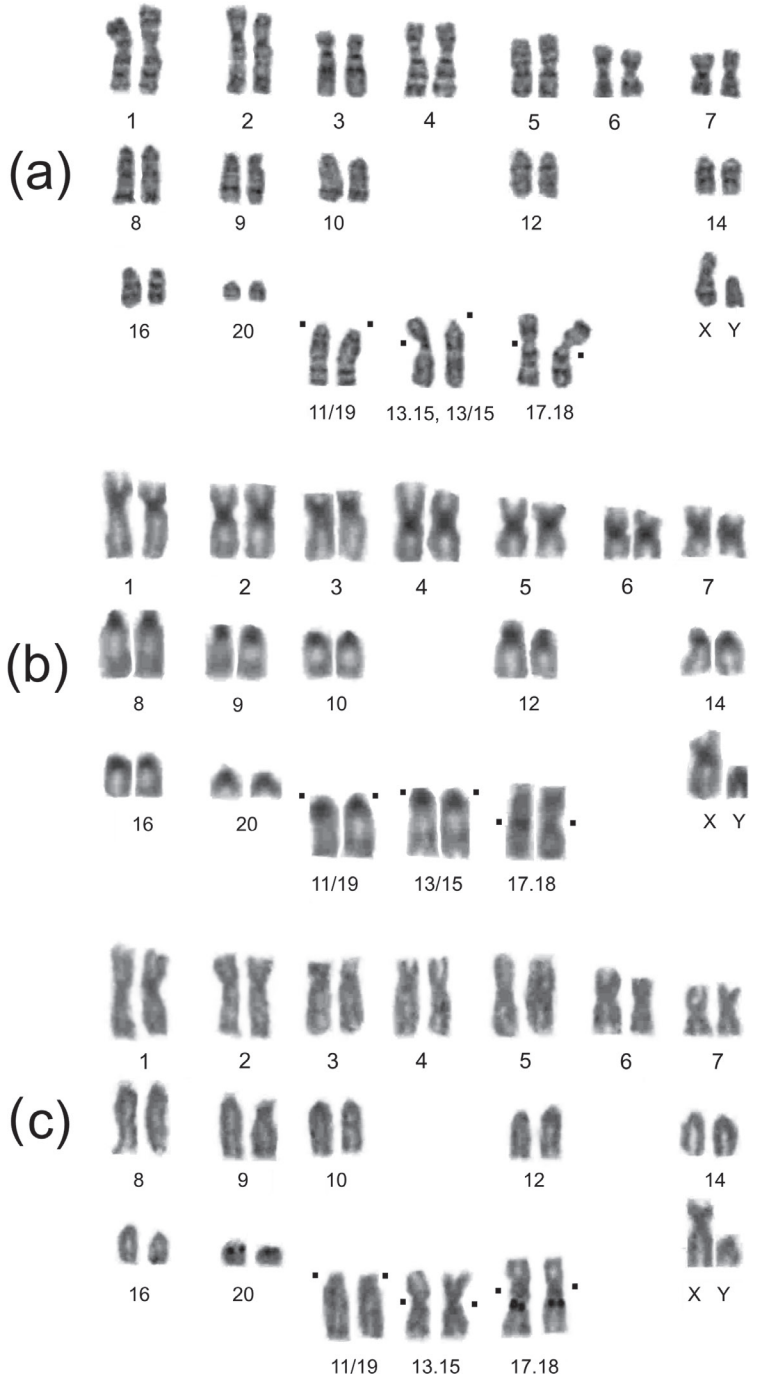

Figure 2. Karyotype of the *Alexandromys evoronensis* animals of the chromosomal race "Argi" with 2n = 36 **a** GTG-banded, 2n = 36c, # 4548, male from population No. 6 **b** C-banded, 2n = 36a, # 3950, male from population No. 7 **c** NORs, 2n = 36b, male of laboratory-bred from population No. 7. Black dots mark centromere positions in three pairs of chromosomes formed by the fusion of acrocentrics of the "Evoron" chromosomal race.

Figure 3. Variants of the *Alexandromys evoronensis* karyotype of the chromosomal race "Argi". The square shows variable chromosomes **a** 2n = 36a, male, laboratory-bred from population No. 7 **b** 2n = 36b, # 4557 female from population No. 6 **c** 2n = 36c, male laboratory-bred from population No. 7 **d** 2n = 36d, # 4567 female, the square shows variable pair Mev17/18, and 17.18 **e** 2n = 37a, # 4554 male, population No. 6 the square shows rearrangement in Mev4, and heterozygous Mev13.15, 13/15 **f** 2n = 34a, # 4553 female, population No. 6, the square shows tandem translocation pairs Mev 6, 7 and 14 in heterozygous state.

The Karyotype variants with 2n = 34

Variant 2n = 34a, NF = 51

Variant 2n = 34a, NF = 51 consists of 15 metacentric and 17 acrocentric autosomes. Both homologs of the Mev13/15 were acrocentrics (Fig. 3f). The large biarmed element Mev6/7/14 was formed by three autosomes Mev6, Mev7 and Mev14 as a result of tandem fusion. Such a karyotype was found in one female (# 4553) from a natural population No. 6.

Variant 2n = 34b, NF = 52

Variant 2n = 34b, NF = 52 includes 16 metacentric and 16 acrocentric autosomes, the chromosomes Mev13/15 and Mev13.15 were heteromorphic (Fig. 4). The large biarmed element Mev6/7/14 was formed by three autosomes Mev6, Mev7 and Mev14 as a result of tandem fusion. This karyotype was found in one male (# 3993) from population No. 7.

A decrease in the chromosome number is associated with the tandem fusion of three autosomes: Mev6, Mev7, Mev14, and the formation of a large biarmed element Mev6/7/14. All four chromosomes are in a heterozygous state (Table 1). The two variants 2n = 34a (Fig. 3f) and 2n = 34b (Fig. 4) differ in the morphology of the Mev13/15 and 13.15. The variability in the size of Mev4 is possibly related to an unknown rearrangement.

Each population (Nos. 6 and Nos. 7) of the "Argi" chromosomal race revealed one individual with 2n = 34 (Table 1), the tandem fusion of autosomes Mev6, Mev7, and Mev14 as well as the formation of a large biarmed element Mev6/7/14. In the karyotype, all four chromosomes look like heterozygotes. With the Mev6/7/14 chromosome in the homozygous state, a karyotype with 2n = 32 is theoretically possible. The detection of tandem chromosome fusion in a heterozygous state in a natural population is interesting enough to be studied further focusing on understanding the DNA transformation system in telomere regions during chromosomal rearrangements. The significance of the variability of telomeric regions and their hot spots in the evolution of chromosomes was summarized in the reviews (Zhdanova et al. 2007; Baird 2018).

The Karyotype variants with 2n = 37

Variant 2n = 37a, NF = 55

Variant 2n = 37a, NF = 55 (Fig. 3e) includes 16 biarmed and 19 acrocentric autosomes. The chromosomes Mev13/15 and Mev13.15 chromosomes are heteromorphic. One of the largest biarmed chromosomes has no pair. The two acrocentric chromosomes may have appeared as a result of a large biarmed chromosome fission. We could not determine the number of the arms since the strong spiralization of chromosomes did not allow us to do it. Chromosome suspensions were prepared in the field. This variant was found in population No. 6.

Variant 2n = 37b, NF = 55

Variant 2n = 37b, NF = 55 (see the Table 1): it consists of 16 biarmed and 19 acrocentric autosomes. The chromosomes Mev13/15 and 13.15 and Mev17/18 and 17.18 are heteromorphic. One of the large biarmed chromosomes has no pair. The two acrocentric chromosomes may have appeared as a result of a fission of a large biarmed chromosome. This variant was found in population No. 6.

Table 1. Chromosomal characteristics of karyotype variants and the scheme of variable pairs of autosomes of *Alexandromys evoronensis* from two localities – the Verkhnebureinskaya Depression (No. 6) and the Verkhnezeiskaya Plain (No. 7).

		Autosome number		Number and morphology of autosome pairs					Population	
									No. 6	No. 7
2n	NF	M	A+ St	13/15 (v) or 13.15 (x)	17/18 (v) or 17.18 (x)	7	10	6/7/14	Zoological number of animals	
37a	55	16	19	x v	x x	x x	v v		4554 m	
37b	55	16	19	x v	x v	x x	v v		4556 f	
36a	54	16	18	**v v**	x x	x x	v v		Lb	3992 f, 3950 m, 3991 m, Lb
36b	56	18	16	**x x**	x x	x x	v v		Lb, 4548 m, 4550 f, 4557 f,	Lb
36c	55	17	17	**xv**	xx	xx	vv		4549 f	3994 m, 3997 f, 3999 m, 3995 m, Lb
36d	55	15	19	**v v**	x v	x x	v v		4567 f	3996 m
34a	51	15	17	**v v**	x x	x	v	**X**	4553 f	
34b	52	16	16	**x v**	x x	x	v	**X**		3993 m
Variations	51–56	16–18	15–19						8	9

M – biarmed (x); m – male, f – female; A +St – acrocentric + subtelocentric (v); Lb – laboratory-bred voles; Pair 6/7/14 is given in capital letters to emphasize its larger sizes.

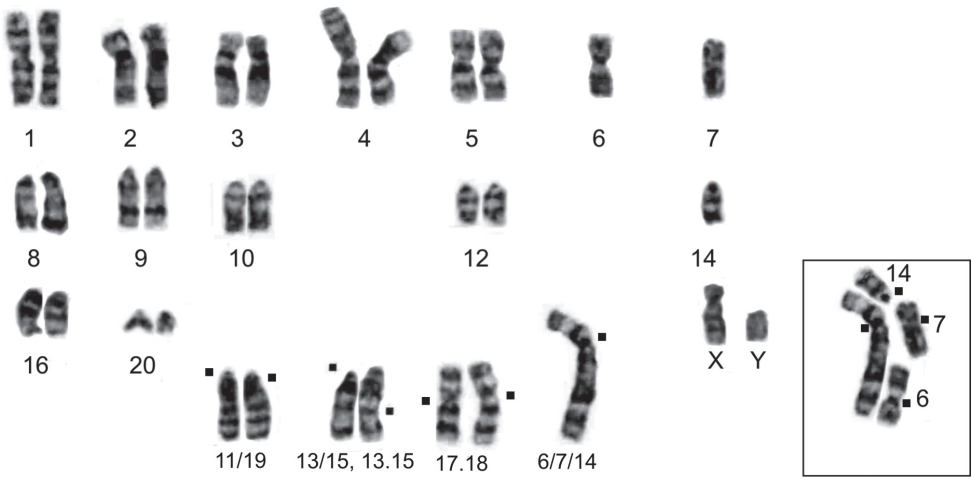

Figure 4. Karyotype of the *Alexandromys evoronensis* with tandem fusion of three autosomes: Mev6, Mev7, Mev14, and formation of a large biarmed element Mev6/7/14, 2n = 34b, # 3993 male. Black dots mark centromere in chromosomes involved in rearrangements.

This study describes Evoron voles of the "Argi" chromosomal race, with their 8 variants of the karyotype and a minimal number of chromosomes (2n = 34) as well as acrocentrics (16), as being previously not found for *A. evoronensis*. All karyotypes of voles from the two populations studied (Nos. 6 and Nos. 7) showed an acrocentric Mev11/19 to be in a homozygous state, which indicates that chromosomes had already stabilized. Chromosomes Mev13/15 and Mev13.15 in the karyotypes of both populations had a different combination (A, A; A, M; M, M), which indicates the inability of this translocation to stabilize. We can assume the possibility of the centromere repositioning as well.

After sixteen months of breeding of animals from population No. 7 in our animal facility, we got 18 litters in the first and second generations with 92 young ones from natural parents with 2n = 36 and their descendants. Twenty-two karyotyped laboratory voles (F1) with 2n = 36 showed the frequency of individuals with variable chromosome morphology of Mev13/15 and Mev13.15 (A, A; A, M; M, M) to meet a 1: 2: 1 distribution. Animals with a different chromosome number were not bred. The distribution of variants of the Mev13/15 and Mev13.15 indicates that this rearrangement has no impact on the fertility and viability of the offspring. The morphological differences in the Mev13/15 and Mev13.15 chromosomes could be explained by assuming two scenarios of chromosome fusion. The first one should be a centromere-centromere, while the second scenario should support a fusion of the centromere and telomere with different centromere inactivation, and thus forming pairs of different morphologies, as was observed for the Mev17/18 and Mev17.18 chromosomes of the "Evoron" chromosomal race (Kartavtseva et al. 2021).

Discussion

Comparative analysis of chromosomal rearrangements in two chromosomal races

We demonstrated that two local populations (Nos. 6 and Nos. 7) of the "Argi" chromosomal race, separated by mountain ranges (Fig. 1), have the same karyotype variants and chromosomal rearrangements. In the karyotype with 2n = 36 we always detected stabilization of Mev11/19, while chromosomal rearrangements Mev13/15 and Mev13.15; Mev17/18 and Mev17.18 had different morphology.

It is noteworthy that the 2n = 36 karyotype with these changed chromosomes exists in two geographically isolated populations, with the distance between these populations being about 500 kilometers. A recent time of divergence for *Alexandromys* was demonstrated using mt DNA data (Haring et al. 2011). The *p*-distance was small (0.0215) and matched the population level only. Two chromosomal races of *A. evoronensis*, "Argi" (2n = 34, 36, 37, NF = 51–56) and "Evoron" (2n = 38–41, NF = 54–59), differed in structural chromosomal rearrangements, which affected the number and morphology of chromosomes, as well as the number of karyotype variants (8 and 12, respectively). For example, Mev1.4 and Mev17/18 and Mev17.18 were detected for the "Evoron" chromosomal race, while Mev11.19; Mev13/15, Mev13.15; Mev6/7/14; Mev17/18 and Mev17.18 were revealed for the "Argi" chromosomal race (Fig. 5). The chromosomes Mev17.18 and Mev17/18 was present in both races.

Analysis of numerous rearrangements in mitosis and meiosis of the *Microtus* species of the Russian fauna showed that in most cases, structural rearrangements that do not affect linkage groups of important genes do not result in disruption of meiosis, nor do they serve as an obstacle to their fixation in populations. In most cases, changes revealed in centromere position are brought about by repeated chromosome fusion, with random

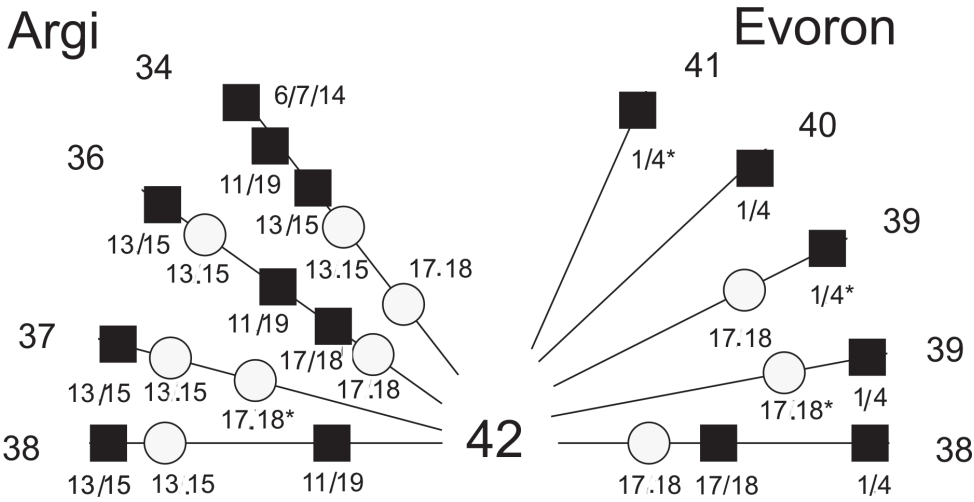

Figure 5. Scheme of the structural chromosomal rearrangements of the chromosome races "Argi" and "Evoron" identified in karyotypes with different numbers of chromosomes. Circles – centromeric, squares – telomeric fusion of chromosomes; asterisk – heterozygous state. The numbers on the edge of the diagram correspond to the diploid numbers found.

inactivation of centromeres belonging to different chromosomes (Meyer et al. 1996). Our opinion is confirmed by the data obtained which makes us believe that the shift of the centromere (or reposition) in chromosomes formed by the fusion of chromosomes is the result of centromeres' inactivation that have different chromosomes. Many examples of centromere repositioning occurring for other reasons in several mammalian lineages (Rocchi et al. 2012; Dobigny et al. 2017) which might be possibly described in voles.

Group "maximowiczii"

The range of voles with an ancestral karyotype (2n = 42) could cover the area from Lake Baikal to the coast of the Sea of Okhotsk in the eastern part of Siberia. According to Pozdnyakov (1996), fluctuations in the climatic conditions of this territory can lead to a significant change in the ranges of many species, including voles. Paleogeographic reconstructions also confirm the representatives of the "maximowiczii" voles (Golenishchev 1982): *A. maximowiczii* (Schrank, 1859), *A. mujanensis* (Orlov et Kovalskaya, 1978), *A. evoronensis* to belong to the boreal subcomplex of the mammoth theriocomplex (Baryshnikov and Markova 2009; Erbajeva et al. 2011) which included vast areas of tundra and meadow steppes during the cold period of the Late Pleistocene in Eurasia. With the beginning of landscape changes in the Holocene, this environment of tundra and meadow steppes decreased, but could be preserved in refugia.

For example, in the Middle Holocene, 7–5 thousand years ago, peculiar meadow steppes were widespread in the intermountain basins of Northern Transbaikalia (Mikheev 1974), very close to the habitats of *A. mujanensis* and *A. evoronensis*. Late

Holocene cooling caused severe changes in vegetation (Neustadt 1957; Bazarov 1968; Mikheev 1974), the disappearance of areas of meadow steppes and, as a result, the reduction of the vole range, its division into parts and the disappearance of species over a wide range. There are no paleontological data on these species, but there are data on *A. maximowiczii*, morphologically close and little distinguishable from *A. mujanensis* and *A. evoronensis* which appeared in the territory of Transbaikalia (Erbajeva 1970; Erbajeva et al. 2011) and the South of the Russian Far East in the Late Pleistocene and Early Holocene (Alekseeva and Golenishchev 1986; Voyta et al. 2019). The vole *A. mujanensis* has intra- and interpopulation variability in the morphology of four pairs of chromosomes (2n = 38; NF = 50–53) (Lemskaya et al. 2015; Kartavtseva et al. 2019).

According to Pozdnyakov (1996), *A. mujanensis* and *A. evoronensis* could have appeared simultaneously, as *A. mujanensis* in Buryatia and Transbaikalia, and *A. evoronensis* in the south of the Russian Far East. If we talk about the rate of chromosomal transformations, our data makes it possible to conclude that five structural rearrangements occurred in the karyotype of the vole *A. evoronensis* over a short geological period. The number of rearrangements from the ancestral karyotype to the *A. mujanensis* karyotype has not been determined, but there should be no less than two of them.

A. maximowiczii karyotype also underwent structural and intrachromosomal rearrangements (Meyer at al. 1996; Kartavtseva et al. 2008). FISH methods revealed intrachromosomal rearrangements in the syntenic regions of several chromosomes (the number of chromosome pairs is unknown) in *A. maximowiczii* (2n = 44), *A. mujanensis* (2n = 38), and *A. evoronensis* (2n = 36) (Romanenko et al. 2018). The authors suggest that intrachromosomal rearrangements in syntenic regions of chromosomes possibly serve as the main evolutionary force modulating the genome architecture. It should also be noted that the study used an *A. evoronensis* specimen (2n = 36) belonging to population No. 6 of the "Argi" chromosomal race, whose karyotype was previously published without differential staining (Sheremetyeva et al. 2017a). We also believe that the FISH analysis of three chromosomal polymorphic species used a pair of chromosomes with a stable morphology; otherwise, the existing differences in chromosomal rearrangements could be attributed not to the listed species differences, but to intraspecific variability.

Previously, for ten Palearctic vole species (whose chromosome number varied from 30 to 50), comparative G-banding and chromosome staining with specific *Microtus agrestis* (Linnaeus, 1961) revealed chromosomal rearrangements that distinguish this species from its ancestral karyotype (2n = 54) (Lemskaya et al. 2010). The greatest number of fusion / fission rearrangements was observed in two species of the genus *Alexandromys* Ognev, 1914 (= *Microtus*) – *A. oeconomus* (2n = 30) and *A. maximowiczii* (2n = 41) (Lemskaya et al. 2010). Based on karyological data and data on the average time of appearance of the *Microtus* sensu lato species, the stabilization of 6 chromosomal rearrangements was established, leading to a change in the number of *A. oeconomus* chromosomes of greater than once every million years of evolution, while, for other rodents this process takes more than 1 million years.

On average, one rearrangement of this type (fusion / fission) was believed to occur once every million years (Schibler et al. 1998). The second studied vole species,

A. maximowiczii has not had its number of such rearrangements determined yet, though at least nine chromosome fusions of the ancestral karyotype have been shown to bring about the formation of a karyotype with 2n = 41 (Lemskaya et al. 2010).

The chromosome painting data that are now available for many species from different orders (Murphy et al. 2001; Ferguson-Smith and Trifonov 2007) help to estimate the average rate of evolutionary rearrangements during different periods in distinct lineages and propose two main modes of karyotype evolution rate: an ancestral slow rate (one or less exchange per 10 mya) and higher rates. Record high rates of karyotype evolution were found in muroid rodents, canids, gibbons and equids (reviewed in Ferguson-Smith and Trifonov 2007). Chromosome rearrangements are central to studies of genome evolution, as our understanding of the evolutionary consequences of the early stages of karyotypic differentiation (i.e. polymorphism), especially the non-meiotic impacts, is surprisingly limited (Dobigny et al. 2017). All known chromosomal rearrangements can be involved in intra- and interpopulation polymorphism in mammals, especially in evolutionarily young species, but tandem fusions are the most deleterious mutations (King 1993; Dobigny et al. 2017). Tandem fusions (i.e. centromere–telomere, or telomere–telomere fusions (Elder and Hsu 1988) are considered as highly deleterious rearrangements because heterozygous carriers were displaying at least a 50% decrease in the production of balanced gametes (White 1973; King 1993). The tandem fusions were detected in a heterozygous state in three mammal species only (Dobigny et al. 2017) in *Uroderma bilobatum* bats (Owen and Baker 2001), South American rodent tuco-tuco *Ctenomys talarum* (Massarini et al. 2002) and in one of southern birch mouse *Sicista subtilis* (Kovalskaya et al. 2011). Later we added three more species to this list (Kartavtseva et al. 2021): Arctic foxes *Alopex lagopus* (Radzhabli and Grafodatskii 1977), voles *Alexandromys maximowiczii* (Meyer et al. 1996; Kartavtseva et al. 2008), and *A. evoronensis* (chromosomal race "Evoron") (Kartavtseva et al. 2021). The study of the "Evoron" chromosomal race revealed a heterozygous state of tandem fusion (Mev1/4) with a frequency of 0.47. For the "Argi" chromosomal race, the frequency of a heterozygous state of tandem fusion (Mev6/7/14) is 0.12 (see the Table 1).

Structural chromosomal rearrangements of "maximowiczii" voles in Asia (*A. maximowiczii* and *A. evoronensis*), as well as species of the genus *Microtus* in Europe, occurred in isolated mountain populations during the Late Pleistocene and Holocene climate change. Studies of karyotype transformation in various species allow us better to understand the role of chromosomal rearrangements in speciation.

Conclusions

Thus, we demonstrated two isolated populations of the "Argi" chromosomal race to have identical polymorphism (2n = 34, 36, 37, NF = 51–56). We revealed the multiple chromosomal rearrangements with the tandem fusions (Mev11/19, Mev13/15, Mev17/18, Mev6/7/14) and the Robertsonian translocations (Mev13.15 and Mev17.18) that led to eight new variants of the karyotype described. We observed the tandem fusion (Mev6/7/14) of chromosomes in heterozygous states in both populations.

For *A. evoronensis*, the variation in the number of chromosomes exceeded the known 2n = 34, 36 up to 2n = 34, 36, 38–41. The combination of all the variations of chromosomes for the species made it possible to describe 20 variants of the *A. evoronensis* karyotype, with 11 chromosomes which being involved in multiple structural rearrangements. In the "Evoron" chromosomal race 4 chromosomes (Mev1, Mev4, Mev17, and Mev18) and in the "Argi" chromosomal race 9 chromosomes (Mev6, Mev7, Mev14, Mev13, Mev11, Mev15, Mev17, Mev18, and Mev19) were observed. Tandem and Robertsonian rearrangements (Mev17/18 and Mev17.18) were revealed in both "Evoron" and "Argi" chromosomal races.

Acknowledgements

We thank Evgenia V. Terekhova, Prof., Chair, Foreign Lang. Dept., Far Eastern Branch, Russian Academy of Sciences for translating the paper. Our thanks also go to Natalia A. Lemskaya, Ph. D., Institute of Molecular and Cellular Biology SB RAS for help in differential standing chromosomes of voles from population No. 6. We also thank Marten Davenport and Lev Fedorov from Oregon Health Science University for proofreading our manuscript and helpful discussion. This study was partially supported by the Russian Foundation for Basic Research, Project No. 15-04-03871; the approved Research Theme is No. 0207-2021-0007.

References

Akhverdyan MR, Lyapunova EA, Vorontsov NN (1992) Karyology and taxonomy of pine voles of the Caucasus and Transcaucasia (Terricola, Arvicolinae, Rodentia). Zoologicheskii Zhurnal 71(3): 96–110. [In Russian]

Alekseeva EV, Golenishchev FN (1986) Fossil remains of grey voles of genus *Microtus* from Cave Bliznetz (Southern Far East) Proceedings of the Zoological Institute of the Russian Academy of Sciences 156: 134–142. [In Russian]

Bakloushinskaya IYu (2016) Chromosomal rearrangements, genome reorganization, and speciation. Biology Bulletin 43(8): 759–775. https://doi.org/10.1134/S1062359016080057

Baird DM (2018) Telomeres and genomic evolution. Philosophical Transaction of the Royal Society B – Biological Sciences 373(1741): e20160437. https://doi.org/10.1098/rstb.2016.0437

Baryshnikov GA, Markova AK (2009) Major theriocomplexes during the Cold Late Pleistocene (Map 23). In: Velichko AA (Ed.) Paleoclimates and paleoenvironments of extra-tropical area of the Northern Hemisphere. GEOS, Moscow, 79–87. [In Russian]

Bazarov DB (1968) Quaternary deposits and the main stages of the development of the relief of the Selenga midlands. Ulan-Ude, 166 pp. [In Russian]

Bulatova NSh, Nadzhafova RS, Kostin DS, Lavrenchenko LA, Spangenberg VE (2020) Tandem Fusions in Evolution of Ethiopian Endemic Rodents. Russian Journal of Genetics 56(10): 1255–1259. https://doi.org/10.1134/S1022795420090045

Dobigny G, Britton-Davidian J, Robinson TJ (2017) Chromosomal polymorphism in mammals: An evolutionary perspective. Biological Reviews 92: 1–21. https://doi.org/10.1111/brv.12213

Elder FFB (1980) Tandem fusion, centric fusion, and chromosomal evolution in the cotton rats, genus *Sigmodon*. Cytogenetics and Cell Genetics 26: 199–210. https://doi.org/10.1159/000131441

Elder FFB, Hsu TC (1988) Tandem fusion in the evolution of Mammalian chromosomes. In: Sandberg AA (Ed.) The Cytogenetics of Mammalian Autosomal Rearrangements. Alan R. Liss, New York, 481–506.

Erbajeva MA (1970) History of the anthropogenic fauna of lagomorphs and rodents of the Selenga midlands. Nauka, Moscow, 132 pp. [In Russian]

Erbajeva MA, Khenzykhenova FI, Alexeeva NV (2011) Late Pleistocene and Holocene environmental peculiarity of the Baikalian region, based on mammal associations and deposits. Quaternary International 237: 39–44. https://doi.org/10.1016/j.quaint.2011.01.014

Ferguson-Smith M, Trifonov V (2007) Mammalian karyotype evolution. Nature Reviews Genetics 8: 950–962. https://doi.org/10.1038/nrg2199

Ford CF, Hamerton JLA (1956) Colchicine hypotonic citrate squash preparation for mammalian chromosomes. Stain Technology 31: 247–251. https://doi.org/10.3109/10520295609113814

Giagia-Athanasopoulou EB, Chondropoulos BP, Fraguedakis-Tsolis SE (1995) Robertsonian chromosomal variation in the subalpine voles *Microtus* (*Terricola*) (Rodentia, Arvicolidae) from Greece. Acta Theriologica 40: 139–143. https://doi.org/10.4098/AT.arch.95-15

Giagia-Athanasopoulou EB, Stamatopoulos C (1997) Geographical distribution and interpopulation variation in the karyotypes of *Microtus* (*Terricola*) *thomasi*. Caryologia 50: 3003–3315. https://doi.org/10.1080/00087114.1997.10797404

Golenishchev FN (1982) The gray voles (subgenus *Microtus*, group "maximowiczii") of Eastern Siberia and the Far East. Abstract of Ph.D. Dissertation, Zoological Institute, Russian Academy of Sciences, Leningrad, 23 pp. [In Russian]

Haring E, Sheremetyeva I, Kryukov A (2011) Phylogeny of Palearctic vole species (genus *Microtus*, Rodentia) based on mitochondrial sequences. Mammalian Biology 76: 258–267. https://doi.org/10.1016/j.mambio.2010.04.006

Huang L, Wang J, Nie W, Su W, Yang F (2006) Tandem chromosome fusions in karyotypic evolution of *Muntiacus*: evidence from *M. feae* and *M. gongshanensis*. Chromosome Research 14: 637–647. https://doi.org/10.1007/s10577-006-1073-2

Kartavtseva IV, Sheremetyeva IN, Korobitsina KV, Nemkova GA, Konovalova EV, Korablev VV, Voyta LL (2008) Chromosomal forms of *Microtus maximowiczii* (Schrenck, 1859) (Rodentia, Cricetidae): variability in 2n and NF in different geographic regions. Russian Journal of Theriology 7: 89–97. https://doi.org/10.15298/rusjtheriol.07.2.05

Kartavtseva IV, Sheremetyeva IN, Romanenko SA, Gladkikh OL (2013) Chromosomes variability of the Maximowicz's vole *Microtus maximowiczii* (Rodentia, Cricetidae, *Microtus*). Tsitologiya 55(4): 261–263.

Kartavtseva IV, Sheremetyeva IN, Pavlenko MV, Vasiljeva TV, Frisman LV (2018) A new chromosomal race of the Evoron voles *Alexandromys evoronensis* of two isolated populations in the Russian Far East, 6th International Conference of Rodent Biology and Management

and 16th Rodents et Spatium (3–7 September, 2018, Potsdam, Germany): Book of Abstracts, Potsdam, 268–268.

Kartavtseva IV, Vasilieva TV, Sheremetyeva IN, Lemskaya NA, Moroldoev IV, Golenishchev FN (2019) Genetic Variability of Three Isolated Populations of the Muya Valley Vole *Alexandromys mujanensis* Orlov et Kovalskaya, 1978 (Rodentia, Arvicolinae). Russian Journal of Genetics 55(8): 978–992. https://doi.org/10.1134/S1022795419080076

Kartavtseva IV, Sheremetyeva IN, Pavlenko MV (2021) Multiple Chromosomal Polymorphism of "Evoron" Chromosomal Race of the Evoron Vole (Rodentia, Arvicolinae). Russian Journal of Genetics 57(1): 70–82. https://doi.org/10.1134/S1022795421010087

King M (1993) Chromosomal Speciation Revisited (Again): Species Evolution. The Role of Chromosome Change. Cambridge Univ. Press, Cambridge, 336 pp. https://doi.org/10.1046/j.1420-9101.1994.7060764.x

Kovalskaya Y, Aniskin V, Bogomolov P, Surov A, Tikhonov I, Thikonova G, Robinson T, Volobuev V (2011) Karyotype reorganization in the subtilis group of Birch Mice (Rodentia, Dipodidae, *Sicista*): unexpected taxonomic diversity within a limited distribution. Cytogenetics and Genome Research 132: 271–288. https://doi.org/10.1159/000322823

Kulemzina AI, Trifonov VA, Perelman PL, Rubtsova NV, Volobuev V, Ferguson-Smith MA, Stanyon R, Yang F, Graphodatsky AS (2009) Cross-species chromosome painting in Cetartiodactyla: reconstructing the karyotype evolution in key phylogenetic lineages. Chromosome Research 17: 419–436. https://doi.org/10.1007/s10577-009-9032-3

Lemskaya NA, Romanenko SA, Golenishchev FN, Rubtsova NV, Sablina OV, Serdukova NA, O'Brien PCM, Fu B, Yiğit N, Ferguson-Smith MA, Yang F, Graphodatsky AS (2010) Chromosomal evolution of Arvicolinae (Cricetidae, Rodentia). III. Karyotype relationships of ten *Microtus* species. Chromosome Research 18: 459–471. https://doi.org/10.1007/s10577-010-9124-0

Lemskaya NA, Kartavtseva IV, Rubtsova NV, Golenishchev FN, Sheremetyeva IN, Graphodatsky AS (2015) Chromosome polymorphism in *Microtus* (*Alexandromys*) *mujanensis* (Arvicolinae, Rodentia). Cytogenetic and Genome Research 146: 238–242. https://doi.org/10.1159/000439096

Liming S, Yingying Y, Xingsheng D (1980) Comparative cytogenetic studies on the red muntjac, *Chinese muntjac*, and their F1 hybrids. Cytogenetics and Cell Genetics 26: 22–27. https://doi.org/10.1159/000131417

Lyapunova EA, Akhverdyan MR, Vorontsov NN (1988) The Robertsonian fan of variability of chromosomes in subalpine voles of Caucasian (*Pitymys*, Microtinae, Rodentia). Doklady Akademii Nauk SSSR 273(5): 1204–1208.

Mazurok NA, Rubtsova NV, Isaenko AA, Pavlova ME, Slobodyanyuk SY, Nesterova TB, Zakian SM (2001) Comparative chromosome and mitochondrial DNA analyses and phylogenetic relationships within common voles (*Microtus*, Arvicolidae). Chromosome Research 9: 107–120. https://doi.org/10.1023/A:1009226918924

Meyer MN, Golenishchev FN, Radjabli SI, Sablina OV (1996) Voles (subgenus *Microtus* Schrank) of Russia and adjacent territories. Russian Academy of Science Preceding of Zoological Institute 232, 320 pp. [In Russian]

Miinke M, Schmiady H (1979) A simple one-step for staining the nucleolus organizer region. Experiential 35: 602–603. https://doi.org/10.1007/BF01960345

Mikheev BC (1974) Verkhnecharskaya depression (experience of topological study of landscape). Nauka, Novosibirsk, 143 pp. [In Russian]

Mitsainas GP, Rovatsos MT, Rizou EI, Giagia-Athanasopoulou EB (2009) Sex chromosome variability outlines the pathway to the chromosomal evolution in *Microtus thomasi* (Rodentia, Arvicolinae). Biological Journal of Linnean Society 96: 685–695. https://doi.org/10.1111/j.1095-8312.2008.01161.x

Modi WS (1987) Phylogenetic analyses of chromosomal banding patterns among the Nearctic Arvicolidae (Mammalia, Rodentia). Systematic Zoology 36(2): 109–136. https://doi.org/10.2307/2413264

Murphy WJ, Stanyon R, O'Brien SJ (2001) Evolution of mammalian genome organization inferred from comparative gene mapping. Genome Biology 2(6): reviews0005.1. https://doi.org/10.1186/gb-2001-2-6-reviews0005

Neishtadt MI (1957) History of forests and paleogeography of USSR in the Holocene. Moscow, 404 pp. [In Russian]

Owen JG, Baker RK (2001) The *Uroderma bilobatum* (Chiroptera, Phyllostomidae) cline revisited. Journal of Mammalogy 82(4): 1102–1113. https://doi.org/10.1644/1545-1542(2001)082%3C1102:TUBCPC%3E2.0.CO;2

Pozdnyakov AA (1996) On the phylogeny of voles of the subgenus *Alexandromys* (Rodentia, Arvicolidae, *Microtus*): variability and paleontological records. Zoologicheskii Zhurnal 75(1): 133–140. [In Russian]

Radzhabli SI, Grafodatskii AS (1977) Evolution of the mammalian karyotype: structural rearrangements of chromosomes and the heterochromatin, in Tsitogenetika gibridov, mutatsii i evolyutsiya kariotipa (Cytogenetics of Hybrids, Mutations and the Karyotype Evolution). Nauka, Novosibirsk, 231–249. [In Russian]

Rocchi M, Archidiacono N, Schempp W, Capozzi O, Stanyon R (2012) Centromere repositioning in mammals. Heredity 108: 59–67. https://doi.org/10.1038/hdy.2011.101

Romanenko SA, Serdyukova NA, Perelman PL, Trifonov VA, Golenishchev FN, Bulatova NSh, Stanyon R, Graphodatsky AS (2018) Multiple intrasyntenic rearrangements and rapid speciation in voles. Scientific Reports 8: e14980. https://doi.org/10.1038/s41598-018-33300-6

Rovatsos MTh, Mitsainas GP, Paspali G, Oruci S, Giagia-Athanasopoulou EB (2011) Geographical distribution and chromosomal study of the underground vole *Microtus thomasi*. Mammalian Biology 76: 22–25. https://doi.org/10.1016/j.mambio.2010.01.003

Rovatsos MT, Marchal JA, Romero-Fernández I, Arroyo M, Athanasopoulou EB, Sánchez A (2017) Extensive sex chromosome polymorphism of *Microtus thomasi* / *Microtus atticus* Species complex associated with cryptic chromosomal rearrangements and independent accumulation of heterochromatin. Cytogenetic and Genome Research 151: 198–207. https://doi.org/10.1159/000477114

Rovatsos M, Marchal JA, Giagia-Athanasopoulou E, Sánchez A (2021) Molecular Composition of Heterochromatin and Its Contribution to Chromosome Variation in the *Microtus thomasi* / *Microtus atticus* Species Complex. Genes 12(6): e807. https://doi.org/10.3390/genes12060807

Schibler L, Vaiman D, Oustry A, Giraud-Delville C, Cribiu EP (1998) Comparative gene mapping: a fine-scale survey of chromosome rearrangements between ruminants and humans. Genome Research 8: 901–915. https://doi.org/10.1101/gr.8.9.901

Seabright M (1971) A rapid banding technique for human chromosomes. The Lancet 298(7731): 971–972. https://doi.org/10.1016/S0140-6736(71)90287-X

Shchetnikov AA, Khenzykhenova FI, Klement'ev AM, Simakova AN, Semenei EY, Filinov IA (2015) Changes of environments and climate during the Late Pleistocene and Holocene reconstructed from aeolian and colluvial deposits of the Zaktui site (Tunka rift valley, Baikal region). Quaternary International 355: 80–89. https://doi.org/10.1016/j.quaint.2014.07.074

Sheremetyeva IN, Kartavtseva IV, Vasiljeva TV (2017a) Does *Alexandromys evoronensis* Inhabit the Northeastern Part of Verkhnezeiskaya Plain? Biology Bulletin 44(9): 1049–1055. https://doi.org/10.1134/S1062359017090126

Sheremetyeva IN, Kartavtseva IV, Vasiljeva TV, Frisman LV (2017b) Voles of the genus *Alexandromys* from the Verkhnebureinskaya Depression. Biology Bulletin 44(7): 813–819. https://doi.org/10.1134/S1062359017070159

Sitnikova NA, Romanenko SA, O'Brien PCM, Perelman PL, Fu B, Rubtsova NV, Serdukova NA, Golenishchev FN, Trifonov VA, Ferguson-Smith MA, Yang F, Graphodatsky AS (2007) Chromosomal evolution of Arvicolinae (Cricetidae, Rodentia). I. The genome homology of tundra vole, field vole, mouse and golden hamster revealed by comparative chromosome painting. Chromosome Research 15(2): 447–456. https://doi.org/10.1007/s10577-007-1137-y

Sumner AT (1972) A simple technique for demonstrating centromeric heterochromatin. Experimental Cell Research 83: 438–442. https://doi.org/10.1016/0014-4827(72)90558-7

Swier VJ, Bradley RD, Rens W, Elder FFB, Baker RJ (2009) Patterns of chromosomal evolution in *Sigmodon*, evidence from whole chromosome paints. Cytogenetics and Cell Genetics 125: 54–66. https://doi.org/10.1159/000218747

Voyta LL, Golenishchev FN, Tiunov MP (2019) Far Eastern grey voles *Alexandromys* (Rodentia: Cricetidae) from Medvezhyi Klyk cave Late Pleistocene-Holocene deposits, Primorskii Kray, Russia. Proceedings of the Zoological Institute 323(3): 313–346. https://doi.org/10.31610/trudyzin/2019.323.3.313 [In Russian]

White MJD (1973) Animal Cytology and Evolution, 3rd edn. Cambridge University, Cambridge, 468 pp.

Zhdanova NS, Rubtsov NB, Minina YuM (2007) Terminal Regions of Mammal Chromosomes: Plasticity and Role in Evolution. Russian Journal of Genetics 43(7): 721–773. https://doi.org/10.1134/S1022795407070022

Zima J, Král B (1984) Karyotypes of European mammals. II. Acta Scientiarum Naturalium Academiae Scientiarum Bohemoslovacae Slovakia, Brno 28: 3–62.

ORCID

Irina V. Kartavtseva https://orcid.org/0000-0003-2136-8253
Irina N. Sheremetyeva https://orcid.org/0000-0003-3464-9009
Marina V. Pavlenko https://orcid.org/0000-0002-7772-7019

CompCytogen 15(4): 413–428 (2021)
doi: 10.3897/compcytogen.v15.i4.73769
https://compcytogen.pensoft.net

RESEARCH ARTICLE

COMPARATIVE Cytogenetics
A peer-reviewed open-access journal
International Journal of Plant & Animal Cytogenetics, Karyosystematics, and Molecular Systematics

Distribution of GC-rich heterochromatin and ribosomal genes in three fungus-farming ants (Myrmicinae, Attini, Attina): insights on chromosomal evolution

Gisele Amaro Teixeira[1,2], Luísa Antônia Campos Barros[3], Hilton Jeferson Alves Cardoso de Aguiar[3], Denilce Meneses Lopes[2]

1 *Programa de Pós-graduação em Biologia Celular e Estrutural, Universidade Federal de Viçosa, Viçosa, MG 36570-900, Brazil* **2** *Laboratório de Citogenética de Insetos, Departamento de Biologia Geral, Universidade Federal de Viçosa, Viçosa, MG 36570-900, Brazil* **3** *Universidade Federal do Amapá, Campus Binacional, n°3051, Bairro Universidade, 68980-000, Oiapoque, Amapá, Brazil*

Corresponding author: Luísa Antônia Campos Barros (luufv@yahoo.com.br)

Academic editor: Rodolpho Menezes | Received 31 August 2021 | Accepted 11 October 2021 | Published 25 November 2021

http://zoobank.org/DD774ADE-CFB0-4292-B229-5A27BE4E6EDA

Citation: Teixeira GA, Barros LAC, de Aguiar HJAC, Lopes DM (2021) Distribution of GC-rich heterochromatin and ribosomal genes in three fungus-farming ants (Myrmicinae, Attini, Attina): insights on chromosomal evolution. CompCytogen 15(4): 413–428. https://doi.org/10.3897/compcytogen.v15.i4.73769

Abstract

Cytogenetic studies on fungus-farming ants have shown remarkable karyotype diversity, suggesting different chromosomal rearrangements involved in karyotype evolution in some genera. A notable cytogenetic characteristic in this ant group is the presence of GC-rich heterochromatin in the karyotypes of some ancient and derivative species. It was hypothesized that this GC-rich heterochromatin may have a common origin in fungus-farming ants, and the increase in species studied is important for understanding this question. In addition, many genera within the subtribe Attina have few or no cytogenetically studied species; therefore, the processes that shaped their chromosomal evolution remain obscure. Thus, in this study, we karyotyped, through classical and molecular cytogenetic techniques, the fungus-farming ants *Cyphomyrmex transversus* Emery, 1894, *Sericomyrmex maravalhas* Ješovnik et Schultz, 2017, and *Mycetomoellerius relictus* (Borgmeier, 1934), to provide insights into the chromosomal evolution in these genera and to investigate the presence the GC-rich heterochromatin in these species. *Cyphomyrmex transversus* (2n = 18, 10m + 2sm + 6a) and *S. maravalhas* (2n = 48, 28m + 20sm) showed karyotypes distinct from other species from their genera. *Mycetomoellerius relictus* (2n = 20, 20m) presented the same karyotype as the colonies previously studied. Notably, *C. transversus* presented the lowest chromosomal number for the genus and a distinct karyotype from the other two previously observed for this species, showing the existence of a possible species complex and the need for its taxonomic revision. Chromosomal banding

data revealed GC-rich heterochromatin in all three species, which increased the number of genera with this characteristic, supporting the hypothesis of a common origin of GC-rich heterochromatin in Attina. Although a single chromosomal pair carries rDNA genes in all studied species, the positions of these rDNA clusters varied. The rDNA genes were located in the intrachromosomal region in *C. transversus* and *M. relictus*, and in the terminal region of *S. maravalhas*. The combination of our molecular cytogenetic data and observations from previous studies corroborates that a single rDNA site located in the intrachromosomal region is a plesiomorphic condition in Attina. In addition, cytogenetic data obtained suggest centric fission events in *Sericomyrmex* Mayr, 1865, and the occurrence of inversions as the origin of the location of the ribosomal genes in *M. relictus* and *S. maravalhas*. This study provides new insights into the chromosomal evolution of fungus-farming ants.

Keywords
Biodiversity, chromatin, chromosomal rearrangements, Formicidae, karyotype evolution, molecular cytogenetics

Introduction

Fungus-farming ants, included in the subtribe Attina (sensu Ward et al. 2015), have an obligatory symbiotic relationship with fungi (Weber 1966). In this symbiosis, these ants cultivate the fungus for food and, in return, provide the fungus with nutrition, propagate it to new locations, and protect it against parasitic microorganisms (Weber 1966; Little et al. 2005). In this agricultural system, these ants use different types of substrates depending on the genus/species (reviewed by Mehdiabadi and Schultz 2010), and with this, they play important roles in natural ecosystems, such as dispersion and increasing the success of seed germination, soil structuring, and nutrient cycling (Leal and Oliveira 1998; Fernandez-Bou et al. 2019).

Several molecular phylogenetic studies have been conducted in Attina to address the relationships between genera and species (Schultz and Brady 2008; Ješovnik et al. 2017; Sosa-Calvo et al. 2017; Solomon et al. 2019). These phylogenies support the monophyly of the group, with an origin of approximately 50–60 million years ago (Schultz and Brady 2008; Nygaard et al. 2016; Sosa-Calvo et al. 2017). This group includes approximately 280 described taxa distributed in 20 genera (Bolton 2021), which are grouped into two monophyletic sister clades: Paleoattina (*Apterostigma* Mayr, 1865, *Mycocepurus* Forel, 1893, and *Myrmicocrypta* Smith, 1860) and Neoattina (the remaining 17 genera) (Sosa-Calvo et al. 2018; Solomon et al. 2019; Cristiano et al. 2020).

Some Attina genera have been extensively revised (Sosa-Calvo et al. 2017, 2018; Solomon et al. 2019; Cristiano et al. 2020), and in this scenario, cytogenetics is a tool that can help in taxonomic issues, since chromosomal rearrangements can lead to reduced gene flow between populations and reproductive isolation, playing an important role in speciation (Riesemberg 2001; reviewed by Faria and Navarro 2010). In addition to evolutionary, phylogenetic, and chromosomal patterns in different groups, cytogenetic studies on ants, using classical and molecular techniques, are important for the

understanding of taxonomically challenging species (Mariano et al. 2012; Santos et al. 2016; Aguiar et al. 2017; Micolino et al. 2019a; Teixeira et al. 2021).

Cytogenetic data are available for 56 taxa of fungus-farming ants with representatives from 12 genera (reviewed by Mariano et al. 2019; Aguiar et al. 2020; Micolino et al. 2020; Barros et al. 2021) and the chromosome number observed for the group ranges from 2n = 8 in *Mycocepurus goeldii* (Forel, 1893) and *Mycocepurus* sp. to 2n = 64 in *Mycetophylax lectus* (Forel, 1911) (as *Cyphomyrmex lectus*) (reviewed by Mariano et al. 2019). A notable cytogenetic characteristic in this ant group is that some Paleoattina and Neoattina species have GC-rich heterochromatin in all chromosomes, with nucleotide composition yet to be determined but may have an origin in the common ancestor needing further investigation (Barros et al. 2018; reviewed by Mariano et al. 2019). Molecular cytogenetic studies using fluorescence *in situ* hybridization (FISH) for mapping ribosomal genes have already been performed in 17 taxa, including six genera showing a single chromosome pair carrying rDNA genes (reviewed in Teixeira et al. 2021).

According to available cytogenetic data, different chromosomal rearrangements have been proposed to explain karyotype evolution in some Attina genera. The occurrence of centric fissions, according to Minimum Interaction Theory (MIT) (Imai et al. 1994), was suggested to explain the remarkable karyotype variation in *Mycetarotes* Emery, 1913 (2n = 14 to 54), *Apterostigma* (2n = 20 to 46), *Cyphomyrmex* Mayr, 1862 (2n = 20 to 42), and in leaf-cutting ants, in which *Amoimyrmex striatus* (Roger, 1863) and *Atta* spp. present 2n = 22, and most *Acromyrmex* spp. show 2n = 38 (reviewed by Mariano et al. 2019; Barros et al. 2021). However, chromosomal fusion has been suggested as the origin of the derived karyotype from *Acromyrmex ameliae* De Souza et al. 2007 (2n = 36) (Barros et al. 2021). In *Mycetophylax* Emery, 1913, both chromosomal fusions and fissions are important for the karyotypic evolution of species (Micolino et al. 2019a). In addition, other mechanisms that do not change the chromosome number were proposed for some species as differential heterochromatin growth in *Acromyrmex* spp. (Barros et al. 2016), duplications of euchromatic regions by unequal crossing-over or non-homologous translocations in *Mycetomoellerius urichii* (Forel, 1893) (as *Trachymyrmex fuscus* Emery, 1934) (Barros et al. 2013a), paracentric inversion in *Acromyrmex echinatior* (Forel, 1899) (Barros et al. 2016; Teixeira et al. 2021) and pericentric inversion in *Mycetomoellerius iheringi* (Emery, 1888) (Micolino et al. 2020).

There are different possible mechanisms involved in the karyotype evolution of Attina genera, highlighting the need to increase the number of studied species for more robust inferences (Barros et al. 2013b, 2018). The remaining genera of fungus-farming ants have little or no cytogenetically studied species; therefore, the processes that shaped their chromosomal evolution remain obscure. Therefore, using classical and molecular cytogenetic techniques, we determined the karyotypes of three fungus-farming ants – *Cyphomyrmex transversus* Emery, 1894, *Mycetomoellerius relictus* (Borgmeier, 1934), and *Sericomyrmex maravalhas* Ješovnik et Schultz, 2017 – to investigate the presence of GC-rich heterochromatin in these species and understand the patterns of chromosomal evolution in their respective genera as well as in Attina in general.

Material and methods

Colonies of *C. transversus*, *M. relictus*, and *S. maravalhas* were collected in Viçosa, in the Minas Gerais state, Brazil (-20.757041, -42.873516) (Table 1). Sampling permission was given by the Instituto Chico Mendes de Conservação da Biodiversidade (ICMBio) (SISBIO accession number 32459). Adult vouchers were identified by Dr. Jacques H. C. Delabie and deposited in the myrmecological collection of the Centro de Pesquisas do Cacau at the Comissão Executiva do Plano da Lavoura Cacaueira (CEPLAC), in Bahia, Brazil.

Mitotic metaphases were obtained from cerebral ganglia of larvae after meconium elimination accordingly to Imai et al. (1988). Chromosome number and morphology of metaphases were analyzed using conventional 4% Giemsa staining. Chromosomes were arranged in order of decreasing size, measured and classified according to the methodology proposed by Levan et al. (1964) that is based on the ratio of the chromosome arm lengths (r = long arm/short arm). The chromosomes were classified as m = metacentric (r = 1–1.7), sm = submetacentric (r = 1.7–3), st = subtelocentric (r = 3–7) and a = acrocentric (r > 7). Chromosomes were organized using Adobe Photoshop CS6 and measured using Image Pro Plus.

The heterochromatin distribution pattern was observed by C-banding technique according to Sumner (1972), with adaptations of Barros et al. (2013b). Metaphases were stained with the fluorochromes chromomycin A_3 (CMA_3) and 4'6-diamidino-2-phenylindole (DAPI), to the detection of GC and AT-rich regions, respectively based on the technique proposed by Schweizer (1980).

The ribosomal 18S gene clusters were detected by FISH, following the protocol of Pinkel et al. (1986) with the use of the 18S rDNA probes obtained via PCR amplification. The genomic DNA from the ant *Camponotus rufipes* (Fabricius, 1775) was used for amplification of 18S rDNA using the primers 18SF1 (5'-GTC ATA GCT TTG TCT CAA AGA-3') and 18SR1.1 (5'-CGC AAA TGA AAC TTT TTT AAT CT-3') (Pereira 2006). These primers amplify the initial portion of 18S rDNA (for details see Menezes et al. 2021). Gene amplification followed Pereira (2006). 18S rDNA probes were labeled by an indirect method using digoxigenin-11-dUTP (Roche Applied Science, Mannheim, Germany), and the FISH signals were detected with anti-digoxigenin-rhodamine (Roche Applied Science), following the manufacturer's protocol.

Table 1. Species of fungus-farming ants cytogenetically analyzed in the present study collected in Viçosa, Minas Gerais, Brazil. Species, total number of colonies and individuals; diploid chromosome numbers; diploid karyotype formulae, presence of GC-rich heterochromatin, and idiogram showing the location of 18S rDNA genes in the karyotype.

Species	Col. / Ind.	2n	Karyotype formulae	GC-rich Het	rDNA 18S location
Cyphomyrmex transversus	1 / 6	18	10m + 2sm + 6a	Yes	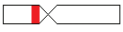
Mycetomoellerius relictus	2 / 7	20	20m	Yes	
Sericomyrmex maravalhas	2 / 14	48	28m + 20sm	Yes	

Chromosomes from ten metaphases of each taxon were measured in order to determine the chromosomal morphology. For C-banding, fluorochrome staining, and FISH techniques, at least 30 metaphases of each taxon were analyzed. The metaphases were photographed using an epifluorescent microscope Olympus BX60 attached to an image system QColor Olympus with the filters WB (450–480 nm), WU (330–385 nm), and WG (510–550 nm) for the fluorochromes CMA_3, DAPI, and rhodamine, respectively.

Results

The chromosome numbers and karyotypic formulae observed in the three fungus-farming ant species were as follows: 2n = 18 (10m + 2sm + 6a) in *C. transversus* (Fig. 1a), 2n = 20 (20m) and n = 10 (10m) in *M. relictus* (Fig. 1b, c), and 2n = 48 (28m + 20sm) in *S. maravalhas* (Fig. 1d).

Heterochromatin was observed in the centromeric/pericentromeric regions of all chromosomes besides short arms of acrocentric chromosomes in *C. transversus* (Fig. 2a). *Mycetomoellerius relictus* presented heterochromatic bands in the centromeric regions of all chromosomes (Fig. 2b). In *S. maravalhas*, heterochromatin was observed in the centromeric and pericentromeric regions of metacentric chromosomes, and short arms of the 7th, 10th, and 13th metacentric and all submetacentric pairs (Fig. 2c). Most of the heterochromatic regions showed GC-rich patterns in all three species (Fig. 3).

The three species showed a single pair of chromosomes bearing rDNA clusters. The 18S ribosomal gene clusters were mapped in the pericentromeric region of the short arm of the 2nd metacentric pair in *C. transversus* (Fig. 4a), in the interstitial region of the long arm of the 5th metacentric pair in *M. relictus* (Fig. 4b, c), and in the terminal region of the short arm of the 7th metacentric pair in *S. maravalhas* (Fig. 4d).

Discussion

The association of cytogenetic and molecular data provided insights into the karyotype evolution of the three genera of fungus-farming ants in this study. In *Sericomyrmex*, the molecular phylogeny proposed by Ješovnik et al. (2017) showed that *S. maravalhas*, a new species recently described by Ješovnik and Schultz (2017), belongs to the *scrobifer* clade, which is basal to the other existing clade, the *amabilis*. Ješovnik and Schultz (2017) highlighted that the distribution data of *S. maravalhas* are clearly incomplete. This is the first report of this species in the Atlantic rainforest since its known occurrence, to this date, was restricted to Cerrado habitats.

Sericomyrmex maravalhas (*scrobifer* clade) has a basal position to *Sericomyrmex amabilis* Wheeler, 1925 (*amabilis* clade) (Ješovnik et al. 2017). The former species has 2n = 48, with more submetacentric chromosomes (this study), whereas the latter species has 2n = 50 with only metacentric chromosomes (Murakami et al. 1998). It is possible to

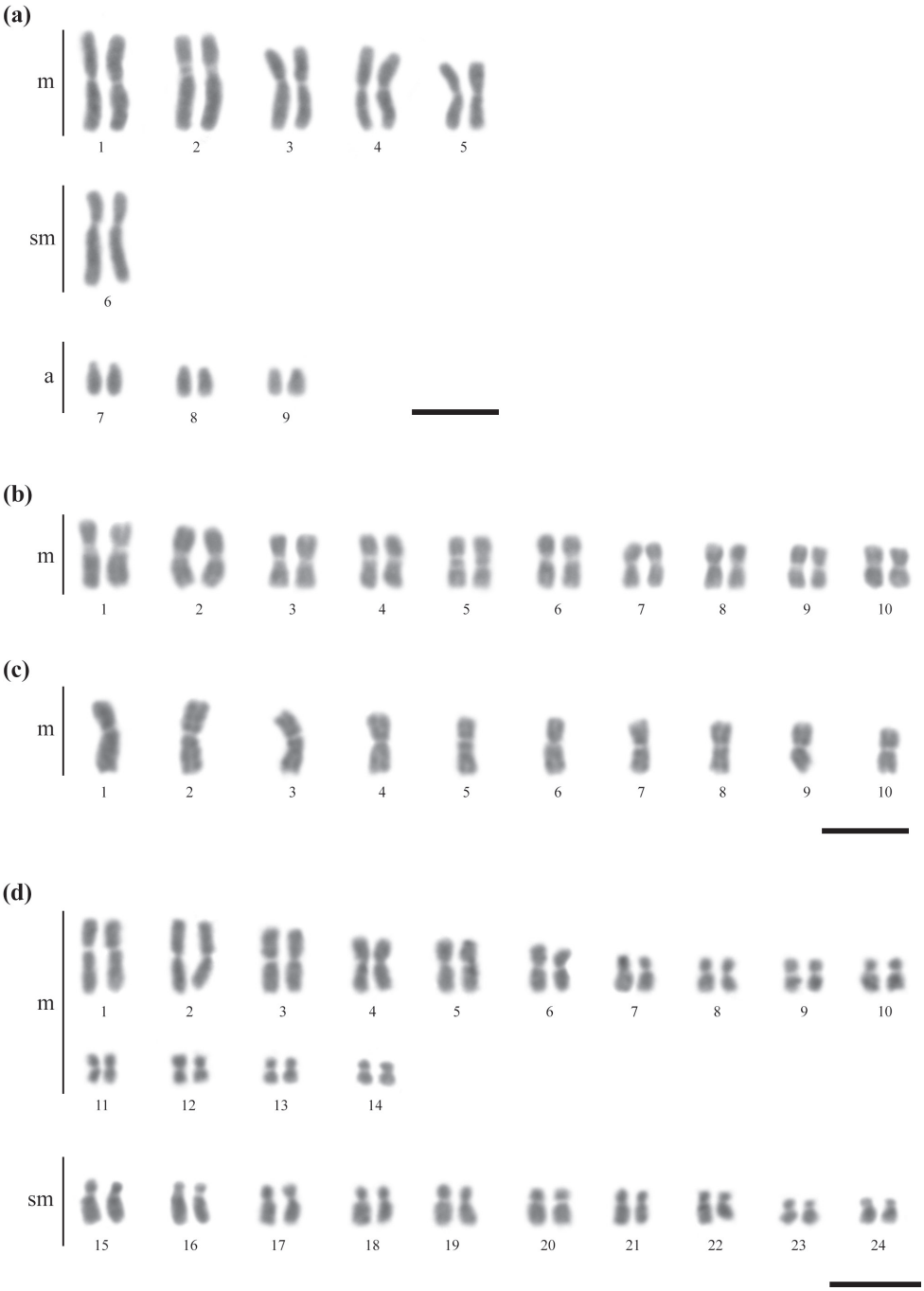

Figure 1. Karyotypes of fungus-farming ants **a** *Cyphomyrmex transversus* (2n = 18, 10m + 2sm + 6a) **b, c** *Mycetomoellerius relictus* (2n = 20, 20m and n = 10, 10m), and **d** *Sericomyrmex maravalhas* (2n = 48, 28m + 20sm). Scale bars: 5 μm.

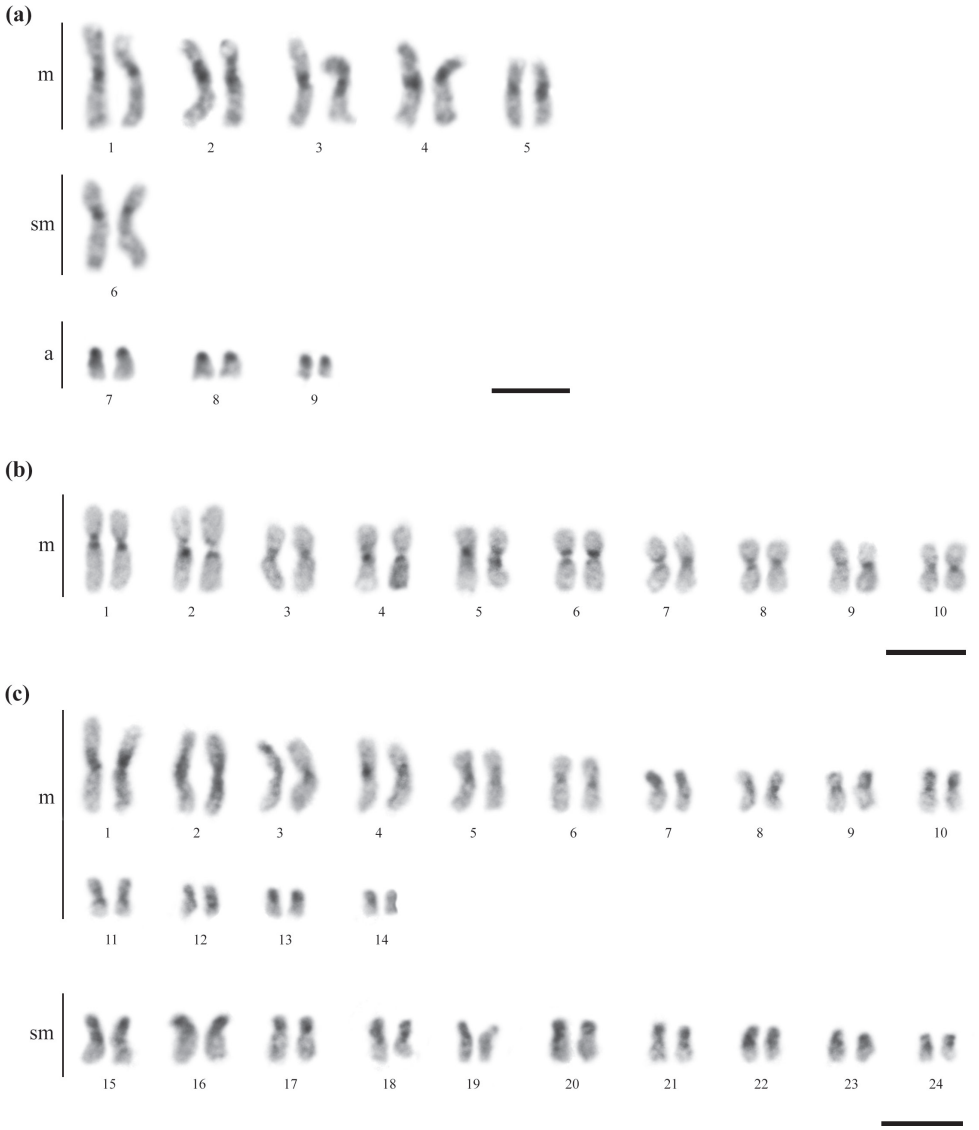

Figure 2. Heterochromatic patterns after C-banding technique in the karyotypes of the studied fungus-farming ants **a** *Cyphomyrmex transversus* (2n = 18) **b** *Mycetomoellerius relictus* (2n = 20), and **c** *Sericomyrmex maravalhas* (2n = 48). Dark blocks indicate heterochromatin in the centromeric/pericentromeric regions and short arms of the chromosomes. Scale bars: 5 μm.

suggest an increase in chromosome number from 2n = 48 to 2n = 50. Additionally, the heterochromatic pattern on the short arms of the submetacentric/metacentric chromosomes of *S. maravalhas* is a strong indicator of centric fission events during the karyotype evolution in *Sericomyrmex*. The absence of subtelocentric/acrocentric chromosomes in the karyotype of *S. maravalhas*, which has also been observed in *S. amabilis*

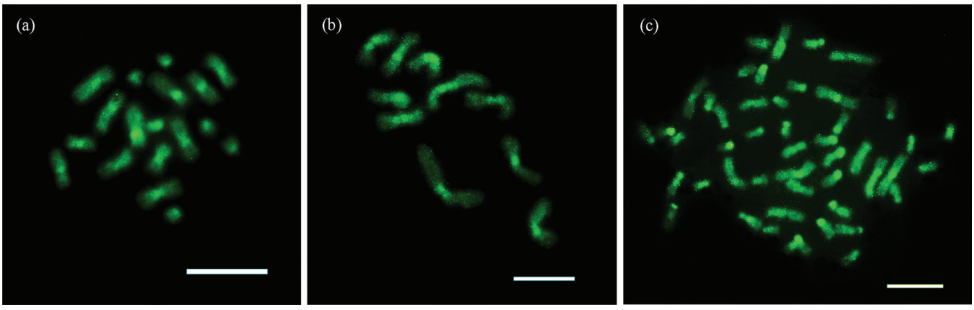

Figure 3. GC-rich chromatin patterns using Chromomycin A_3 fluorochrome on metaphases of the studied fungus-farming ants **a** *Cyphomyrmex transversus* (2n = 18) **b** *Mycetomoellerius relictus* (n = 10), and **c** *Sericomyrmex maravalhas* (2n = 48). The GC-rich bands in the centromeric/pericentromeric regions and short arms of the chromosomes are colocalized with heterochromatic blocks. Scale bars: 5 μm.

and *Sericomyrmex* sp. (Murakami et al. 1998; Barros et al. 2013b), can be associated with tandem growth of heterochromatin for telomeric stability after fission, which should have changed the chromosome's morphology from acrocentric to submetacentric/metacentric. These events of heterochromatin growth may have contributed to differences in chromosomal morphology observed in *S. maravalhas* in relation to *Sericomyrmex* sp. and *S. amabilis*. A similar mechanism has also been suggested to explain interspecific chromosomal variations in leaf-cutting ants *Acromyrmex* (Barros et al. 2016) and trap-jaw ants *Odontomachus* (Aguiar et al. 2020).

The molecular phylogeny of *Mycetomoellerius*, proposed by Solomon et al. (2019), showed two main clades. One clade includes *M. urichii* with 2n = 18 chromosomes (Barros et al. 2013a), *Mycetomoellerius holmgreni* (Wheeler, 1925), and *M. iheringi*, both of which have 2n = 20 chromosomes (Barros et al. 2018; Cardoso et al. 2018; Micolino et al. 2020; Table 2). *Mycetomoellerius relictus* belongs to the other clade and has 2n = 20 chromosomes (present study; Barros et al. 2013b). *Mycetomoellerius* sp. (as *Trachymyrmex* sp.) from the Atlantic rainforest has 2n = 22 (Barros et al. 2013b). Therefore, an ancestor of *Mycetomoellerius* with the chromosome number between 2n = 18–22 and with a predominance of metacentric chromosomes seems likely.

The cytogenetic data obtained in this study for *C. transversus* (2n = 18) showed the lowest chromosome number for this genus. This karyotype is different from the other two previously studied karyotypes in French Guiana (2n = 24) and Brazil (2n = 42) (Mariano et al. 2019; Aguiar et al. 2020; Table 2). The chromosomal morphology also differs among the three karyotypes of *C. transversus*, with a notable increase in the number of acrocentric pairs in the karyotype from São Paulo-Brazil, which has a higher chromosome number. These data suggest that *C. transversus* may be a species complex and, therefore, cytogenetic data highlight the need for taxonomic revision of this species. Based on cytogenetic studies available for *Cyphomyrmex*, Mariano et al. (2019) suggested that centric fissions play a major role in the karyotype evolution within this genus due to an increase in acrocentric chromosome pairs in species with high chromosome numbers. Further molecular phylogenetic studies associated with

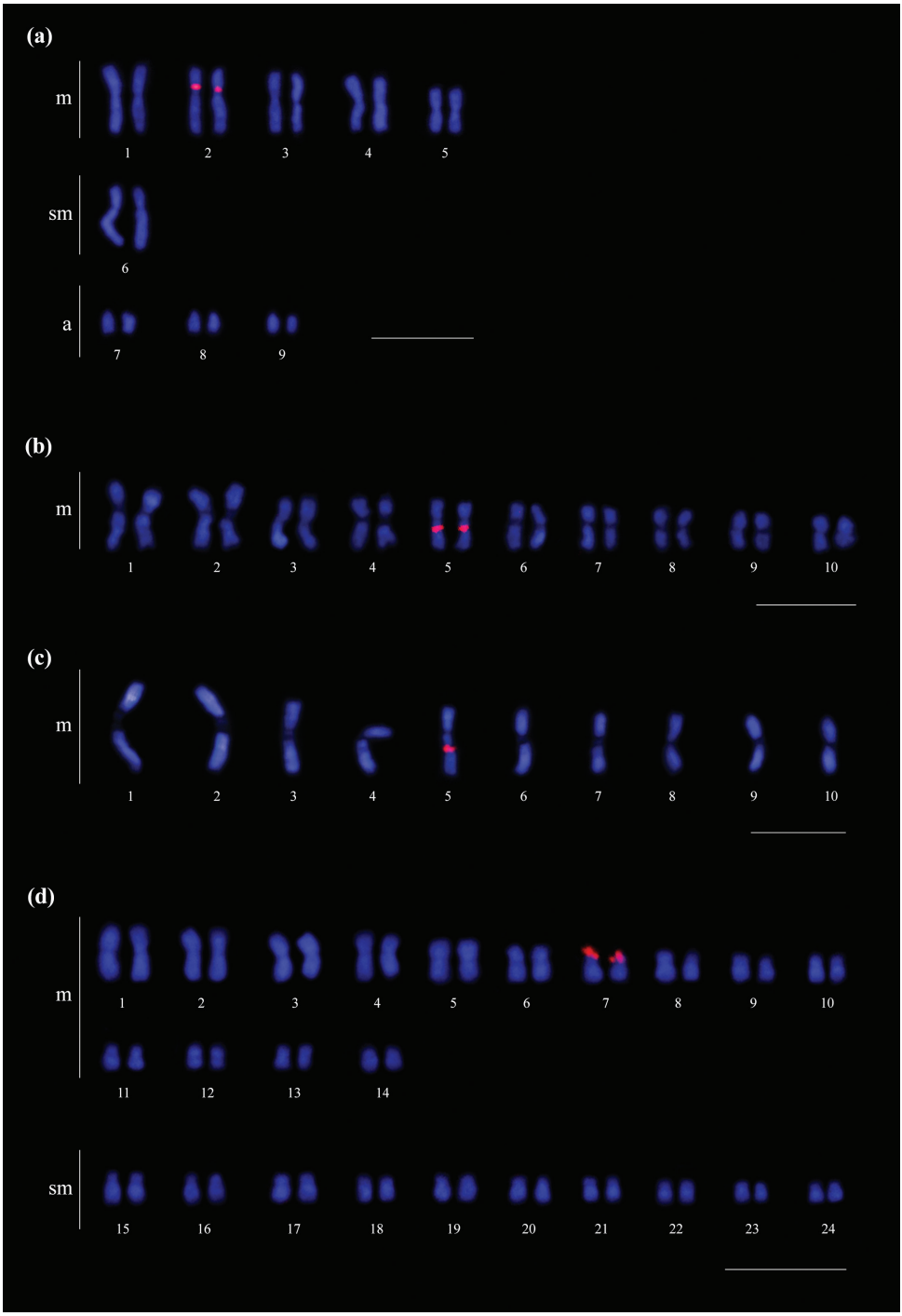

Figure 4. 18S rDNA clusters (red blocks) location on the karyotypes of the studied fungus-farming ants **a** *Cyphomyrmex transversus* (2n = 18) **b, c** *Mycetomoellerius relictus* (2n = 20, n = 10), and **d** *Sericomyrmex maravalhas* (2n = 48). Scale bars: 5 μm.

Table 2. Summary of available cytogenetic data in the literature and this study for the genera of fungus-farming ants *Cyphomyrmex*, *Sericomyrmex*, and *Mycetomoellerius*. Species, localities, chromosome numbers: diploid (2n)/haploid (n), diploid karyotype formulae, and references. The terminology used for karyotype formulae is in accordance to the published data.

Species	Localities	2n/(n)	Karyotype formulae	References
Cyphomyrmex				
C. costatus	Panama	20	20M	Murakami et al. (1998)
C. cornutus	French Guiana	22	10M + 12SM	Mariano et al. (2011)
C. rimosus	Panama	32	28M + 4A	Murakami et al. (1998)
C. transversus	French Guiana	24/(12)	14m + 6sm + 4a	Aguiar et al. (2020)
C. transversus	SP - Brazil	42	42A	Mariano et al. (2019)
C. transversus	MG - Brazil	18	10m + 2sm + 6a	**Present study**
Cyphomyrmex sp. §	MG - Brazil	32	14M + 18A	Mariano et al. (2019)
Sericomyrmex				
S. amabilis	Panama	50	50M	Murakami et al. (1998)
S. maravalhas	MG - Brazil	48	28m + 20sm	**Present study**
Sericomyrmex sp.	MG - Brazil	50/(25)	44m + 6sm	Barros et al. (2013b)
Mycetomoellerius				
*M. urichii**	MG - Brazil	18	16m + 2sm	Barros et al. (2013a)
M. holmgreni	MG - Brazil	20	20m	Barros et al. (2018) / Cardoso et al. (2018)
M. iheringi	SC - Brazil	20	18M + 2SM	Micolino et al. (2020)
M. relictus	MG - Brazil	20/(10)	20m	Barros et al. (2013b) / **Present study**
Mycetomoellerius sp.†	MG - Brazil	22	18m + 4sm	Barros et al. (2013b)

* As *Trachymyrmex fuscus* in Barros et al. (2013a); † According to new revision by Solomon et al. (2019); § *Cyphomyrmex* sp. group *rimosus*. MG: Minas Gerais State; SP: São Paulo State; SC: Santa Catarina State.

cytogenetic data will help in the discussion of the karyotype evolution of this genus and the taxonomy of *C. transversus*.

Regarding heterochromatin constitution, the three species of the present study showed GC-rich heterochromatin, as evidenced by the colocalization of the heterochromatic and CMA_3^+ bands. These data were first reported in *Sericomyrmex* and *Cyphomyrmex*. Other fungus-farming ants showed the same heterochromatic composition such as *M. goeldii* (Paleoattina) (Barros et al. 2010), *M. urichii* (Barros et al. 2013a), and *M. holmgreni* (Barros et. al. 2018), included in Neoattina. This pattern is not common in ants, with few examples in the *Dolichoderus* genus, which belongs to another subfamily (Santos et al. 2016). Barros et al. (2018) suggested that GC-rich heterochromatin observed in different species of Attina, with representatives in Paleoattina and Neoattina, may have a common origin within the subtribe. The heterochromatic pattern rich in GC observed in this study supports this hypothesis, increasing the number of genera with this characteristic. Further investigation of the chromatin composition of these species should corroborate this hypothesis.

The physical mapping of rDNA genes showed a single chromosome pair bearing these genes for the three species in this study. This pattern is similar to that observed for other fungus-farming ants, which is suggested to be a plesiomorphic characteristic in Formicidae (reviewed by Teixeira et al. 2021), and aculeate Hymenoptera as well (Menezes et al. 2021). Regarding the location of these rDNA genes on the chromosomes in Attina, most species presented these genes in the intrachromosomal region (pericentromeric or interstitial). This characteristic is observed in ancient species such

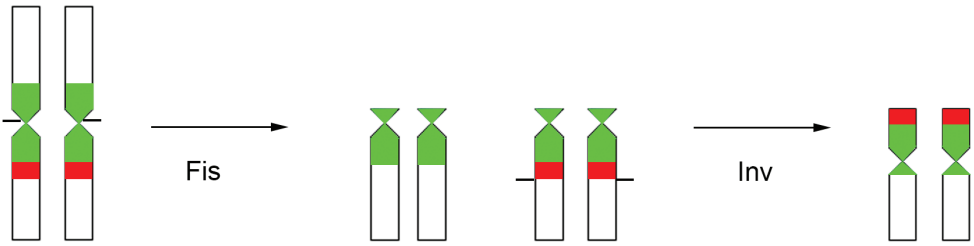

Figure 5. Diagram of origin of terminal rDNA clusters in metacentric chromosome from *Sericomyrmex maravalhas*, considering its ancestor with intrachromosomal rDNA clusters. Black bars: chromosomal breaks; Fis: centric fission; Inv: pericentric inversion; Green blocks: GC-rich regions; Red blocks: 18S ribosomal clusters.

as *M. goeldii*, *Myrmicocrypta* sp., *Mycetophylax* spp., and *C. tranversus*, in the transition species *M. holmgreni* and *M. relictus*, and leaf-cutting ants, most derived from the group, *Am. striatus* and *Atta* spp. (reviewed by Teixeira et al. 2021; this study). These data suggest that the intrachromosomal position of rDNA genes seems to be a plesiomorphic character in fungus-farming ants.

However, in *S. maravalhas*, the rDNA clusters were mapped in the terminal region of the heterochromatic short arm of the 7th metacentric pair (see Figs 2c, 4c). Considering an ancestor with a low chromosome number and intrachromosomal rDNA clusters, after centric fission events, the occurrence of pericentric inversion would change the pericentromeric rDNA genes to the terminal positions, as observed in *S. maravalhas* (Fig. 5). In some other fungus-farming ants, rDNA genes are also located in the terminal region, such as *Acromyrmex* spp. (Barros et al. 2016; Teixeira et al. 2017), *Mycetophylax conformis* (Mayr, 1884), and *M. morschi* (Emery, 1888) (2n = 30) (Micolino et al. 2019a), which are species with derived karyotypes within their respective phylogenetic branches. In the case of *M. conformis*, the terminal rDNA cluster located on the metacentric chromosome (Micolino et al. 2019a) seems to represent a derived pattern, explained by a single paracentric inversion, considering its ancestor with intrachromosomal rDNA clusters. The rDNA terminal location in *Acromyrmex* seems to be a derived condition among leaf-cutting ants (Barros et al. 2021).

In addition, a difference in the location of rDNA clusters was observed between *M. relictus* in this study and *M. holmgreni* (Barros et al. 2018; Micolino et al. 2019b). The former showed 18S rDNA clusters located in the interstitial region of the 5th metacentric pair while the latter presented these genes in the pericentromeric region of the 4th metacentric pair (Barros et al. 2018; Micolino et al. 2019b). This difference may reflect the phylogenetic position of these species, as they are included in distinct branches of *Mycetomoellerius*, in which *M. holmgreni* has a basal position to *M. relictus* (Solomon et al. 2019). However, the size variation between the 4th and 5th metacentric pairs was very subtle in *M. relictus* (see Fig. 4b, c). This suggests homeology of the chromosome pair carrying rDNA clusters between *M. relictus* and *M. holmgreni*. Therefore, the difference in the location of ribosomal genes between *M. relictus* and *M. homlgreni* may be

the result of paracentric inversion. In addition, the occurrence of a paracentric inversion involving rDNA genes has already been observed in leaf-cutting ant *A. echinatior* (Teixeira et al. 2021). Thus, inversions seem to be important rearrangements that generate changes in the position of rDNA genes in the karyotype of fungus-farming ants.

Conclusions

In this study, the distribution of 18S ribosomal genes and GC-rich heterochromatin in *Sericomyrmex* and *Cyphomyrmex*, which were reported for the first time, suggest the origin of this heterochromatin in the common ancestor of Attina. The karyotype observed in *C. tranversus* shows the lowest chromosomal number for the genus, and chromosomal variability among populations of the species highlights the need for taxonomic revision of this species using an integrative approach. Although *Sericomyrmex* spp. are morphologically complex (Ješovnik and Schultz 2017), karyotype differences were observed in this study, highlighting cytogenetics as an important tool for integrative taxonomy. Cytogenetic data obtained for *S. maravalhas* suggested centric fission events during chromosomal evolution in *Sericomyrmex*. Inversions seem to be involved in the origin of location of 18S ribosomal genes in *M. relictus* and *S. maravalhas*. Therefore, this study provides new insights into chromosomal evolution in *Sericomyrmex*, *Cyphomyrmex*, and *Mycetomoellerius*. Our data suggest that chromosomal rearrangements have contributed to the species diversification in Attina. We also believe that the increase in the number of species studied using classical and molecular cytogenetic techniques will continue to contribute to discussions about the evolution of fungus-farming ants.

Acknowledgements

We are grateful to Dr. Jacques H. C. Delabie for species identification. GAT thanks the Coordenação de Aperfeiçoamento de Pessoal de Nível Superior (CAPES) for the scholarship granted. This study was supported by Programa de Auxílio ao Pesquisador PAPESQ/UNIFAP.

References

Aguiar HJAC, Barros LAC, Alves DR, Mariano CSF, Delabie JHC, Pompolo SG (2017) Cytogenetic studies on populations of *Camponotus rufipes* (Fabricius, 1775) and *Camponotus renggeri* Emery, 1894 (Formicidae: Formicinae). PLoS ONE 12(5): e0177702. https://doi.org/10.1371/journal.pone.0177702

Aguiar HJAC, Barros LAC, Silveira LI, Petitclerc F, Etienne S, Orivel J (2020) Cytogenetic data for sixteen ant species from North-eastern Amazonia with phylogenetic insights into three

subfamilies. Comparative Cytogenetics 14(1): 43–60. https://doi.org/10.3897/CompCytogen.v14i1.46692

Barros LAC, Aguiar HJAC, Mariano CSF, Delabie JHC, Pompolo SG (2010) Cytogenetic characterization of the lower-Attine *Mycocepurus goeldii* (Formicidae: Myrmicinae: Attini). Sociobiology 56: 57–66.

Barros LAC, Aguiar HJAC, Mariano CSF, Delabie JHC, Pompolo SG (2013a) Cytogenetic characterization of the ant *Trachymyrmex fuscus* Emery, 1934 (Formicidae: Myrmicinae: Attini) with the description of a chromosomal polymorphism. Annales de la Société Entomologique de France 49: 367–373. https://doi.org/10.1080/00379271.2013.856201

Barros LAC, Mariano CSF, Pompolo SG (2013b) Cytogenetic studies of five taxa of the tribe Attini (Formicidae: Myrmicinae). Caryologia: International Journal of Cytology, Cytosystematics and Cytogenetics 66(1): 59–64. https://doi.org/10.1080/00087114.2013.780443

Barros LAC, Aguiar HJAC, Mariano CSF, Andrade-Souza V, Costa MA, Delabie JHC, Pompolo SG (2016) Cytogenetic data on six leafcutter ants of the genus *Acromyrmex* Mayr, 1865 (Hymenoptera, Formicidae, Myrmicinae): insights into chromosome evolution and taxonomic implications. Comparative Cytogenetics 10: 229–243. https://doi.org/10.3897/CompCytogen.v10i2.7612

Barros LAC, Teixeira GA, Aguiar HJAC, Lopes DM, Pompolo SG (2018) Cytogenetic studies in *Trachymyrmex holmgreni* Wheeler, 1925 (Formicidae: Myrmicinae) by conventional and molecular methods. Sociobiology 65(2): 185–190. https://doi.org/10.13102/sociobiology.v65i2.2214

Barros LAC, Aguiar HJAC, Teixeira GA, Souza DJ, Delabie JHC, Mariano CSF (2021) Cytogenetic studies on the social parasite *Acromyrmex ameliae* (Formicidae: Myrmicinae: Attini) and its hosts reveal chromosome fusion in *Acromyrmex*. Zoologischer Anzeiger 293: 273–281. https://doi.org/10.1016/j.jcz.2021.06.012

Bolton B (2021) An online catalog of the ants of the world. http://antcat.org [Accessed 15 January 2021]

Cardoso DC, Heinze J, Moura MN, Cristiano MP (2018) Chromosomal variation among populations of a fungus-farming ant: implications for karyotype evolution and potential restriction to gene flow. BMC Evolutionary Biology 18(1): 1–10. https://doi.org/10.1186/s12862-018-1247-5

Cristiano MP, Cardoso DC, Sandoval-Gómez VE, Simões-Gomes FC (2020) *Amoimyrmex* Cristiano, Cardoso & Sandoval, gen. nov. (Hymenoptera: Formicidae): a new genus of leaf-cutting ants revealed by multilocus molecular phylogenetic and morphological analyses. Austral Entomology 59(4): 643–676. https://doi.org/10.1111/aen.12493

Faria R, Navarro A (2010) Chromosomal speciation revisited: rearranging theory with pieces of evidence. Trends in Ecology & Evolution 25(11): 660–669. https://doi.org/10.1016/j.tree.2010.07.008

Fernandez-Bou AS, Dierick D, Swanson AC, Allen MF, Alvarado AGF, Artavia-León A, Carrasquillo-Quintana O, Lachman DA, Oberbauer S, Pinto-Tomás AA, Rodríguez-Reyes Y, Rundel P, Schwendenmann L, Zelikova TJ, Harmon TC (2019) The role of the ecosystem engineer, the leaf-cutter ant *Atta cephalotes*, on soil CO_2 dynamics in a wet tropical

rainforest. Journal of Geophysical Research: Biogeosciences 124(2): 260–273. https://doi.org/10.1029/2018JG004723

Imai H, Taylor RW, Crosland MW, Crozier RH (1988) Modes of spontaneous chromossomal mutation and karyotype evolution in ants with reference to the minimum interaction hypothesis. Japanese Journal of Genetics 63: 159–185. https://doi.org/10.1266/jjg.63.159

Imai HT, Taylor RW, Crozier RH (1994) Experimental bases for the minimum interaction theory. Chromosome evolution in ants of the *Myrmecia pilosula* species complex (Hymenoptera: Formicidae: Myrmeciinae). Japanese Journal of Genetics 69: 137–182. https://doi.org/10.1266/jjg.69.137

Ješovnik A, Schultz TR (2017) Revision of the fungus-farming ant genus *Sericomyrmex* Mayr (Hymenoptera, Formicidae, Myrmicinae). Zootaxa 670: 1–109. https://doi.org/10.3897/zookeys.670.11839

Ješovnik A, Sosa-Calvo J, Lloyd MW, Branstetter MG, Fernández F, Schultz TR (2017) Phylogenomic species delimitation and host-symbiont coevolution in the fungus-farming ant genus *Sericomyrmex* Mayr (Hymenoptera: Formicidae): ultraconserved elements (UCEs) resolve a recente radiation. Systematic Entomology 42: 523–542. https://doi.org/10.1111/syen.12228

Leal IR, Oliveira PS (1998) Interactions between fungus-growing ants (Attini), fruits, and seeds in cerrado vegetation in southeast Brazil. Biotropica 30: 170–178. https://doi.org/10.1111/j.1744-7429.1998.tb00052.x

Levan A, Fredga K, Sandberg A (1964) Nomenclature for centromeric position on chromosomes. Hereditas 52: 201–220. https://doi.org/10.1111/j.1601-5223.1964.tb01953.x

Little AEF, Murakami T, Mueller UG, Currie CR (2005) Defending against parasites: fungus-growing ants combine specialized behaviours and microbial symbionts to protect their fungus gardens. Biology Letters 2(1): 12–16. https://doi.org/10.1098/rsbl.2005.0371

Mariano CSF, Santos IS, Groc S, Leroy C, Malé PJ, Ruin-González MX, Cerdan P, Dejean A, Delabie JHC (2011) The karyotypes of *Gigantiops destructor* (Fabricius) and other ants from French Guiana (Formicidae). Annales de la Société Entomologique de France 47(1–2): 140–146. https://doi.org/10.1080/00379271.2011.10697705

Mariano CSF, Pompolo SG, Silva JG, Delabie JHC (2012) Contribution of cytogenetics to the debate on the paraphyly of *Pachycondyla* spp. (Hymenoptera, Formicidae, Ponerinae). Psyche: A Journal of Entomology 2012: 1–9. https://doi.org/10.1155/2012/973897

Mariano CSF, Barros LAC, Velasco YM, Guimarães IN, Pompolo SG, Delabie JHC (2019) Citogenética de hormigas de la región neotropical. In: Fernández F, Guerrero R, Delsinne T (Eds) Hormigas de Colombia. Universidad Nacional de Colombia, Bogotá, 131–157. [In Spanish]

Mehdiabadi NJ, Schultz TR (2010) Natural history and phylogeny of the fungus-farming ants (Hymenoptera: Formicidae: Myrmicinae: Attini). Myrmecological News 13: 37–55.

Menezes RS, Cabral-de-Mello DC, Milani D, Bardella VB, Almeida EA (2021) The relevance of chromosome fissions for major ribosomal DNA dispersion in hymenopteran insects. Journal of Evolutionary Biology 34(9): 1466–1476. https://doi.org/10.1111/jeb.13909

Micolino R, Cristiano MP, Travenzoli NM, Lopes D, Cardoso DC (2019a) Chromosomal dynamics in space and time: evolutionary history of *Mycetophylax* ants across past

climatic changes in the Brazilian Atlantic coast. Scientific Reports 9(1): 1–13. https://doi.org/10.1038/s41598-019-55135-5

Micolino R, Cristiano MP, Cardoso DC (2019b) Population-based cytogenetic banding analysis and phylogenetic relationships of the neotropical fungus-farming ant *Trachymyrmex holmgreni* Wheeler, 1925. Cytogenetic and Genome Research 159(3): 151–161. https://doi.org/10.1159/000503913

Micolino R, Cristiano MP, Cardoso DC (2020) Karyotype and putative chromosomal inversion suggested by integration of cytogenetic and molecular data of the fungus-farming ant *Mycetomoellerius iheringi* Emery, 1888. Comparative Cytogenetics 14(2): 197–210. https://doi.org/10.3897/CompCytogen.v14i2.49846

Murakami T, Fujiwara A, Yoshida MC (1998) Cytogenetics of ten ant species of the tribe Attini (Hymenoptera, Formicidae) in Barro Colorado Island, Panama. Chromosome Science 2: 135–139.

Nygaard S, Hu H, Li C, Schiøtt M, Chen Z, Yang Z, Xie Q, Ma C, Deng Y, Dikow RB, Rabeling C, Nash DR, Wcislo WT, Brady SG, Schultz TR, Zhang G, Boomsma JJ (2016) Reciprocal genomic evolution in the ant–fungus agricultural symbiosis. Nature Communications 7(1): 1–9. https://doi.org/10.1038/ncomms12233

Pereira JOP (2006) Diversidade genética da abelha sem ferrão *Melipona quinquefasciata* baseada no sequenciamento das regiões ITS1 parcial e 18S do DNA ribossômico nuclear. Thesis, Universidade Federal do Ceará, Fortaleza, Brazil, 141 pp. [In Portuguese]

Pinkel D, Straume T, Gray JW (1986) Cytogenetic analysis using quantitative, high-sensitivity, fluorescence hybridization. Proceedings of the National Academy of Sciences of the United States of America 83: 2934–2938. https://doi.org/10.1073/pnas.83.9.2934

Riesemberg LH (2001) Chromosomal rearrangements and speciation. Trends in Ecology & Evolution 7(1): 351–358. https://doi.org/10.1016/S0169-5347(01)02187-5

Santos IS, Mariano CSF, Delabie JHC, Costa MA, Carvalho AF, Silva JG (2016) "Much more than a neck": karyotype differentiation between *Dolichoderus attelaboides* (Fabricius, 1775) and *Dolichoderus decollatus* F. Smith, 1858 (Hymenoptera: Formicidae) and karyotypic diversity of five other Neotropical species of *Dolichoderus* Lund, 1831. Myrmecological News 23: 61–69.

Schultz TR, Brady SG (2008) Major evolutionary transitions in ant agriculture. Proceedings of the National Academy of Sciences of the United States of America 105: 5435–5440. https://doi.org/10.1073/pnas.0711024105

Schweizer D (1980) Simultaneous fluorescent staining of R bands and specific heterocromatic regions (DA/DAPI-bands) in human chromosomes. Cytogenetics and Cell Genetics 27: 190–193. https://doi.org/10.1159/000131482

Solomon SE, Rabeling C, Sosa-Calvo J, Lopes CT, Rodrigues A, Vasconcelos HL, Bacci Jr M, Mueller UG, Schultz TR (2019) The molecular phylogenetics of *Trachymyrmex* Forel ants and their fungal cultivars provide insights into the origin and coevolutionary history of 'higher-attine' ant agriculture. Systematic Entomology 44(4): 939–956. https://doi.org/10.1111/syen.12370

Sosa-Calvo J, Ješovnik A, Vasconcelos HL, Bacci Jr M, Schultz TR (2017) Rediscovery of the enigmatic fungus-farming ant "*Mycetosoritis*" *asper* Mayr (Hymenoptera: Formicidae):

implications for taxonomy, phylogeny, and the evolution of agriculture in ants. PLoS ONE 12: e0176498. https://doi.org/10.1371/journal.pone.0176498

Sosa-Calvo J, Schultz TR, Ješovnik A, Dahan RA, Rabeling C (2018) Evolution, systematics, and natural history of a new genus of cryptobiotic fungus-growing ants. Systematic Entomology 43: 549–567. https://doi.org/10.1111/syen.12289

Sumner AT (1972) A simple technique for demonstrating centromeric heterochromatin. Experimental Cell Research 83: 304–306. https://doi.org/10.1016/0014-4827(72)90558-7

Teixeira GA, Barros LAC, Aguiar HJAC, Pompolo SG (2017) Comparative physical mapping of 18S rDNA in the karyotypes of six leafcutter ant species of the genera *Atta* and *Acromyrmex* (Formicidae: Myrmicinae). Genetica 145: 351–357. https://doi.org/10.1007/s10709-017-9970-1

Teixeira GA, Aguiar HJAC, Peticlerc F, Jerome O, Lopes DM, Barros LAC (2021) Evolutionary insights into the genomic organization of major ribosomal DNA in ant chromosomes. Insect Molecular Biology 30(3): 340–354. https://doi.org/10.1111/imb.12699

Ward PS, Brady SG, Fisher BL, Schultz TR (2015) The evolution of Myrmicinae ants: phylogeny and biogeography of a hyperdiverse ant clade (Hymenoptera: Formicidae). Systematic Entomology 40: 61–81. https://doi.org/10.1111/syen.12090

Weber NA (1966) Fungus-Growing Ants. Science 153: 587–604. https://doi.org/10.1126/science.153.3736.587

ORCID

Gisele Amaro Teixeira https://orcid.org/0000-0002-7106-5798
Luísa Antônia Campos Barros https://orcid.org/0000-0002-1501-4734
Hilton Jeferson Alves Cardoso de Aguiar https://orcid.org/0000-0001-7738-1460
Denilce Meneses Lopes https://orcid.org/0000-0001-7209-4411

CompCytogen 15(4): 429–445 (2021)
doi: 10.3897/compcytogen.v15.i4.69638
https://compcytogen.pensoft.net

RESEARCH ARTICLE

COMPARATIVE Cytogenetics
A peer-reviewed open-access journal
International Journal of Plant & Animal Cytogenetics, Karyosystematics, and Molecular Systematics

Comparative cytogenetic patterns in Carangidae fishes in association with their distribution range

Rodrigo Xavier Soares[1], Clóvis Coutinho da Motta-Neto[1], Gideão Wagner Werneck Félix da Costa[1], Marcelo de Bello Cioffi[2], Luiz Antônio Carlos Bertollo[2], Amanda Torres Borges[1], Wagner Franco Molina[1]

1 *Departament of Cell Biology and Genetics, Biosciences Center, Universidade Federal do Rio Grande do Norte, Natal, RN, 59078970, Brazil* **2** *Fish Cytogenetics Laboratory, Departament of Genetics and Evolution, Universidade Federal de São Carlos, São Carlos, SP, C.P. 676, Brazil*

Corresponding author: Wagner Franco Molina (molinawf@yahoo.com.br)

Academic editor: Petr Rab | Received 2 June 2021 | Accepted 11 October 2021 | Published 1 December 2021

http://zoobank.org/A5857084-62D9-4DCE-8F97-1412F6986C79

Citation: Soares RX, da Motta-Neto CC, da Costa GWWF, de Bello Cioffi M, Bertollo LAC, Borges AT, Molina WF (2021) Comparative cytogenetic patterns in Carangidae fishes in association with their distribution range. CompCytogen 15(4): 429–445. https://doi.org/10.3897/compcytogen.v15.i4.69638

Abstract

Carangidae are an important and widespreaded family of pelagic predatory fishes that inhabit reef regions or open ocean areas, some species occupying a vast circumglobal distribution. Cytogenetic comparisons among representatives of its different tribes help to understand the process of karyotype divergence in marine ecosystems due to the variable migratory ability of species. In this sense, conventional cytogenetic investigations (Giemsa staining, Ag-NORs, and C-banding), GC base-specific fluorochrome staining and FISH mapping of ribosomal DNAs were performed. Four species, *Elagatis bipinnulata* (Quoy et Gaimard, 1825) and *Seriola rivoliana* (Valenciennes, 1883) (Naucratini), with circumtropical distributions, *Gnathanodon speciosus* (Forsskål, 1775) (Carangini), widely distributed in the tropical and subtropical waters of the Indian and Pacific oceans, and *Trachinotus carolinus* (Linnaeus, 1766) (Trachinotini), distributed along the western Atlantic Ocean, were analyzed, thus encompassing representatives of three out its four tribes. All species have diploid chromosome number 2n = 48, with karyotypes composed mainly by acrocentric chromosomes (NF = 50–56). The 18S rDNA/Ag-NORs/GC+ and 5S rDNA loci were located on chromosomes likely homeologs. Karyotypes showed a pattern considered basal for the family or with small variations in their structures, apparently due to pericentric inversions. The migratory capacity of large pelagic swimmers, in large distribution areas, likely restricts the fixation of chromosome changes in Carangidae responsible for a low level of karyotype diversification.

Keywords

Conservative karyotype, Fish cytogenetics, karyotype evolution, pelagic fishes

Introduction

The spatial distribution of biodiversity is related to the existing or past physical and environmental conditions. In this context, fishes provide good models for investigating the association between chromosome diversity and environmental characteristics of different regions and ecosystems (Molina et al. 2014). Some fish groups show a high congruence between their high biodiversity and patterns of karyotype diversifications (Bertollo et al. 2000). Among freshwater fishes, the species diversity is linked to an evident allopatric isolation scenarios leading to the fixation of chromosome rearrangements (Moreira-Filho and Bertollo 1991; Costa et al. 2019). In marine fishes, in addition to environmental physical barriers, the karyotype diversification is also associated with the limited dispersion or colonization capacity of the species (Molina and Galetti 2004; Molina et al. 2014), together with the effective size of the populations (Riginos et al. 2016; Motta-Neto et al. 2019).

The marine environment is both extensive and multidimensional due to its varied ecological patterns, thus providing complex evolutionary conditions that impacts the genetic structure of species (Rocha 2003). Egg types and length of the larval period are not the only biological factors predicting the geographic structure of the reef fish populations (Shulman and Bermingham 1995). Larval behavior and habitat availability are equally important ones for maintaining the population structure (Kohn and Clements 2011). In demersal species, for example, the association of biogeographic barriers physical factors such as currents, and the dispersion of eggs and larvae, can promote larval retention and the maintenance of genetically connected populations over long distances (Taylor and Hellberg 2003; Craig et al. 2007; Saenz-Agudelo et al. 2011). The maintenance of widely distributed populations is particularly more limited in reef species, as exemplified by the absence of circumglobal distribution in any Gobiidae species, the most species-rich marine group (Gaither et al. 2016). On the other hand, in groups with pelagic habits and vast oceanic distributions, genetic patterns are established by migrating adults, larval behavior, and dispersal under limits of physical or ecological barriers (Palumbi 1994).

The investigation of environmental effects on the genetic diversity of marine fish species depends on favorable spatial models, which have been used to identify causes and factors that promote their karyotype differentiation (Accioly et al. 2012; Molina et al. 2012; Amorim et al. 2017; Motta-Neto et al. 2019). Additionally, it is also advantageous to add an integrated view of contemporary ecological and environmental patterns associated with the historical biogeography of the groups (Molina 2007; Molina et al. 2014; Amorim et al. 2017).

A negative correlation was found when associating the dispersive potential of the pelagic larvae with the karyotype diversification in reef fish (Molina and Galetti 2004; Sena and Molina 2007). Although an increasing number of large pelagic species have recently been the target of more detailed cytogenetic analyses (Soares et al. 2013, 2014, 2017), studies on the dispersive potential and chromosome diversification have been neglected in pelagic fish. It is estimated that almost three hundred of marine fish species have a circumtropical distribution (Gaither et al. 2016), and, among them, the Carangidae family (Carangoidei, Carangiformes) stands out with several species reaching wide oceanic distributions (Froese and Pauly 2020).

Carangidae are pelagic fishes with high swimming capacity, composed of 31 genera and 150 presently recognized species (Nelson et al. 2016; Fricke et al. 2020), with very variable hydrodynamic body adaptations, ranging from slender to deep-bodied ones (Honebrink 2000). Their phylogenetic relationships based on morphological (Smith-Vaniz 1984) and molecular data (Damerau et al. 2017) point out four monophyletic tribes, namely Naucratinae, Scomberoidinae, Caranginae, and Trachinotinae. The ancient origin of this group and its radiation during the Cretaceous period offer extensive spatial scenarios (Honebrink 2000) for analyzing its genetic diversity (Santini and Carnevale 2015). Thus, cytogenetic analyses in groups with such a wide geographic distribution, provide favorable tools for understanding the role of biogeographic barriers and the dispersive potential on karyotype changes.

In view of the environmental complexity to which the marine fish groups are subjected, the investigation of their chromosome change patterns must consider wide taxonomic, biogeographic, and different biological models. In the context of the marine environment, cytogenetic analyses in groups with a wide geographic distribution, such as Carangidae, provide an understanding of the role of biogeographic barriers and the dispersive potential on karyotype changes. Therefore, we performed cytogenetic analyses using conventional and molecular protocols in *Elagatis bipinnulata* (Quoy et Gaimard, 1825) (Rainbow runner), *Seriola rivoliana* (Valenciennes, 1883) (Greater amberjack), *Gnathanodon speciosus* (Forsskål, 1775) (Golden trevally), and *Trachinotus carolinus* (Linnaeus, 1766) (Florida pompano), which have extensive geographical distribution. The patterns of their karyotype evolution were discussed in relation with the dispersive potential estimated by their geographic distribution.

Material and methods

Individuals and mitotic chromosome preparation

Cytogenetic analyses were performed on the species *Elagatis bipinnulata* (n = 15; 10 males; 5 females), and *Seriola rivoliana* (n = 4; 1 male; 3 females), both from off the São Pedro and São Paulo archipelago (00°56'N, 29°22'W) located in the Meso-Atlantic region; in *Gnathanodon speciosus* (n = 2; juveniles), from the Pacific and Indo-Pacific, obtained through ornamental fish traders, and *Trachinotus carolinus* (n = 10; 4 males; 6 females), from cultivated stock of the coast of Florida (USA). The samples were collected with the authorization of the Brazilian environmental agency ICMBio/ SISBIO (License #19135-4, #131360-1 and #27027-2).

The individuals were subjected to in vivo mitotic stimulation according to Molina et al. (2010). Chromosome preparations were obtained from short-term culture (Gold et al. 1990) using tissue suspensions from the anterior portion of the kidney. All the experiments followed ethical protocols and anesthesia conducted with clove oil prior the animals were sacrified. The process was approved by the Animal Ethics Committee of Federal University of Rio Grande do Norte (Protocol 44/15).

Standard cytogenetic procedures

The nucleolus organizing regions (**NORs**) and the chromosomal heterochromatin content were analyzed according to the C-banding and Ag-NOR methods, reported by Sumner (1972) and Howell and Black (1980), respectively. The CG rich sites were vizualized with the base-specific mithramycin (**MM**) fluorochrome and DAPI staining (Schweizer 1976).

Fluorescence in situ hybridization (FISH)

FISH was performed according to Pinkel et al. (1986). The 18S and 5S rDNA probes were obtained using PCR with DNA template from *Rachycentron canadum* (Linnaeus, 1766) (Euteleostei, Rachycentridae) and primer pairs NS1 5'-GTA GTC ATA TGC TTG TCT C-3' and NS8 5'-TCC GCA GGT TCA CCT ACG GA-3' (White et al., 1990) and A 5'-TAC GCC CGA TCT CGT CCG ATC-3' and B 5'-CAG GCT GGT ATG GCC GTA AGC-3' (Pendás et al. 1994), respectively. The probes were labeled by nick translation (Invitrogen, Thermo Fisher Scientific, Waltham, MA, USA) with digoxigenin-11-dUTP and biotin-14-dATP for the 18S rDNA, and 5S rDNA, respectively. Hybridization signals were detected using anti-digoxygenin-rhodamine (Roche, Mannheim, Alemanha) and streptavidin-FITC (Vector Laboratories, Burlingame, CA, USA), for the 18S and 5S rDNA probes, respectively, according to the manufacturer's specifications. The chromosomes were counterstained with Vectashield/DAPI (Vector Laboratories, Burlingame, CA, USA).

Cytogenetic analyses

At least 30 metaphase spreads per individual were analyzed to confirm the chromosome number, karyotype structure, and FISH results. Images were photographed using an Olympus BX51 epifluorescence microscope coupled to an Olympus DP73 digital image capture system (Olympus Corporation, Ishikawa, Japan) with the cellSens (Version 1.9 Digital, Tokyo, Kanto, Japan) software. Chromosomes were classified as metacentric (m), submetacentric (sm), subtelocentric (st), and acrocentric (a) according to their arm ratios (Levan et al. 1964). To count the chromosome arms (NF), the m, sm, and st chromosomes were considered with two arms and the acrocentric chromosomes (or if classified indistinctly as st/a) with only one arm.

Estimation of maximum linear geographic distribution and total area occupied by species

The maximum linear geographic distribution distance (MLD) and the occupied area by each species (OA) were obtained through the Ocean Biogeographic Information System (Obis 2020). The OBIS platform performs analyses using an online management software that accesses spatial distribution databases associated with the highest taxonomic levels, geographic area, time, and depth, providing a map of localities

related to environmental data. Based on the maps for each species, the corresponding files were loaded in the public domain software Image J (Rasband 2018), allowing us to measure the distribution areas and the linear distribution axis distances of each species and tribe, as presented in Table 1. To calculate the proportionality of the distances and distribution areas, the data for each species and each tribe were defined proportionally to the data of *Elagatis bipinnulata*, a species chosen as a representative parameter of the maximum circumglobal distribution for the family.

Statistical analysis

The descriptive statistical analysis (Table 1) and Spearman's rank correlation coefficient were calculated using the RStudio software. The Shapiro-Wilk test was used to normality afferition. These tests were conducted to determine the correlation between the number of chromosome arms (NF) and the measure of the species' geographic distribution, as indicated by the maximum axis of linear geographic distribution (MLD) and total area occupied (OA). The level of significance adopted was $p < 0.05$. The cytogenetic database for the Carangidae species was obtained from an exhaustive up-to-date online review. The cytogenetic data (2n, karyotype composition, NF) covered the studies published among the years 1974 and 2021, and was used in comparative intra- and inter-group analyses. The search was developed in representative research portals, encompassing Google Scholar (https://scholar.google.com.br/), SciELO (http://www.scielo.br/), Portal de Periodicos (http://www.periodicos.capes.gov.br/), Web of Science ResearchGate (http://www.researchgate.net), and included the extensive review by Arai (2011).

Results

Cytogenetic data

All species had 2n = 48, but with different karyotypes. While *E. bipinnulata* and *G. speciosus* shared karyotypes with 2st+46a (NF = 50), *S. rivoliana* has 2sm+2st+44a (NF = 52), and *T. carolinus* has 4m+4sm+40a (NF = 56). No evidence of the presence of differentiated sex chromosomes was found.

C-positive heterochromatic blocks were located mainly in the pericentromeric regions and in the terminal regions of some chromosome pairs to a lesser extent (Fig. 1). An unique Ag-NOR site, coincident with conspicuous heterochromatic and MM^{+}/$DAPI^{-}$ regions was found in the four species. In *E. bipinnulata* and *G. speciosus*, these regions were located in the end of the short arms of the large st pair No. 1. In *S. rivoliana* and *T. carolinus*, they were located in the same position, but in the similarly sized subtelocentric pair No. 2 in *S. rivoliana*, and in a large a element marked as pair No. 5 in *T. carolinus* (Fig. 1). In all species, the Ag-NOR sites corresponded to the positive 18S rDNA hybridization signals.

Table 1. Cytogenetic data from species of the family Carangidae and their maximum linear geographic distribution (MLD) and occupied area (OA) and ratio with the maximum distribution values defined for the family. Vertical bars represent the set of parameters available to the species.

Species	MLD Km × 10^4	% LGDmax	OA Km^2 × 10^4	% OAmax	2n	Karyotype	NF	Ref.
Naucratini								
Elagatis bipinnulata (Quoy et Gaimard, 1825)	3.80	100	977.05	100	48	2st+46a	50	1
Seriolina nigrofasciata (Rüppell, 1829)	1.34	40	213.16	30	48	48a	48	2
Seriola rivoliana Valenciennes, 1833	3.14	90	446.50	50	48	2sm+2st+44a	52	1
Seriola dumerili (Risso, 1810)	2.05	60	526.26	60	48	2sm+46a	50	3
					48	2sm+2st+44a	52	4
Seriola quinqueradiata Temminck et Schlegel, 1845	0.13	10	18.54	20	48	2sm+2st+44a	52	5
Seriola lalandi Valenciennes, 1833	1.43	40	454.94	50	48	2m+2sm+6st+38a	58	6
Average values	1.98	**60**	439.41	**50**			**51.7**	
Scomberoidini								
Scomberoides lysan (Forsskål, 1775)	2.15	60	523.60	60	48	4m/sm+44a	52	7
Oligoplites saliens (Bloch, 1793)	0.60	20	36.95	10	48	4m/sm+44st/a	52	8
Average values	1.37	**40**	280.28	**30**			**52**	
Carangini								
Alectis ciliaris (Bloch, 1787)	2.75	80	579.72	60	48	48a	48	9
Alepes djedaba (Forsskål, 1775)	1.33	40	161.50	20	56	56a	56	10
Alepes melanoptera (Swainson, 1839)	0.83	30	122.57	20	48	2sm+46a	50	10
Atropus atropos (Bloch et Schneider, 1801)	0.71	20	43.83	10	48	48a	48	7
Atule mate (Cuvier, 1833)	1.48	40	483.84	50	50	14sm+36a	64	11
Carangoides armatus (Rüppell, 1830)	0.99	30	197.62	30	48	2st+46a	50	7
Carangoides equula (Temminck et Schlegel, 1844)	1.48	40	221.06	30	48	2st+46a	50	9
Carangoides bartholomaei (Cuvier, 1833)	0.73	20	219.65	30	48	6sm+42a	54	12
Caranx praeustus Anonymous (Bennett), 1830	0.67	20	41.97	10	48	10m/sm+28a	58	7
Caranx latus Agassiz, 1831	1.14	40	212.55	30	48	2sm+46a	50	12
Caranx lugubris Poey, 1860	3.59	100	379.16	40	48	2sm+46a	50	13
Caranx ignobilis (Forsskål, 1775)	2.21	60	590.42	70	48	2sm+46a	50	14
Caranx sexfasciatus Quoy et Gaimard, 1825	2.48	70	875.01	90	48	2st+46a	50	9
Chloroscombrus chrysurus (Linnaeus, 1766)	1.33	40	422.56	50	48	48a	48	15
Gnathanodon speciosus (Forsskål, 1775)	2.47	70	615.10	70	48	2st+46a	50	1
Megalaspis cordyla (Linnaeus, 1758)	1.06	30	336.44	40	50	2st+48a	50	10
Selene setapinnis (Mitchill, 1815)	1.23	40	298.39	40	46	2sm+44a/2m+44a	48	16
Selene vomer (Linnaeus, 1758)	0.69	20	289.54	30	48	2st+46a	50	16
Selene brownii (Cuvier, 1816)	0.40	20	46.20	10	48	48a	48	16
Trachurus japonicus (Temminck et Schlegel, 1844)	0.23	10	40.34	10	48	4m+14sm+12st+18a	78	9
T. mediterraneus (Steindachner, 1868)	0.58	20	122.38	20	48	4m+6sm+38st/a	58	17
	0.69				48	4m+4sm+14st+26a	70	18
T. trachurus (Linnaeus, 1758)	1.32	20	423.31	50	48	2sm+46a	50	18
Average values	2.75	**40**	327.54	**40**			**53.4**	
Trachinotini								
Trachinotus goodei Jordan et Evermann, 1896	0.67	20	89.73	10	48	4m/sm+44a	52	19
T. carolinus (Linnaeus, 1766)	0.69	20	122.06	20	48	8m/sm+40a	56	19
	0.19	10	25.22	10	48	4m+4sm+40a	56	1
T. falcatus (Linnaeus, 1758)	1.30	40	265.56	30	48	10m/sm+38a	58	19
			125.64	20	48	2m+2st+44a	52	20
T. ovatus (Linnaeus, 1758)	0.67	20	89.73	10	48	2m+4sm+42st/a	54	10
Average values	0.69	**20**	122.06	**20**			**54.4**	

Notes: 1 – present study; 2 – Tripathy and Das (1988); 3 – Vitturi et al., (1986); 4 – Sola et al. (1997); 5 – Ida et al. (1978); 6 – Chai et al. (2009); 7 – Das et al. (1980); 8 – Castro-Leal et al. (1998); 9 – Murofushi and Yosida (1979); 10 – Choudhury et al. (1993); 11 – Lee and Loo (1975); 12 – Jacobina et al. (2014a); 13 – Jacobina et al. (2014b); 14 – Patro and Prasad (1979); 15 – Accioly et al. (2012); 16 – Jacobina et al. (2013); 17 – Vasiliev (1978); 18 – Caputo et al. (1996); 19 – Jacobina et al. (2012); 20 – Nirchio et al. 2014.

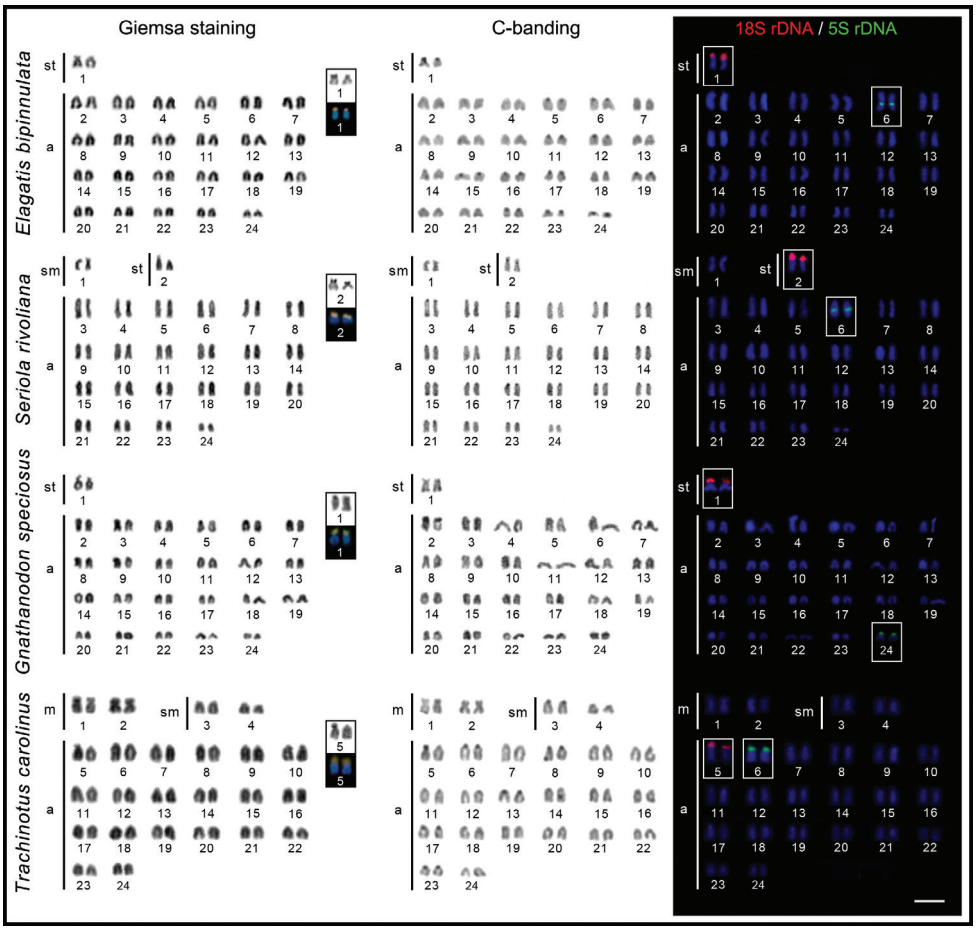

Figure 1. Karyotypes of *Elagatis bipinnulata*, *Seriola rivoliana*, *Gnathanodon speciosus*, and *Trachinotus carolinus* arranged after Giemsa staining (Ag-NORs and $MM^{+}/DAPI^{-}$ sites, highlighted), C- banding, and double-FISH with 18S rDNA (red) and 5S rDNA (green) probes. The chromosome pairs were tentatively numbered. Scale bar: 5 μm.

The 5S rDNA loci were also unique, but with an interstitial or terminal distribution in a pairs of similar size among the species, and non-syntenic with the 18S ones. In *E. bipinnulata* and *S. rivoliana*, they were interstitially located in the q arms of the pair labelled as No. 6; in the terminal region of the short arms of the pair labelled as No. 6 in *T. carolinus*, and in the pericentromeric region of the smallest chromosome pair No. 24 in *G. speciosus* (Fig. 1).

NF average and geographic distribution

The average number of the chromosome arms (NF average) showed an negative correlation with the averages of linear distances of distribution and areas occupied for each

tribe. In fact, the NF average showed be progressively divergent on the NF considered as basal for the family (NF = 50) in Naucratini (51.7), that encompass an average linear distribution distance equivalent to 60% of the greatest distance established for the family (LD), and 50% concerning the largest occupied area (LOA); Scomberoidini (52), with 40% (LD) and 30% (LOA), Carangini (53.4), with 40% (LD) and 40% (LOA) and Trachinotini (54.4), with 20% (LD) and 20% (LOA) (Table 1).

Statistical data

The average of the two distribution measures (MLD and OA) and NF values showed evidences on an statistically supported relationship between karyotype and geographic distribution, that encompass a synergic set of ecological, adaptive, and migratory characteristics. The variables MLD (p = 0.001), OA (p = 0.001), and NF (p < 3.097e-07) did not present a normal distribution (Shapiro-Wilk test). The analysis revealed a high correlation between the MLD and OA (Pearson's correlation r = 0.829, $p \leq 0.05$). The NF values showed a moderate negative Pearson's correlation coefficient with the MLD (r = -0.419, p = 0.0144) and modest negative correlation with OA (r = -0.876, p = 0.043).

Discussion

In contrast to other marine fish groups, Carangidae have a representative set of cytogenetic data (Table 1), now including new data for species of the genera *Elagatis* Bennett, 1840, *Seriola* Cuvier, 1816, *Gnathanodon* Bleeker, 1850, and *Trachinotus* Lacepède, 1801, reaching 22% of its species, encompassing all tribes. This repertoire shows remarkable conservation of the diploid number, with 2n = 48 occuring in 88% of the species. On the other hand, divergences exits in the karyotype compositions, with variation in chromosome arms (NF) from 48 to 78 (Table 1). Karyotypes with NF = 50 (composed by one pair of two-armed chromosomes – m, sm, or st) plus 46 acrocentric elements) are shared by 35% of the species and constitute the most widespread condition among Carangidae tribes (Chai et al. 2009; present data). However, this probable basal constitution for the family shows increasing evolutionary divergences among tribes mainly modeled by pericentric inversions (Sola et al. 1997; Rodrigues et al. 2007). Other chromosome rearragements, such as centric fissions and fusions, have a lesser extent on the karyotype differentiation. In fact, fissions are phylogenetically restricted and detected only in three Carangini species, leading to the increase from the basal 2n = 48 to 2n = 50 and 2n = 56 (Table 1). Likewise, Robertsonian fusions are also rare events, with a polymorphic pattern in *Seriola dumerili* (Risso, 1810) (2n = 48/47) (Vitturi et al. 1986) and a stable condition in *Selene setapinnis* (Mitchill, 1815) (2n = 46) (Jacobina et al. 2013).

Pericentric inversions are predominant changes in the order, but to a lesser extent in the syntenic composition of gene groups. If so, the chromosome conservation

evidenced among the four Carangidae genera could encompass a wide shared synteny among the species. Indeed, genetic maps of *Seriola* species evidenced a high collinearity among their linkage groups (Ohara et al. 2005), thus supporting this hypothesis. Additionally, comparison of carangid genome assemblies (Zhang et al. 2019), including *Trachinotus ovatus* (Linnaeus, 1758) (2m+4sm+42st/a; Choudhury et al. 1993), *Seriola quinqueradiata* Temminck et Schlegel, 1845 (2sm+2st+44a; Ida et al. 1978), *S. dumerili* (2sm+2st+44a; Sola et al. 1997), and *S. rivoliana* Valenciennes, 1833 (2sm+2st+44a; present data) revealed synteny with *T. ovatus* 24 linkage groups, indicating that fission and/or fusion events are unlikely during their karyotype evolution.

If pericentric inversions are the most common rearrangements in Carangidae, and if they are equally likely to occur in all tribes, a similar level of karyotype divergence among them would be expected. However, this does not occur, as seen by cytogenetic data covering representative species from most genera of each tribe (Table 1). Since tribes share a common origin, what factors would be linked with this differential fixation of chromosome rearrangements? Data show that, on average, species of the Naucratinae tribe has NF = 51.7, the closest one to that considered basal (NF = 50) for the family, followed by species from the Scomberoidini (NF = 52), Caranginae (NF = 53.4), and Trachinotini (NF = 54.4) tribes. Notably, the level of karyotype diversification of these groups was inversely proportional to their geographic distribution, thus suggesting that the dispersive potential and, consequently, the level of gene flow maintained by migrants) are agents driving the karyotype evolution in the group.

The geographic variables MLD and OA showed a high positive correlation with each other and both showed a negative correlation with the NF ($p \leq 0.05$). In fact, the data set revealed that the probability of chromosomal variations decreases as the geographical distribution of the species expands. Between the two distribution variables, MLD exhibited a more pronounced negative correlation with the NF. Although both parameters are negatively associated with chromosomal variation, they have different prediction intervals. The modest correlation between OA and NF, was statistically significant, and probably related to lower precision in the definition of the ecological areas occupied by the species. In contrast, MLD, despite being a simpler parameter, proved to be a more effective predictor of differences in the dispersive potential of migratory species.

Large pelagic fish populations, whose life histories include migratory behavior, planktonic larval stages, and broadcast spawning, maintain high levels of gene flow among vast oceanic areas (Pla and Pujolar 1999; Tripp-Valdez et al. 2010), thus finding fewer opportunities for fixing chromosome rearrangements and, essentially, maintaining a more conservative karyotype evolution (Molina 2007; Accioly et al. 2012; Soares et al. 2013; Molina et al. 2014; Motta-Neto et al. 2019). Having that in mind, the low rate of NF divergence in Naucratini is probably due to the wide distribution of some *Elagatis*, *Seriola*, and *Seriolina* Wakiya, 1924 species reaching circumglobal scales (Froese and Pauly 2020). In contrast, Carangini, the most diverse Carangidae tribe, shows the largest ranges in the diploid number and NF, from 46 to 56 and 48 to 78, respectively (Table 1). In this group, several species have a circumglobal distribution

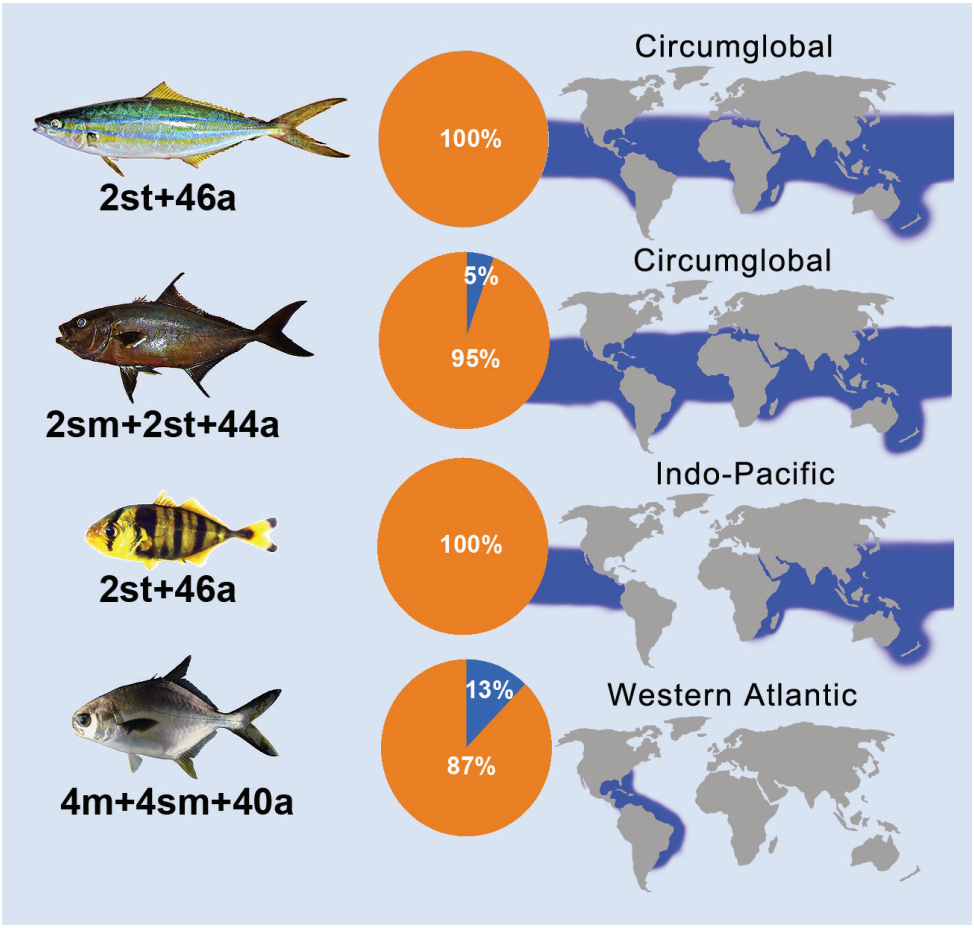

Figure 2. Karyotype index of chromosomal similarity (orange) and divergence (blue) regarding the probable basal karyotype for Carangidae studied species. Maps show the magnitude of the geographic distribution of *Elagatis bipinnulata*, *Seriola rivoliana*, *Gnathanodon speciosus*, and *Trachinotus carolinus* (top to bottom).

(e.g., *Gnathanodon speciosus* and *Caranx lugubris* Poey, 1860), which show the basal karyotype pattern for the family. In spite of this group has an average NF conspicuously higher than that of Naucratini, this value is strongly biased by *Trachurus* Rafinesque, 1810, species, which have higher NF values (NF = 50–78). In fact, *Trachurus* diverge markedly from other Carangini groups because its species have a limited distribution (FAO 2020), with evidence of strong genetic structuring between broad and distant regions (Karaiskou et al. 2004). Thus, the analysis of the structural diversification of Carangini karyotypes, removing the particular group *Trachurus* (Fig. 2), drastically reduces the NF values for this tribe, making the NF = 51.3, thus very close to that of the Naucratini subfamily. On the other hand, Trachinotini species showed the lowest geographic distributions among the other tribes and the more divergent NF values.

Significantly, a conservatism pattern can also be seen at microstructural cytogenetic level. For example, the 18S rDNA sites, that are usually characterized by a high

evolutionary dynamism among fishes (Gornung 2013), have a stable distribution pattern among the four species now analyzed, as well as in several other Carangidae species (Accioly et al. 2012; Jacobina et al. 2012, 2014a). Their similarity in number and chromosomal location probably represent a homeolog linkage group among them. Although the 5S rDNA sites exhibit a more dynamic evolutionary pattern in other species (Accioly et al. 2012; Jacobina et al. 2012, 2013, 2014a, b), they also reveal here signs of microstructural conservatism.

The distribution of some *Trachinotus* species in the Western Atlantic is subdivided by the Amazonas and Orinoco rivers barrier. In this context, *T. carolinus* from Caribbean, first analyzed here, shows no variable karyotypes compared to those previously reported for populations from the southeast and northeast Brazilian coasts (Rodrigues et al. 2007; Jacobina et al. 2012).

Biogeographic barriers in marine oceans affect the karyotype diversification (Molina et al. 2012), but have different effects among the species (Motta-Neto et al. 2019). In this context, cytogenetic analyses in fish populations from different biogeographic regions help to decipher the karyotype evolution in groups with large distribution.

Conclusions

Carangidae constitute a marine fish group in which many species are vagrant/nomadic pelagic swimmers, ranging from a single ocean to circumglobal distributions. Gene flow among marine fish populations with significant population sizes and extensive distributions can mitigate genetic differentiation. The cytogenetical/geographical approach suggest negative correlation between active migratory capacity and cytogenetic divergence in marine fish. This genetic context could restrains evolutionary diversification and speciation, in the Carangidae, a clade in which many genera are monotypic or formed by a few species. As a whole, our data provide preliminary data of high gene flow in minimize chromosomal rearrangements in large oceanic spaces, highlighting new scenarios of the karyotype evolution in pelagic species.

Acknowledgements

The authors thank to the Conselho Nacional de Desenvolvimento Científico e Tecnológico (CNPq) for financial support (#442664/2015-0; #442626/2019-3 and #301458/2019-7 to WFM), to the Coordenação de Aperfeiçoamento de Pessoal de Nível Superior (CAPES) to scholarship grant to RXS, and to ICMBio/SISBIO (#19135-4, #131360-1 and #27027-2) for the authorization in collecting specimens. We also thank to Dr. José Garcia Júnior for the taxonomic identification of the specimens and the University of Miami's RSMAS (Rosenstiel School of Marine and Atmosferic Science) for the partnership and for making available the specimens of *Trachinotus carolinus* used in this study.

Authors' contributions

Rodrigo Xavier Soares: Conceptualization, Methodology, Writing – Original draft preparation, Data curation. **Gideão Wagner Werneck Félix da Costa:** Investigation, Validation. **Clóvis Coutinho da Motta-Neto, Amanda Torres Borges:** Supervision, Visualization. **Marcelo de Bello Cioffi, Luiz Antônio Carlos Bertollo:** Writing – Reviewing and Editing. **Wagner Franco Molina:** Conceptualization, Methodology, Writing – Original draft preparation, Funding acquisition, Project administration. Writing – Reviewing and Editing.

Data availability statement

The data that support the findings of this study are available from the corresponding author upon reasonable request.

References

Accioly IV, Bertollo LAC, Costa GWWF, Jacobina UP, Molina WF (2012) Chromosomal population structuring in carangids (Perciformes) between the north-eastern and south-eastern coasts of Brazil. African Journal of Marine Science 34(3): 383–389. https://doi.org/10.2989/1814232X.2012.689671

Amorim KDJ, Cioffi MB, Bertollo LAC, Soares RX, Calado LL, Borges AT, Costa GWWF, Molina WF (2017) Interregional cytogenetic comparisons in *Halichoeres* and *Thalassoma* wrasses (Labridae) of coastal and insular regions of the southwestern Atlantic. Genetics and Molecular Research 16(2): gmr16029650. https://doi.org/10.4238/gmr16029650

Bertollo LAC, Born GG, Dergam JA, Fenocchio AS, Moreira-Filho O (2000) A biodiversity approach in the neotropical Erythrinidae fish, *Hoplias malabaricus*. Karyotypic survey, geographic distribution of cytotypes and cytotaxonomic considerations. Chromosome Research 8: 603–613. https://doi.org/10.1023/A:1009233907558

Caputo V, Marchegiani F, Olmo E (1996) Karyotype differentiation between two species of carangid fishes, genus *Trachurus* (Perciformes: Carangidae). Marine Biology 127: 193–199. https://doi.org/10.1007/BF00942103

Castro-Leal ME, Brum MJI, Corrêa MMO (1998) Estudos citogenéticos em *Oligoplites saliens* (Perciformes, Carangidae) da Baía de Sepetiba, RJ – Resultados Preliminares. Simpósio de Citogenética Evolutiva e Aplicada de Peixes Neotropicais VII. Londrina – PR, Universidade Estadual de Londrina. Londrina, 14 pp.

Chai X, Lu LR, Clarke S (2009) Karyotype analysis of the yellowtail kingfish *Seriola lalandi lalandi* (Perciformes: Carangidae) from South Australia. Aquaculture Research 40(15): 1735–1741. https://doi.org/10.1111/j.1365-2109.2009.02278.x

Choudhury RC, Prasad R, Das CC (1993) Karyomorphology of four carangids from the Indian Ocean (Carangidae: Perciformes). La Kromosomo 69(2): 2329–2335.

Costa GWWF, Cioffi MB, Liehr T, Feldberg E, Bertollo LAC, Molina WF (2019) Extensive chromosomal reorganization in *Apistogramma* fishes (Cichlidae, Cichlinae) fits the complex evolutionary diversification of the genus. International Journal of Molecular Sciences 20(17): e4077. https://doi.org/10.3390/ijms20174077

Craig MT, Eble JA, Bowen BW, Robertson DR (2007) High genetic connectivity across the Indian and Pacific Oceans in the reef fish *Myripristis berndti* (Holocentridae). Marine Ecology Progress Series 334: 245–254. https://doi.org/10.3354/meps334245

Damerau M, Freese M, Hanel R (2017) Multi-gene phylogeny of jacks and pompanos (Carangidae), including placement of monotypic vadigo *Campogramma glaycos*. Journal of Fish Biology 92(1): 190–202. https://doi.org/10.1111/jfb.13509

Das NK, Prasad R, Das CC (1980) Chromosomes of four species of marine fishes (Fam: Carangidae). Indian Biologist 12: 21–25.

FAO (2020) FishFinder – Web Site. About FAO FishFinder. FI Institutional Websites. In: FAO Fisheries and Aquaculture Department, Rome. http://www.fao.org/fishery/ [Accessed 31-March-2020]

Fricke R, Eschmeyer WN, Fong JD (2020) Eschmeyer's catalog of fishes: species by family/subfamily. California Academy of Sciences. http://researcharchive.calacademy.org/research/ichthyology/catalog/SpeciesByFamily.asp [Accessed 10-April-2020]

Froese R, Pauly D (2020) FishBase. World Wide Web electronic publication. www.fishbase.org [Accessed 10-April-2020]

Gaither MR, Bowen BW, Rocha LA, Briggs JC (2016) Fishes that rule the world: circumtropical distributions revisited. Fish and Fisheries 17(3): 664–679. https://doi.org/10.1111/faf.12136

Gold JR, Li YC, Shipley NS, Powers PK (1990) Improved methods for working with fish chromosomes with a review of metaphase chromosome banding. Journal of Fish Biology 37(4): 563–575. https://doi.org/10.1111/j.1095-8649.1990.tb05889.x

Gornung E (2013) Twenty years of physical mapping of major ribosomal RNA genes across the Teleosts: A review of research. Cytogenetic and Genome Research 141: 90–102. https://doi.org/10.1159/000354832

Honebrink RR (2000) A review of the biology of the family Carangidae, with emphasis on species found in Hawaiian waters. DAR Technical Report 20-01. Hawai'i Department of Land and Natural Resources, Division of Aquatic Resources, Honolulu, 37 pp.

Howell WM, Black DA (1980) Controlled silver-staining of nucleolus organizer regions with a protective colloidal developer a 1-step method. Experientia 36: 1014–1015. https://doi.org/10.1007/BF01953855

Ida H, Murofushi M, Fujiwara S, Fujino K (1978) Preparation of fish chromosomes by in vitro colchicine treatment Japanese. Journal of Ichthyology 24(5): 281–284. https://doi.org/10.1016/0030-4018(78)90011-1

Jacobina UP, Bertollo LAC, Cioffi MB, Molina WF (2014a) Physical mapping of 18S and 5S genes in pelagic species of the genera *Caranx* and *Carangoides* (Carangidae). Genetics and Molecular Research 13: 9628–9635. https://doi.org/10.4238/2014.November.14.7

Jacobina UP, Martinez PA, Cioffi MB, Garcia Jr J, Bertollo LAC, Molina WF (2014b) Morphological and karyotypic differentiation in *Caranx lugubris* (Perciformes: Carangidae) in

the St. Peter and St. Paul Archipelago, mid-Atlantic Ridge. Helgoland Marine Research 68: 17–25. https://doi.org/10.1007/s10152-013-0365-0

Jacobina UP, Vicari M, Bertollo LAC, Molina WF (2012) Discriminatory profile of rDNA sites and trend for acrocentric chromosome formation in the genus *Trachinotus* Lacépède, 1801 (Perciformes, Carangidae). Comparative Cytogenetics 6(4): 359–369. https://doi.org/10.3897/compcytogen.v6i4.3062

Jacobina UP, Vicari M, Martinez PA, Cioffi MB, Bertollo LAC, Molina WF (2013) Atlantic moonfishes: independent pathways of karyotypic and morphological differentiation. Helgoland Marine Research 67: 499–506. https://doi.org/10.1007/s10152-012-0338-8

Karaiskou N, Triantafyllidis A, Triantaphyllidis C (2004) Shallow genetic structure of three species of the genus *Trachurus* in European waters. Marine Ecology Progress Series 281: 193–205. https://doi.org/10.3354/meps281193

Kohn YY, Clements KD (2011) Pelagic larval duration and population connectivity in New Zealand triplefin fishes (Tripterygiidae). Environmental Biology of Fishes 91: 275–286. https://doi.org/10.1007/s10641-011-9777-3

Lee MH, Loh PC (1975) Some properties of an established fish cell line from the marine fish, *Caranx mate* (Omaka). Experimental Biology and Medicine 150(1): 40–48. https://doi.org/10.3181/00379727-150-38970

Levan A, Fredga K, Sandberg A (1964) Nomenclature for centromeric position on chromosomes. Hereditas 52(2): 201–220. https://doi.org/10.1111/j.1601-5223.1964.tb01953.x

Molina WF (2007) Chromosomal changes and stasis in marine fish groups. In: Pisano E, Ozouf-Costaz C, Foresti F, Kapoor BG (Eds) Fish Cytogenetics. Science Publishers Inc., Enfield, 69–110. https://doi.org/10.1201/b10746-4

Molina WF, Costa GWWF, Cioffi MB, Bertollo LAC (2012) Chromosomal differentiation and speciation in sister-species of Grammatidae (Perciformes) from the Western Atlantic. Helgoland Marine Research 66: 363–370. https://doi.org/10.1007/s10152-011-0276-x

Molina WF, Galetti Jr PM (2004) Karyotypic changes associated to the dispersive potential on Pomacentridae (Pisces, Perciformes). Journal of Experimental Marine Biology and Ecology 309(1): 109–119. https://doi.org/10.1016/j.jembe.2004.03.011

Molina WF, Martinez PA, Bertollo LAC, Bidau CJ (2014) Evidence for meiotic drive as an explanation for karyotype changes in fishes. Marine Genomics 15: 29–34. https://doi.org/10.1016/j.margen.2014.05.001

Moreira-Filho O, Bertollo LAC (1991) *Astyanax scabripinnis* (Pisces, Characidae): a species complex. Revista Brasileira de Genética 14(2): 331–357. https://doi.org/10.1590/S1984-46702012000200008

Motta-Neto CC, Cioffi MB, Costa GWWF, Amorim KDJ, Bertollo LAC, Artoni RF, Molina WF (2019) Overview on karyotype stasis in Atlantic grunts (Eupercaria, Haemulidae) and the evolutionary extensions for other marine fish groups. Frontiers in Marine Science 6: e628. https://doi.org/10.3389/fmars.2019.00628

Motta-Neto CC, Lima-Filho PA, Araújo WC, Bertollo LAC, Molina WF (2012) Differentiated evolutionary pathways in Haemulidae (Perciformes): karyotype stasis versus morphological differentiation. Reviews in Fish Biology and Fisheries 22: 457–465. https://doi.org/10.1007/s11160-011-9236-4

Murofushi M, Yosida TH (1979) Cytogenetical studies on fishes, II. Karyotypes of four carangid fishes. The Japanese Journal of Genetics 54(5): 367–370. https://doi.org/10.1266/jjg.54.367

Nelson JS, Grande TC, Wilson MVH (2016) Fishes of the world. 5th edn. John Wiley and Sons, New Jersey, 707 pp. https://doi.org/10.1002/9781119174844

Nirchio M, Rossi AR, Foresti F, Oliveira C (2014) Chromosome evolution in fishes: a new challenging proposal from Neotropical species. Neotropical Ichthyology 12(4): 761–770. https://doi.org/10.1590/1982-0224-20130008

OBIS (2020) Ocean Biogeographic Information System. Intergovernmental Oceanographic Commission of UNESCO. www.iobis.org [Acessed 20-October-2020]

Ohara E, Nishimura T, Nagakura Y, Sakamoto T, Mushiake K, Okamoto N (2005) Genetic linkage maps of two yellowtails (*Seriola quinqueradiata* and *Seriola lalandi*). Aquaculture 244(1–4): 41–48. https://doi.org/10.1016/j.aquaculture.2004.10.022

Palumbi SR (1994) Genetic divergence, reproductive isolation, and marine speciation. Annual Review of Ecology and Systematics 25(1): 547–572. https://doi.org/10.1146/annurev.es.25.110194.002555

Patro R, Prasad R (1979) Chromosomes of six marine percoids from the Indian Sea. Indian Biologist 11: 9–12.

Pendás AM, Morán P, García-Vázquez E (1994) Organization and chromosomal location of the major histone cluster in brown trout, Atlantic salmon and rainbow trout. Chromosoma 103: 147–152. https://doi.org/10.1007/BF00352324

Pinkel D, Straume T, Gray JW (1986) Cytogenetic analysis using quantitative, high-sensitivity, fluorescence hybridization. Proceedings of the National Academy of Sciences of the United States of America 83(9): 2934–2938. https://doi.org/10.1073/pnas.83.9.2934

Pla C, Pujolar JM (1999) Genetic homogeneity of dolphinfish (*Coryphaena hippurus*) in the western Mediterranean and the eastern Atlantic. Scientia Marina 63(3–4): 337–341. https://doi.org/10.3989/scimar.1999.63n3-4337

Rasband WS (2018) ImageJ. US National Institutes of Health, Bethesda, Maryland. https://imagej.nih.gov/ij/ [1997–2018]

Riginos C, Crandall ED, Liggins L, Bongaerts P, Treml EA (2016) Navigating the currents of seascape genomics: how spatial analyses can augment population genomic studies. Current Zoology 62(6): 581–601. https://doi.org/10.1093/cz/zow067

Rocha LA (2003) Patterns of distribution and processes of speciation in Brazilian reef fishes. Journal of Biogeography 30(8): 1161–1171. https://doi.org/10.1046/j.1365-2699.2003.00900.x

Rodrigues MM, Baroni S, Almeida-Toledo LF (2007) Karyological characterization of four marine fish species, genera *Trachinotus* and *Selene* (Perciformes: Carangidae), from the Southeast Brazilian coast. Cytologia 72(1): 95–99. https://doi.org/10.1508/cytologia.72.95

Saenz-Agudelo P, Jones GP, Thorrold SR, Planes S (2011) Connectivity dominates larval replenishment in a coastal reef fish metapopulation. Proceedings of the Royal Society of London – Series B: Biological Sciences 278: 2954–2961. https://doi.org/10.1098/rspb.2010.2780

Santini F, Carnevale G (2015) First multilocus and densely sampled timetree of trevallies, pompanos and allies (Carangoidei, Percomorpha) suggests a Cretaceous origin and Eocene

radiation of a major clade of piscivores. Molecular Phylogenetics and Evolution 83: 33–39. https://doi.org/10.1016/j.ympev.2014.10.018

Schweizer D (1976) Reverse fluorescent chromosome banding with chromomycin and DAPI. Chromosoma 58: 307–324. https://doi.org/10.1007/BF00292840

Sena DCS, Molina WF (2007) Robertsonian rearrangements and pericentric inversions in Scaridae fish (Perciformes). Genetics and Molecular Research 6(3): 575–580.

Shulman M, Bermingham E (1995) Early life histories, ocean currents, and the population genetics of Caribbean reef fishes. Evolution 49(5): 897–910. https://doi.org/10.1111/j.1558-5646.1995.tb02325.x

Smith-Vaniz WF (1984) Carangidae: relationships. In: Moser HG, Richards WJ, Cohen DM, Fahay MP, Kendall AWJ, Richardson SL (Eds) Ontogeny and Systematics of Fishes, American Society of Ichthyologists and Herpetologists, Lawrence, KA, 522–530.

Soares RX, Bertollo LAC, Cioffi MB, Costa GWWF, Molina WF (2014) Chromosomal distribution of two multigene families and the unusual occurrence of an $X_1X_1X_2X_2/X_1X_2Y$ sex chromosome system in the dolphinfish (Coryphaenidae): An evolutionary perspective. Genetics and Molecular Research 13(2): 2470–2479. https://doi.org/10.4238/2014.April.3.19

Soares RX, Bertollo LAC, Costa GWWF, Molina WF (2013) Karyotype stasis in four Atlantic Scombridae fishes: mapping of classic and dual-color FISH markers on chromosomes. Fisheries Science 79: 177–183. https://doi.org/10.1007/s12562-013-0602-0

Soares RX, MB Cioffi, LAC Bertollo, AT Borges, GWWF Costa, WF Molina (2017) Chromosomal evolution in large pelagic oceanic apex predators, the barracudas (Sphyraenidae, Percomorpha). Genetics and Molecular Research 16(2): gmr16029644. https://doi.org/10.4238/gmr16029644

Sola L, Cipelli O, Gornung E, Rossi AR, Andaloro F, Crosetti D (1997) Cytogenetic characterization of the greater amberjack, *Seriola dumerili* (Pisces: Carangidae), by different staining techniques and fluorescence in situ hybridization. Marine Biology 128: 573–577. https://doi.org/10.1007/s002270050123

Sumner AT (1972) A simple technique for demonstrating centromeric heterochromatin. Experimental Cell Research 75(1): 304–306. https://doi.org/10.1016/0014-4827(72)90558-7

Taylor MS, Hellberg ME (2003) Genetic evidence for local retention of pelagic larvae in a Caribbean reef fish. Science 299(5603): 107–109. https://doi.org/10.1126/science.1079365

Tripathy ANK, Das CC (1988) Karyotypes of five Indian Perciform fishes. Copeia 1988(1): 231–233. https://doi.org/10.2307/1445939

Tripp-Valdez MA, León FJG, Ortega-García S, Lluch-Cota D, López-Martínez J, Cruz P (2010) Population genetic structure of dolphinfish (*Coryphaena hippurus*) in the Gulf of California, using microsatellite loci. Fisheries Research 105(3): 172–177. https://doi.org/10.1016/j.fishres.2010.03.023

Vasiliev VP (1978) Karyotypes of 5 species of fishes (Pisces) from the Black Sea. Tsitologiya 20: 1092–1094.

Vitturi R, Mazzola A, Macaluso M, Catalano E (1986) Chromosomal polymorphism associated with Robertsonian fusion in *Seriola dumerili* (Risso, 1810) (Pisces: Carangidae). Journal of Fish Biology 29(5): 529–534. https://doi.org/10.1111/j.1095-8649.1986.tb04969.x

White TJ, Bruns T, Lee S, Taylor J (1990) Amplification and direct sequencing of fungal ribosomal RNA genes for phylogenetics. In: Innis M, Gelfand D, Sninsky J, White T (Eds) PCR Protocols: A Guide to Methods and Applications, Academic Press Inc., Orlando, 315–322. https://doi.org/10.1016/B978-0-12-372180-8.50042-1

Zhang DC, Guo L, Guo HY, Zhu KC, Li SQ, Zhang Y, Zhang N, Liu BS, Jiang SG, Li JT (2019) Chromosome-level genome assembly of golden pompano (*Trachinotus ovatus*) in the family Carangidae. Scientific Data 6: e216. https://doi.org/10.1038/s41597-019-0238-8

ORCID

Wagner Franco Molina https://orcid.org/0000-0002-6695-0952
Marcelo de Bello Cioffi https://orcid.org/0000-0003-4340-1464
Clóvis Coutinho da Motta-Neto https://orcid.org/0000-0002-0592-6131
Rodrigo Xavier Soares https://orcid.org/0000-0002-3735-3649

CompCytogen 15(4): 447–458 (2021)
doi: 10.3897/compcytogen.v15.i4.73135
https://compcytogen.pensoft.net

RESEARCH ARTICLE

COMPARATIVE Cytogenetics
A peer-reviewed open-access journal
International Journal of Plant & Animal Cytogenetics, Karyosystematics, and Molecular Systematics

Karyotype and *COI* gene sequence of *Chironomus heteropilicornis* Wülker, 1996 (Diptera, Chironomidae) from the Gydan Peninsula, Russia

Viktor V. Bolshakov[1], Alexander A. Prokin[1,2], Sergey V. Artemenko[3]

1 *Papanin Institute for Biology of Inland Waters Russian Academy of Sciences, Yaroslavl reg., Nekouz prov., Borok, 152742, Russia* **2** *Cherepovets State University, Lunacharski 5,Cherepovets, 162600, Vologda Oblast', Russia* **3** *AquaBioSafe Laboratory, University of Tyumen, 625003, Tyumen, Russia*

Corresponding author: Viktor V. Bolshakov (victorb@ibiw.ru)

Academic editor: Paraskeva Michailova | Received 17 August 2021 | Accepted 19 October 2021 | Published 7 December 2021

http://zoobank.org/54180A42-09A1-4E94-96AC-D9C103F7B8E7

Citation: Bolshakov VV, Prokin AA, Artemenko SV (2021) Karyotype and *COI* gene sequence of *Chironomus heteropilicornis* Wülker, 1996 (Diptera, Chironomidae) from the Gydan Peninsula, Russia. CompCytogen 15(4): 447–458. https://doi.org/10.3897/compcytogen.v15.i4.73135

Abstract

The karyotype features and gene *COI* sequence of *Chironomus heteropilicornis* Wülker, 1996 from the Gydan Peninsula are presented for the first time. Nine banding sequences were determined, eight of them hpiA2, hpiB1, hpiC1, hpiC2, hpiD1, hpiE1, hpiF3 and hpiG1 were previously known from European, Georgian (South Caucasus) and Siberian populations. One new banding sequence for *Ch. heteropilicornis*, hpiB2, was found. The hpiA2 banding sequence was found in all individuals, and this is its second finding after the Georgian population (Karmokov 2019). The hpiF3 banding sequence was found only in the homozygous state. Additional B-chromosomes are absent. The genetic distances (K2P) between *Ch. heteropilicornis COI* gene sequence from Gydan Peninsula and Norway are 1.1–1.3%, and Georgia – 1.8%, much lower than the commonly accepted threshold of 3% for species of genus *Chironomus* Meigen, 1803. The phylogenetic tree for *COI* gene sequences estimated by Bayesian inference showed geographically determined clusters of Norway and Gydan and a separate lineage of the Georgian population of *Ch. heteropilicornis*. The analysis of karyotype and *COI* gene sequences shows that the population of *Ch. heteropilicornis* from the Gydan Peninsula has an intermediate position within the *Ch. pilicornis* group between Georgian, Yakutian and Norwegian populations. The position of *Ch. pilicornis* Fabricius, 1787 from Canada and Greenland on the phylogenetic tree is discussed.

Keywords

Chironomidae, *Chironomus heteropilicornis*, *COI*, Diptera, DNA-barcode, Gydan Peninsula, karyotype

Introduction

The water bodies of the Gydan Peninsula remain poorly studied. In 2012 during the investigation of the zonal distribution of macrozoobenthos in lakes of the Tyumen Oblast', in the Tundra zone, larvae of *Chironomus* Meigen, 1803 were not recorded (Aleshina and Uslamin 2012). Later, the single species *Chironomus heterodentatus* Konstantinov, 1956 identified by larval morphology, was recorded from two unnamed inundated lakes on the Gydan Peninsula (Stolbov et al. 2017).

Chironomus heteropilicornis Wülker, 1996 belongs to *Chironomus pilicornis*-group, which includes one more species *Ch. pilicornis* Fabricius, 1787. In Russia larvae with unknown karyotype were found in a few populations of Sakha Republic (Yakutia): channel in the vicinity of the Yakutsk city; Bakyl pond in Khoro village, Verkhnevilyuyskiy District; Erien-Kuta lake in Antonovka village; unnamed pond for irrigation in Nyurba village; unnamed lake in Antonovka village, Nyurbinskiy District; Irelyakh River near Mirnyy city, Mirninskiy District. These larvae were initially named *Chironomus* sp. *Ya2* (Kiknadze et al. 1996), later identified as *Ch. heteropilicornis* (Kiknadze and Istomina 2000). One population is known from an unnamed lake in the Republic of Georgia (South Caucasus), Kvemo Kartli reg., Tsalka District (Karmokov 2019). This species was also recorded from Sweden, Finland (Wülker 1996), and North Germany (Kiknadze and Istomina 2011; Kiknadze et al. 2016).

At present, 16 banding sequences are known for the banding sequences pool of *Ch. heteropilicornis*: 15 of them are described by Kiknadze et al. (2016), and one additional banding sequence hpiA2 described from Georgia (Karmokov 2019).

The *COI* gene sequences of *Ch. heteropilicornis* from Norway and Georgia are present in genetic information databases, GenBank and Barcode of Life Data Systems (BOLD). In addition, COI sequences of *Ch. pilicornis* from Canada, Greenland, and Sweden were also present in aforementioned databases.

The present research aims at describing the karyotype and *COI* gene features of the *Ch. heteropilicornis* from the Gydan peninsula (Russia) in a comparison with known populations.

Material and methods

Four IV instar larvae were collected from a small bay overgrown with sedge (*Carex* sp.) of an unnamed lake in Gydan Peninsula, Tazovskiy District, Yamalo-Nenets Autonomous Region (Fig. 1): 70°24'51.54"N, 76°06'42.08"E (70.414317, 76.111689) in August 4, 2018. Depth – 0.8 m, bottom – silt, detritus; water temperature – 10.5 °C, mineralization – 0.06 ppm. The total abundance of *Chironomus* spp. specimens in this habitat was estimated at 700 ind./m^2 (67% of the total number of benthic animals) and total biomass was 6.6 g/m^2 (38%). All larvae were used for karyotype analysis by the ethanol-orcein technique (Dyomin 1989). A Micromed-6C (LOMO,

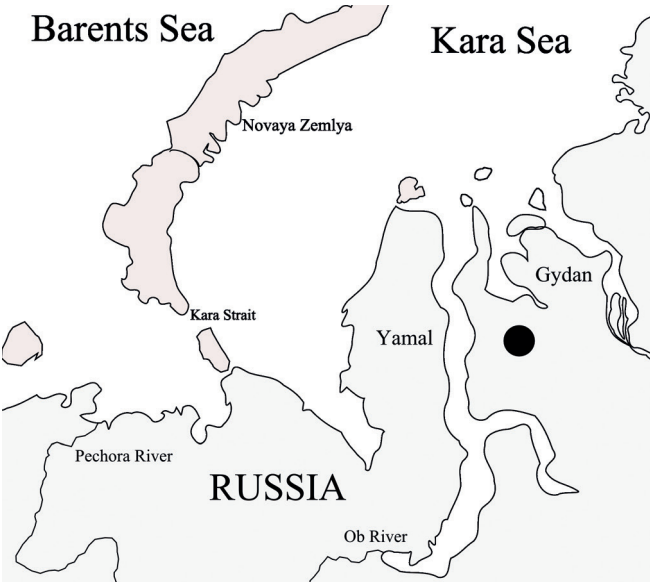

Figure 1. Collection site of *Ch. heteropilicornis* in Gydan Peninsula, Russia. The collection site is marked by a black circle.

St. Petersburg) light microscope equipped with standard (kit) oil objective x100, and camera ToupCam5.1 (China) were used for microscopy analysis.

The head capsule of one larva was mounted on a slide in the Fora-Berlese solution (fig. 2), the morphological terminology proposed by Sæther (1980) was used.

The larvae were determined by karyology. To identify chromosome banding sequences in arms A, E and F the cytophotomaps of Wülker (1996), Kiknadze et al. (1996, 2016), Karmokov (2019) were used, the mapping performed in the system of Keyl (1962), and for arms C and D cytophotomaps of Wülker (1996), Kiknadze et al. (1996, 2016) were used in the system of Dévai et al. (1989).

One larva which was studied karyologically was taken for the total DNA extraction using a «M-sorb-OOM» (Sintol, Moscow) kit with magnet particles according to the manufacturer's protocol. For amplification of *COI* gene (cytochrome oxidase subunit I) we used primers LCO1490 (5'-GGTCAACAAATCATAAAGATATTGG-3') and HCO2198 (5'-TAAACTTCAGGGTGACCAAAAAATCA -3') (Evrogen, Moscow) (Folmer et al. 1994). The amplification reaction was carried out in 25 µl reaction mixture (1x buffer, 1.5 µM MgCl2, 0.5 mM of each primer, 0.2 µM dNTP of each nucleotide, 17.55 µL deionized water, 1 µL template DNA, 1 unit Taq-polymerase (Evrogen, Moscow). PCR performed at 94 °C (3 min), followed by 30 cycles at 94 °C (15 s), 50 °C (45 s), 72 °C (60 s) and a final one at 72 °C (8 min). PCR products were visualized on 1% agarose gels and later purified by ethanol and ammonium acetate (3 M). Both strands were sequenced on an Applied Biosystems 3500 DNA sequencer (Thermo Scientific, USA) following the manufacturer's instructions.

For alignment of *COI* nucleotide sequences we used MUSCLE algorythm in the MEGA6 software (Tamura et al. 2013). The MEGA6 was used to calculate pairwise genetic distances Kimura 2-parameter (K2P) with codon position preferences: 1st, 2nd, 3rd and noncoding sites (Kimura 1980). The Bayesian analysis was performed using MrBayes v.3.2.6 software (Ronquist and Huelsenbeck 2003; Ronquist et al. 2012) with settings suggested by Karmokov (2019), for 1 000 000 iterations and 1000 iterations of burn-in, nst = 6 (GTP + I + G). The phylogenetic trees resulting in Bayesian inference analyses were visualized and edited using FigTree v.1.4.3 software (http://tree.bio.ed.ac.uk/software/figtree/).

In addition, the forty one COI sequences of the genus *Chironomus* from "GenBank" and "Barcode of Life Data Systems" (BOLD)* were used for comparison. Accession numbers of used sequences in GenBank and BOLD: *Chironomus acutiventris* Wülker, Ryser et Scholl 1983 (AF192200.1), *Ch. annularius* Meigen, 1818 (AF192189.1), *Ch. aprilinus* Meigen, 1830 (KC250746.1), *Ch. balatonicus* Devai, Wulker et Scholl, 1983 (JN016826.1), *Ch. bernensis* Wülker et Klötzli,, 1973 (AF192188.1), *Ch. borokensis* Kerkis, Filippova, Schobanov, Gunderina et Kiknadze, 1988 (AB740261), *Ch. cingulatus* Meigen, 1830 (AF192191.1), *Ch. commutatus* Keyl, 1960 (AF192187.1), *Ch. curabilis* Belyanina, Sigareva et Loginova, 1990 (JN016810.1), *Ch. dilutus* Shobanov, Kiknadze et Butler, 1999 (KF278335.1), *Ch. entis* Shobanov, 1989 (KM571024.1), *Ch. heterodentatus* Konstantinov, 1956 (AF192199.1), *Ch. heteropilicornis* Wülker, 1996 (MK795770.1, MK795771.1, MK795772.1, CHMNO268-15*, CHMNO413-15, CHMNO267-15, CHMNO269-15, CHMNO266-15), *Ch. luridus* Strenzke, 1959 (AF192203.1), *Ch. maturus* Johannsen, 1908 (DQ648204.1), *Ch. melanescens* Keyl, 1961 (MG145351.1), *Ch. nipponensis* Tokunaga, 1940 (LC096172.1), *Ch. novosibiricus* Kiknadze, Siirin et Kerkis, 1993 (AF192197.1), *Ch. nuditarsis* Keyl, 1961 (KY225345.1), *Ch. obtusidens* Goetghebuer, 1921 (CHMNO207-15*); *Ch. piger* Strenzke, 1959 (AF192202.1), *Ch. pilicornis* Fabricius, 1787 (BSCHI736-17, BSCHI735-17, HM860166.1, ARCHR033-11, INNV033-08, ARCHR026-11, KR593529.1), *Ch. plumosus* Linnaeus, 1758 (KF278217.1), *Ch. riparius* Meigen, 1804 (KR756187.1), *Ch. tentans* Fabricius, 1805 (AF110157.1), *Ch. tuvanicus* Kiknadze, Siirin et Wülker, 1993 (AF192196.1), *Ch. whitseli* Sublette et Sublette, 1974 (KR683438.1). The *COI* gene sequence of *Ptychoptera minuta* Tonnoir, 1919 (KF297888) was used as outgroup in phylogenetic analysis.

Results and discussion

The morphological characteristics of mentum, antenna, mandible and ventromental plate of the larva are presented in Fig. 2. In general the morphological characteristics are similar to those previously described in Kiknadze et al. (1996).

The head capsule is dark yellow. The mentum is black-brown with sharp teeth. The central tooth with small additional teeth (Fig. 2a). The third to fifth teeth are almost the same size and lighter in color than the first and second teeth. The sixth tooth a

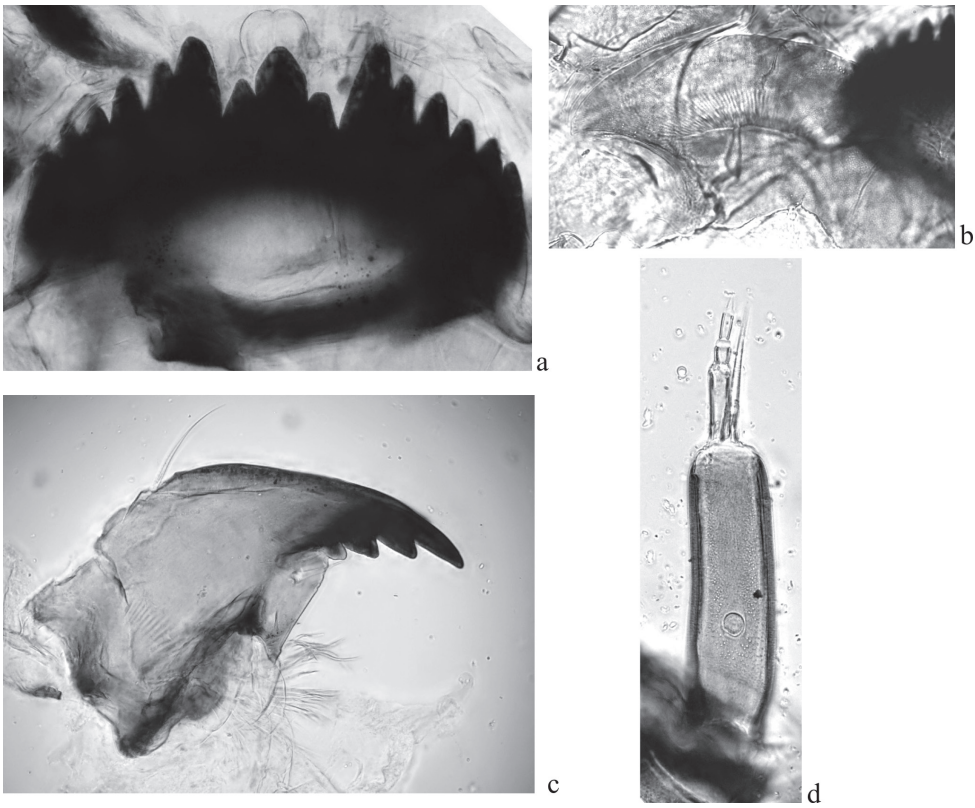

Figure 2. Larva morphology of *Ch. heteropilicornis* from the Gydan peninsula, Russia **a** mentum **b** ventromental plate **c** mandible **d** antenna.

small and light. Basal segment of antenna (Fig. 2d) is cone-shaped, length 119–167 μm. Antenna blade is extended to the base of a fourth segment (Kiknadze et al. 1996), but on the fig. 6 (Kiknadze et al. 1996) it is extended to the middle of a fifth segment and similar to Fig. 2d. Ventromental plates (Fig. 2b) with small outer hooks, the number of striae is 64–84 (Kiknadze et al. 1996). Mandible (Fig. 2c) with black first and brownish second teeth. Three lower teeth are black. The fourth tooth is small, it is color varied from light to dark brown.

Karyotype of *Chironomus heteropilicornis* Wülker, 1996 from the Gydan Peninsula

The chromosome set of the species is 2n = 8. The chromosome arm combination is AB, CD, EF and G (the *Chironomus* "*thummi*" cytocomlex). The additional B-chromosomes are absent. The chromosomes AB and CD are metacentric, EF is submetacentric, and G is telocentric. Nucleoli were found in arms B, D, E and G, Balbiani rings in arms B and G. The homologues in arm G usually laying closely to each other or are tightly paired (Kiknadze et al. 2016).

We found three different karyotypes in four larvae from the Gydan Peninsula: hp iA2.2.B1.1.C.1.1.D1.1.E.1.1.F.3.3.G1.1. (in two larvae), hpiA2.2.B1.2.C1.1.D.1.1. E.1.1.F.3.3. G1.1. and hpiA2.2.B1.1.C2.2.D.1.1.E.1.1.F.3.3.G1.1. They consist of 9 banding sequences out of 16 known for the banding sequences pool of this species (Kiknadze et al. 2016; Karmokov 2019) and one new hpiB2 sequence reported for the first time (Fig. 3). Sequences hpiA2 and hpiE1 mapped according to Karmokov (2019).

Arm A. One banding sequence hpiA2 1a-e 2d-3c 9e-7a 14f-13a 4a-6e 3i-d 12c-10a 2g-1f 14g-19f C.

Arm B. Two banding sequences: hpiB1was found in homozygous and heterozygous state with hpiB2, which was described for the first time. Frequency of sequences hpiB1 – 0.875 and hpiB2 – 0.125. Both banding sequences are still not mapped.

Arm C. Two banding sequences: hpiC1 1a-2i 15c-e 8a-11c 6b-3a 15b-13a 16a-17a 6gh 11d-12d 7d-a 6f-c17b-22g C and hpiC2 1a-2i 15c-e 8a-11c 13a-15b 3a-6b 16a-17a 6hg 11d-12d 7d-a 6f-c 17b-22g C. Frequency of sequences hpiC1 – 0.750 and hpiC2 – 0.250. Both sequences founded in homozygous state.

Arm D. One banding sequence: hpiD1 1a-3g 17f-11a 18f-a 7d-4a 10e-7e 18g-24g C.

Arm E. One banding sequence: hpiE1 1a-3e 8d-10b 10c-13g C.

Arm F. One banding sequence: hpiF3 1a-9b 12d-13d 11e-i 12a-c 16a-17d 10d-9c 15i-14a 11b-a 18a-23f C.

Arm G. One banding sequence: hpiG1 was found. Not mapped.

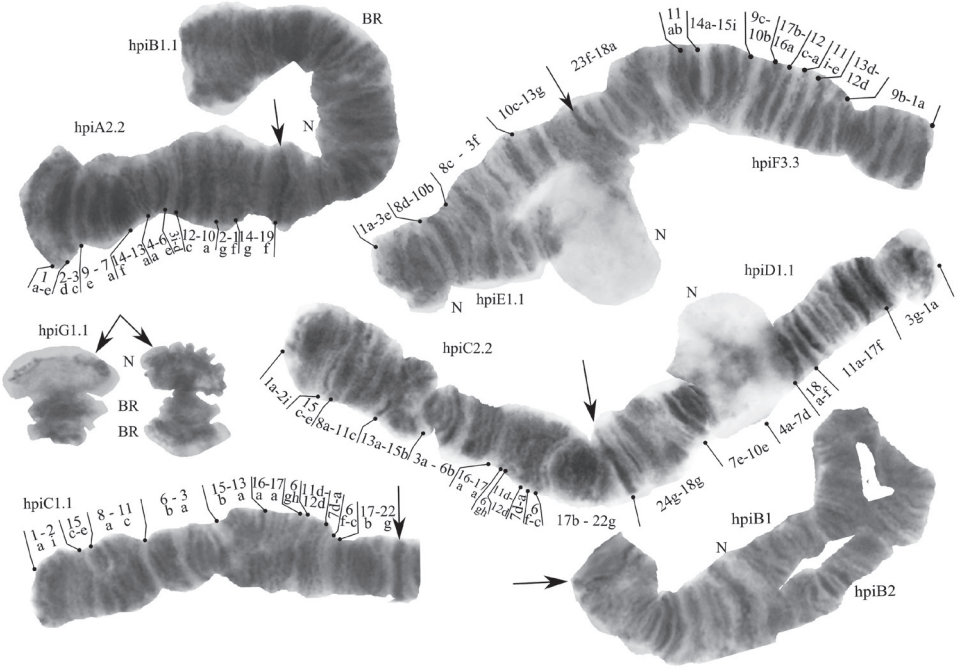

Figure 3. Karyotype of *Chironomus heteropilicornis* from the Gydan Peninsula, Russia. Arrows indicate centromeric band, hpiA2.2, hpiB1.1 and etc. – genotypic combinations of banding sequences in chromosome arms, BR – Balbiani rings, N – nucleous.

In total, nine banding sequences were found. The main feature of the population is the presence of rare banding sequences hpiA2 and hpiF3 only in the homozygous state. Another interesting moment is the large nucleous in D (7e-10e) and E (10c-11a) arms, usually, it is not so big. By the morphology, the chromosomes are similar to the karyotype of *Ch. heteropilicornis* from Netherlands (fig. 2.27.2, Kiknadze et al. 2016). Probably, it is a result of some non-obvious similar characteristics of water bodies, for example, a temperature. As we know, the characteristics of the karyotype and distribution of inversion variants in *Chironomus* depends more on the conditions in the local water body than on their geographic location (Gunderina et al. 1999), and the physiological condition of the organism (Iliinskaya 1984; Dyomin and Iliinskaya 1988; Dyomin 1989).

DNA-barcoding and phylogenetic analysis

Eight sequences for *Ch. heteropilicornis* and seven for *Ch. pilicornis* were found in genetic information databases, GenBank and BOLD (see access numbers in material and methods), there are populations from Canada, Greenland, Sweden, Norway, and Georgia. We obtained the *COI* sequence barcode for *Ch. heteropilicornis* with the length of 617 nucleotides (percentage A: 25; T: 36; G: 18; C: 21) and deposited it into the GenBank database with accession number – MZ450155. The pairwise genetic distances between the members of the *Ch. pilicornis* group obtained by K2P model (Kimura 1980) shown high variability. Distance between sequences of *Ch. heteropilicornis* from the Gydan Peninsula and: Georgia was 1.8%, Norway – 1.1–1.3%, with *Ch. pilicornis* from Sweden – 1.1%, Canada and Greenland – 5.3%. According to Proulx et al. (2013) *Chironomus COI* interspecific sequence distances are about 3%. In our study, the distances between different populations of *Ch. heteropilicornis* varies from 1.1 to 1.8%, that is much lower than the 3% accepted interspecific threshold.

The analysis of the phylogenetic tree constructed by Bayesian inference showed groups of sibling species (Fig. 4), and the *Ch. pilicornis* group is divided into geographically determined clusters: 1) Canada and Greenland, 2) Georgia, and Scandinavia (Norway, Sweden) and Gydan, with support value 0.98. Another interesting moment is the presence of two *Ch. pilicornis* sequences (BSCHI735-17, BSCHI736-17) along with the *Ch. heteropilicornis* sequences inside the Scandinavian cluster. If this is not a result of species misidentification, it could be a result of interspecific hybridization and horizontal transfer of mitochondrial genes with fixation in one of the parental species in the population (Guryev and Blinov 2002; Polukonova 2009; Polukonova and Dyomin 2010, 2013; Karmokov 2019; Bolshakov and Prokin 2021). About possibilities of hybridization between sibling-species in *Chironomus* are well known: *Camptochironomus tentans* × *C. pallidivittatus* (Tichy 1975), *Ch. plumosus* × *Ch. muratensis* Ryser, Scholl et Wülker 1983, *Ch. muratensis* × *Ch. nudiventris* Ryser, Scholl et Wülker 1983, *Ch. plumosus* × *Ch. borokensis* (Butler et al. 1999), *Ch. riparius* × *Ch. piger* (Petrova et al. 2014). Karmokov (2019) suppose that interspecific hybridization event between *Ch. heteropilicornis* (female) and *Ch. pilicornis* (male) in the population of Swe-

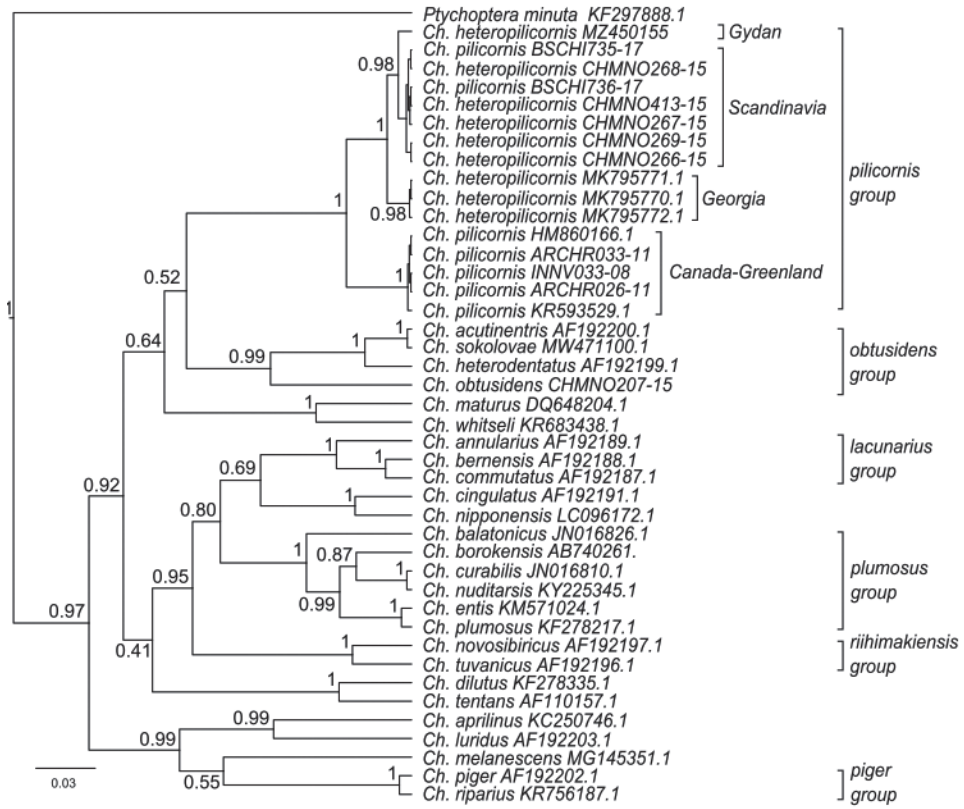

Figure 4. Bayesian tree of the analyzed samples of *Chironomus* spp. inferred from *COI* sequences. Species name, GenBank accession numbers and group name are shown to the right of the branches. Support values are given if they exceed 0.4. The numbers at the nodes indicate posterior probabilities.

den, because according to Wülker (1996) both species occurred sympatrically in collection site Kyrkösjärvi, Seinajöki-area (South Ostrobothnia, western Finland) which not so far from the place where were collected specimens of *C. pilicornis* (BSCHI735-17, BSCHI736-17) from BOLD.

Conclusions

Chironomus heteropilicornis is recorded from the Gydan Peninsula for the first time. Three different karyotypes in four larvae were found. The hpiB2 banding sequence is new for the species. The karyotypes of the population have a characteristic feature, possession of hpiA2 only in a homozygous state and phiF3 has been observed only in the homozygous state for the first time, and unusually large nucleous in D and E arms. We found sequences hpiA2.2, hpiC1.1, hpiD1.1 and hpiE1.1 in all larvae. The same

situation with the occurrence of these banding sequences was in all of 33 Georgian individuals (Karmokov 2019). The sequence hpiF3 was found in all larvae from the Gydan Peninsula, absent in Georgia (Karmokov 2019), but present in Yakutian populations with an occurrence from 9 to 22.5% (Kiknadze et al. 1996).

On the phylogenetic tree constructed by the Bayesian inference, we can see clusters of the sibling species groups: *Ch. obtusidens*, *Ch. lacunarius*, *Ch. plumosus*, *Ch. riihimakiensis*, *Ch. piger* and *Ch. pilicornis*, that were independently identified based on morphological and cytogenetic characteristics. In the *Ch. pilicornis* group, we can see the clusters explained geographically: Canada-Greenland and Georgia-Scandinavia-Gydan. The geographic distance in latitudes between Gydan and Georgian populations is about 3000 km, with Scandinavian populations 400–800 km and 400–1000 km with Greenland and Canada. We can conclude that the conditions in closely located sites will be similar, for example, in the Tundra zone it is the predominance of negative air temperatures per year, a predominance of oligotrophic waters, etc.

Unfortunately, we have no opportunity to examine the karyotype of the *Ch. pilicornis* from Canada. The genetic distances between most of the Palearctic and Canadian populations are 5.1%, as well as Greenland one (Karmokov 2019), that is more than the 3% accepted interspecific threshold (Proulx et al. 2013). A similar situation is known in the *Camptochironomus* group, for karyotypes and morphological characteristics of *C. tentans* and *C. dilutus*, which diverged during a long period of continental isolation to independent species (Shobanov et al. 1999; Kiknadze et al. 2007). Thus, the Canada-Greenland cluster is characterized by long isolation from other populations and can, possibly, represent one new, separate species.

Four larvae are not enough for complete chromosomal polymorphism analysis. Based on all the available data on karyotype and *COI* gene sequences, we can conclude that the population of *Ch. heteropilicornis* from the Gydan Peninsula has an intermediate position between Georgian (hpiA2.2), Yakutia (hpiF3.3) and Scandinavian (*COI*) populations within the European cluster. The absence of Yakutian population DNA-sequencing and data from other Asian regions gives no chance to establish a phylogeographical scenario for *Ch. heteropilicornis* at the moment.

Acknowledgements

The work was realized according to the Russia state projects 121050500046-8 and 121051100109-1. This research was funded by the Tyumen Oblast Government, as part of the West-Siberian Interregional Science and Education Center's project No. 89-DON (2). The authors are grateful to I. A. Stolbunov, D.D. Pavlov (IBIW RAS) for the provided material; to E.A. Movergoz, B.A. Levin, A.A. Bobrov (IBIW RAS) and M.Kh. Karmokov (IEMT RAS) for their help and consultations during all stages of the investigation and manuscript preparation; D.D. Pavlov (IBIW RAS) for the linguistic corrections of the text.

References

Aleshina OA, Uslamin DV (2012) Zonal distribution of macrozoobenthos in fresh water lakes of the Tyumen region. Vestnik Tyumenskogo gosudarstvennogo universiteta. Ekologiya i prirodopol'zovanie. 12: 160–172. [In Russian]

Bolshakov VV, Prokin AA (2021) Karyotype and COI sequences of *Chironomus sokolovae* Istomina, Kiknadze et Siirin, 1999 (Diptera, Chironomidae) from the bay of Orkhon River, Mongolia. CompCytogen 15(2): 149–157. https://doi.org/10.3897/CompCytogen.v15.i2.66549

Butler MG, Kiknadze II, Golygina VV, Martin J, Istomina AG, Wülker W, Sublette J (1999) Cytogenetic differentiation between Palearctic and Nearctic populations of *Chironomus plumosus* L.(Diptera, Chironomidae). Genome 42: 797–815. https://doi.org/10.1139/g99-014

Dévai Gy, Miskolczi M, Wülker W (1989) Standardization of chromosome arms B, C and D in *Chironomus* (Diptera, Chironomidae). Acta Biologica Debricina. Supplementum Oecologica Hungarica 2(1): 79–92.

Dyomin SYu (1989) Variability of the degree of condensation of polytene chromosomes in the cells of different organs of *Chironomus plumosus* larvae from nature. PhD Thesis, Institute of Cytology of the USSR Academy of Sciences, Leningrad, 25 pp. [In Russian]

Dyomin SYu, Il'inskaya NB (1988) Changes in the compactness of polytene chromosomes from different organs of the larvae of *Chironomus plumosus*. Tsitologiya 30(4): 407–415. [In Russian]

Folmer O, Black M, Hoeh W, Lutz R, Vrijenhoek R (1994) DNA primers for amplification of mitochondrial cytochrome c oxidase subunit I from diverse metazoan invertebrates. Molecular Marine Biology and Biotechnology 3: 294–299.

Gunderina LI, Kiknadze II, Golygina VV (1999) Intraspecific differentiation of the cytogenetic structure in natu ral populations of *Chironomus plumosus* L., the central species in the group of sibling species (Chironomidae: Diptera). Russian Journal of Genetics 35(2): 142–150.

Guryev VP, Blinov AG (2002) Phylogenetic relationships among Holarctic populations of *Chironomus entis* and *Chironomus plumosus* in view of possible horizontal transfer of mitochondrial genes. Russian Journal of Genetics 38(3): 239–243. https://doi.org/10.1023/A:1014842415628

Il'inskaya NB (1984) Characteristics of polytene chromosomes of various levels of density in larvae of the natural population of *Chironomus*. Tsitologiya. 26(5): 543–551. [In Russian].

Karmokov MK (2019) Karyotype characteristics, chromosomal polymorphism and gene COI sequences of *Chironomus heteropilicornis* Wülker, 1996 (Diptera, Chironomidae) from the South Caucasus. Comparative Cytogenetics 13(4): 339–357. https://doi.org/10.3897/CompCytogen.v13i4.35572

Keyl H-G (1962) Chromosomenevolution bei *Chironomus*. II. Chromosomenumbauten und phylogenetische Beziehungen der Arten. Chromosoma 13(4): 464–514. https://doi.org/10.1007/BF00327342

Kiknadze II, Istomina AG (2011) Karyological study of *Chironomus* species from the Netherlands. Contemporary Chironomid Studies. In: Wang X, Liu W (Eds) Contemporary Chi-

ronomid Studies. Proceedings of 17th International Symposium on Chironomidae (6–10 July 2009, Nankai University, China), Nankai, 41–72. [412 pp.]

Kiknadze II, Istomina AG, Gunderina LI, Aimanova KG, Salova TA, Savvinov DD (1996) Banding sequence pools of chironomid of Yakutian Permafrost. Tribe Chironomini. Novosibirsk, 166 pp. [In Russian with English summary]

Kiknadze II, Istomina AG (2000) Karyotypes and Chromosomal Polymorphisms in Siberian Chironomids (Diptera, Chironomidae). Sibirskiy ekologicheskiy zhurnal 4: 445–460. [In Russian]

Kiknadze II, Istomina AV, Golygina VV, Gunderina LI (2016) Karyotypes of Palearctic and Holarctic species of the genus *Chironomus* [Electronic resource]. Russian Academy of Sciences, Siberian Branch, Federal Research Center Institute of Cytology and Genetics. Novosibirsk, 489 pp.

Kimura M (1980) A simple method for estimating evolutionary rate of base substitutions through comparative studies of nucleotide sequences. Journal of Molecular Evolution 16: 111–120. https://doi.org/10.1007/BF01731581

Petrova NA, Zhirov SV, Harutyunova K, Harutyunova M (2014)On the possibility of spontaneous interspecific hybridization in the nature of representatives of sibling-species Chironomus riparius Kieffer and Chironomus piger Strenzke (DIPTERA, CHIRONOMIDAE) from Armenia. Tsitologiya 56(2): 170–174. [In Russian]

Polukonova NV, Djomin AG, Mugue NS (2013) Molecular criteria in insects systematics: barcoding gene COI range of variability as a taxonomic criterion for genus, tribe, and subfamily, with Chironominae and Orthocladiinae midges (chironomidae, diptera) as a case study. Zhurnal Obshchei Biologii 74(1): 66–76. [In Russian]

Polukonova NV, Djomin AG, Mugue NS, Shaikevich EV (2009) Comparison of Chironomus usenicus and Chironomus curabilis with species of the group plumosus (Diptera) inferred from the mitochondrial DNA gene COI and by the polytene chromosomes banding pattern. Russian Journal of Genetics 45(8): 899–905. https://doi.org/10.1134/S102279540908002X

Polukonova NW, Dyomin AG (2010) The results of complex analysis species of *Chironomus* group obtusidens (Diptera, Chironomidae) based on morphology, karyotype and molecular-genetic data. Entomologicheskie i paraziticheskie issledovaniya v Povolzhe 8: 8–13. [In Russian]

Proulx I, Martin J, Carew M, Hare L (2013) Using various lines of evidence to identify *Chironomus* species (Diptera: Chironomidae) in eastern Canadian lakes. Zootaxa 3741: 401–458. https://doi.org/10.11646/zootaxa.3741.4.1

Ronquist F, Huelsenbeck JP (2003) MRBAYES 3: Bayesian phylogenetic inference under mixed models. Bioinformatics 19: 1572–1574. https://doi.org/10.1093/bioinformatics/btg180

Ronquist F, Teslenko M, van der Mark P, Ayres DL, Darling A, Hohna S, Larget B, Liu L, Suchard MA, Huelsenbeck JP (2012) MrBayes 3.2: efficient Bayesian phylogenetic inference and model choice across a large model space. Systematic Biology 61: 539–542. https://doi.org/10.1093/sysbio/sys029

Sæther O (1980) Glossary of Chironomid morphology terminology (Diptera, Chironomidae). Entomologica Scandinavica. Supplement 14: 1–51.

Shobanov NA, Kiknadze II, Butler MG (1999) Palearctic and Nearctic *Chironomus* (*Camptochironomus*) *tentans* (Fabricius) are different species (Diptera: Chironomidae). Entomologica Scandinavica 30: 311–322. https://doi.org/10.1163/187631200X00147

Stolbov VA, Aleshina OA, Prokin AA, Allayarov DA (2017) The study of the hydrochemical composition, zooplankton and macrozoobenthos of some floodplain lakes of the typical tundra of the Gydan Peninsula. Voda: Khimiya i Ekologiya 8: 11–18. [In Russian]

Tamura K, Stecher G, Peterson D, Filipski A, Kumar S (2013) MEGA6: Molecular Evolutionary Genetics Analysis version 6.0. Molecular Biology and Evolution 30: 2725–2729. https://doi.org/10.1093/molbev/mst197

Tichy H (1975) Nature genetic basis and evolution of the hemoglobin polymorphysm in *Chironomus*. Journal of Molecular Evolution 6: 39–50. https://doi.org/10.1007/BF01732672

Wülker W (1996) *Chironomus pilicornis* Fabricius, 1787 and *Ch. heteropilicornis* sp. n. (Diptera: Chironomidae) in Fennoscandian reservoirs: Kariosystematics and morphological results. Aquatic Insects 8(4): 209–221. https://doi.org/10.1080/01650429609361624

ORCID

Viktor V. Bolshakov https://orcid.org/0000-0002-8028-3818
Alexander A. Prokin https://orcid.org/0000-0002-9345-5607
Sergey V. Artemenko https://orcid.org/0000-0002-8512-4795

Supplementary material 1

Fig. 6 from Kikanadze et al. 1996
Authors: Kikanadze et al.
Data type: pdf file
Explanation note: Karyotypes of kryolitozone of Yakutya.

Link: https://doi.org/10.3897/compcytogen.v15.i4.73135.suppl1

CompCytogen 15(4): 459–465 (2021)
doi: 10.3897/compcytogen.v15.i4.71295
https://compcytogen.pensoft.net

SHORT COMMUNICATION

COMPARATIVE Cytogenetics
A peer-reviewed open-access journal
International Journal of Plant & Animal Cytogenetics, Karyosystematics, and Molecular Systematics

A rare chromosomal polymorphism in a Kangayam bull (*Bos indicus*) of south India

Vemula Harshini[1], P. Kumarasamy[1], S.M.K. Karthickeyan[1]

1 *Department of Animal Genetics and Breeding, Madras Veterinary College, Tamil Nadu Veterinary and Animal Sciences University, Chennai-600 007, Tamil Nadu, India*

Corresponding author: Vemula Harshini (kashuvemula15@gmail.com)

Academic editor: Nina Bulatova | Received 11 July 2021 | Accepted 11 October 2021 | Published 15 December 2021

http://zoobank.org/55232ED5-A017-456D-B118-13E7CB9E62DC

Citation: Harshini V, Kumarasamy P, Karthickeyan SMK (2021) A rare chromosomal polymorphism in a Kangayam bull (*Bos indicus*) of south India CompCytogen 15(4): 459–465. https://doi.org/10.3897/compcytogen.v15.i4.71295

Abstract

A chromosomal polymorphism was detected on karyological screening of Kangayam breeding sires prior to subjecting them for frozen semen collection. One bull possessed the chromosomal complement 2n = 60, consisting of 58 acrocentric autosomes, one large sub-metacentric X-chromosome, and one small acrocentric Y-chromosome with a small visible p-arm, which was further confirmed using CBG- and GTG-banding. This polymorphism was attributed to a heterochromatin variation of the acrocentric Y-chromosome routine in the *Bos indicus* Linnaeus, 1758 cattle.

Keywords

Heterochromatin variation, individual chromosomal polymorphism, karyological screening

Introduction

The Kangayam breed of cattle is a pride of Tamil Nadu and native to south India. It is well known for its excellent draught qualities, adaptation to poor nutrition and longevity (Kandasamy 2001). Despite large scale transformation and decline in agricultural practices, there is still a demand for the Kangayam cattle from the neighboring states such as Kerala, Karnataka and Andhra Pradesh. The breed has been transported to

countries like Brazil, Malaysia, Philippines and Sri Lanka. Given its importance, the breed has been characterized phenotypically as well as through cytogenetic (Kumarasamy et al. 2006) and microsatellite analyses (Karthickeyan et al. 2009).

In the process of evolution, chromosomes have undergone rearrangements and form species-specific karyotypes. Iannuzzi and Di Meo (1995) stated that centric fusion translocations, and peri- or paracentric inversions along with the loss or gain of heterochromatin appeared to be the main chromosomal rearrangements occurred and thus differentiated the chromosomal complements across the bovid species. The variations in the size of the Y-chromosomes among subspecies are proportional to the amount of heterochromatin present (Cabelova et al. 2012). It shows the involvement of heterochromatin in the karyotype evolution of taxa of higher as well as lower ranks.

The chromosomal complements of *Bos indicus* Linnaeus, 1758 and *Bos taurus* Linnaeus, 1758 cattle are highly similar except for the Y-chromosome morphology being acrocentric (one arm) and sub-meta/metacentric (two arms), respectively. This morphological difference is due to the pericentric inversion which might have been occurred at the time of divergence (Goldammer et al. 1997; Di Meo et al. 2005). In the present study, a phenotypically healthy Kangayam bull was found carrying a different type of Y-chromosome on routine karyological screening, which was subjected to banding for unequivocal identification of chromosome morphology.

Material and methods

A total of 46 blood samples of Kangayam bulls were received for routine cytogenetic screening before using them for semen collection (14 from Buffalo Frozen Semen Station, 16 from Kangayam Cattle Research Station and 16 from field progeny tested animals in Tamil Nadu).

Metaphase chromosomes were obtained using short term lymphocyte culture technique (Moorhead et al. 1960), standardized with minor modifications in the Cytogenetics Laboratory of Department of Animal Genetics and Breeding, Madras Veterinary College, Chennai, India. The chromosome spreads were examined under Olympus microscope (BX61, USA) and more than 200 metaphases were screened. The good metaphase spreads were photographed using applied spectral imaging software. The cell fixation from one Kangayam bull carrying an unusual Y-chromosome was subsequently further studied using different cytogenetic banding techniques.

The chromosome preparations were CBG-banded using barium hydroxide [$Ba(OH)_2$] treatment as described by Sumner et al. (1972) with minor modifications (Harshini et al. 2020). GTG-banding technique was done as described by Seabright (1971) with modifications in concentration of the trypsin and exposure time. Slides aged for 5–7 days were immersed in Sorenson's phosphate buffer for 2–3 seconds and transferred to 0.025 per cent trypsin solution for 10–14 seconds. Then the slides were immediately transferred to Sorenson's phosphate buffer to stop the action of trypsin, washed twice in double distilled water and subsequently air-dried. The chromosomes

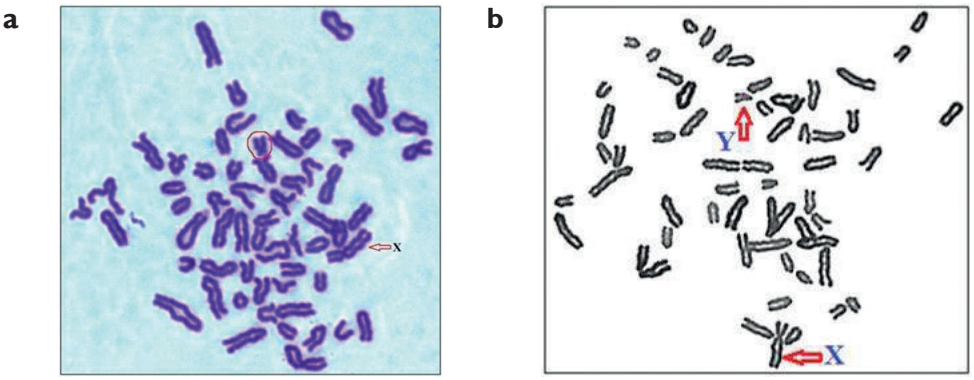

Figure 1. Giemsa-stained metaphase spreads of Kangayam bulls showing general similarity of acrocentric autosome set and X-chromosome, and different morphology of Y-chromosome: subacrocentric with small p-arm (**a**, encircled) and typical acrocentric (**b**).

were stained with 4 per cent Giemsa for 15 minutes and rinsed thoroughly in two consecutive washes in double distilled water. The chromosomes were then observed under microscope, photographed and karyotyped.

Results and discussion

All the Kangayam bulls, except the one investigated in detail, found to have 60 chromosomal diploid set with 29 pairs of acrocentric autosomes, one large sub-metacentric X- and the smallest acrocentric Y-chromosome. One bull showed similar chromosomal profile except for the presence of an unpaired smallest subacrocentric chromosome possessing a small p-arm (Fig. 1) in all the spreads screened. A similar kind of chromosomal complement was reported earlier by Iannuzzi et al. (2001) in Chainina cattle (*Bos taurus*) and considered as a sex-autosomal reciprocal translocation between the chromosomes Y and 9. Therefore, this Kangayam sample was further investigated using CBG- and GTG-banding techniques.

CBG-banding revealed that all the acrocentric chromosomes each showed characteristically a positive C-band as a distinctly-stained centromeric region. The X-chromosome was stained lightly across its entire length (Fig. 2). This is like the standard CBG-banding pattern of cattle as reported for Red Danish (Hansen 1973), *Bos taurus* L. (Iannuzzi and Berardino 1985), Jersey crossbreds (Chauhan et al. 2009), Tho-Tho cattle (Longkumer et al. 2015), mithun (Ezung 2016) and Nellore cattle (Amancio et al. 2019). However, the unpaired acrocentric chromosome with a small p-arm also stained darkly throughout the length showing no centromere banding (Fig. 2). Thus, it was confirmed as a sex chromosome (Y) and its small extra p-arm was not a translocated portion of any autosome which arms are lightly C-stained.

Upon GTG-banding, the Y-chromosome displayed a rearrangement in the distribution of G-bands divided for two arms (p, q) in the subacrocentric Y-chromo-

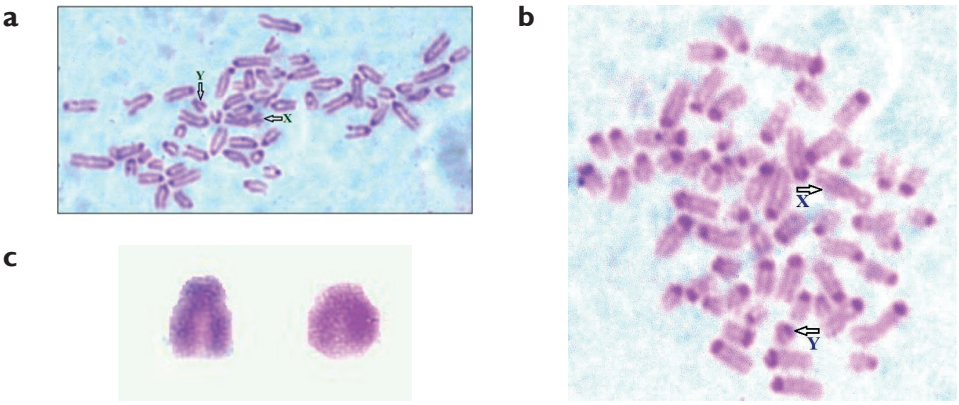

Figure 2. CBG-banded metaphase spreads of Kangayam bulls (**a, b**) bearing C-positive heterochromatic Y chromosome of two alternative types - subacrocentric (**c**, left) or acrocentric (**c**, right).

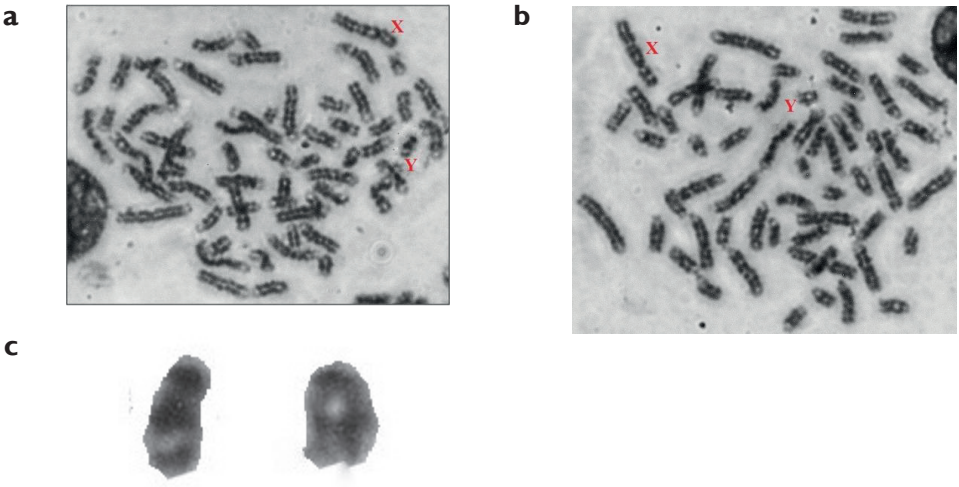

Figure 3. GTGbanded metaphase spreads of Kangayam bulls (**a**, **b**) with different Y-chromosome showing visible dark band in p-arm (**c,** left) and no prominent p-arm (**c**, right).

some and being situated together in the one arm (q) of acrocentric structure (Fig. 3), which is comparable to the standard G-banding pattern of *Bos indicus* cattle *viz.* Red Kandhari (Katkade 2005), Khillari (Nakod 2013), Malnad Gidda (Suresh et al. 2015), Indonesian native bulls (Ciptadi et al. 2017) and Nellore cattle (Amancio et al. 2019). The GTG-banding results also confirmed that there was no translocation between autosomes and Y-chromosome, as all the autosomes were having the typical G-banding pattern, as those of Iannuzzi and Di Meo (1995) and ISCNDB 2000 (Cribiu et al. 2001).

Of many studies pertaining to variations in morphology of cattle Y-chromosome, only a few cytogeneticists detected the polymorphisms. Halnan and Watson (1982) studied the Y-chromosome of *Bos indicus* breeds Sahiwal, Sindhi, Brahman, Santa Gertrudis and Belmont Red, derived from Zebu males, and reported as acrocentric though the centromere was found at a variable distance from the terminal point of the small p-arm; sometimes there would be no visible chromatin beyond the centromere and at other times the Y-chromosome would have distinct p-arms. Further, they also found visible subtelocentric Y-chromosome in every Sahiwal bull studied which they considered as differing only insignificantly from acrocentric according to the definition of Potter and Upton (1979) or Potter et al. (1979). According to them, these points served to raise the question of possible Y-chromosome polymorphism in *Bos indicus* in contradiction to the relative stability of the Y-chromosome in *Bos taurus*. Iannuzzi and Di Meo (1995) noticed that even though, there are size and morphological differences in the sex chromosomes (X and Y), R-banding patterns are conserved among cattle, river buffalo, sheep and goat. The differences are due to peri/paracentric inversions in sex chromosomes with loss or gain of heterochromatin.

In the present case also, there is a distinct p-arm in Y-chromosome of a Kangayam bull, when other bulls were possessing acrocentric Y-chromosomes with no prominent p-arm. As for the criteria for chromosome classification, the terms 'acrocentric' and 'subtelocentric' belong to different nomenclature systems, and their common use in the description of the same karyotype should be incorrect. Subtelocentric means the presence of telocentric, that is the chromosomes being strictly one-armed. It has been known from classic cytogenetics that the centromere is always distanced, at least minimally (very short arm) from the side opposite to the main (long) arm. Because of some uncertainty in definition of arm proportions in small chromosomes, such as the Y-chromosome of many mammals, including bovid taxa, and to stress a disproportion in arms of Y-chromosomes of the bulls studied, the term "subacrocentric" for the Y variant with a visible p-arm should be appropriate in recognition to the typical acrocentric of other breeding sires.

This visible p-arm appears attributable to heterochromatin variation and this can be considered as a possible Y-chromosomal polymorphism in Kangayam bull of south India. Even though, it is not a chromosomal abnormality, the productive and reproductive performance of the bull and its descendents should be studied to know the effect of the subacrocentric Y-chromosome; if the bull is allowed to breed without being usually culled upon receipt of the screening results.

References

Amancio AP, Duarte SSM, Silva RC, da Cruz AS, Silva DC, da Silva CC, da Cruz AD (2019) Banded karyotype of Nellore cattle (*Bos taurus indicus Linnaeus*, 1758). Comparative Cytogenetics 13(3): 265–275. https://doi.org/10.3897/CompCytogen.v13i3.36449

Cabelova K, Kubickova S, Cernohorska H, Rubes J (2012) Male specific repeats in wild Bovidae. Journal of Applied Genetics 53: 423–433. https://doi.org/10.1007/s13353-012-0108-y

Chauhan JB, Patel RK, Singh KM, Soni KJ (2009) A dicentric Robertsonian translocation, rob (1; 29) in Indian Jersey crossbred (*Bos taurus* × *Bos indicus*) bull. Nucleus 52: 119–123.

Ciptadi G, Ihsan MN, Nurgiartiningsih VMA, Ardyah IP, Mudawamah M (2017) The normal karyotyping result of Indonesian native breed bull qualified for artificial insemination. Biodiversitas 18(4): 1462–1467. https://doi.org/10.13057/biodiv/d180423

Cribiu EP, Di Berardino D, Di Meo GP, Eggen A, Gallagher DS, Gustavsson I, Hayes H, Iannuzzi L, Popescu CP, Rubes J, Schmutz S, Stranzinger G, Vaiman A, Womack J (2001) International system for chromosome nomenclature of domestic bovids (ISCNDB 2000). Cytogenetics and Cell Genetics 92(34): 283–299. https://doi.org/10.1159/000056917

Di Meo GP, Perucatti A, Floriot S, Incarnato D, Rullo R, Caputi Jambrenghi A, Ferretti L, Vonghia G, Cribiu E, Eggen A, Iannuzzi L (2005) Chromosome evolution and improved cytogenetic maps of the Y chromosome in cattle, Zebu, River buffalo, sheep and goat. Chromosome Research 13(4): 349–355. https://doi.org/10.1007/s10577-005-2688-4

Ezung NM (2016) Comparative cytogenetic studies of Mithun and Mithun X Cattle Cross. M.V.Sc. thesis, Maharashtra Animal and Fishery Sciences University, Nagpur, 102 pp.

Goldammer T, Brunner RM, Schwerin M (1997) Comparative analysis of Y-chromosome structure in *Bos taurus* and *Bos indicus* by FISH using region specific, microdissected, and locus specific DNA probes. Cytogenetic and Genome Research 77(3–4): 238–241. https://doi.org/10.1159/000134584

Halnan CRE, Watson JI (1982) Y chromosome variants in cattle *Bos taurus* and *Bos indicus*. Annales de Génétique et de Sélection Animale 14(1): 1–16. https://doi.org/10.1186/1297-9686-14-1-1

Hansen KM (1973) Heterochromatin (C-bands) in bovine chromosomes. Hereditas 73(1): 65–69. https://doi.org/10.1111/j.1601-5223.1973.tb01068.x

Harshini V, Kumarasamy P, Karthickeyan SMK, Cauveri D, Gowri AM, Rangasamy S (2020) Ascertaining the paternal lineage in crossbred calves. Journal of Genetics 99(1): 1–3. https://doi.org/10.1007/s12041-020-01193-y

Iannuzzi L, Di Berardino D (1985) Diagrammatic representation of RBA-banded chromosomes of swamp buffalo (*Bubalus bubalis* L.) and sex chromosome banding homologies with cattle (*Bos taurus* L.). Caryologia 38 (3–4): 281–295. https://doi.org/10.1080/00087114.1985.10797751

Iannuzzi L, Di Meo GP (1995) Chromosomal evolution in bovids: a comparison of cattle, sheep and goat G-and R-banded chromosomes and cytogenetic divergences among cattle, goat and river buffalo sex chromosomes. Chromosome Research 3(5): 291–299. https://doi.org/10.1007/BF00713067

Iannuzzi L, Molteni L, Di Meo GP, De Giovanni A, Perucatti A, Succi G, Incarnato D, Eggen A, Cribiu EP (2001) A case of azoospermia in a bull carrying a Y-autosome reciprocal translocation. Cytogenetics and Cell Genetics 95(3–4): 225–227. https://doi.org/10.1159/000059349

Kandasamy N (2001) Kangayam breed of cattle: present status and management practices. Proceedings of the Workshop on Indigenous Cattle and Their Role in the New Millennium. Erode, March, 2001. Tamil Nadu, 24–25.

Karthickeyan SMK, Sivaselvam SN, Selvam R, Thangaraju P (2009) Microsatellite analysis of Kangayam cattle (*Bos indicus*) of Tamilnadu. Indian Journal of Science and Technology 2(10): 38–40. https://doi.org/10.17485/ijst/2009/v2i10.11

Katkade BS (2005) Cytogenetic Studies on Indian Domestic Cattle (*Bos indicus*). M.V.Sc. thesis, Maharashtra Animal and Fishery Sciences University, Nagpur, India, 40 pp.

Kumarasamy P, Sivaselvam SN, Thara S, Thangaraju P, Nainar AM (2006) Chromosomal studies on Kangayam cattle. Indian Veterinary Journal 83(10): 1072–1073.

Longkumer I, Mukherjee A, Yenisetti SC, Mukherjee S, Mech M (2015) Complete cytogenetic insight of Tho-Tho cattle. Journal of Agriculture, Science and Techonology 5: 277–285. https://doi.org/10.17265/2161-6256/2015.04.006

Moorhead PS, Nowell PC, Mellman WJ, Battips DM, Hungerford DA (1960) Chromosome preparation of leucocytes cultured from human peripheral blood. Experimental Cell Research 20(3): 613–616. https://doi.org/10.1016/0014-4827(60)90138-5

Nakod N (2013) Karyological evaluation of Khillar cattle. M.V.Sc. thesis, Maharashtra Animal and Fishery Sciences University, Nagpur, India, 27 pp.

Potter WL, Upton PC (1979) Y Chromosome morphology of cattle. Australian veterinary Journal 55: 539–541. https://doi.org/10.1111/j.1751-0813.1979.tb07026.x

Potter WL, Upton PC, Blackshaw AW (1979) Presumptive 1/29 autosomal translocation in Australian cattle. Australian Veterinary Journal 55: 209–213. https://doi.org/10.1111/avj.1979.55.5.209

Seabright M (1971) A rapid banding technique for human chromosomes. Lancet 2: 971–972. https://doi.org/10.1016/S0140-6736(71)90287-X

Sumner AT (1972) A simple technique for demonstrating centromeric heterochromatin. Experimental Cell Research 75: 304–306. https://doi.org/10.1016/0014-4827(72)90558-7

Suresh SC, Nagaraja CS, Satheesha GM (2015) Cytogenetic studies in Malnad Gidda cattle. Wayamba Journal of Animal Science 1424965516: 1059–1065.

ORCID

Vemula Harshini https://orcid.org/0000-0001-9484-3444
P. Kumarasamy https://orcid.org/0000-0001-9444-577X
S.M.K. Karthickeyan https://orcid.org/0000-0002-2064-2321

CompCytogen 15(4): 467–505 (2021)
doi: 10.3897/compcytogen.v15.i4.78718
https://compcytogen.pensoft.net

RESEARCH ARTICLE

COMPARATIVE Cytogenetics
A peer-reviewed open-access journal
International Journal of Plant & Animal Cytogenetics, Karyosystematics, and Molecular Systematics

A new species of the genus *Rhaphidosoma* Amyot et Serville, 1843 (Heteroptera, Reduviidae), with data on its chromosome complement

Dmitry A. Gapon[1], Valentina G. Kuznetsova[1], Anna Maryańska-Nadachowska[2]

1 *Zoological Institute, Russian Academy of Sciences, 1 Universitetskaya Emb., St Petersburg 199034, Russia*
2 *Institute of Systematics and Evolution of Animals, Polish Academy of Sciences, Sławkowska 17, 31-016 Kraków, Poland*

Corresponding authors: Dmitry A. Gapon (tentatdag@gmail.com),
Valentina G. Kuznetsova (valentina_kuznetsova@yahoo.com)

Academic editor: Snejana Grozeva | Received 1 December 2021 | Accepted 7 December 2021 | Published 15 December 2021

http://zoobank.org/5787D425-5890-4C6A-A3FB-E9F971CA2DE9

Citation: Gapon DA, Kuznetsova VG, Maryańska-Nadachowska A (2021) A new species of the genus *Rhaphidosoma* Amyot et Serville, 1843 (Heteroptera, Reduviidae), with data on its chromosome complement. CompCytogen 15(4): 467–505. https://doi.org/10.3897/compcytogen.v15.i4.78718

Abstract

A new species, *Rhaphidosoma paganicum* **sp. nov.** (Heteroptera: Reduviidae: Harpactorinae: Rhaphidosomatini), is described from the Dry Zone of Myanmar. It is the fifth species of *Rhaphidosoma* Amyot et Serville, 1843, known from the Oriental Region, and the first record of the genus for Myanmar and Indochina. The structure of the external and internal terminalia of the male and female is described and illustrated in detail. The completely inflated endosoma is described for the first time in reduviids. The complex structure of the ductus seminis is shown; it terminates with a voluminous seminal chamber which opens with a wide secondary gonopore and may be a place where spermatophores are formed. The new species is compared with all congeners from the Oriental Region and Western Asia. It is characterised by the absence of distinct tubercles on the abdominal tergites of the male, the presence only two long tubercles and small rounded ones on the abdominal tergites VII and VI, respectively, in the female, the presence of short fore wing vestiges which are completely hidden under longer fore wing vestiges, and other characters. In addition to the morphological description, an account is given of the male karyotype and the structure of testes of *Rh. paganicum* **sp. nov.** and another species of Harpactorinae, *Polididus armatissimus* Stål, 1859 (tribe Harpactorini). It was found that *Rh. paganicum* **sp. nov.** has a karyotype comprising 12 pairs of autosomes and a multiple sex chromosome system (2n♂=24A+$X_1X_2X_3Y$), whereas *P. armatissimus* has a karyotype comprising five pairs of autosomes and a simple sex chromosome system (2n♂=10A+XY). The males of these species were found to have seven and nine follicles per testis, respectively. FISH mapping of *18S* ribosomal DNA (major *rDNA*) revealed hybridisation signals on two of the four sex chromosomes

(Y and one of the Xs) in *Rh. paganicum* **sp. nov.** and on the largest pair of autosomes in *P. armatissimus*. The presence of the canonical "insect" $(TTAGG)_n$ telomeric repeat was detected in the chromosomes of both species. This is the first application of FISH in the tribe Raphidosomatini and in the genus *Polididus* Stål, 1858.

Keywords

18S rDNA, completely inflated aedeagus, FISH, karyotype, male and female genitalia, morphology, Myanmar, new species, Oriental Region, Reduviidae, *Rhaphidosoma*, taxonomy, testes, $(TTAGG)_n$

Introduction

Harpactorinae are the largest subfamily of Reduviidae, comprising approximately 2,330 species and 320 genera in its worldwide distribution (Swanson 2020). The subfamily is composed of seven tribes: Apiomerini, Diaspidiini, Dicrotelini, Ectinoderini, Harpactorini, Rhaphidosomatini, and Tegeini (Weirauch et al. 2014; Zhang et al. 2015; Schuh and Weirauch 2020). The tribe Rhaphidosomatini Distant, 1904 has unclear circumscription and taxonomic status. Davis (1969) included five genera in this tribe: *Rhaphidosoma* Amyot et Serville, 1843, *Lopodytes* Stål, 1855, *Leptodema* Carlini, 1892, *Hoffmanocoris* China, 1940, and *Harrisocoris* Miller, 1959, while Maldonado Capriles (1990), only three genera: *Rhaphidosoma*, *Lopodytes*, and *Kibonotocoris* Miller, 1953. Swanson (2020), considering the taxonomic history of the tribe, concludes that it "became a 'dumping ground' or 'trash bin taxon' for any long, slender Old World harpactorine assassin bug". The genera *Elongicoris* Hidaka et Miller, 1959, *Floresocoris* Miller, 1958, *Heterocorideus* Schouteden, 1952, *Pseudolopodes* Putshkov, 1985, *Pseudolopodytes* Schouteden, 1957, and *Vibertiola* Horváth, 1909 were not formally assigned to the tribe, but in the descriptions, they were compared with its representatives and share some of the distinctive characters of this tribe.

The genus *Rhaphidosoma* includes about 50 species distributed mainly in the Afrotropical Region. Twelve species are known in the Palaearctic, namely in North Africa and Western Asia, and only three species have so far been known in the Indian and Ceylonese subregions of the Oriental Region. In this article, a new species from the Indo-Chinese Subregion is described. As far as is known, species of this genus live in deserts and savannas in grass or low bushes (Miller 1956; Schuh and Weirauch 2020), and the find of a new species in the Dry Zone of Myanmar corresponds to these conditions.

To clarify the circumscription and status of the tribe Rhaphidosomatini, a detailed examination of the morphology of the listed taxa, with the involvement of new characters, including karyological ones, is necessary, and this work is a small step towards this goal. In particular, the completely inflated endosoma of a new *Rhaphidosoma* species, which has a complex structure and is rich in characters significant for taxonomy, is described for the first time for reduviids, and the structure of the female internal genitalia is also examined.

Our work was aimed also to describe the karyotype of a new species of *Rhaphidosoma* and search for the molecular composition of telomeres and localisation of *45S rDNA* loci in chromosomes of this species and another harpactorine species, *Polididus armatissimus* Stål, 1859 (tribe Harpactorini), distributed in the Oriental and eastern Palaearctic regions. The standard karyotype of *P. armatissimus* was first studied by Banerjee (1958). Data on chromosomal FISH-mapping of repetitive DNAs are the first such data for the tribe Rhaphidosomatini in general. In addition, for both species, we studied the structure of the testes in terms of the number of testicular follicles they contain.

Karyology of Harpactorinae

Previous original papers and revisions reported the chromosome complements of approximately 80 species (3% of the described ones) in about 40 genera (10% of the recognised ones) of Harpactorinae (Kpordugbe 1979; Ueshima 1979; Poggio et al. 2007; Kaur et al. 2012; Kaur and Kaur 2013; Bardella et al. 2014; Souza et al. 2014; Tiepo 2016; Grozeva et al. 2019). The vast majority of the studied species belong to the most species-rich tribe Harpactorini; however, several species have also been studied in the tribes Apiomerini (six species, two genera), Rhaphidosomatini (two species, two genera), and Dicrotelini (one species). Data available today suggest a high karyotypic uniformity of Harpactorinae, regarding the number of autosomes in their karyotypes. Despite the holokinetic nature of chromosomes, which is believed to facilitate karyotype evolution through chromosomal fusions and fissions (fragmentations), most harpactorine species have a diploid autosomal number of 24 (24A) as was concluded earlier by Poggio et al. (2007) based on an almost three times smaller data set. Species with a different number of autosomes (numbers 26, 22, 20, 18, 12, and 10 are presently known) are very rare, the second most common number, 22, being found mainly in the tribe Apiomerini (see Tiepo 2016). Another characteristic feature of harpactorines is multiple sex chromosome systems, with the number of X-chromosomes varying from one to five in different species (XY, X_1X_2Y, $X_1X_2X_3Y$, $X_1X_2X_3X_4Y$, $X_1X_2X_3X_4X_5Y$), while the system $X_1X_2X_3Y$ clearly predominates in the subfamily. Other mechanisms observed in other heteropterans (see Ueshima 1979; Poggio et al. 2007), such as X(0) and its multiple variant $X_n(0)$ as well as XY_n and neo-XY, have not been reported in harpactorines. A simple XY system seems to be characteristic of the tribe Apiomerini (all so far studied species of this small tribe have 2n=22A+XY) and is rarely found in the Harpactorini. It is generally argued that multiple systems usually arise from the simple systems XY or X(0) through chromosome fissions (Ueshima 1979; Poggio et al. 2013), although other mechanisms could also have taken place, e.g. non-disjunctions (Ueshima 1979) or duplications of the X-chromosome (Sadílek et al. 2019). It is also believed that autosomal translocation remnants can be fixed in population as extra sex chromosomes (Perez et al. 2004).

In recent years, knowledge of true bug cytogenetics has advanced significantly due to the use of modern techniques and approaches including chromosomal band-

ings, FISH, GISH, DNA content analysis, etc. (see for review Papeschi and Bressa 2007; Kuznetsova et al. 2021). This is also the case for the family Reduviidae (e.g. Bardella et al. 2014; Pita et al. 2016, 2021; Grozeva et al. 2019; Panzera et al. 2021). In particular, using fluorescence *in situ* hybridisation (FISH), it was shown that assassin bugs of the hematophagous subfamily Triatominae (Pita et al. 2016) and the subfamily Harpactorinae (Grozeva et al. 2019) display the "insect" telomere motif $(TTAGG)_n$. This telomere sequence is considered as the ancestral one in the evolution of Heteroptera (Grozeva et al. 2011) and Hexapoda as a whole (Frydrychová et al. 2004; Vitková et al. 2005; Kuznetsova et al. 2020). It is important to emphasise that this motif was presumably lost by other families of Cimicomorpha; in any case, it could not be found in the families Cimicidae, Nabidae, Tingidae, and Miridae despite repeated attempts to detect it (Grozeva et al. 2011, 2019; Golub et al. 2018 and references therein). FISH with markers that identify specific chromosomes in a karyotype provides a powerful approach to studying general patterns and processes of evolution within a particular group (e.g. Sharakhov 2015). Repetitive DNAs are the main components of eukaryotic genome. FISH mapping of the major *rDNA* (tandemly arrayed *45S rDNA* repeating units encoding for the *28S*, *18S* and *5.8S rRNA*s), the most popular chromosomal landmark used in insect molecular cytogenetics, to reduviid chromosomes has been conducted multiple times. The largest amount of such data has been accumulated for the blood-feeding subfamily Triatominae (known as kissing bugs), in which as many as 92 species belonging to three of the five tribes, and ten of the 18 recognised genera have been studied to date (see Pita et al. 2021). As data accumulated on *rDNA* in triatomine karyotypes, it became clear that the conclusions reached from research on separate triatomine taxa apply to the subfamily as a whole. That is, triatomines are a significantly diverse subfamily in terms of the number and chromosomal location of the *45S rDNA* clusters. Triatomines have from one to four clusters per haploid genome and six distinct chromosomal location patterns (on one or two autosomes, on one, two or three sex chromosomes, on the X chromosome plus one to three autosomes). In triatomines, both number and chromosomal location of the *45S rDNA* clusters are species-specific, and the evolutionary mobility of *rDNA* clusters is supposed to be a driver of species diversification (Panzera et al. 2021; Pita et al. 2021).

The subfamily Harpactorinae is much less studied regarding chromosomal distribution of *rDNA*. Currently, data are available only for seven species in six genera (of the 2330 species described and 320 genera recognised; Swanson 2020), all these species belong to the most species-rich tribe Harpactorini (Bardella et al. 2014; Grozeva et al. 2019).

According to various authors, the tribe Rhaphidosomatini includes five (Davis 1969) down to three (Maldonado Capriles 1990) genera and approximately 90 species. Karyotype data are available for two genera, *Lopodytes* Stål, 1853 and *Rhaphidosoma* Amyot et Serville, 1843; all of them are obtained exclusively using routine methods of chromosomal staining. Different karyotypes were found in the two stud-

ied species, 2n=26(24A+XY) in *Rh. truncatum* Jeannel, 1914 (Kpordugbe 1979) and 2n=27(24A+X_1X_2Y) in *L. quadrispinosus* Villiers, 1948 (Louis and Kumar 1973). It was also shown that *L. quadrispinosus* has testes containing seven follicles (per testis) and ovaries containing seven ovarioles (per ovary); a similar structure of testes and ovaries was also discovered in two other studied species of Rhaphidosomatini, *Lopodytes armatus* Villiers, 1948 and *Rhaphidosoma occidentale* Jeannel, 1914 (Louis and Kumar 1973).

Material and methods

The material for this study was collected by the first author during his expedition to Myanmar. The detailed data on the locality and the quantity of the material is provided in the section "Results and Discussion": in the description of the new species (for *Rhaphidosoma paganicum* sp. nov.) and in the section "Chromosomal analysis" (for *Polididus armatissimus*).

Morphological studies. The male and female terminalia were examined in wet preparations; the aedeagus was also examined in an entirely inflated condition in dry preparations made using the method of inflation by means of glass microcapillaries (Gapon 2001). The pygophores of several pinned specimens were removed and boiled for 2–3 min in 15–20% KOH solution. The abdomen of the female was boiled whole in a similar solution, whereupon the membrane between dorsal and ventral laterotergites was dissected, the abdominal dorsum was removed, and then the boiling of the abdomen without tergites was repeated. Gynatrial membranes and one of the aedeagi were stained with methylene blue. One male was boiled in alkali entirely to study the body sculpture and the endoskeleton. The phallobase and theca are described in repose.

The terminology for male genitalia partly follows Davis (1966); for endosoma, is based on the topographic principle and follows Konstantinov and Gapon (2005); for internal ectodermal genitalia of female, follows Scudder (1959), Štys (1961), Davis (1966), and Gapon (2007). In particular, although the term "gynatrial cone" was proposed by the first author for a morphologically separate part of the gynatrium, which accommodates the male vesica during copulation in Pentatomomorpha, this term is used here for a species that does not have a vesica, since the part of its gynatrium, into which the common oviduct opens, is also morphologically separated and has a distinct structure similar to that of Pentatomomorpha. Membranous elements of the sculpture of the endosoma, which are wider or subequal to their length, are here named tubercles, those that are longer than their width are named lobes.

All measurements are given in millimetres.

The holotype and paratypes of the new species are stored at the Zoological Institute of the Russian Academy of Sciences, St Petersburg, Russia (ZISP).

Chromosome studies. One male of the new species and eight males of *Polididus armatissimus* were studied using conventional chromosome staining and FISH with *18S rDNA* and $(TTAGG)_n$ probes.

Fixation and slide preparation. Whole individuals were fixed immediately after collecting in 3:1 (ethanol: acetic acid) fixative. Chromosome preparations were made from the male gonads. The testes were extracted from the abdomen; testicular follicles were separated from each other in order to determine their number and shape, placed on a slide in a drop of 45% acetic acid, covered with a coverslip, and squashed by gently pressing it. No more than one or two follicles were placed on each slide. The coverslip was removed with a razor blade after freezing with dry ice, and the slide was then dehydrated in fresh fixative (3:1) and air dried.

Routine staining. For this staining, we followed the Schiff-Giemsa method (Grozeva and Nokkala 1996), with 30 min Schiff staining and 40 min Giemsa staining.

Fluorescence in situ hybridisation (FISH). Probes for *18S rDNA* and $(TTAGG)_n$ were prepared and two-colour FISH was carried out as described by Grozeva et al. (2019); for primer information, see Grozeva et al. (2011). The telomere probe was amplified by PCR and labelled with rhodamine-5-dUTP (GeneCraft, Köln, Germany). An initial denaturation period of 3 min at 94 °C was followed by 30 cycles of 45 s at 94 °C, annealing for 30 s at 50 °C and extension for 50 s at 72 °C, with a final extension step of 3 min at 72 °C. The *18S rDNA* probe was amplified by PCR and labelled with biotin-11-dUTP (Fermentas, Vilnius, Lithuania) using genomic DNA of the firebug, *Pyrrhocoris apterus* (Linnaeus, 1758). An initial denaturation period of 3 min at 94 °C was followed by 33 cycles of 30 s at 94 °C, annealing for 30 s at 50 °C and extension for 1.5 min at 72 °C, with a final extension step of 3 min at 72 °C. The chromosome preparations were treated with 100 μg/ml RNase A and 5 mg/ml pepsin solution to remove excess RNA and proteins. Chromosomes were denatured in the hybridisation mixture containing labelled *18S rDNA* and $(TTAGG)_n$ probes (80–100 ng per slide) with an addition of salmon sperm blocking reagent and then hybridised for 42 h at 37 °C. *18S rDNA* probes were detected with NeutrAvidin-Fluorescein conjugate (Invitrogen, Karlsbad, CA, USA). The chromosomes were mounted in an antifade medium (ProLong Gold antifade reagent containing 40,6-diamidino-2-phenylindole (DAPI) (Invitrogen) and covered with a glass coverslip. All nine males examined in both species showed a large number of dividing meiotic cells, then, dozen cells were scanned. We had unfortunately no females to study, and therefore the female karyotypes cannot be mentioned.

Microscopy and imaging. The routinely stained preparations were analysed using an Olympus BX 51 light microscope with an Olympus C-35 AD-4 camera. FISH images were taken using a Leica DM 6000 B microscope with a 100×objective, Leica DFC 345 FX camera, and Leica Application Suite 3.7 software with an Image Overlay module (Leica Microsystems, Wetzlar, Germany). The filter sets applied were A, L5 and N21 (Leica Microsystems). The specimens, from which the chromosome preparations have been obtained, are stored at the Zoological Institute RAS (St Petersburg, Russia).

Results and discussion

Family Reduviidae
Subfamily Harpactorinae
Tribe Rhaphidosomatini
Genus *Rhaphidosoma* Amyot et Serville, 1843

***Rhaphidosoma paganicum* Gapon, sp. nov.**
http://zoobank.org/32F81B06-1A3A-4111-A923-48E7F1A861BA
Figs 1–9

Material examined. ***Holotype*.** Male (glued to rectangular piece of card), **Myanmar**, **Mandalay Region**, nr Nyaung-U Town, 21°10'47.2"N, 94°53'37.9"E, 31.X.2019, D.A. Gapon leg. (ZISP).

***Paratypes*.** Same data as for holotype, 5 males, 1 female mounted as holotype, 3 males in ethanol, 1 male in fixative, with a series of karyological preparations on slides (ZISP).

Description. Body strongly elongated, rod-shaped, with subparallel lateral margins, slightly widened at level of thoracic segments. Antennae and legs long and thin. Both sexes with vestigial fore and hind wings.

***Colouration and integument*.** Body dark reddish-brown, often with blackish sides; ventral surface of abdomen with a more or less distinct median yellowish stripe; tarsi and last two segments of antennae yellowish brown; claws and apex of last segment of rostrum black. Body entirely, except for last two segments of rostrum, covered with dense, adpressed, whitish scale-like setae; they rather long on head, slightly shorter on thorax and abdomen, and very short and sparse on antennae and legs. On abdomen of female, they are shorter than on that of male, therefore looking less dense. Head ventrobasally with very long and dense erect setae; similar long setae, directed anteriorly, located at anterior angles of pronotum; thoracic sternites in their anterior and posterior parts near coxal cavities with dense, rather long, raised setae.

Some setae all over body, including legs and antennae, semierect, located on sparse, rounded, minute setiferous tubercles, those being visible only on wet preparations and hidden by setae on dry specimens. Such tubercles on dorsal and lateral surfaces of postocular part of head larger (looking like granules on dry specimens), bearing relatively long setae. Semierect setae on preocular part of head slightly shorter, becoming longer and denser on dorsal surface of clypeus; several longer setae located laterally anterior to eyes and on antennal tubercles. Ventral surfaces of head and thorax with less long semierect setae, dorsal surface of thorax and whole abdomen with short semierect setae; first segment of each antenna in basal part with semierect setae slightly shorter than thickness of the segment and increasing in length towards its apex; second segment with setae not exceeding its thickness and also with sparse, longer setae; third and fourth segments with very short, semierect setae. Semierect setae on coxae, trochanters and femora rather short, longer, denser on tibiae and becoming longer towards apices of tibia.

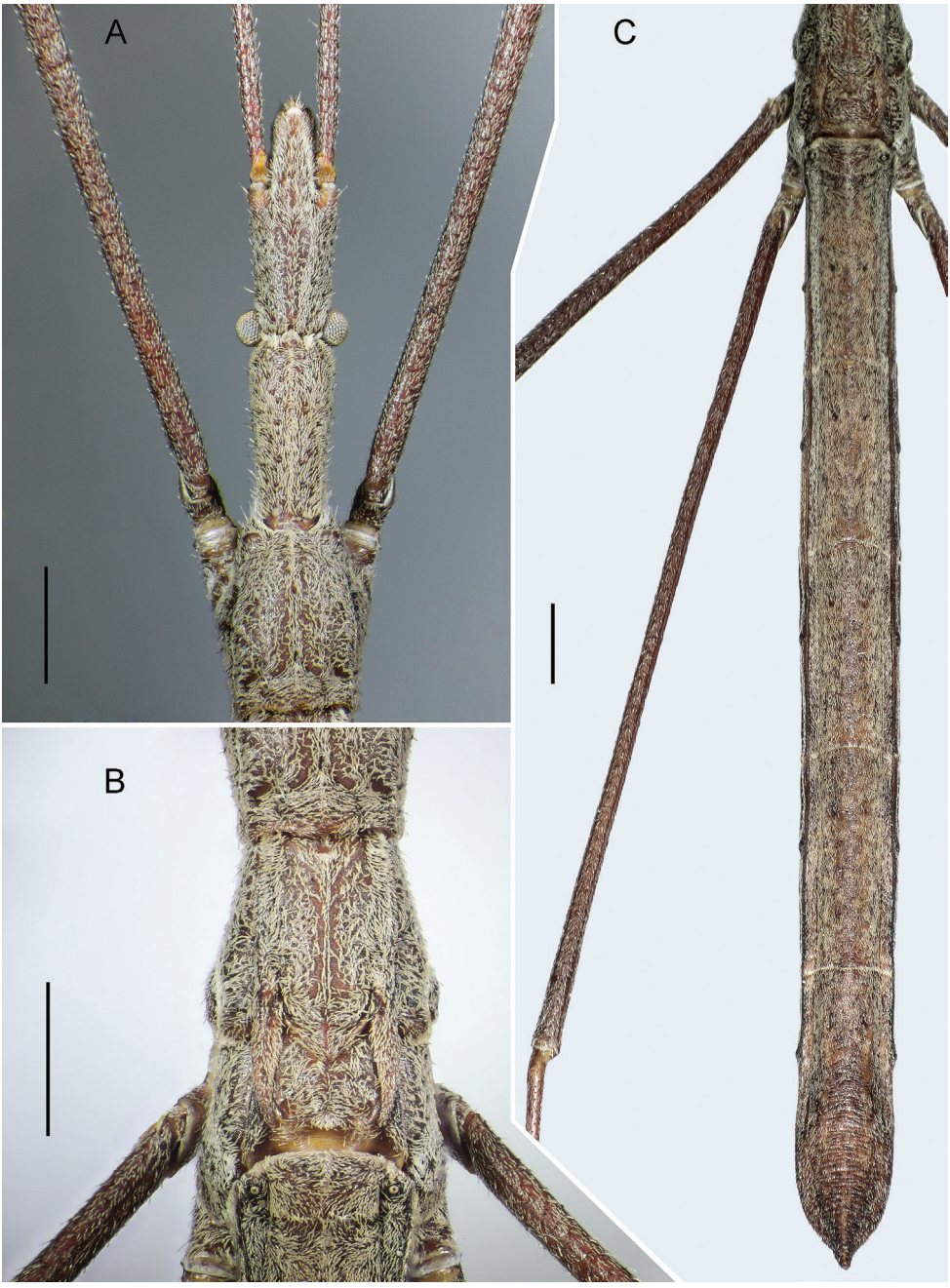

Figure 1. *Rhaphidosoma paganicum* sp. nov., holotype in dorsal view **A** head and prothorax **B** meso- and metathorax **C** abdomen. Scale bars: 1 mm.

V-shaped spot on dorsal surface of preocular part of head, longitudinal stripes on sides of ventral surface of head, a thin medial stripe on ventral surface of abdomen, lateral irregular stripes and extreme margins of abdominal ventrites with very sparse, almost absent pubescence. Rostrum shining, with sparse, very short, semierect setae, only its first visible segment with adpressed pubescence and several longer, semierect setae. Small, round, dark, shining, slightly depressed scarlike marks located in pairs on abdominal tergites: approximately in middle of combined tergites I–III and before middle of each subsequent tergite; the same markings, longitudinal anterior and rounded posterior, located at anterior angle of each abdominal ventrite.

Simple scale-like setae and cuticle between them covered with a white waxy coating, that being especially abundant and thick on ventral surface of body.

Head (Figs 1, 2) long, linear, with deep transverse interocular sulcus. Postocular part of head slightly widened laterally just behind eyes, slightly narrower than anteocular part at level of antenniferous tubercles; its anterior margin with a small medial triangular projection directed anteriad. The part of head anterior to sulcus faintly widening towards antenniferous tubercles. Head dorsally and ventrally almost flat, only slightly convex just posterior to clypeus base. Eyes moderate, hemispherical. Ocelli absent. Clypeus rather wide, conical, slightly flattened laterally, obtuse at apex, without sharp spine anteriorly. Antenniferous tubercles large, far removed from eyes, faintly diverging, completely visible from above. Segments II–IV of antennae thinner than segment I, gradually thinning distally. Maxillary plate triangular, flat. Gena convex. Rostrum straight, reaching middle of fore coxae; its first visible segment significantly not reaching base of antenna, second segment reaching posterior margin of head, but not protruding beyond it; third segment slightly shorter than first one. Labrum short, about three-fifths of first rostral segment.

Thorax (Figs 1–3). Anterior margin of pronotum deeply notched; lateral margins without carinae, almost parallel in posterior half, converging anteriorly in anterior half; posterior margin slightly concave laterally, convex, raised medially. Anterior angles slightly elongated, angularly rounded. Anterior lobe of the pronotum long, slightly convex, with a thin medial sulcus posteriorly; its posterior margin looking like two letters W, i.e. with four triangular projections rising above posterior lobe of pronotum. The latter short, rim-like; its medial area flat, with extremely smoothed medial and lateral carinae converging posteriorly; lateral areas deeply depressed. Pleural areas of prothorax relatively weakly convex, but clearly visible from above. Each epimeron continuing ventrally like a long plate; together they enclose the posterior part of sternite and touch with their inner margins. Rather large, rounded spiracle located on a plate surrounded by membrane under each epimeron and not visible from outside.

Labial sulcus wedge-shaped, tapering posteriorly, with thinnest transverse stridulation ribs, bounded by rounded keels, tapering and converging posteriorly. Coxal cavities located near anterior margin of prothorax, closed posteriorly and open anteriorly, separated from each other by a very narrow, sharp carina. Fore coxae contiguous. Each coxal cavity posteriorly with rather large, rounded fossa, corresponding to large inter-

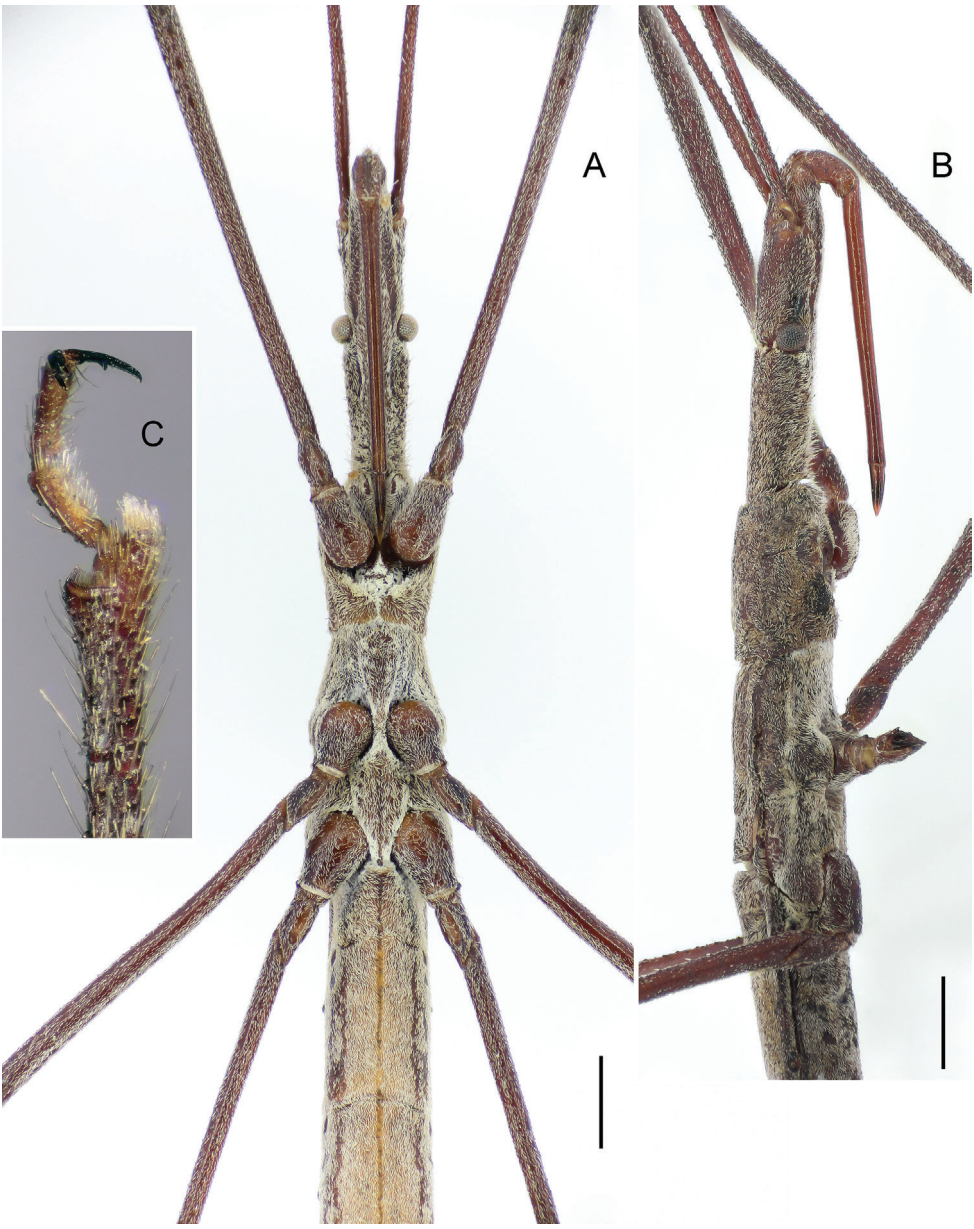

Figure 2. *Rhaphidosoma paganicum* sp. nov. **A** anterior part of body in ventral view **B** anterior part of body in right lateral view (right fore and middle legs omitted) **C** extreme apex of fore leg in anterior view. Holotype (**A**) and paratype (**B, C**). Scale bars: 1 mm.

nal hook-shaped apodeme lying in transverse plane, having flattened apex directed medially and ventrally.

Mesothorax wider than prothorax, trapezoidal, its pleural areas wide, with margins converging anteriorly in dorsal view. Mesonotum narrower than pronotum, its

lateral margins almost parallel, slightly convex in middle, slightly concave anteriorly and posteriorly. Disc slightly convex, without a distinct medial sulcus or carina, laterally bounded along its entire length by a pair of wide flattened carinae, those being strongly smoothed anteriorly and passing into vestiges of fore wings posteriorly. The latter narrow, elongate-triangular, incumbent on metanotum, reaching its posterior margin, slightly curved medially before pointed apices. Scutellum distinct, slightly shorter than its width, convex, fused with mesonotum without distinct suture, with sharp apex and posterior margin bordered by rounded carina thickening towards middle. Small, rounded spiracle located under convex posterior margin of epimeron near dorsal margin of pleurite.

Middle coxal cavities open anteriorly, separated each from other by wider than in prosternum, flat, raised carina. Middle coxae slightly more widely spaced than anterior ones.

Metathorax short, slightly wider than mesothorax, its pleural areas wide in dorsal view, with lateral margins subparallel in anterior part and diverging posteriorly in posterior part. Metanotum slightly wider than mesonotum; its disc rather convex, without a medial sulcus or carina, laterally bounded by lateral carinae. They narrow, subparallel, hidden by vestiges of fore wings in anterior half and, in posterior half, wide, flat, tapering towards posterior ends, reaching posterior margin of metathorax and diverging. Base of each hind wing vestige looking like a narrow longitudinal carina, medially adjacent to anterior half of each lateral carina of metanotum (Fig. 3). Distal part of each vestige shaped as narrow platelike flap with narrowly rounded apex. Vestiges of hind wings completely hidden under those of fore wings. Posterior margin of metanotum tapering trapezoidally posteriorly, roundly convex laterally, finely concave in middle, with small triangular median projection, and framed by thin rounded carina starting from base of posterior part of each hind wing vestige. Posterior part of tergite flat, smooth. Small rounded spiracle located near posterior margin of pleurite in its dorsal part at level of posterior end of metanotal lateral carina.

Hind coxal cavities closed anteriorly, open posteriorly. Hind coxae wider moved apart than middle ones. Space between middle and hind coxal cavities monolithic, rhomboid, elongated posteriorly, with almost flat, barely depressed surface and thin medial sulcus. Ostiole of metathoracic scent gland and evaporatorium absent. Epimeron shaped as large, triangular, convex plate with rounded posterior margin.

Note. It seems that in the description of some species of *Rhaphidosoma*, posterior ends of lateral carinae of the mesonotum are confused with vestiges of the hind wings, which are actually absent in these species. Genuine vestiges of the fore and hind wings are described in this article, and the representation of this character in the genus requires clarification.

Legs. Coxae of all legs longitudinal, swollen; femora and tibiae evenly slender, without any denticles. Anteromedial surface of each fore tibiae subapically with distinct comb (Fig. 2C). Tarsi three-segmented, with a very small first segment. Claws long, thin, slightly curved, with a long thin denticle before middle.

Abdomen (Figs 1, 2, 4) with lateral margins parallel in male and slightly convex towards middle in female. Tergites I, II and III seamlessly merged; on preparations

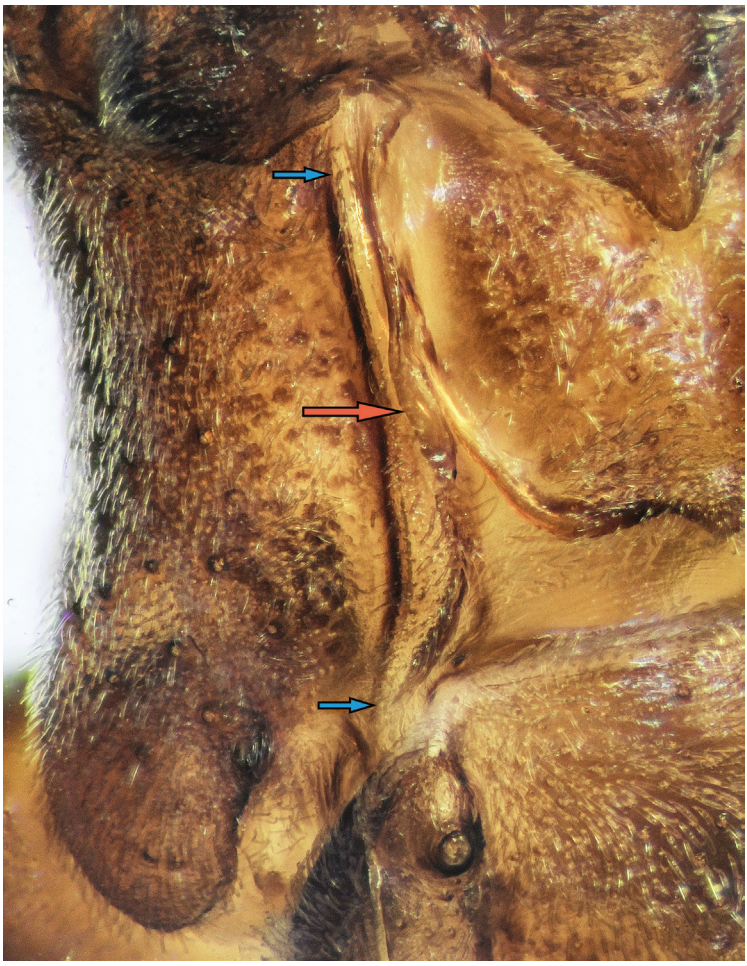

Figure 3. *Rhaphidosoma paganicum* sp. nov., metanotum in left dorsolateral view at a wet preparation, under high magnification. Vestige of the left forewing is removed. Red arrow indicates a vestige of the hind wing, and blue arrows, lateral carina of the metanotum.

cleared in alkali, border between tergites II and III barely discernible as area of weaker sclerotisation. Inner surface of combined tergite I–III at border of short I and longer II tergites with large fragma looking like two contiguous, wide, rather high crests with semicircular ventral margins, anteriorly concave surfaces, and rather long apodeme at each of lateral ends. Tergites evenly, not strongly convex, only base of combined tergite I–III rather strongly elevated. Posterior margins of tergites from III to V rather deeply concave; posterior margin of tergite VI weakly and smoothly concave. Male and female with only two dorsal abdominal scent glands located at anterior margin of tergites IV and V, with openings shaped like an eight (Fig. 4A).

Figure 4. *Rhaphidosoma paganicum* sp. nov. **A** boundary between tergites IV and V, and opening of abdominal scent gland in male (paratype) **B** boundary between tergites V and VI in male (paratype) **C** boundary between tergites VI and VII in male (paratype) **D** apex of abdomen of male (paratype) in right lateral view **E** abdomen of female in dorsal view **F** apex of abdomen of female in right dorsolateral view. Wet preparations (**A–C**) and dry specimens (**D–F**). Red arrows indicate small tubercles on the posterior margin of tergite VI in female. Scale bars: 1 mm.

Ventrites rather strongly convex; boundaries between ventrites II and III on inner side with two slightly spaced, concave, transverse cristae having a cupped shape, concave anteriorly. Posterior margins of ventrites from II to IV rather deeply concave and less concave in subsequent ventrites.

Connexivum separated dorsally by a rather deep depression. Ventral connexival suture present. Dorsal and ventral laterotergites flat, almost vertical.

Spiracles located on small tubercles. First pair of spiracles located dorsally close to anterior margins of corresponding laterotergites; their tubercles directed slightly posteriad (Fig. 1). Spiracles of second pair small, lying very close to spiracles of first pair; third pair of spiracles larger, located slightly behind middle of combined tergite I–III and before middle of ventrite III; other pairs of spiracles located slightly anterior to middle of corresponding tergite and ventrite.

Posterior margin of median tergite VI in male with low, smoothed, transverse medial elevation only with a row of 5–6 setiferous tubercles at posterior margin (Fig. 4C); such elevation on tergite V even less distinct, also with a row of setiferous tubercles (Fig. 4B). Posterior margins of previous tergites only slightly convex in middle. Tergite VII posteriorly weakly widened, with smoothly rounded lateral margins in dorsal view. Posterior margin of this tergite transversely wrinkled, elongated, pointed, strongly raised, protruding far beyond posterior margin of pygophore, carinate at extreme apex (Figs 1C and 4D). Laterotergites VII terminated behind middle of the median tergite, fused with it in dorsal view and, in lateral view, gradually narrowing posteriorly and smoothly passing into thin carina bordering posterior margin of tergite VII. Segment VIII completely retracted into previous segment; its ventral sclerotised part represented by rather long semicircle with oblique anterior margin.

Tergites in female with three weak longitudinal carinae disappearing anteriorly. Posterior margin of tergite VII medially with two long, digitiform, contiguous throughout tubercles, those being located on rather high common elevation and directed dorsoposteriorly (Figs 4E, F and 8A). Posterior margin of tergite VI weakly raised in middle, with two small, rounded tubercles contiguous anteriorly and slightly spaced posteriorly (Fig. 8B). Previous tergites without any distinct tubercles. Tergite VIII short, with medial sulcus and two rather long, slightly spaced conical processes of posterior margin, those being directed posteriorly and slightly dorsally (Fig. 8C). Connexival membrane between dorsal and ventral laterotergites extensive, with multiple thin and one large longitudinal folds (Fig. 8A). Dorsal and ventral laterotergites of segment VIII fused with each other; dorsal ones fused with the median tergite; ventral laterotergite with small spiracle in anterior part. Posterior margin of ventrite VII with small medial triangular projection.

Pygophore (Fig. 5A–C) 2.5 times as long as wide. Its dorsal wall straight, ventral wall strongly and rather smoothly convex before middle, lateral walls almost parallel. Basal foramen large, longitudinally oval, oblique. Lateral and ventral walls sclerotised (ventral one stronger), covered with dense, appressed scale-like setae, as well as sparser, thickened, semierect setae. At extreme base of pygophore, these walls weaker sclerotised, without pubescence. Ventral wall with light medial stripe. Lateral walls membranous

dorsodistally, each with triangular, strongly sclerotised isolated area above base of paramere and anterior to base of proctiger. Paramere attached at anterioventral margin of this membranous area. Dorsal wall of pygophore membranous, deeply folded along midline, without visible border passing into large, cone-shaped, membranous proctiger posteriorly hanging over apex of pygophore. Dorsal and ventral valves of proctiger reinforced with thin horseshoe-shaped sclerites. Laterally, dorsal wall with two longitudinal, weakly sclerotised areas anteriorly covered with thin oblique wrinkles and, posteriorly, with thin, semierect setae. Apex of pygophore rounded in ventral view; medial process highly sclerotised, shaped as wide base with two wide denticles directed ventroposteriad. Genital opening located terminally, bounded by sclerotised apex of pygophore, membranous ventral wall of proctiger and membranous portions of lateral walls of pygophore; it small in repose, but able to stretch strongly due to elasticity of the membranes.

Paramere (Fig. 5D) long and narrow. Corpus cylindrical, without any projections, slightly curved at base, almost straight in rest part. Hypophysis slightly widened and slightly flattened laterally, slightly curved dorsally and medially; its ventral margin more convex than dorsal one; apex rounded; lateral surface, dorsal and ventral margins covered with rather long setae. Parameres located horizontally along lateral walls of pygophore, posteriorly protruding far beyond its apex.

***Aedeagus*.** Basal plates of phallobase (Fig. 6B, C) very long, almost parallel, slightly widening posteriorly in lateral view; their posterior ends C-shaped, curved ventrally and diverging, extreme ends widened, with spoon-shaped depression. Suspensory apodemes short, attached laterally to almost extreme apices of posterior ends of basal plates. Dorsal apodemes very short, attached to ends of basal plates medially and subterminally. Capitate processes large, broadly oval, with irregular margin and extremely short stalk. Plate bridge narrow and rather short. Pedicel short, ductifer absent.

Theca (Fig. 6A–C) cylindrical, slightly flattened dorsoventrally, with almost parallel lateral walls, tapering anteriorly and posteriorly, narrowly rounded at anterior end. Dorsal wall of theca entirely sclerotised ("dorsal phallothecal sclerite"), except for two small weakly sclerotised windows located on either side of place of attachment of phallobase. Basal foramen of theca (Fig. 6D) rather large, located at base of its dorsal wall, longitudinal, bordered by flat, rather wide edging with distinct outer margins fused with membrane connecting theca and basal plates of phallobase. Inner margins of this plate in middle with a pair of triangular projections, posteriorly with a pair of large rectangular inner processes directed slightly into cavity of theca; anterior angle of each of these processes and margin of basal foramen in its anterior part connected by very thin transparent cord.

Ventral wall of theca in basal half with two longitudinal, almost rectangular areas of strong sclerotisation, those being separated by rather wide membranous interval. At extreme base, these areas fused with sclerotisation of dorsal wall of theca, extending onto its lateral sides. In middle of theca length, dorsal sclerotisation extending even further to sides and almost touching lateroapical angles of strongly sclerotised parts of ventral wall. Lateral walls of theca in its basal half between described areas of sclerotisation remain membranous. Apical half of ventral wall of theca membranous, with two

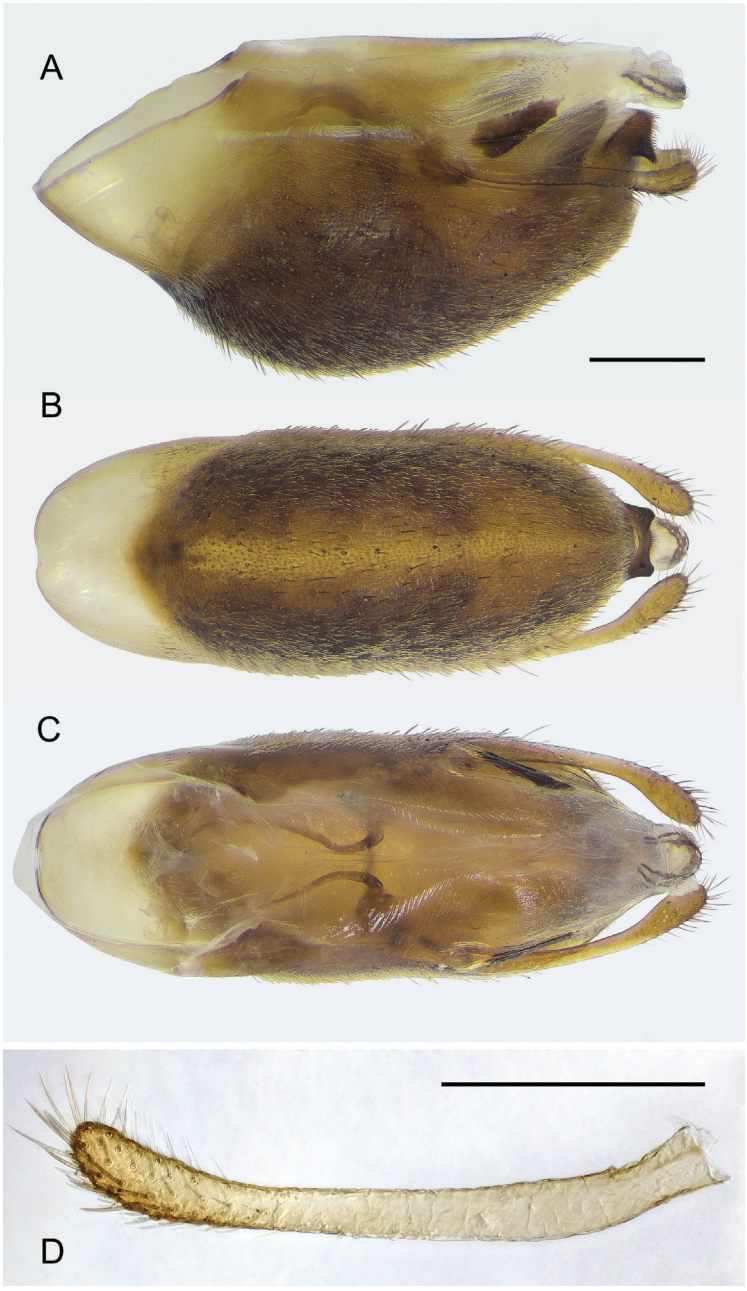

Figure 5. *Rhaphidosoma paganicum* sp. nov., pygophore (**A–C**) and right paramere (**D**) at wet preparations (paratype) **A** left lateral view **B** ventral view (ventral and lateral branches of basolateral lobes of endosoma are slightly protruding beyond theca under the action of osmotic pressure **C** dorsal view **D** right lateral view. Scale bars: 0.5 mm.

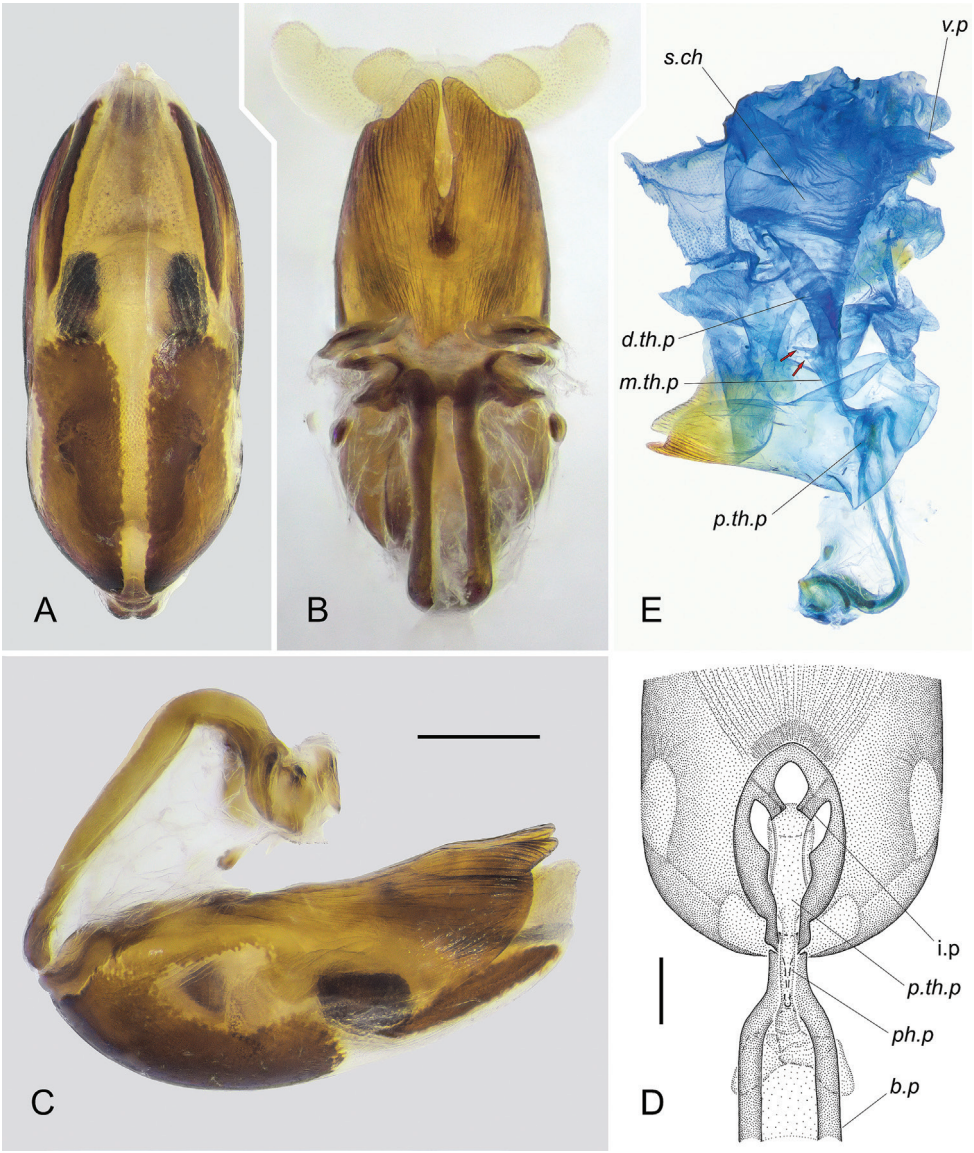

Figure 6. *Rhaphidosoma paganicum* sp. nov., aedeagus (paratype) at wet preparations **A–C** theca and phallobase in ventral (**A**), dorsal (**B**) and left lateral (**C**) view **D** basal foramen of theca in anteriodorsal view (phallobase is strongly unbent anteriad, membrane connecting the basal plates and theca is removed and not shown) **E** ductus seminis in dissected aedeagus, right lateral view. Abbreviations: *b.p* – basal plate of phallobase; *i.p* – inner process of thecal basal foramen; *ph.p* – phallobasal part of ductus seminis; *d.th.p* – distal thecal part of ductus seminis; *m.th.p* – middle thecal part of ductus seminis; *p.th.p* – proximal thecal part of ductus seminis; *s.ch* – seminal chamber; *v.p* – ventral pouch of seminal chamber. Red arrows indicate cords attached to the middle thecal part of ductus seminis. Scale bars: 0.5 mm.

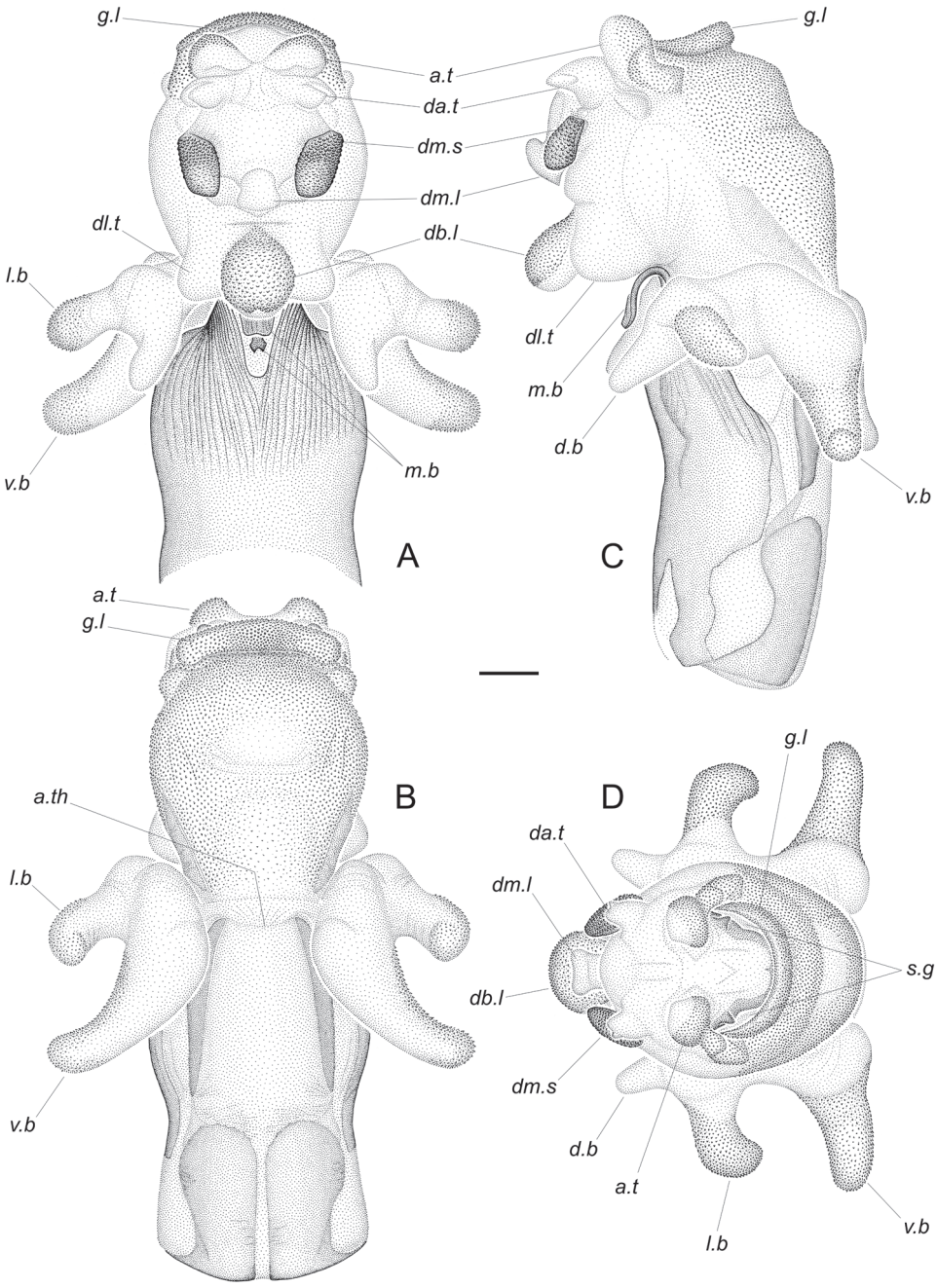

Figure 7. *Rhaphidosoma paganicum* sp. nov., completely inflated aedeagus (paratype) at dry preparations **A** dorsal view **B** ventral view **C** left lateral view **D** caudal view. Phallobase not shown. Abbreviations: *a.t* – apical tubercle; *a.th* – apical margin of theca; *d.b* – dorsal branch of basolateral lobe; *da.t* – dorsoapical tubercle; *db.l* – dorsobasal lobe; *db.t* – dorsolateral tubercle; *dm.l* – dorsomesial lobe; *dm.s* – dorsomesial sclerite; *g.l* – gonoporal lip; *l.b* – lateral branch of basolateral lobe; *m.b* – medial band of the basal part of endosoma; *s.g* – secondary gonopore; *v.b* – ventral branch of basolateral lobe. Scale bar: 0.5 mm.

narrow, highly sclerotised stripes laterally, those being tapering anteriorly and posteriorly. Extreme thecal apex represented by two lobes tapering apically. Dorsal lobe completely sclerotised, with deep, narrow medial notch and external surface striated with dense longitudinal wrinkles. Ventral lobe membranous, trapezoidally rounded apically, with lateral margins reinforced with narrow stripes of strong sclerotisation described above, basally extending under lateral margins of dorsal lobe.

Short unpaired ectodermal vas deferens entering cavity of aedeagus near place of fusion of basal plates (near posterior end of pedicel). Ductus seminis morphologically subdivided into five parts (Fig. 6E): (1) phallobasal part short, narrow, extending into cavity of theca at anterior margin of its basal foramen; (2) proximal thecal part sharply widening at base, wide, running along plane of basal foramen and connecting to inner processes of the latter; (3) middle thecal part curved at right angles to the previous part, narrow at base and gradually widening distally; (4) distal thecal part widening very strongly, funnel-shaped and passing into (5) voluminous seminal chamber opening by very wide secondary gonopore. Ventral wall of seminal chamber with large triangular pouch jutting into cavity of endosoma. At distal end of middle thecal part of ductus seminis, two thin cords (indicated by red arrows in Fig. 6D) attached to its dorsal wall (in another specimen, they are fused with each other into a ring-shaped structure; their functional significance is unclear).

Endosoma (Fig. 7) subdivided into basal and apical parts. Basal part with two large basolateral lobes, each having three branches. Ventral branches long, swollen at base, narrowed in distal part, directed ventrolaterally, with extreme apices rounded, slightly curved dorsoposteriorly; dorsal branches short, tapering towards pointed apices, directed dorsoanteriorlly and slightly diverging; lateral branches located strongly close to dorsal ones on common with them, slightly swollen base, slightly longer than dorsal branches, directed laterally and slightly anteriorly, widened before rounded apices, those being C-shaped, rather strongly curved ventrally. Lateral and posterior surfaces of ventral and lateral branches densely covered with finest microspines directed to apex of corresponding branch. Dorsal wall of basal part of endosoma with narrow, highly sclerotised medial band; distally it passes into a long plate, that being C-shaped, sharply curved anteriad (only on completely inflated endosoma; in repose, this plate almost straight, adjacent to dorsal wall of endosoma), slightly widening distally, with rounded lateroapical angles and notched apical margin. Ventral wall of basal part of endosoma extremely short, delimited from the apical part by transverse fold.

Apical part of endosoma large, obovoid. Its base convex on dorsal side, bearing unpaired dorsobasal lobe and paired dorsobasal tubercles located laterally and slightly more basal than base of the latter. Dorsobasal lobe short, rounded, slightly tapering towards base, directed dorsoanteriorlly. Posterior surface of this lobe with sharply outlined field of microsculpture represented by dense, larger than on basolateral lobes, rather strongly sclerotised, tangentially flattened microspines decreasing towards base of lobe. Apex of lobe with two tiny contiguous tubercles. Dorsobasal tubercles shorter than dorsobasal lobe, tapering broadly to rounded apices directed anterolaterally; surfaces of tubercles without microspines. Distal part of dorsal wall of endosomal apical part smoothly convex, with unpaired dorsomesial lobe, paired dorsomesial sclerites

lying on either side of the latter, and with paired membranous dorsoapical tubercles located even more distally. Dorsomesial lobe small, narrowed basally, widening distally, directed dorsoanteriorlly, slightly curved posteriad, without microsculpture. Dorsomesial sclerites rather large, diamond, with rounded angles, posteriorly fused with wall of endosoma, with anterior ends slightly elevated above the wall. Dorsal surface of each sclerite convex, densely and very finely granulated. Dorsoapical tubercles widely spaced, small, conical, with pointed apices directed dorsally, without microsculpture.

Apex of apical part of endosoma broadly dome-shaped, with paired membranous apical tubercles on dorsal side and transverse membranous protuberance on ventral side. Apical tubercles rather large, almost hemispherical, spaced apart. Membranous protuberance crescent, wide, rounded in cross section, rather thick in middle, thinning dorsally towards ends, bordering secondary gonopore ventrally, and here named gonoporal lip. Secondary gonopore looking like a wide gap between gonoporal lip and apex of endosoma, very short in middle, widening laterally; its dorsal margin at each end with a small conical membranous tubercle and very densely covered with finest microsculpture, resulting in it looking dark brown. Ventral half of each apical tubercle, lateral portions of endosomal apex, and entire gonoporal lip densely covered with microspines becoming denser towards middle of the latter.

Ventral wall of apical part of endosoma flat in proximal part and convex distally, with shallow transversal depression behind middle, entirely covered with finest microspines (those being smaller than at apex of endosoma). Distally, this area of microspines somewhat continuing onto lateral walls and, basally on each side, edged by oblique, very weakly sclerotised band.

Notes on functional morphology, dissection and terminology of the aedeagus. In repose, the basal part of endosoma is simply retracted into the theca, while the large apical part is turned inside out like a glove, and when straightened, it should turn back through a relatively small opening at the basal part of endosoma. This mode of folding the endosoma greatly complicates making preparations of completely inflated aedeagi. Perhaps for that reason and because of the high water pressure required in this case, the only completely inflated preparation that the first author (D.G.) obtained well, burst in two places, on the dorsal ends of the gonoporal lip, and these places were reconstructed in the drawings. It should also be noted that all the microspines in the drawings are shown slightly larger than they are, since D.G. did not have the technical ability to draw them very thin.

Perhaps the sclerotised medial band of the basal part of endosoma corresponds to the merged "struts" of some other reduviids, although D.G. does not quite comprehend what "struts" are as described by Davis (1966); he points out that in "Rhaphidosominae", "the struts are short, widely separated, and attached to the proximal [sic!] edge of the dorsal phallothecal sclerite", but D.G. did not find such structures in the aedeagus of the species described, and he believes that no endosomal structures can attach to the proximal part of the theca.

It is hard not to associate the complex structure of the ductus seminis, the extreme distal part of which is represented by the extensive seminal chamber with the large

pouch and opens by the wide secondary gonopore possessing soft margins, with the presence of spermatophores in insemination in reduviids (about this see e.g. Ambrose and Vennison 1990). It can be assumed that the seminal chamber is the place where spermatophores form or complete their formation.

Female external terminalia (Fig. 8C–E). Gonocoxites I not fused with paratergites VIII, large, convex, trapezoidal, slightly wider than long, with anterior margins laterally straight, slightly concave medially, medioposterior angles truncated, other angles rounded. Gonocoxites I along their entire medial margins connected to each other by long membrane. Gonapophyses I shaped as small triangular plates located at truncate medioposterior angles of gonapophyses I; they slightly more sclerotised than the latter, with rounded apices. First rami absent. Thin, long, sclerotised, slightly S-shaped band beginning from apex of each gonapophysis I and passing in middle of its ventral membranous wall, and then continuing on ventral wall of gynatrium. Tergite IX oblique downward, roof-shaped, with long dorsal slope and short ventral one; in ventral view, it tapers trapezoidally caudad, with two short tubercles on sides of posterior margin, that being shallowly notched between them. Paratergites IX fused with their median tergite (suture between them retained), small, triangularly tapering anteriorly, articulated with lateral margins of gonocoxites I. Gonocoxites II shaped as rather long, narrow plates tapering towards their anterior and posterior ends; the latter continuing under tergite IX; each gonocoxite I in middle of its lateral margin articulated with posterior limb of gonangulum. Gonapophyses II rather large, membranous, acutely tapering towards narrowly rounded apices directed posteriorly. Second rami distinct, looking like strongly sclerotised and rather wide bands running along lateral margins of gonapophyses II; their posterior ends slightly not reaching apices of the gonapophyses, anterior ends arcuate and connected with anterior ends of gonocoxites II. Each gonoplac short and wide, oval, convex medially and shaped as flat, triangular plate laterally. Both gonoplacs connected to each other by narrow membranous suture into single arcuate structure with convex part facing posteriad. Tergite IX, gonocoxites I, gonapophyses I, and medial parts of gonoplacs covered with setae, some of them semierect. Proctiger membranous, retracted inward under tergite IX, with dorsal and ventral valves reinforced with thin horseshoe-shaped sclerites. Wide, rather short, tapering anteriorly, inner membranous fold, that probably being subrectal gland, located between proctiger and dorsal wall of gynatrium; dorsal wall of this fold connecting posterior ends of gonocoxites II.

Gynatrium (bursa copulatrix) (Fig. 9) shaped as voluminous, longitudinally elongated sac reaching anterior margin of ventrite VII. In extreme base, it narrow, sharply widening anteriorly; lateral walls of its base at the level of anterior ends of gonocoxites II with two large depressions jutting into cavity of gynatrium. Distal to base, gynatrium widening gradually, with subparallel lateral walls in anterior half. Anterior wall almost straight, anteriolateral angles broadly rounded. Ventral wall with very large unpaired ring sclerite shaped like very thin edging, that being oval posteriorly and smoothly concave anteriorly. Dorsal wall of gynatrium in its anterior part forming large, external (protruding into body cavity) semicircular fold; its convex part facing posteriad, anterior ends reaching

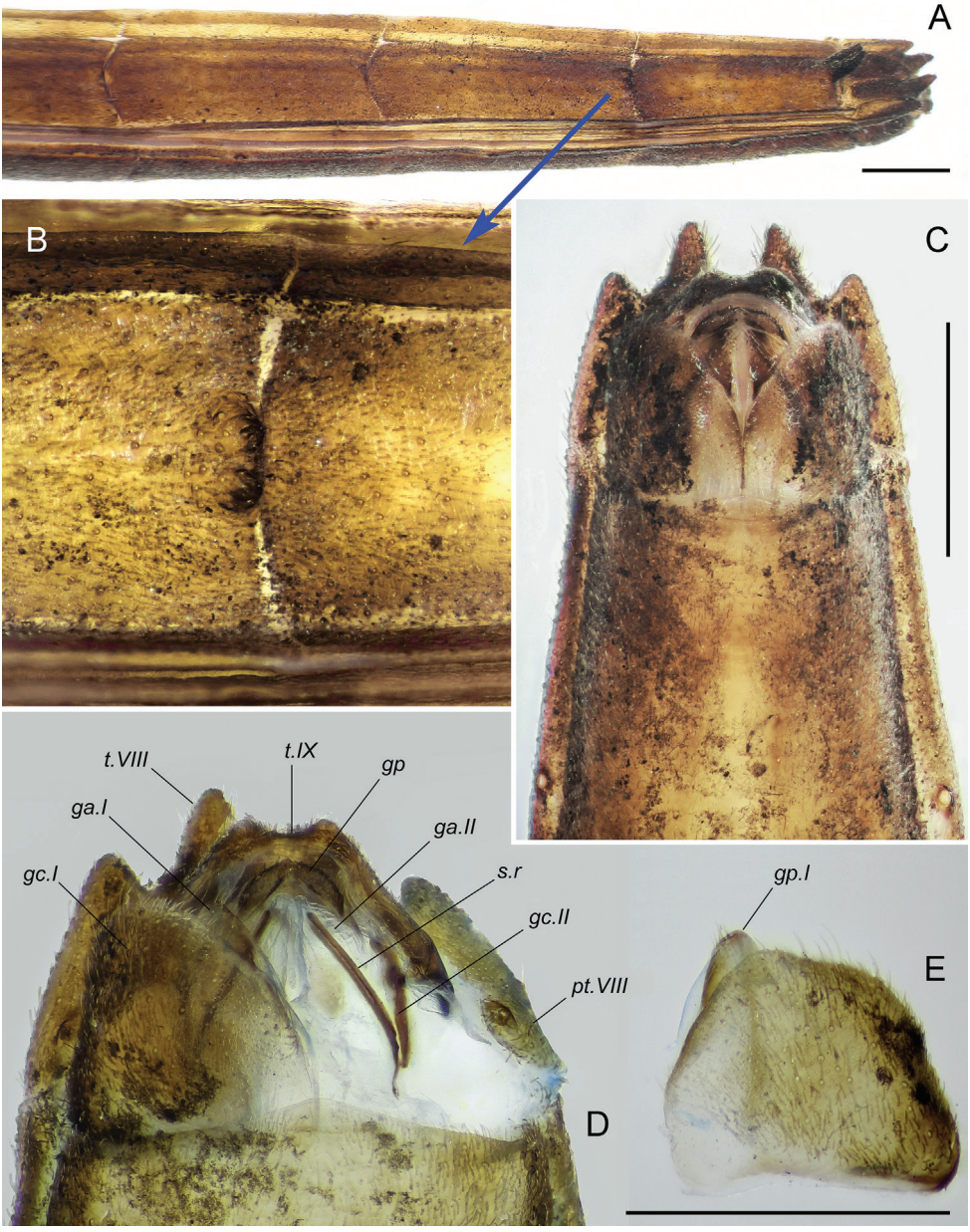

Figure 8. *Rhaphidosoma paganicum* sp. nov., details of the structure of female abdomen, at wet preparations **A** apical part of abdomen in left dorsolateral view **B** boundary between tergites VI and VII under high magnification **C** extreme apex of abdomen in ventral view **D** terminalia in ventral view (right gonocoxite I is removed) **E** right gonocoxite I. Abbreviations: *ga.I* – gonapophyse I; *ga.II* – gonapophyse II; *gc.I* – gonocoxite I; *gc.II* – gonocoxite II; *gp* – gonoplacs; *pt.VIII* – ventral paratergite VIII; *s.r* – second ramus; *t.VIII* – tergite VIII; *t.IX* – tergite IX. Scale bars: 1 mm.

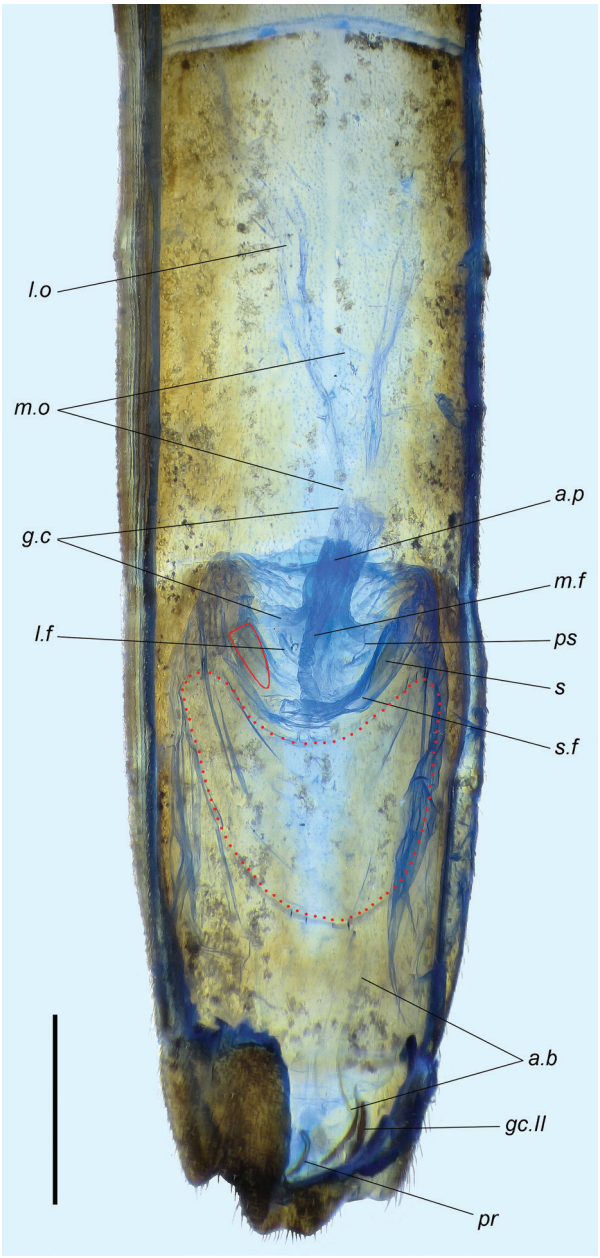

Figure 9. *Rhaphidosoma paganicum* sp. nov., gynatrium in dorsal view, at a wet preparation. Abbreviations: *a.b* – anterior band of gonapophyse I; *a.p* – anterior pouch of gynatrial cone; *g.c* – gynatrial cone; *gc.II* – gonocoxite II; *l.f* – lateral fold of dorsal wall of gynatrium; *l.o* – lateral ectodermal oviduct; *m.f* – median fold of dorsal wall of gynatrium; *m.o* – medial oviduct; *pr* – proctiger; *ps* – supposed duct of pseudospermatheca; *s* – sclerite of semicircular fold (contour of the left sclerite is outlined with a red line); *s.f* – semicircular fold of dorsal wall of gynatrium. Red dotted line outlines the ring sclerite. Scale bar: 1 mm.

anterolateral angles of gynatrium. Ventral (anterior) wall of this fold on each side forming rather large longitudinal sclerite with parallel margins, subrectangular anterior end and triangularly narrowed posterior one. Gynatrial cone large, broadly funnel-shaped, flattened dorsoventrally at extreme base, distally cylindrical, directed anteriad, protruding beyond anterior margin of gynatrium; its walls thick in proximal part and thin, with longitudinal folds in extreme distal part. Deep external median fold extending from semicircular fold to approximately middle of gynatrial cone; its walls posteriorly accordion-folded; anteriorly, this fold forming longitudinal pouch directed anteriad. A pair of small, arcuate folds located posterior to base of gynatrial cone. Just anterior to each of these folds, very thin and rather long thread attaching to dorsal wall of gynatrium [these structures are probably pseudospermathecae, because fragments of a membrane were visible at the distal end of one of the threads, and this membrane is probably part of the destroyed bulb]. Vermiform gland not found. Common oviduct thin-walled, rather long, narrow in place of connection with gynatrial cone, strongly widening anteriorly; ectodermal lateral oviducts rather wide, long, extending beyond anterior margin of ventrite VI.

Measurements (males / female). Body length 19.04–19.89 / 20.23; length of head 3.55–3.78 / 3.58; length of head anterior to transverse sulcus 1.93–2.05 / 2.03; length of head posterior to transverse sulcus 1.73–1.63 / 1.55; width across eyes 0.91–0.95 / 0.93; synthlipsis 0.50–0.53 / 0.50; length of prothorax at midline 1.48–1.70 / 1.58; width of prothorax 1.23–1.30 / 1.28; length of mesothorax 1.28–1.56 / 1.45; width of mesothorax 1.43–1.53 / 1.50; length of metathorax 0.43–0.50 / 0.43; width of metathorax 1.50–1.63 / 1.63; width of abdomen at level of first spiracles 1.13–1.25 / 1.30; length of abdomen 13.40–14.50 / 14.70; length of first antennal segment 6.15–6.50 / 5.50; length of second antennal segment 3.45–3.60 / 3.20; length of third antennal segment 2.55–2.90 / 2.25; length of fourth antennal segment 2.15; total length of labium 3.73–3.93 / 3.75; length of second visible labial segment 2.78–2.98 / 2.78; length of third visible labial segment 0.50–0.55 / 0.53; length of fore coxa 0.78–0.85 / 0.78; length of fore femur 6.70–7.10 / 6.30; length of fore tibia 8.80–9.10 / 8.10; length of middle coxa 0.70–0.78 / 0.73; length of middle femur 5.40–5.90 / 5.70; length of middle tibia 6.70–7.20 / 6.50; length of hind coxa 0.83–0.88 / 0.88; length of hind femur 9.70–10.60 / 9.40; length of hind tibia 11.4–12.6 / 11.3.

Distribution and bionomics. The species was found within the Dry zone in central Myanmar, whose climate, according to the classification of Beck et al. (2018), is dry, steppe, hot, with a low average annual rainfall of less than 1,000 mm and a dry season lasting nine months or longer (Gupta 2005). The specimens were collected by sweeping over grass in areas of a herb-grass steppe with individual thorny shrubs and low trees, particularly from the genus *Acacia* Mill., 1754, interspersed with agricultural landscapes and Buddhist religious buildings (Fig. 10).

Etymology. The specific name *paganicum* is a Latin adjective meaning "heathen"; it is given after the type locality that belonged to the Kingdom of Pagan in the XI–XIII centuries AD.

Comparison. Being predominantly Afrotropical, the genus is represented by only four species in the Oriental Region (*Rh. atkinsoni* Bergroth, 1893, *Rh. tuberculatum*

Figure 10. Habitat in the type locality of *Rhaphidosoma paganicum* sp. nov.

Distant, 1904, *Rh. greeni* Distant, 1906, and *Rh. madukaraiensis* Ravichandran et Livingstone, 1994). Four species are also known from Western Asia (*Rh. argillaceum* Horváth, 1929, *Rh. bergevini* Poppius, 1911, *Rh. lutescens* Poppius, 1911, and *Rh. davatchiae* Dispons et Villiers, 1967), and they must be taken into account in comparison with the new species. All these species were described very superficially, more often from one or two specimens of the same sex, and only one of them, *Rh. atkinsoni*, was recently redescribed in sufficient detail (not counting the male and female terminalia) by Pansare et al. (2017). Since I have no material on these species, except for specimens from Iran and Afghanistan, identified by me as *Rh. tuberculatum*, I consider it necessary to compare all the characters given in the original descriptions of these species with those of the new species.

Differences from Rh. argillaceum [described by Horváth (1929: 331) from one male and one immature shrunken female]. In new species, body dark reddish-brown, often with blackish sides, ventral surface of abdomen with a more or less distinct median yellowish stripe, tarsi and last two segments of antennae yellowish brown [*vs.* body argillaceous, head ventrally and thorax laterally except for coxal cavities black]; head 1.18–1.32 times as long as pronotum and mesonotum combined [*vs.* they of equal length]; preocular part of head 1.18–1.30 times as long as postocular part [*vs.* postocular part slightly longer than preocular part]; first antennal segment 0.88–0.93 times in males and 0.87 times in female as long as fore tibia [*vs.* 0.80 times in male]; mesonotum posteriorly with distinct triangular scutellum and vestiges of fore wings [*vs.* mesonotum posteriorly truncate]; abdomen dorsally without distinct tubercles in male, with a pair of long finger-like tubercles on tergite VII and a pair of small rounded tubercles on tergite VI in female [*vs.* abdomen dorsally unarmed in both sexes; but according to Linnavuori (1973), dorsum of abdomen in female with a longitudinal row of three pairs of erect plug-shaped median tubercles]; longer, body length 19.04–19.89 in males, 20.23 in female [*vs.* 18.50 in male, 19.50 in female].

Differences from Rh. bergevini [described by Poppius (1911: 101) from two males]. Body colouration as stated above [*vs.* yellow-grey, thorax (Mittelkörper) sometimes darkened, abdomen (Hinterkörper) black-brown above, sometimes more or less extensively pale, with pale apex, laterally with yellow spots or completely yellow with regularly broken row of black spots, ventral surface brown, with more or less extensive yellow pattern, antennae and legs yellow, extreme apices of tibiae and last article of tarsus black, femora with black ring before apex]; head 1.18–1.32 times as long as pronotum and mesonotum combined [*vs.* head as long as pro- and mesonotum combined]; first antennal segment not thickened towards base, 1.19–1.24 times in males and 1.09 times in female as long as head and pronotum combined [*vs.* slightly thickened towards base, about 0.71 times (etwa 2/7 kürzer) in males as long as head and pronotum combined]; first antennal segment 1.74–1.81 times in males and 1.72 times in female as long as second segment, second and third segments combined about three times as long as fourth segment [*vs.* first segment a little more than three times as long as second one, fourth segment about as long as previous two segments combined]; second segment of rostrum about five times as long as first segment [*vs.* about four times]; pronotum without median carina [*vs.* pronotum in middle with slightly raised longitudinal carina]; tubercles on abdominal tergites as stated above [*vs.* dorsum of abdomen in female with longitudinal row of four pairs of erect plug-shaped median, according to Linnavuori (1973)]. Body length 19.04–19.89 in males [*vs.* 19.50–20.00].

Differences from Rh. lutescens [described by Poppius (1911: 102) from one female]. Body colouration as stated above [*vs.* yellow, some narrow longitudinal lines and small spots on each side of abdominal dorsum, large spot on each side at base of each dorsal segment, sides of head, sides of thorax, transverse band at base of each ventral segment, first antennal segment basally, extreme apex of tibiae and apex of last tarsal segment brown to brown-black; according to Linnavuiri (1973), body testaceous, sides of head and thorax with longitudinal black band, dorsum of abdomen and connexivum with irregular dark pattern, antennae and legs yellowish]; head 1.18–1.32 times as long as pro- and mesonotum combined [*vs.* head about as long as pro- and mesonotum combined]; preocular part of head long, clypeus apically obtuse [*vs.* head short anteriorly, but clearly pointed]; first antennal segment not thickened towards base, 1.19–1.24 times in males and 1.09 times in female as long as head and pronotum combined, last three segments combined 1.33 times as long as first one, second segment 1.21–1.37 times in males and 1.16 times in females as long as third one and together they almost three times as long as fourth segment [*vs.* first segment slightly and gradually thickened towards base, almost 0.71 times as long as head and pronotum combined, last three segments combined hardly shorter than first one, second and third segments about of equal length, together hardly longer than last segment]; mesonotum without sulci [*vs.* mesonotum at base with two longitudinal sulci]; metanotum without middle carina [*vs.* with three longitudinal carinae, one of which slightly curved on each side, and middle one straight]; dorsum of female abdomen along its entire length with three thin carinae and with tubercles as stated above [*vs.* abdominal dorsum in middle with longitudinal carina completely smoothed anteriorly and slightly raised in

posterior part, from segment II onwards with tubercle, that being small and simple on segment II, gradually becoming stronger on following segments, with clearly forked, darkened tips, tubercle on genital segment (sic!) divided almost to base]; longer, body length 20.23 in female [*vs.* 20].

Differences from Rh. davatchiae [described by Dispons and Villiers (1967: 1070) from one male]. Body colouration as stated above [*vs.* head brown, with postocular part yellowish dorsally, pronotum brown with yellowish base, meso- and metanotum light brown with yellowish lateral carinae, ventrally thorax brown with yellowish margins of coxal cavities (? le pourtour des hanches), abdomen brown with yellowish base of first visible tergite, base of apical "horn" and small spots on connexivum]; head 2.22–2.51 times in males, 2.27 times in female as long as pronotum [*vs.* head relatively robust, 1.50 times in male as long as pronotum]; preocular part of head 1.18–1.23 times in males, 1.31 times in female as long as postocular part [*vs.* 1.50 times in male]; distance between eye and apex of antenniferous tubercle about 3.50 times as long as eye in dorsal view [*vs.* 2.25 times]; interocular space 2.29–2.47 times in males, 2.35 times in female as wide as eye in dorsal view [*vs.* twice as wide as eye in male]; clypeus without prominence [*vs.* clypeus with short triangular prominence anteriorly]; mesonotum approximately 1.60 times as long as wide, its posterior angles rounded, posterior margin with distinct triangular scutellum and vestiges of fore wings [*vs.* mesonotum subrectangular, almost 1.50 times as long as wide (39:27), its posterior angles obliquely truncated, base concave with outline of median carina; according to the drawing (Dispons and Villiers 1967, fig. 1), posterior margin with medial notch, without distinct scutellum and wing vestiges]; metanotum wider than length, without distinct medial carina, its posterior margin with convex lateral parts, concave medially, with small triangular projection, vestiges of hind wings present [*vs.* metanotum slightly longer than wide, distinctly shorter than mesonotum, with three longitudinal carinae; according to the drawing (Dispons and Villiers 1967, fig. 1), posterior margin uniformly concave, vestiges of wings apparently absent, and what is mistaken for the latter in the description is a continuation of the lateral carina]; tergite VII of male almost three times as long as wide, smoothly and slightly widened anterior to apex, apical carina narrow [*vs.* tergite VII twice as long as wide, with greatest width at level of apical five seventh, where its sides slightly angular; according to the drawing (Dispons and Villiers 1967, fig. 1), apical carina of tergite VII wide]; longer, body length in males 19.04–19.89 [*vs.* 16.00].

Distinguished from Rh. atkinsoni [described based on an unspecified number of specimens (presumably males), redescribed by Pansare et al. (2017) from two males and two females] by following main characters. In male, thorax and abdomen with more or less evenly distributed setae, dorsally without lateral stripes of dense setae; pubescence on abdomen ventrally less dense. Lateral margins of head just posterior to transversal sulcus less convex; entire dorsum of head, including area just posterior to sulcus, almost flat [*vs.* tumescent]. First segment of rostrum noticeably shorter than preantennal part of head [*vs.* almost as long as preantennal region]. Pronotum only slightly convex dorsally [*vs.* tumescent above], its posterior margin slightly convex in middle and concave laterally [*vs.* straight]. Metanotum uniformly convex in posterior part of disc, without

carina [*vs.* with median raised area or blunt carina along its length], with posterior margin convex laterally, concave in middle [*vs.* sinuate]. Ventral parts of posterior lobe of prothorax (epimera) contiguous [*vs.* not meeting each other, with a noticeable gap in the midline]. Thoracic segments dorsally and ventrally without granules [*vs.* provided with few dark brown granules]. Boundary between metasternite and abdominal ventrite II distinct [*vs.* indistinct]. In males, medial part of abdominal tergites not shining, all tergites without mid-dorsal tubercles [*vs.* median part of each tergite shining; third and fourth tergites with small mid-dorsal tubercle]; posterior margin of tergite VI in middle slightly elevated, that of tergite V elevated even less strongly, these areas not shining [*vs.* posterior border of tergites III–VI medially slightly elevated as small shining tubercle]. In female, tergite V in middle of posterior margin without distinct tubercle, tergite VI with two small rounded tubercles, tergite VII with two large finger-like tubercles located on strongly raised base [*vs.* tergite V with small mediodorsal tubercle at posterior border, tergite VI with a pair of small tubercles, and tergite VII with a pair of small, posteriorly directed blunt tubercular projections on either side of midline]. Posterior margins of laterotergites and median tergite VIII with rather long triangular projections [*vs.* posterior margins of laterotergites rounded, posterior margin of tergite with very short, smoothed projections]. Male and female terminalia are not well described for comparison. Pygophore more smoothly convex ventrally in lateral view, with more parallel lateral margins and two denticles of medial process at apex in ventral view [*vs.* sharply and almost triangularly convex ventrally, rhomboid-like widening before apex, the latter with one triangular denticle in ventral view, according to the photographs (Pansare et al. 2017, figs 32–34)]. Paramere less strongly curved at base and more strongly at slightly widening apex [*vs.* apex uniformly narrow, straight, according to the photographs (Pansare et al. 2017, figs 32–34)]. Shorter, body length 19.04–19.89 in males, 20.23 in female [*vs.* 25.10 in males, 23.50 in females].

Differences from Rh. tuberculatum [described by Distant (1904: 330) based on an unspecified number of specimens, presumably from female(s)]. Body colouration as stated above [*vs.* pale greyish, tibiae and last two joints of antennae pale ochraceous]; thorax dorsally without small tubercles [*vs.* with marginal series of small tubercles on each side of thorax above, a number of small discal tubercles to pronotum]; only tergites V and VI in females with paired tubercles [*vs.* two prominent tubercles at posterior margins of third (IV), fourth (V), fifth (VI), and sixth (VII) abdominal segments]; apex of head tapered, obtuse [*vs.* distinctly porrectly spinous]; first antennal segment 1.21–1.46 times in males, 1.20 times in female as long as distance from eye to base of thorax [*vs.* first joint of antenna about as long as from eyes to base of thorax]; head very slightly swollen laterally behind eyes [*vs.* head distinctly tumid behind eyes]; pronotum slightly convex, its anterior angles angularly rounded [*vs.* convexly tumid, its anterior angles sinuously produced]; vestiges of both pairs of wings present [*vs.* absent in available for me specimens]. Shorter, body length 19.04–19.89 in males, 20.23 in female [*vs.* 23].

Differences from Rh. greeni [described by Distant (1906: 367) based on an unspecified number of specimens, presumably from male(s)]. Body colouration as stated

above [*vs.* piceous black, intermediate and hind tibiae dull ochraceous, tarsal claws piceous, antennae pale castaneous brown, abdomen above pale piceous brown, a central longitudinal fascia and the lateral margins black]; preocular part of head 1.18–1.30 times as long as postocular part [*vs.* head elongate, ante- and postocular portions almost subequal in length]; first antennal segment 1.10–1.12 times in males and 0.96 times in female as long as middle femora [*vs.* antennae first joint as long as middle femora]; second antennal segment 1.21–1.37 times in males, 1.42 times in female as long as third one and they combined approximately equal to first segment [*vs.* second and third joints subequal in length and each considerably shorter than first]; fore femora longer than middle femora [*vs.* fore and middle femora subequal in length]; hind femora 0.71–0.78 times in males, 0.64 times in female as long as abdomen, hind tibia 0.87–0.91 times in males, 0.77 times in female as long as abdomen [*vs.* hind femora a little shorter and hind tibiae a little longer than abdomen]. Shorter, body length 19.04–19.89 in males, 20.23 in female [*vs.* 25].

Differences from Rh. madukaraiensis [described by Ravichandran and Livingstone (1994: 106) from males (and presumably female)]. Body colouration as stated above [*vs.* concolourous, griseous, antennae concolourous, castaneous, connexivum (abdomen?) ventrally griseous, with a median longitudinal line]; preocular part of head 1.18–1.30 times as long as postocular part [*vs.* anteocular and postocular areas subequal in length]; postocular part of head slightly tapering to base [*vs.* tumid throughout]; second antennal segment 1.21–1.38 times in males, 1.42 times in female as long as third segment and 1.6 times as long as fourth one, third and fourth segments combined 0.70 times as long as second segment [*vs.* pedicel and flagellar segments equal]; pronotum slightly convex dorsally, its lateral margins almost parallel posteriorly and converging anteriorly, pubescence as on other segments of thorax [*vs.* pronotum slightly globose, spotted, almost bare]; mesonotum trapezoidal, rather weakly convex [*vs*. nodule like]; matanotum without medial carina, its posterior margin with convex lateral parts, distinctly concave medially, with small medial prominence [*vs.* metanotum medially carinate, posteriorly obscurely concave]; abdominal tergites without distinct tubercles in male, with small paired rounded tubercles on tergite VI and long tubercles on tergite VII in female [*vs.* second (III), third (IV), fourth (V) and fifth (VI) segments dorsally with a forked tubercle]. Shorter, body length 19.04–19.89 in males [*vs.* 20 in males].

Note. According to the description of *Rh. madukaraiensis*, it differs from *Rh. tuberculatum* "by the total absence of thoracic tubercles, cephalic spine and by the obscure development of scutellum, wing pads and mesonotal median carina". In the specimens of *Rh. tuberculatum* available to the first author, vestiges of the fore and hind wings are completely absent. The relief triangular structures in the posterior angles of the metanotum, which can be mistaken for vestiges of the hind wings, are in fact lateral carinae. Scutellum of *Rh. tuberculatum* is very small, much smaller than that of the new species; the mesonotal median carina is absent in both of these species. According to the description of *Rh. madukaraiensis*, the type series (holotype and several paratypes) consists of males only, but the listed characters of the sculpture of abdominal tergites

and the phrase “behind the fifth segment the abdomen abruptly terminates” correspond to the female. The median tergite and paratergites VIII in the female of the new species have rather large triangular prominences on the posterior margins.

Chromosomal analysis

Karyotypes

Rhaphidosoma paganicum sp. nov.

Based on the analysis of the only male (paratype) available for such a study, we conclude that the male chromosome complement of the species comprises 12 pairs of autosomes and a multiple sex chromosome system, $X_1X_2X_3Y$, i.e., n=16(12AA+$X_1X_2X_3$Y) and 2n=28(24A+$X_1X_2X_3$Y). The autosomal bivalents make up a decreasing size range; of the four sex chromosomes, Y is the largest, and all three X-chromosomes are approximately the same size (Fig. 11A–D). At early condensation stage of the first meiotic prophase, sex chromosomes are grouped together as four heteropycnotic bodies, with all X-chromosomes located in a train and the Y placed away from them (Fig. 11A). At metaphase I (MI), the sex chromosomes appear clearly separated from one another; they are lying side by side inside the ring formed by autosomal bivalents and show no visible physical connection with each other (Fig. 11B, C). FISH with two repetitive DNA probes, *18S rDNA* and telomeric $(TTAGG)_n$, visualised, on the one hand, clusters of *rRNA* genes on the Y-chromosome and on one of the X-chromosomes, and, on the other hand, the $(TTAGG)_n$-signals at both ends of each chromosome (Fig. 11D) and also in spermatids (Fig. 11E).

As mentioned in Introduction, the most common karyotype of Harpactorinae includes 2n=28(24A+$X_1X_2X_3$Y), and *Rh. paganicum* sp. nov., thus, shares this modality with regard to both the number of autosomes and the sex chromosome system. Previously, there was only one species in the genus *Rhaphidosoma* with a known (standard) karyotype, *Rh. truncatum* Jeannel, 1914. According to Kpordugbe (1979), this species possesses the karyotype of 2n=26(24A+XY), i.e., *Rh. truncatum* has 24A as *Rh. paganicum* but, unlike it, a simple sex chromosome system. We can assume that the multiple sex chromosome system of *Rh. paganicum* arose because of the fragmentation of the X-chromosome in the ancestral karyotype with the XY-system. This character is interesting in light of the fact that the new species seems to have several more primitive morphological characters than in *Rh. truncatum*, in particular, distinct vestiges of the fore and hind wings, which are not mentioned for the latter in the description by Jeannel and are not shown in his drawing (Jeannel 1919, fig. 60).

Polididus armatissimus Stål, 1859

Material examined. **Thailand**, **Mae Hong Son Prov.**, Pai Distr., near Pai Town, 19°21'25.8"N, 98°27'01.0"E, 12,13.XI.2019, at light, D.A. Gapon leg., 8 males (ZISP).

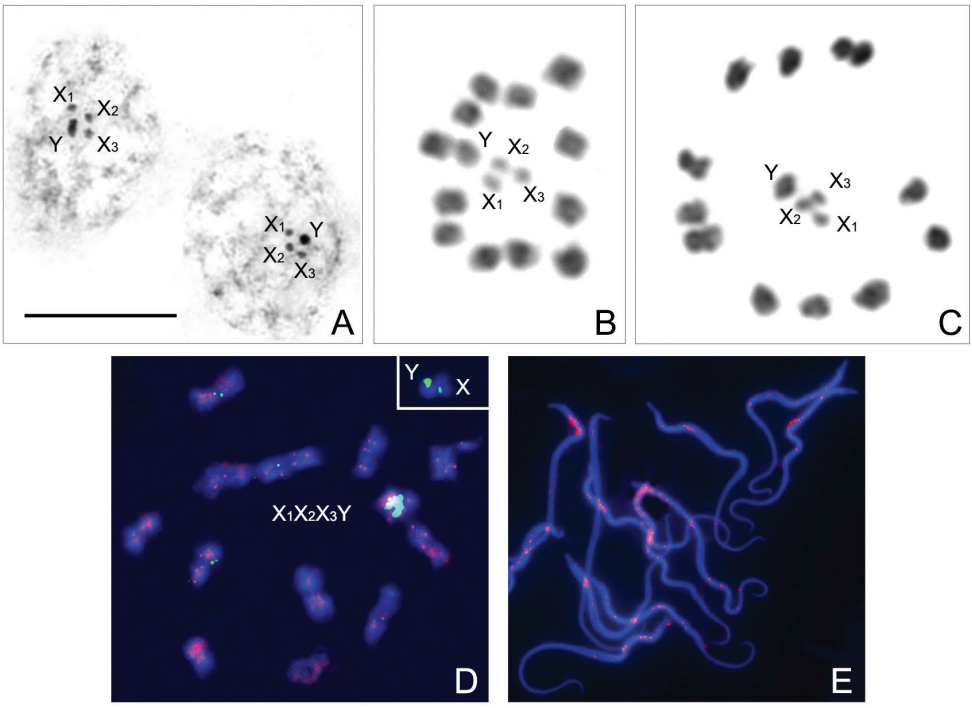

Figure 11. Male meiotic chromosomes of *Rhaphidosoma paganicum* sp. nov., n=12AA+$X_1X_2X_3Y$ (2n=24A+ $X_1X_2X_3Y$) **A** first prophase, early condensation stage (chromosomes $X_1X_2X_3$ are located in a train and the Y is located slightly away from them) **B, C** metaphase I (sex chromosomes $X_1X_2X_3Y$ are lying side by side inside the ring formed by autosomal bivalents) **D** hybridisation signals of *18S rDNA*-FISH (green) and $(TTAGG)_n$-FISH (red) are visible on Y and one of the X-chromosomes (small green signals are also seen in some autosomal bivalents, but they proved to be not specific), and on both ends of each chromosome, respectively; **Inset**, Y and an X-chromosome with *18S rDNA* signals **E** $(TTAGG)_n$-FISH-signals are visible in spermatids. Scale bar: 10 μm.

Based on the analysis of eight males, we conclude that the male chromosome complement of *P. armatissimus* comprises five pairs of autosomes and a simple sex chromosome system, XY, i.e., n=7(5AA+XY) and 2n=12(10A+XY) as previously noted by Banerjee (1958). The autosomal bivalents are clearly larger than in *Rh. paganicum* sp. nov. and make up a decreasing size series. The X- and Y-chromosomes are close to each other in size being at the same time significantly smaller than autosomes (Fig. 12A–E). At the first meiotic prophase, sex chromosomes are grouped together and appear as two heteropycnotic bodies (Fig. 12A). The autosomes are associated by one or, in some bivalents, two chiasmata, and the sex chromosomes form a pseudo-bivalent (Fig. 12B–D). FISH with probes for *18S rDNA* and $(TTAGG)_n$ visualised *rDNA* clusters located on the largest autosomal bivalent (AA1) and positive $(TTAGG)_n$-signals at both ends of each chromosome (Fig. 12E).

It should be noted that *P. armatissimus* has the lowest number of autosomes (10A) ever recorded in Harpactorinae. It was previously shown that males of this species orig-

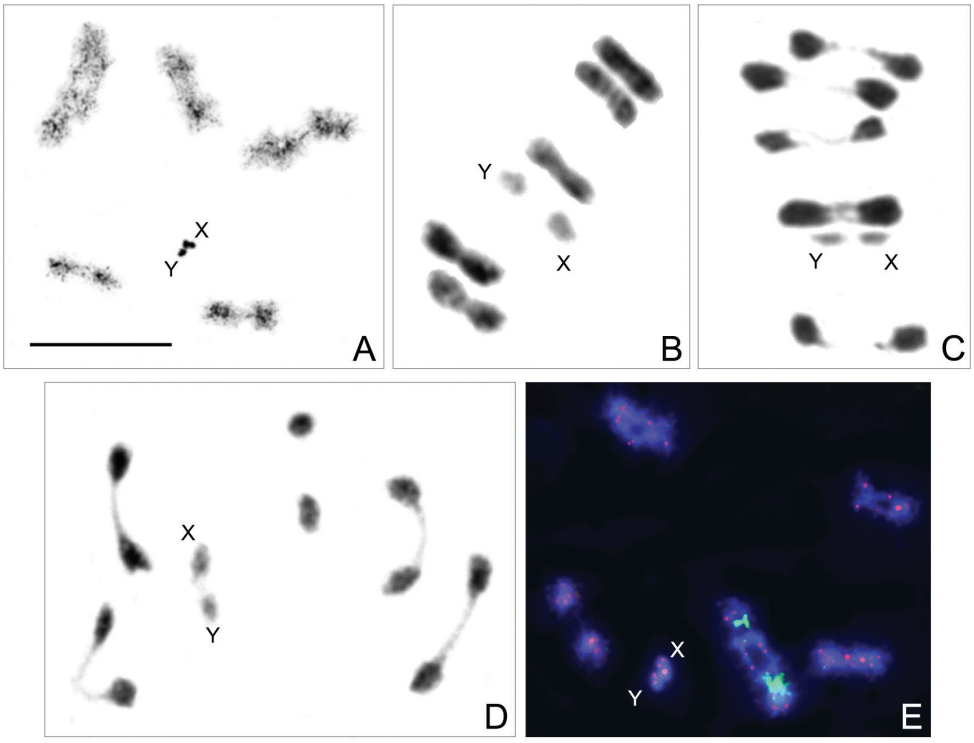

Figure 12. Male meiotic chromosomes of *Polididus armatissimus* Stål, 1859, n=5AA+XY (2n=10A+XY) **A** diplotene/diakinesis; heteropycnotic X- and Y-chromosomes form a pseudo-bivalent **B, C, D** metaphase I/anaphase I transition; X- and Y-chromosomes form a pseudo-bivalent **E** hybridisation signals of *18S rDNA*-FISH (green) and $(TTAGG)_n$-FISH (red) are visible on AAI and on both ends of each chromosome, respectively. Scale bar: 10 μm.

inated from Japanese and Indian (Calcutta) populations also have 2n=12(10A+XY), although males from northwest India were reported to have 2n=14(12A+XY) (see for references Ueshima 1979).

Telomeres

Telomeres of both *Rh. paganicum* sp. nov. and *P. armatissimus* have clearly demonstrated presence of the TTAGG repeat, which constitutes the first report of the $(TTAGG)_n$ telomere motif in the tribe Raphidosomatini and in the genus *Polididus* (Harpactorini). This so-called "insect" repeat is considered an ancestral DNA motif of insect telomeres (Frydrychová et al. 2004; Kuznetsova et al. 2020). Recent research has revealed several examples of heterogeneity for presence/absence of the $(TTAGG)_n$ motif in different insect groups (see for references Kuznetsova et al. 2020), and such heterogeneity was also found in Heteroptera, including the infraorder Cimicomorpha. Thus, no hybridisation signals were detected in the families Nabidae, Miridae, Tingidae, and Cimicidae in the

experiments using FISH with the $(TTAGG)_n$ telomeric probe; moreover, the TTAGG telomeric sequence was not found in the sister to Cimicomorpha infraorder Pentatomomorpha (see for references Grozeva et al. 2019). On the contrary, the telomere motif $(TTAGG)_n$ appears to be characteristic of all studied species of the family Reduviidae (in total, eight species and six genera of the largest reduviid subfamilies, Triatominae and Harpactorinae). These species are as follow: *Dipetalogaster maxima* Uhler, 1894, *Rhodnius prolixus* Stål, 1859, *Triatoma infestans* Klug, 1834, and *T. dimidiata* Latreille, 1811 from Triatominae (Pita 2016), as well as *Rhaphidosoma paganicum*, *P. armatissimus*, *Rhynocoris punctiventris* (Herrich-Schäffer, 1846), and *Rh. iracundus* (Poda, 1761) from Harpactorinae (Grozeva et al. 2019; present study). Although the available data are still sparse, they allow suggestion that the $(TTAGG)_n$ motif is characteristic of the whole family Reduviidae. Moreover, it was hypothesised that an ancestor of the branch Cimicomorpha + Pentatomomorpha possessed this motif that retained in the Reduviidae but was then repeatedly lost by other families of this branch (Grozeva et al. 2019). This character together with other plesiomorphic characters such as the presence of the first pair of abdominal spiracles, the spermatophore insemination, and a place of fertilisation in the ectodermal parts of the female oviducts confirms the hypothesis (Schuh and Štys 1991; Schuh et al. 2009) of the basal position of the superfamily Reduvioidea on the phylogenetic tree of Cimicomorpha.

18S rDNA

We found that the genes encoding the major *rRNA*s were located differently in *Rh. paganicum* sp. nov. and *P. armatissimus*. These species have different numbers of autosomes (24A and 10A, respectively) and different sex chromosome systems ($X_1X_2X_3Y$ and XY, respectively); however, there seems to be no correlation between these two characters and the *rDNA* chromosomal location in Harpactorinae (Table 1). Table 1 summarises the location of the *18S rDNA* clusters in nine species of Harpactorinae studied until now. These species belong to six genera and three of the seven recognised tribes, Apiomerini (1 species), Harpactorini (7 species), and Rhaphidosomatini (1 species). The species analysed present three (10A, 12A and 24A) of the six numbers of autosomes (excluding 18A, 20A, and 22A) and two (XY and $X_1X_2X_3Y$) of the five sex chromosome systems (excluding X_1X_2Y, $X_1X_2X_3X_4Y$ and $X_1X_2X_3X_4X_5Y$) described in Harpactorinae. The studied species are still very few. Despite this, we can identify four distinct patterns of *rDNA* location in Harpactorinae. First, *rDNA* clusters can be located on the largest pair of autosomes (found in three species with XY and different autosome numbers). Second, they can be located on both sex chromosomes (in one species with XY). Third, they can be located on X-chromosome (in one species with XY). Fourth, they can be located on Y-chromosome and one of the X-chromosomes (in all four species with 24A and $X_1X_2X_3Y$). We can assume that the subfamily Harpactorinae has a very high level of *rDNA* location diversity that is comparable to the diversity observed in the much better studied subfamily Triatominae (see Introduction). Moreover, it is very likely that such diversity is characteristic of the family Reduviidae as a whole.

Table 1. Chromosomal location of genes for *18S rRNA* in karyotypes of nine species of the subfamily Harpactorinae studied to date.

N	Species	2n	Location of *18S rDNA*	Reference
	Tribe Apiomerini			
1	*Apiomerus lanipes* (Fabricius, 1803)	24(22A+XY)	X and Y	Bardella et al. 2014
	Tribe Harpactorini			
2	*Cosmoclopius nigroannulatus* (Stål, 1860)	28(24A+$X_1X_2X_3Y$)	Y and one of Xs	Bardella et al. 2014
3	*Montina confusa* (Stål, 1859)	14(12A+XY)	AAI	Bardella et al. 2014
4	*Polididus armatissimus* Stål, 1859	12(10A+XY)	AAI	Present paper
5	*Repipta flavicans* (Amyot et Serville, 1843)	20(18A+XY)	One of sex chromosomes	Bardella et al. 2014
6	*Rhynocoris iracundus* (Poda, 1761)	28(24A+$X_1X_2X_3Y$)	Y and one of Xs	Grozeva et al. 2019
7	*Rhynocoris punctiventris* (Herrich-Schäffer, 1846)	28(24A+$X_1X_2X_3Y$)	Y and one of Xs	Grozeva et al. 2019
8	*Zelus laticornis* (Herrich-Schäffer, 1853)	26(24A+XY)	AAI	Bardella et al. 2014
	Tribe Rhaphidosomatini			
9	*Rhaphidosoma paganicum* sp. nov.	28(24A+$X_1X_2X_3Y$)	Y and one of Xs	Present paper

Testes

We found that the testes of *Rh. paganicum* sp. nov. and *P. armatissimus* males are located laterally at the sides of the alimentary tract, approximately in the middle of the abdominal cavity. The species have seven and nine elongated follicles per testis, respectively. In *Rh. paganicum*, the follicles have similar length and width; they are arranged side by side being connected by bases. In *P. armatissimus*, the structure of the testis turned out to be more complex. The follicles are folded three times onto each other and wrapped with a reddish peritoneal sheath. Moreover, they form two groups, one consisting of seven long and wide follicles and the other consisting of two smaller follicles. The same testis structure, although with a different ratio of large and small follicles, is also characteristic of some other species of Reduviidae (Louis and Kumar 1973; Freitas et al. 2007). In Rhaphidosomatini, all the three species studied so far (*Rhaphidosoma occidentale*, *Lopodytes armatus*, and *L. quadrispinosus*) also have seven follicles per testis (Louis and Kumar 1973) and it is so with other Harpactorinae species (e.g. Gomes et al. 2013). Moreover, the testis comprising seven follicles seems to be the plesiomorphic condition for Reduviidae, because this number was found in many species throughout the group (Louis and Kumar 1973 and references therein), and for Heteroptera as a whole (Akingbohungbe 1983). Since this number corresponds to the number of pre-genital segments in adult males, it is considered as the initial character state in insects in general (Sharov 1966). The initial number can decrease or increase in oligomerisation or polymerisation processes, which proceed independently in different Heteroptera lineages (Pendergrast 1957).

Author contributions

Conception and design of the project, D.G. and V.K.; material collection and description of the new species, D.G.; cytogenetic study, V.K. and A.M-N.; writing the paper, D.G. and V.K.; final approval of the version to be published, all authors.

Acknowledgements

The work is based on the taxonomic collection of ZISP and was performed in the frames of the state research projects Nos AAAA-A17-117030310210-3 and AAAA-A19-119020790106-0, and supported by the Presidium RAS program No. 41 "Biodiversity of natural systems and biological sources of Russia". V.G. and A.M-N. are grateful to Boris Anokhin for technical assistance with FISH. D.G. is grateful to Ilya Gavrilov-Zimin who shared with him the joys and hardships of the expedition to Myanmar and did not greatly interfere with his collecting material. Lastly, thanks are extended to David Redei and Snejana Grozeva for their helpful comments on the article.

References

Akingbohungbe AE (1983) Variation in testis follicle number in the Miridae (Hemiptera, Heteroptera) and its relationship to the higher classification of the family. Annals of the Entomological Society of America 76: 37–43. https://doi.org/10.1093/aesa/76.1.37

Ambrose PD, Vennison JS (1990) Diversity of spermatophore capsules in Reduviids (Insecta, Heteroptera, Reduviidae) of South India. Mitteilungen aus dem Zoologischen Museum in Berlin 66(2): 309–317. https://doi.org/10.1002/mmnz.19900660205

Banerjee MK (1958) A study of the chromosomes during meiosis in twenty eight species of Hemiptera (Heteroptera, Homoptera). Proceedings of the Zoological Society of Calcutta 11: 9–37.

Bardella VB, Gil-Santana HR, Panzera F, Vanzela ALL (2014) Karyotype diversity among predators of Reduviidae (Heteroptera). Comparative Cytogenetics 8(4): 351–367. https://doi.org/10.3897/CompCytogen.v8i4.8430

Beck H, Zimmermann N, McVicar T, Vergopolan N, Berg A, Wood EF (2018) Present and future Köppen-Geiger climate classification maps at 1-km resolution. Scientific Data 5: 180214. [updated 17 August 2020] https://doi.org/10.1038/sdata.2018.214

Davis NT (1966) Contributions to the morphology and phylogeny of the Reduvioidea (Hemiptera: Heteroptera). Part III. The male and and female genitalia. Annals of the Entomological Society of America 59(5): 911–924. https://doi.org/10.1002/mmnz.19900660205

Davis NT (1969) Contribution to the morphology and phylogeny of the Reduvioidea. Part IV. The harpactoroid complex. Annals of the Entomological Society of America 62(1): 74–94. https://doi.org/10.1093/aesa/62.1.74

Dispons P, Villiers A (1967) Contribution à la faune de l'Iran. 2. Heteroptera Reduviidae. Annales de la Société entomologique de France (N.S.) 3(4): 1067–1085.

Distant WL (1904) The Fauna of British India, including Ceylon and Burma. Rhynchota (Heteroptera), 2. Taylor & Francis, London, 503 pp.

Distant WL (1906) LIII Oriental Reduviidae. The Annals and Magazine of Natural History, Series 7, 18: 363–370. https://doi.org/10.1080/00222930608562629

Freitas SPC, Santos-Mallet JR, Costa J, Souza ALB, Serrão JE, Gonçalves TCM (2008) A comparative study of testis follicles in species of *Triatoma* (Hemiptera, Triatominae) Animal Biology 58: 227–233. https://doi.org/10.1163/157075608X328062

Frydrychová R, Grossmann P, Trubač P, Vítková M, Marec F (2004) Phylogenetic distribution of TTAGG telomeric repeats in insects. Genome 47: 163–178. https://doi.org/10.1139/g03-100

Gapon DA (2001) Inflation of Heteropteran aedeagi using microcapillaries (Heteroptera, Pentatomidae). Zoosystematica Rossica 9(1)[2000]: 157–160.

Gapon DA (2007) Structure, function, and morphological conformity of the male and female genitalia in the true bug genus *Pyrrhocoris* Fall. (Heteroptera, Pyrrhocoridae). Entomologicheskoe Obozrenie 86(4): 729–741. [in Russian] [English translation: Entomological Review 2007, 87(9): 1099–1108.] https://doi.org/10.1134/S0013873807090011

Golub NV, Golub VB, Kuznetsova VG (2018) New data on karyotypes of lace bugs (Tingidae, Cimicomorpha, Hemiptera) with analysis of the 18S rDNA clusters distribution. Comparative Cytogenetics 12(4): 515–528. https://doi.org/10.3897/CompCytogen.v12i4.30431

Gomes MO, Castanhole MMU, Souza HV, Murakami AS, Firmino TSS, Saran PS, Banho CA, Monteiro LS, Silva JCP, Itoyama MM (2013) Morphological aspects of the testes of 18 species of terrestrial of Heteroptera from Northwestern São Paulo (Brazil). Biota Neotropica 13(3). https://doi.org/10.1590/S1676-06032013000300016

Grozeva S, Nokkala S (1996) Chromosomes and their meiotic behavior in two families of the primitive infraorder Dipsocoromorpha (Heteroptera). Hereditas 125: 189–192. https://doi.org/10.1111/j.1601-5223.1996.t01-1-00031.x

Grozeva S, Kuznetsova VG, Anokhin BA (2011) Karyotypes, male meiosis and comparative FISH mapping of 18S ribosomal DNA and telomeric $(TTAGG)_n$ repeat in eight species of true bugs (Hemiptera, Heteroptera). Comparative Cytogenetics 5(4): 355–374. https://doi.org/10.3897/compcytogen.v5i4.2307

Grozeva S, Anokhin BA, Simov N, Kuznetsova VG (2019) New evidence for the presence of the telomere motif $(TTAGG)_n$ in the family Reduviidae and its absence in the families Nabidae and Miridae (Hemiptera, Cimicomorpha). Comparative Cytogenetics 13(3): 283–295. https://doi.org/10.3897/CompCytogen.v13i3.36676

Gupta A (2005) The physical geography of Southeast Asia. Oxford University Press Inc, New York, 440 pp. https://doi.org/10.1093/oso/9780199248025.003.0013

Horváth G (1929) Rhynchoten aus Palästina und Syrien (Zoologische Studienreise von R. Ebner 1928 mit Unterstützung der Akademie der Wissenschaften in Wien). Sitzungsberichte der Akademie der Wissenschaften in Wien. Mathematisch-Naturwissenschaftliche Klasse 138: 329–333.

Jeannel R (1919) Henicocephalidae et Reduviidae. Voyage de Ch. Alluaud et R. Jeannel en Afrique orientale (1911–1912). Résultats scientifiques 8. Insectes Hémiptères 3: 131–314 + 12 pls. Paris: Librairie des Sciences Naturelles, Léon Lhomme.

Kaur R, Kaur H (2013) Chromosomes and their meiotic behavior in twelve species of the subfamily Harpactorinae (Hemiptera: Heteroptera: Reduviidae) from north India. Zootaxa 3694(4): 358–366. https://doi.org/10.11646/zootaxa.3694.4.4

Kaur H, Kaur R, Patial N (2012) Studies on internal male reproductive organs and course of meiosis in a predator species *Repipta taurus* (Fabricius, 1803) (Heteroptera: Reduviidae: Harpactorinae). Journal of Entomological Research 36(3): 247–250.

Konstantinov FV, Gapon DA (2005) On the structure of the aedeagus in shield bugs (Heteroptera, Pentatomidae): 1. Subfamilies Discocephalinae and Phyllocephalinae. Entomo-

logicheskoe Obozrenie 84(2): 334–352. [in Russian] [English translation: Entomological Review, 2005 85(3): 221–235.] https://doi.org/10.1002/zamm.200590013

Kpordugbe PGO (1979) Karyotypes of some tropical reduviids and cytotaxonomy of Reduviidae (Hemiptera: Heteroptera). MSc. Dissertation, Legon, University of Ghana, Ghana, 146 pp. [+ references + tables I–IX + tests I–VII] http://ugspace.ug.edu.gh

Kuznetsova VG, Grozeva S, Gokhman VE (2020) Telomere structure in insects: A review. Journal of Zoological Systematics and Evolutionary Research 58: 127–158. https://doi.org/10.1111/jzs.12332

Kuznetsova VG, Gavrilov-Zimin IA, Grozeva SM, Golub NV (2021) Comparative analysis of chromosome numbers and sex chromosome systems in Paraneoptera (Insecta). Comparative Cytogenetics 15(3): 279–327. https://doi.org/10.3897/CompCytogen.v15.i3.71866

Linnnavuori R (1973) Studies on the hemipterous fauna of Israel and Sinai. Israel Journal of Entomology 8: 35–54.

Louis D, Kumar R (1973) Morphology of the alimentary and reproductive organs in Reduviidae (Hemiptera: Heteroptera) with comments on interrelationships within the family. Annals of the Entomological Society of America 66(3): 635–639. https://doi.org/10.1093/aesa/66.3.635

Maldonado Capriles J (1990) Systematic catalogue of the Reduviidae of the World (Insecta: Heteroptera). Caribbean Journal of Science. University of Puerto Rico, Mayagüez, Special Edition, 694 pp.

Miller NCE (1956) The biology of the Heteroptera. Leonard Hill, London, 162 pp.

Pansare PP, Joshi NU, Boyane SS, Ghate HV (2017) First record of *Rhaphidosoma atkinsoni* (Heteroptera: Reduviidae: Harpactorinae) from Maharashtra, India, with redescription and observations on its bionomics. Zootaxa 4303(2): 253–263. https://doi.org/10.11646/zootaxa.4303.2.5

Panzera F, Pita S, Lorite P (2021) Chromosome structure and evolution of Triatominae: a review. In: Guarneri AA, Lorenzo MG (Eds) Triatominae: the biology of chagas disease vectors. Vol. 5. Entomology in focus. Cham: Springer Nature Switzerland, 65–99. https://doi.org/10.1007/978-3-030-64548-9

Papeschi AG, Bressa MJ (2007) Classical and molecular cytogenetics in Heteroptera. In: Mohan RM (Ed.) Research Advances in Entomology, Kerala, 1–9.

Pendergrast JG (1957) Studies on the reproductive organs of the Heteroptera with a consideration of their bearing on classification. Transactions of the Royal Entomological Society of London 109: 1–63. https://doi.org/10.1111/j.1365-2311.1957.tb00133.x

Pérez R, Calleros L, Rose V, Lorca M, Panzera F (2004) Cytogenetic studies on *Mepraia gajardoi* (Heteroptera: Reduviidae). Chromosome behaviour in a spontaneous translocation mutant. European Journal of Entomology 101(2): 211–218. https://doi.org/10.14411/eje.2004.027

Pita S, Panzera F, Mora P, Vela J, Palomeque T, Lorite P (2016) The presence of the ancestral insect telomeric motif in kissing bugs (Triatominae) rules out the hypothesis of its loss in evolutionarily advanced Heteroptera (Cimicomorpha). Comparative Cytogenetics 10(3): 427–437. https://doi.org/10.3897/compcytogen.v10i3.9960

Pita S, Lorite P, Cuadrado A, Panzera Y, De Oliveira J, Alevi KCC, Rosa JA, Freitas SPC, Gómez-Palacio A, Solari A, Monroy C, Dorn PL, Cabrera-Bravo M, Panzera F (2021) High chromosomal mobility of rDNA clusters in holocentric chromosomes of Triatomi-

nae, vectors of Chagas disease (Hemiptera-Reduviidae). Medical and Veterinary Entomology. https://doi.org/10.1111/mve.12552

Poggio MG, Bressa MJ, Papeschi AG (2007) Karyotype evolution in Reduviidae (Insecta: Heteroptera) with special references to Stenopodainae and Harpactorinae. Comparative Cytogenetics 1(2): 159–168. http://www.zin.ru/journals/compcyt/pdf/1/poggio.pdf

Poggio MG, Provecho YM, Papeschi AG, Bressa MJ (2013) Possible origin of polymorphism for chromosome number in the assassin bug *Zelurus femoralis longispinis* (Reduviidae: Reduviinae). Biological Journal of the Linnean Society 110(4): 757–764. https://doi.org/10.1111/bij.12168

Poppius B (1911) Zwei neue palaearktische Arten der Reduviidengattung Rhaphidosoma Am. et Serv. Wiener Entomologische Zeitung 30: 101–102.

Ravichandran G, Livingstone D (1994) A new species of *Rhaphidosoma* (Heteroptera–Reduviidae–Harpactorinae) from western Ghats. Journal of Bombay Natural History Society 91: 105–107.

Sadílek D, Urfus T, Vilímová J, Hadrava J, Suda J (2019) Nuclear genome size in contrast to sex chromosome number variability in the human bed bug, *Cimex lectularius* (Heteroptera: Cimicidae). Cytometry 95(7): 746–756. https://doi.org/10.1002/cyto.a.23729

Schuh RT, Weirauch Ch (2020) True bugs of the world (Hemiptera: Heteroptera). Classification and natural history (2nd edn). Siri Scientific Press, Manchester, 767 pp. [+ 32 pls]

Schuh RT, Štys P (1991) Phylogenetic analysis of cimicomorphan family relationships (Heteroptera). Journal of the New York Entomological Society 99: 298–350.

Schuh RT, Weirauch Ch, Wheeler WC (2009) Phylogenetic relationships within the Cimicomorpha (Hemiptera: Heteroptera): a total-evidence analysis. Systematic Entomology 34(1): 15–48. https://doi.org/10.1111/j.1365-3113.2008.00436.x

Scudder GGE (1959) The female genitalia of the Heteroptera: morphology and bearing on classification. Transactions of the Royal Entomological Society of London 111(14): 405–467. https://doi.org/10.1111/j.1365-2311.1959.tb02873.x

Sharakhov IV [Ed.] (2015) Protocols for cytogenetic mapping of arthropod genomes. Taylor & Francis Ltd, 526 pp. https://doi.org/10.1201/b17450

Sharov AG (1966) Basic Arthropodan stock with special reference to insects. Oxford University Press, New York, 277 pp.

Souza HV, Castanhole MM, Gomes MO, Murakami AS, Firmino TSS, Saran PS, Banho CA, Monteiro LS, Silva JCP, Itoyama MM (2014) Meiotic behavior of 18 species from eight families of terrestrial heteroptera. Journal of Insect Science 14(1): e149. https://doi.org/10.1093/jisesa/ieu011

Štys P (1961) Morphology of the abdomen and female ectodermal genitalia of the Trichophorous Heteroptera and bearing on their classification. In: Strouhal H, Beier M (Eds) XI. Internationaler Kongress für Entomologie, Wien, 17. bis 25: verhandlungen, Bd. 1. Organisationskomittee des XI. Internationalen Kongresses für Entomologie, Wien, 37–43.

Swanson DR (2020) *Hoffmannocoris sinuatus* sp. nov. and a new generic synonym in the Harpactorinae (Hemiptera: Reduviidae) of Africa, with a brief history of 'Rhaphidosomatini'. Austral Entomology 59: 88–101. https://doi.org/10.1111/aen.12445

Tiepo AN, Pezenti LF, Lopes TBF, da Silva CRM, Dionisio JF, Fernandes JAM, Da Rosa R (2016) Analysis of the karyotype structure in *Ricolla quadrispinosa* (Linneus, 1767): in-

ferences about the chromosomal evolution of the tribes of Harpactorinae (Heteroptera, Reduviidae). Comparative Cytogenetics 10(4): 719–729. https://doi.org/10.3897/CompCytogen.v10i4.10392

Ueshima N (1979) Animal cytogenetics. Insecta 6. Hemiptera II: Heteroptera. Gebrüder Borntraeger, Berlin, Stuttgart, 117 pp.

Vítková M, Král J, Traut W, Zrzavý J, Marec F (2005) The evolutionary origin of insect telomeric repeats, $(TTAGG)_n$. Chromosome Research 13: 145–156. https://doi.org/10.1007/s10577-005-7721-0

Weirauch Ch, Bérenger J-M, Berniker L, Forero D, Forthman M, Frankenberg S, Freedman A, Gordon E, Hoey-Chamberlain R, Hwang WS, Marshall SA, Michael A, Paiero SM, Udah O, Watson C, Yeo M, Zhang G, Zhang J (2014) An illustrated identification key to assassin bug subfamilies and tribes (Hemiptera: Reduviidae). Canadian Journal of Arthropod Identification 26(2): 1–115. https://doi.org/10.3752/cjai.2014.26

Zhang J, Weirauch C, Zhang G, Forero D (2015) Molecular phylogeny of Harpactorinae and Bactrodinae uncovers complex evolution of sticky trap predation in assassin bugs (Heteroptera: Reduviidae). Cladistics 32(5): 1–17. https://doi.org/10.1111/cla.12140

ORCID

Dmitry A. Gapon https://orcid.org/0000-0002-4927-9845
Valentina G. Kuznetsova https://orcid.org/0000-0001-8386-5453
Anna Maryanska-Nadachowska https://orcid.org/0000-0003-3270-825X

CompCytogen 15(4): 507–525 (2021)
doi: 10.3897/compcytogen.v15.i4.75990
https://compcytogen.pensoft.net

RESEARCH ARTICLE

COMPARATIVE Cytogenetics
A peer-reviewed open-access journal
International Journal of Plant & Animal Cytogenetics, Karyosystematics, and Molecular Systematics

Comparative chromosome studies in species of subtribe Orchidinae (Orchidaceae)

Alessio Turco[1], Antonella Albano[1], Pietro Medagli[1], Robert P. Wagensommer[2], Saverio D'Emerico[3]

1 *Dept. of Biological and Environmental Sciences and Technologies, University of Salento, Strada Provinciale Lecce-Monteroni, 73100 Lecce, Italy* **2** *Dept. of Biology, Via E. Orabona 4, "Aldo Moro" University of Bari, 70125 Bari, Italy* **3** *"Aldo Moro" University of Bari, 70125 Bari, Italy*

Corresponding author: Robert P. Wagensommer (robert.wagensommer@uniba.it)

Academic editor: Viktoria Shneyer | Received 1 October 2021 | Accepted 22 November 2021 | Published 17 December 2021

http://zoobank.org/9217943B-7061-4819-8FE4-C0C6112E8D2F

Citation: Turco A, Albano A, Medagli P, Wagensommer RP, D'Emerico S (2021) Comparative chromosome studies in species of subtribe Orchidinae (Orchidaceae). CompCytogen 15(4): 507–525. https://doi.org/10.3897/compcytogen.v15.i4.75990

Abstract

In our study, FISH mapping using 18S-5.8S-25S rDNA and 5S rDNA sequences was performed for the first time on *Ophrys tenthredinifera* Willdenow, 1805, *Serapias vomeracea* (Burman f., 1770) Briquet, 1910 and *Himantoglossum hircinum* (Linnaeus, 1753) Sprengel, 1826. A detailed study was also performed on *O. tenthredinifera* using Giemsa-staining, silver-staining, CMA fluorescence banding and fluorescence *in situ* hybridisation (FISH) with rDNA probes. We analysed two subspecies, i.e. *O. tenthredinifera* subsp. *neglecta* (Parlatore, 1860) E.G. Camus, 1908 and *O. tenthredinifera* subsp. *grandiflora* (Tenore, 1819) Kreutz, 2004 by the traditional Feulgen method and constructed the karyotype. The cytotaxonomic implications for both taxa are also discussed. In *Himantoglossum hircinum*, FISH and silver staining highlighted differences in the number of two rDNA families (35S and 5S) with respect to *Barlia robertiana* (Loiseleur-Deslongchamps, 1807) Greuter, 1967. In addition, fluorescence *in situ* hybridisation was also applied to diploid ($2n = 2x = 36$) and triploid ($2n = 3x = 54$) *Anacamptis morio* (Linnaeus, 1753) R.M. Bateman, Pridgeon et M.W. Chase, 1997. As far as we are aware, this is the first case of autotriploidy observed in *A. morio*.

Keywords

Anacamptis, C-banding, Cytotaxonomy, FISH, *Himantoglossum*, Karyotype, *Ophrys*, *Serapias*

Introduction

Over the years, various karyological aspects including ploidy level, total length of the chromosome set, symmetry indices and amount of nuclear DNA (Siljak-Yakovlev and Peruzzi 2012) have proved to be useful tools for studying cytotaxonomy and for understanding chromosome evolution (Stace 2000; Guerra 2012; Ilnicki 2014; Sharma and Mukai 2015), as have other studies of structural variation looking at chromosomal features (e.g. secondary constrictions, AgNors and rDNA sites). In this context, these studies help to elucidate phylogenetic relationships between taxa. For example, analysis of differences in karyotype asymmetry have been shown to be good indicators of chromosomal diversification in terms of size and morphology within a group (Levitsky 1931; Stebbins 1971; Peruzzi and Eroğlu 2013; Astuti et al. 2017).

These cytogenetic studies have also played an important role in describing the main features in the systematics and phylogeny of orchids, based on both chromosomal analysis by traditional techniques (D'Emerico 2001 and references therein) and analyses of the structural variation of chromosomes (e.g. Giemsa C-banding, FISH, etc.) (Schwarzacher and Schweizer 1982; D'Emerico et al. 1999; D'Emerico et al. 2001; Moscone et al. 2007; Lan and Albert 2011).

The subtribe *Orchidinae* Vermeulen, 1977 comprises about 35 genera of mostly terrestrial orchids (Pridgeon et al. 2001), 15 of which occur in Italy (GIROS 2016; Bartolucci et al. 2018; Martellos et al. 2020). In this context, *Ophrys* Linnaeus, 1753 is probably the richest in species, many of which are endemic to restricted areas and are more or less threatened with extinction (Wagensommer et al. 2020; Turco et al. 2021). From a cytogenetic point of view, the chromosome numbers of at least 23 of these genera have been investigated by various researchers (D'Emerico 2001 and references therein). On the other hand, detailed investigations of the morphology of *Orchidinae* chromosomes have only been performed on the genera *Anacamptis* Richard, 1817, *Chamorchis* Richard, 1817, *Dactylorhiza* Necker ex Nevski, 1935, *Himantoglossum* Sprengel, 1826, *Neotinea* Reichenbach f., 1852, *Ophrys* Linnaeus, 1753, *Orchis* Linnaeus, 1753, *Platanthera* Richard, 1817, and *Serapias* Linnaeus, 1753 (D'Emerico 2005). Comparison of plant karyotypes using conventional cytological techniques can contribute to taxonomy and can provide insight into genome organisation and evolution in various genera (Turco et al. 2018).

The first systematic study of the karyomorphology of *Orchidinae* in Europe was undertaken by Bianco et al. (1988, 1989), who described the karyotypes of six different *Ophrys* species. In cytogenetic studies, in addition to the study of morphological chromosome features by traditional techniques, banding techniques with Giemsa and fluorochromes have also been used. These techniques have revealed variations in heterochromatin content in the chromosomal complements of some groups of *Orchidinae* (D'Emerico et al. 1996, 2000; D'Emerico et al. 2002a, 2002b; Pellegrino et al. 2000; D'Emerico et al. 2005; Baumann et al. 2012; Turco et al. 2020).

Molecular cytogenetic techniques such as fluorescence *in situ* hybridisation (FISH), used to identify repetitive sequence families and their distribution in plant chromo-

somes, have proven to be powerful tools for characterising chromosomes and investigating taxonomic relationships in plant groups (Maluszynska and Heslop-Harrison 1993a, 1993b; Galasso et al. 1995, 1997; Zoldos et al. 1999). D'Emerico et al. (2001) reported the physical distribution of 18S-5.8S-25S and 5S rDNA sequences in the chromosomes of five *Orchidinae* taxa for the first time.

Seeking to increase our knowledge and acquire data on the karyology and systematics of *Orchidinae*, we used FISH and other techniques to study the karyotypes and heterochromatin distribution of *Ophrys tenthredinifera* s.l. and three other *Orchidinae*, i.e. *Himantoglossum hircinum* (Linnaeus, 1753) Sprengel, 1826, *Serapias vomeracea* (Burman f., 1770) Briquet, 1910 and *Anacamptis morio* (Linnaeus, 1753) R.M. Bateman, Pridgeon et M.W. Chase, 1997, specifically their distribution of 18S-5.8S-25S and 5S rDNA loci, in order to elucidate their importance in the plants' systematics and evolution.

Methods

The taxa examined and their collection sites are shown in Table 1. Mitotic chromosomes were observed in tissues of immature ovaries. A total of fifteen individuals of *Ophrys tenthredinifera* Willdenow, 1805 and five *Himantoglossum hircinum* were first analysed by Feulgen and C-banding methods. For these two species, at least ten metaphases were examined and the karyotype was constructed from well-spread metaphase plates. Four well-spread metaphase plates were then examined with the FISH technique. In addition, four specimens of *Anacamptis morio* and four of *Serapias vomeracea* were analysed by the FISH technique and five metaphase plates were selected.

Immature ovary tissues were pre-treated with 0.3% colchicine at room temperature for 2 h. For Feulgen staining they were fixed for 5 min in 5:1:1:1 (v/v) absolute ethanol, chloroform, glacial acetic acid and formalin. Hydrolysis was performed at 20 °C in 5.5 N HCl for 20 min (Battaglia 1957a, b). The material was then stained in freshly prepared Feulgen stain. For C-banding, immature ovaries were fixed in 3:1 (v/v) ethanol–glacial acetic acid and stored in the deep-freeze for up to several months. Subsequently, they were squashed in 45% acetic acid; coverslips were removed by the dry ice method and the preparations air-dried overnight. Slides were then immersed in 0.2 N HCl at 60 °C for 3 min, thoroughly rinsed in distilled water and then treated

Table 1. Specimens of taxa analysed in this study.

Taxon	Provenance	Collector
Ophrys tenthredinifera subsp. *grandiflora*	Sicily, Francavilla di Sicilia (Messina); Niscemi (Caltanissetta)	Bartolo et Pulvirenti
Ophrys tenthredinifera subsp. *neglecta*	Apulia, Cassano Murge (Bari); Torre Canne (Brindisi), Gargano promontory (Foggia)	D'Emerico et Medagli
Himantoglossum hircinum	Apulia, Cassano Murge (Bari)	D'Emerico et Medagli
Serapias vomeracea	Apulia, Adelfia (Bari)	D'Emerico
Anacamptis morio	Apulia, Cassano Murge (Bari)	D'Emerico

with 4% Ba(OH)2 at 20 °C for 4 min. After thorough rinsing they were incubated in 2× SSC at 60 °C for 1 h. The stain used was 3–4% Giemsa (BDH) at pH 7.

For DAPI (4–6-diamidino-2-phenylindole) staining, ovaries were treated as for C-banding and stained using a buffered DAPI solution (0.6 mg/mL) for 5 min. after which they were rinsed and mounted in 1:1 (v/v) buffer and glycerol. For chromomycin A3 (CMA) staining, slides were stained with 0.5 mg/mL CMA for 1 h and mounted in 1:1 (v/v) McIlvaine's pH 7.0 buffer–glycerol. For identification of the nucleolus, AgNO3 precipitation was used (Lacadena and Cermeno 1985).

For *Ophrys tenthredinifera* Willd., 1805, chromosome measurements were performed using the freeware MicroMeasure 3.3 (http://www.colostate.edu/Depts/Biology/MicroMeasure). Chromosome pairs were identified and arranged on the basis of length. The nomenclature used for describing karyotype composition followed Levan et al. (1964). Karyotype morphometric characters were evaluated by calculating the haploid complement, while the karyotype asymmetry indices M_{CA} (Mean Centromeric Asymmetry) and CV_{CL} (Coefficient of Variation of Chromosome Length) were used for the evaluation of karyotype asymmetry. Moreover, CV_{CI} (Coefficient of Variation of the Centromeric Index) was used to evaluate heterogeneity in the position of the centromeres (Paszko 2006, Zuo and Yuan 2011, Peruzzi and Eroğlu 2013).

For fluorescence *in situ* hybridisation, the ribosomal sequences 18S-5.8S-25S (pTa71 - red signals) and 5S (pTa794 - green signals) were used as probes. Clone pTa71 was labelled with rhodamine-4-dUTP by nick translation, while pTa794 was labelled with digoxigenin-11-dUTP using polymerase chain reaction. The former contains a 9kb *EcoBl* repeat unit of 18S-5.8S-25S rDNA and intergenic spacer regions, isolated from *Triticum aestivum* Linnaeus, 1753 (Gerlach and Bedbrook 1979), and the latter corresponds to a complete 410 bp 5S gene unit, containing the 5S gene and intergenic spacer regions, isolated from *Triticum aestivum* (Gerlach and Dyer 1980). Pre-treatment of slides and the FISH procedure followed the protocol in Heslop-Harrison et al. (1991). The chromosomes and DNA probes were denatured together at 70 °C for 5 min and hybridisation was performed at 37 °C overnight. After hybridisation, the coverslips were removed in 2× SSC at room temperature and then washed thoroughly for 10 min in 20% (v/v) formamide in 0.1× SSC at 42 °C to remove sequences with less than 85% homology; the slides were then incubated in immunoflorescent reagents.

For detection of the digoxigenin-labelled probe, the slides were equilibrated in 4× SSC/0.1% (v/ v) Tween 20 and blocked in 5% (w/v) bovine serum albumin in 4× SSC/0.1% (v/v) Tween 20 for 5 min. Slides were incubated with sheep anti-digoxigenin antibody conjugated with FITC in a moist chamber at 37 °C for 1 h. The slides were washed in 4× SSC/Tween 20 3× 5 min and subsequently counterstained with DAPI prior to observation. They were finally mounted in antifade solution AF1 (Citifluor) and examined with a Leitz epifluorescence microscope with single and triple band pass filters. The resulting images were processed with freeware image-editing software, applying the functions to the whole image.

Results

The chromosomes of the studied species are shown in Figs 1–5. Unfortunately, in the analysed species it is rather difficult to obtain good metaphasic plates for FISH staining. Therefore, we considered only the visible signals with the pTa71 and pTa794 probes to document sites rich in GC and AT. The cytogenetic analysis showed the following characteristics.

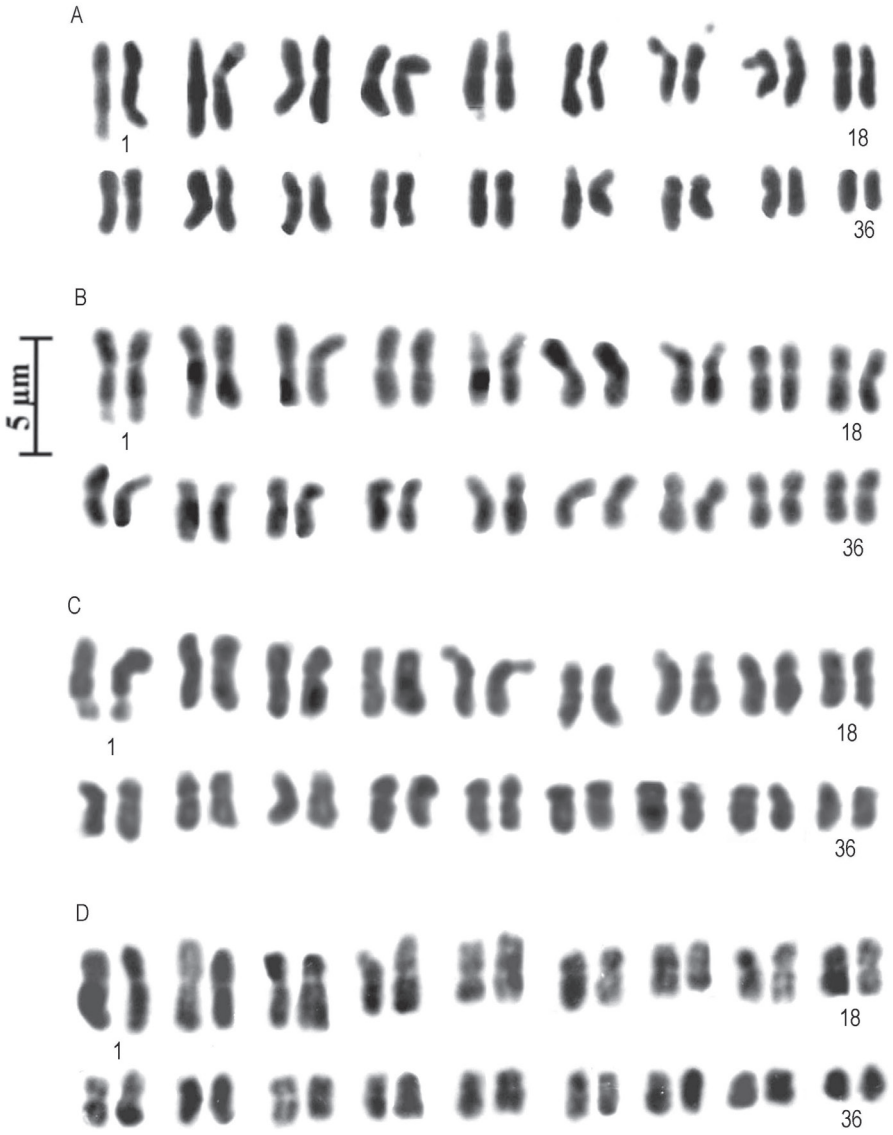

Figure 1. A, B Diploid karyotype of *Ophrys tenthredinifera* subsp *neglecta* **C** diploid karyotype of *O. tenthredinifera* subsp. *grandiflora* **D** diploid karyotype of *Himantoglossum hircinum*.

Table 2. Taxon, chromosome number, formula and morphometric parameters (mean ± SE) in *Ophrys tenthredinifera*. MCA (Mean Centromeric Asymmetry), CVCL (Coefficient of Variation of Chromosome Length), CVCI (Coefficient of Variation of Centromeric Index). Chromosome abbreviations: m, metacentric; sm, submetacentric.

Taxon	Number of individuals	Chromosome number (2n)	Formula	M_{CA}	CV_{CL}	CV_{CI}
Ophrys tenthredinifera subsp. *grandiflora*	5	36	32m + 4sm	12.44 ± 2.59	16.83 ± 0.84	8.43 ± 1.41
O. tenthredinifera subsp. *neglecta*	10	36	32m + 4sm	13.29 ± 0.11	16.56 ± 0.88	10.80 ± 0.79

Genus *Ophrys*: Mitotic metaphases in *Ophrys tenthredinifera* showed the chromosome number $2n = 2x = 36$. We analysed two subspecies of *O. tenthredinifera*, *O. tenthredinifera* subsp. *neglecta* (Parlatore, 1860) E.G. Camus, 1908 and *O. tenthredinifera* subsp. *grandiflora* (Tenore, 1819) Kreutz, 2004, with the traditional Feulgen method and composed the karyotype. The results are shown in Table 2. The karyotypes of both subspecies were similar in terms of both the satellite pairs and the asymmetry indices. It is possible to observe four pairs of chromosomes, each with a satellite on the short arm (Figs 1A, B, C). The karyological formula shows 32 metacentrics plus 4 submetacentrics in both subspecies. The karyotype is the most symmetrical, having a low intrachromosomal asymmetry (M_{CA}) index (12.44–13.29) and a low interchromosomal asymmetry (CV_{CL}) index (16.56–16.83).

In *O. tenthredinifera*, C-banding showed the presence of centromeric heterochromatin, with a pair of chromosomes with a telomeric band. A large number of chromocentres were observed in interphase nuclei (Fig. 2A, B). The nucleolus organiser regions (NORs) revealed by Ag-NOR staining were located in the telomeric region of the third chromosome pair (Fig. 2D), evidence that the six rDNA sites were active. However, in interphase nuclei it was possible to count up to three nucleoli (Fig. 2C). Moreover, in *O. tenthredinifera*, CMA staining revealed a positive signal on the NOR-bearing pair only (Fig. 2E). FISH analyses with the pTa71 (18S-5.8S-25S) probe showed three signals (Fig. 4B), as revealed by the Ag-NOR staining in interphase nuclei (Fig. 2C). In addition, this species showed two pairs of 5S rDNA sites (Fig. 4C).

Genus *Serapias*: Mitotic metaphases in *Serapias vomeracea* had $2n = 2x = 36$ chromosomes. *In situ* hybridisation shows that there are three pairs of 18S-5.8S-25S rDNA sites (Fig. 4E). The 5S rDNA sequence was present on two pairs of chromosomes (Fig. 4F).

Genus *Himantoglossum*: All specimens of *Himantoglossum hircinum* had $2n = 2x = 36$ chromosomes. The *H. hircinum* karyotype consists of 28m + 8sm. In *H. hircinum* a secondary constriction was seen in the short arm of pairs 4, 5 and 7 (Fig. 1D). C-banding revealed that some chromosomes in *H. hircinum* possess small amounts of centromeric and telomeric constitutive heterochromatin (Fig. 3A). In interphase nuclei it was possible to count up to four nucleoli (Fig. 3B). Moreover, FISH revealed the location of four 18S-5.8S-25S rDNA sites (Fig. 4H) and four 5S rDNA sites (Fig. 4I).

Genus *Anacamptis*: In diploid *Anacamptis morio* (2*n* = 2*x* = 36), silver nitrate staining in interphase nuclei counted up to four nucleoli. In this study, *in situ* hybridisation revealed the location of six 18S-5.8S-25S rDNA sites (Fig. 5A) and two 5S rDNA sites (Fig. 5B). Fluorescence *in situ* hybridisation in triploids (2*n* = 3*x* = 54) revealed nine 18S-5.8S-25S rDNA sites (Fig. 5D) and three 5S rDNA sites (5E).

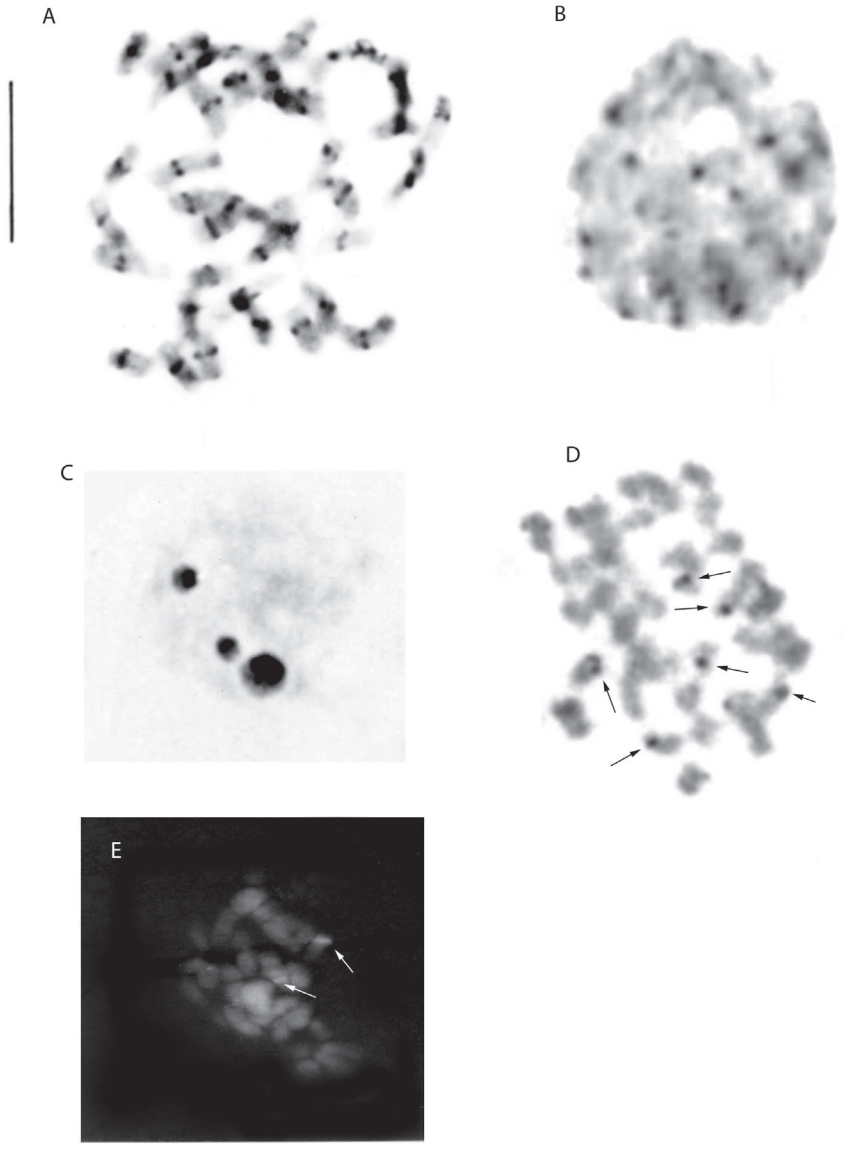

Figure 2. *Ophrys tenthredinifera* **A** Giemsa C-banding metaphase plate **B** Giemsa C-banding, interphase nucleus **C** silver staining, interphase nucleus **D** silver staining, mitotic metaphase **E** CMA staining, mitotic metaphase. Arrows indicate NOR sites. Scale bar: 5 μm.

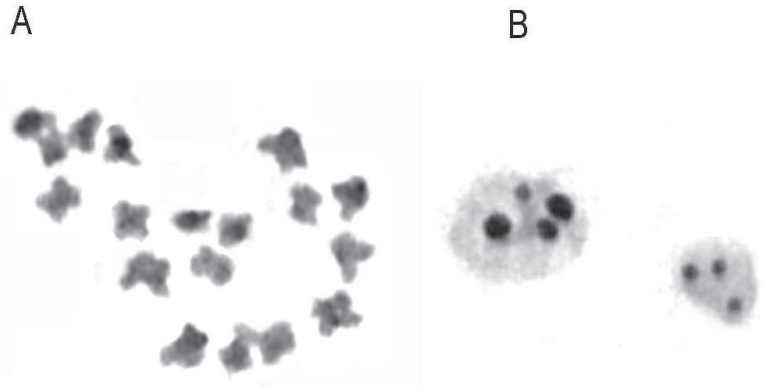

Figure 3. *Himantoglossum hircinum* **A** Giemsa C-banding, haploid metaphase *n* = 18 **B** silver staining, interphase nucleus.

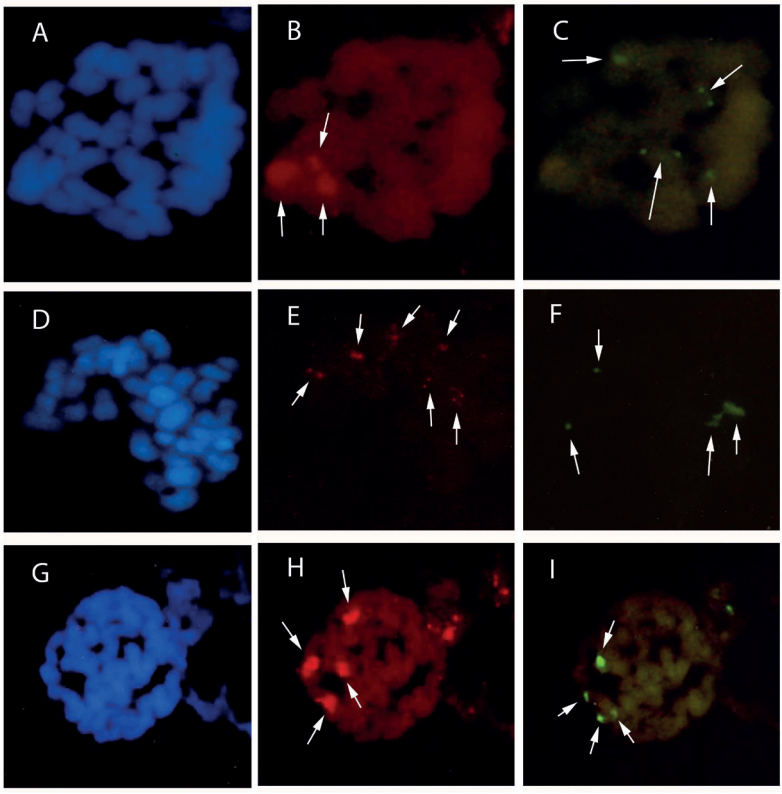

Figure 4. In situ hybridisation applied to chromosomes of orchid species. Blue DAPI staining shows chromosomal DNA (**A, D, G**, respectively *Ophrys tenthredinifera*, *Serapias vomeracea* and *Himantoglossum hircinum*); red and green signals show sites of hybridisation of 18S-25S rDNA and 5S rDNA respectively (**B, E, H, C, F, I**). Arrows indicate sites. *Ophrys tenthredinifera* (**B**) three 18S-25S rDNA sites and (**C**) four 5S rDNA sites. *Serapias vomeracea* (**E**) six 18S-25S rDNA sites and (**F**) four 5S rDNA sites. *Himantoglossum hircinum* (**H**) four 18S-25S rDNA sites and (**I**) four 5S rDNA sites.

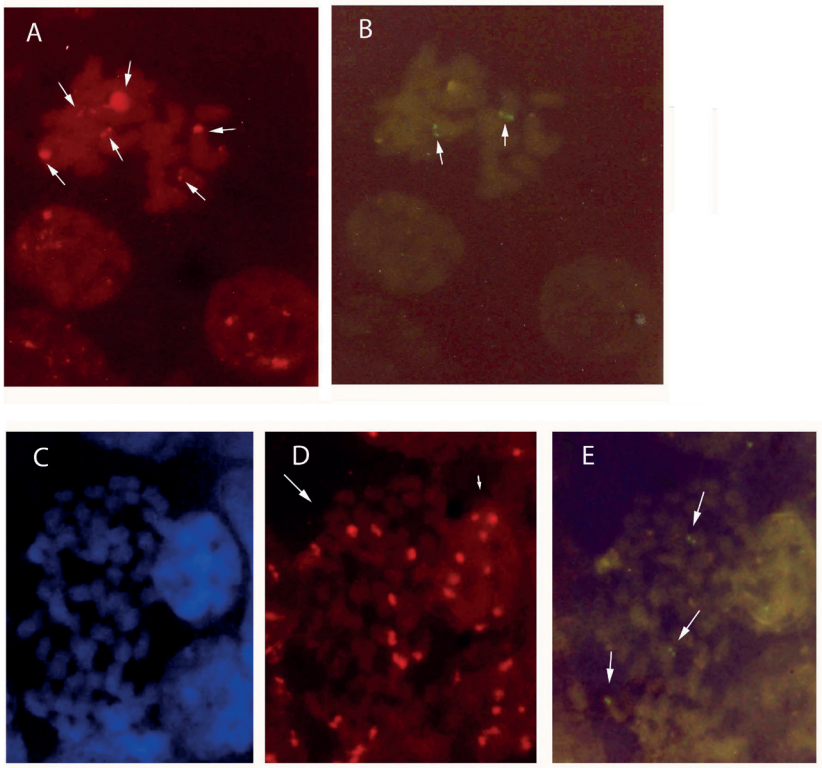

Figure 5. In situ hybridisation applied to chromosomes of *Anacamptis morio*. Blue DAPI staining shows chromosomal DNA (**C**); red and green signals show sites of hybridisation of 18S-25S rDNA and 5S rDNA respectively (**A**, **D**, **B**, **E**). Arrows indicate sites. Mitotic metaphase $2n = 2x = 36$ with (**A**) six 18S-25S rDNA sites and (**B**) two 5S rDNA sites. Mitotic metaphase $2n = 3x = 54$ with (**D**) nine 18S-25S rDNA sites and (**E**) three 5S rDNA sites. Interestingly, a large number of 18S-5.8S-25S rDNA sites (9) were observed in interphase nuclei (small arrow).

Discussion

This paper reports the physical locations of rDNA loci on the somatic chromosomes of *Ophrys tenthredinifera*, *Serapias vomeracea* and *Himantoglossum hircinum* for the first time. Our analyses showed 18S-5.8S-25S rDNA sites and 5S rDNA sites in triploid specimens of *Anacamptis morio*.

The chromosome numbers, karyotype asymmetry and heterochromatin content of spontaneous populations of *Ophrys tenthredinifera* were determined. Mitotic metaphase plates showed $2n = 2x = 36$ chromosomes in all studied populations of *O. tenthredinifera*, which confirms the karyological stability of this taxon throughout its area of distribution (Scrugli 1977; Bianco et al. 1991; Bernardos et al. 2003; D'Emerico et al. 2005). Bernardos et al. (2003) reported $2n = 38 + 4B$ and $2n = 38$ chromosomes for *O. tenthredinifera* in Iberia and North Africa respectively, while $2n = 3x = 54$ was reported by Bianco et al. (1991) in only one case. The first chromosome pair

clearly shows a secondary constriction on the long arm, as observed in other works (D'Emerico et al. 2005; Deniz et al. 2017).

Regarding the infraspecific taxonomy of *Ophrys tenthredinifera*, this study analysed two subspecies, namely *O. tenthredinifera* subsp. *neglecta*, endemic to Sardinia and peninsular Italy from Tuscany to Calabria, and *O. tenthredinifera* subsp. *grandiflora*, endemic to Sicily and southern Calabria (GIROS 2016). The present study showed few intraspecific karyotype variations between populations of *O. tenthredinifera* subsp. *neglecta* and *O. tenthredinifera* subsp. *grandiflora*. These data do not therefore support a separation of these two taxa, as suggested in the World Checklist of selected Plant Families (WCSP), http://wcsp.science.kew.org/home.do, by Hennecke and Galano (2020).

Silver nitrate staining in interphase nuclei showed three nucleoli, although some meristematic cells had one large nucleolus. Moscone et al. (1995) suggest that the maximum number of nucleoli per nucleus generally coincides with the maximum number of NORs detected with silver nitrate. However, the number may be lower, due to frequent nucleoli fusions.

The 18S-5.8S-25S rRNA genes are normally located on the nucleolus organizing secondary constriction and adjacent heterochromatin, of which the nucleolar organiser region (NOR) is constituted. Whereas 5S rDNA sites are exclusively detected by FISH, they do not form chromosome constrictions in metaphase chromosomes (Fuchs et al. 1998). *In situ* hybridisation shows that there are two pairs of 5S rDNA sites in *Ophrys tenthredinifera*. However, in *O. tenthredinifera*, the pTa794 signals were not intense.

The two subspecies *O. tenthredinifera* subsp. *neglecta* and *O. tenthredinifera* subsp. *grandiflora* may be affected by the epigenetic effects of heterochromatic sequences present on chromosomes. Indeed, Paun et al. (2010) analysed three sibling allotetraploid orchid species differing radically in terms of their geographical and ecological contexts, and showed that ecological divergence in *Dactylorhiza* species is mostly due to epigenetic factors regulating gene expression in response to environmental stimuli. Unfortunately, in the genus *Ophrys*, as far as we know, no study of this kind has been conducted.

Previous cytological studies in *Serapias vomeracea* have shown $2n = 2x = 36$ chromosomes (Heusser 1938; Del Prete 1977; Mazzola et al. 1981; Bianco et al. 1987). This species shows a moderately asymmetrical karyotype consisting of mainly submetacentric chromosomes (D'Emerico et al. 1992). Giemsa C-banding analysis showed conspicuous bands in centromeric positions on many chromosomes, together with euchromatic telomeric regions (D'Emerico et al. 2000). In *Serapias vomeracea* the 5S rDNA signals on one pair were much more intense than those on the other pair. The presence of a major site of 5S rDNA gene clusters could be regarded as further evidence of recent chromosomal restructuring (Abbo et al. 1994) of this species, reinforcing previous reports (D'Emerico et al. 2001 and references therein).

Serapias comprises about 25 species (Delforge 2016), and cytological studies have shown that most of them have $2n = 2x = 36$ chromosomes (D'Emerico et al 2000; Bernardos et al. 2004; Bellusci and Aquaro 2008). Polyploidy has been observed in *S. lingua* Linnaeus, 1753 (Brullo et al. 2014), *S. olbia* Verguin, 1908, *S. gregaria* Godfrey,

1921 and *S. strictiflora* Welwitsch ex Veiga, 1887 (Bellusci and Aquaro 2008), all with $2n = 4x = 72$ chromosomes. The karyotype of numerous species of the genus *Serapias* has been observed using the Giemsa technique, with interesting results. Indeed, C-banded somatic metaphase plates showed broad centromeric bands on almost all chromosomes where heterochromatin occupies most of the chromosome, leaving a euchromatic segment in a telomeric position (D'Emerico et al. 2000). The karyology of *Serapias lingua* is interesting from the data obtained through conventional analyses alone, with numerous bivalents compared to the few tetravalents observed at metaphase I in EMC. Unfortunately, for this genus, the only data obtained with FISH in this study are reported for *S. vomeracea*.

Himantoglossum s.l. (including *Comperia* K. Koch, 1849 and *Barlia* Parlatore, 1860) is a group of species found in Portugal, Spain and across the Mediterranean region, including North Africa, the Aegean islands, Syria and Turkey, as well as the Crimea, the Caucasus and western and northern Iran (Wood 2001). The species *Himantoglossum hircinum* and *H. adriaticum* H. Baumann, 1978 have a chromosome number of $2n = 2x = 36$. Ströhlein and Sundermann (1972) reported $2n = 2x = 30$ in *Himantoglossum comperianum* (Steven, 1829) P. Delforge, 1999, and Bernardos et al. (2006) reported $2n = 2x = 36$ for *Himantoglossum metlesicsianum* (W.P. Teschner, 1982) P. Delforge, 1999. The chromosomal numbers of the other species of the genus such as *H. formosum* (Steven, 1813) K. Koch, 1849, *H. calcaratum* (Beck, 1887) Schlechter, 1927, *H. caprinum* Sprengel, 1826 and *H. montis-tauri* Kreutz et W. Lüders, 1997 (Bateman et al. 2017) are unknown. Cases of aneuploidy with $2n = 36+1B$ are known in both *H. hircinum* and *H. adriaticum* (Capineri and Rossi 1987; D'Emerico et al. 1993).

It is interesting to note that the World Checklist of selected Plant Families (WCSP) reports *Barlia robertiana* (Loiseleur-Deslongchamps, 1807) Greuter, 1967 as a synonym for *Himantoglossum robertianum* (Loiseleur-Deslongchamps, 1807) P. Delforge, 1999. Furthermore, in the new classification based on morphological and molecular data (Sramkó et al. 2014), Bateman et al. (2017) place *Barlia robertiana* in the new subgenus *Barlia* (Parlatore, 1860) R.M. Bateman, Molnar et Sramkó, 2017 within the genus *Himantoglossum*.

Comparative investigations of *Himantoglossum hircinum* and *Barlia robertiana* show similar karyotype morphologies, with mainly metacentric chromosomes, low asymmetry and little constitutive heterochromatin. *H. hircinum* was found to have four nucleoli in interphase nuclei. Moreover, in situ hybridisation showed four 18S-5.8S-25S rDNA sites and four 5S rDNA sites. In contrast, double-target in situ hybridisation in *Barlia robertiana* revealed one pair of chromosomes carrying both the pTa794 and pTa71 signals on opposite arms (D'Emerico et al. 2001). In addition, interphase nuclei in *Barlia robertiana* had two nucleoli.

Giemsa C-banding and FISH yielded few data for *Himantoglossum hircinum* and *Barlia robertiana*, while for *H. adriaticum*, on which only the conventional Feulgen method was used, only the karyotype was established. As already mentioned, the asymmetry indices and karyological formulas of *Himantoglossum hircinum* and *Barlia robertiana* are so similar that it is hard to clearly distinguish between them. Furthermore, we did not obtain important data with Giemsa C-banding; the few discriminating data are visible

only with silver staining and FISH. Therefore, in the future it will be useful to continue with the above analyses in order to obtain clarification regarding the phylogenetic relationships between *Barlia robertiana* and the other species of the genus *Himantoglossum*.

In *Anacamptis morio*, the chromosome number $2n = 2x = 36$ is consistent with previous reports (D'Emerico et al. 1996 and references therein). The karyotype consists of 30m + 6sm. This species possesses the most symmetrical karyotype, comprising mainly metacentric chromosomes. Three satellited chromosomes were visible. In our study, neither the chromosomes nor the interphase nuclei of this species showed any differential reaction when stained with Giemsa or DAPI. Fluorescence *in situ* hybridisation mapping in diploid *Anacamptis morio* showed six 18S-5.8S-25S rDNA sites and two 5S rDNA sites. In contrast, in a previous paper, D'Emerico et al. (2001) reported four 18S-5.8S-25S rDNA sites and two 5S rDNA sites.

In this study we report analyses of a triploid individual of *Anacamptis morio* with chromosome number $2n = 3x = 54$ for the first time. The same count has been reported in specimens of *A. coriophora* (Linnaeus, 1753) R.M. Bateman, Pridgeon et M.W. Chase, 1997, *A. laxiflora* (Lamarck, 1779) R.M. Bateman, Pridgeon et M.W. Chase, 1997 and *A. pyramidalis* (Linnaeus, 1753) Richard, 1817 (D'Emerico et al. 1992, 1993; Pegoraro et al. 2016, 2019; Doro 2020). Fluorescence *in situ* hybridisation mapping in this triploid showed nine 18S-5.8S-25S rDNA sites and three 5S rDNA sites.

Conclusions

Fluorescence in situ hybridisation may authentically substantiate the genome structure and distribution of repetitive DNA families. In this context, our results provide new data on the cytogenetic differences between four genera within the Orchidinae and investigations of other species are expected to yield further insight. Moreover, these data constitute basic knowledge for facilitating the study of taxonomic relationships in other species of this subtribe. Some examples are given below.

In relation to the triploid individuals observed in the genus *Anacamptis* s.l., it is possible to add some interesting notes about *A. pyramidalis*, useful for other species where polyploid individuals have been observed. The species *A. pyramidalis* has $2n = 2x = 36, 54, 72$ chromosomes (D'Emerico et al. 1992, 1993; Pegoraro et al. 2016, 2019). Recently the new species *A. berica* Doro, 2020 has been reported by Doro (2020), with $2n = 4x = 72$ chromosomes. In both cases, polyploid species with $2n = 4x = 72$ are referred to as autotetraploid, although Bianco et al. (1991) reported 36 bivalents with occasional quadrivalents at metaphase I in EMC. Giemsa C-banding has not yielded good results, but it would be interesting to analyse these species with other banding methods and FISH.

Also interesting from the karyological point of view are the *Neotinea* s.l. group, with $2n = 2x = 42$ chromosomes, and the polyploid insular neoendemic *N. commutata* (Todaro, 1842) R.M. Bateman, 2003 with $2n = 4x = 84$ (Mazzola et. al. 1981). An interesting result for *N. commutata* was reported by Pavarese et al (2013), who showed

42 bivalents at Metaphase I in EMC, hypothesising that the species arose from allopolyploidisation. In this case, no further data was obtained by the FISH method.

The *Orchis* s.s. group, with a chromosomal number of $2n = 2x = 42$, is characterised by small chromosomes and a fairly complex structure. Polyploidy has been observed in *Orchis canariensis* Lindley, 1835, *O. olbiensis* Reuter ex Grenier, 1860 and *O. patens* Desfontaines, 1799, with $2n = 4x = 84$ chromosomes (Pellegrino et al. 2000; Bernardos et al. 2002; Bernardos et al. 2006). The *O. mascula* (Linnaeus, 1753) Linnaeus, 1755 complex, which includes the species *O. mascula*, *O. provincialis* Balbis ex Lamarck et Candolle, 1806, *O. pauciflora* Tenore, 1811 and *O. patens*, is still undergoing taxonomic evaluation. Cytogenetic analyses using differential banding methods based on Giemsa and fluorochromes such as DAPI and CMA3 have revealed a remarkable affinity between these species. In *O. mascula*, C-banded somatic metaphase chromosomes show distinctive heterochromatin distribution. In ten chromosome pairs of the complement, heterochromatin occupies most of the chromosomes, with euchromatin occupying only the telomeric region, while eleven pairs were euchromatic, characterised by the presence of thin centromeric bands. After staining with fluorochrome DAPI, the chromosomes of this species showed blocks of heterochromatin in telomeric and subtelomeric regions (D'Emerico et al. 2002a). The results reveal that the species of the *O. mascula* s.l. complex are cytogenetically different from those belonging to the remaining species of *Orchis* s.s. These differences open up interesting avenues of investigation regarding the involvement of heterochromatin in the evolutionary processes of these species. The presence of these chromosomal structures needs to be studied further, through these and other techniques.

Acknowledgements

We thank Giuseppina Bartolo and Santa Pulvirenti for helping us with the collection of *O. tenthredinifera* subsp *grandiflora*. Domenico Pignone and Incoronata Galasso for technical analysis as part of the FISH experiments. The reviewers Lorenzo Peruzzi and Quanwen Dou for corrections and suggestions that helped us to improve the early version of the manuscript.

References

Abbo S, Miller TE, Reader SM, Dunford RP, IP King (1994) Detection of ribosomal DNA sites in *lentil* and *chickpea* by fluorescent in situ hybridisation. Genome 37: 713–716. https://doi.org/10.1139/g94-101

Astuti G, Roma-Marzio F, Peruzzi L (2017) Traditional karyomorphological studies: can they still provide a solid basis in plant systematics? Flora Mediterranea 27: 91–98 https://doi.org/10.7320/FlMedit27.091

Bartolucci F, Peruzzi L, Galasso G, Albano A, Alessandrini A, Ardenghi NMG, Astuti G, Bacchetta G, Ballelli S, Banfi E, Barberis G, Bernardo L, Bouvet D, Bovio M, Cecchi L, Di Pietro R, Domina G, Fascetti S, Fenu G, Festi F, Foggi B, Gallo L, Gottschlich G, Gubellini L, Iamonico D, Iberite M, Jiménez-Mejías P, Lattanzi E, Marchetti D, Martinetto E, Masin RR, Medagli P, Passalacqua NG, Peccenini S, Pennesi R, Pierini B, Poldini L, Prosser F, Raimondo FM, Roma-Marzio F, Rosati L, Santangelo A, Scoppola A, Scortegagna S, Selvaggi A, Selvi F, Soldano A, Stinca A, Wagensommer RP, Wilhalm T, Conti F (2018) An updated checklist of the vascular flora native to Italy. Plant Biosystems 152(2): 179–303. https://doi.org/10.1080/11263504.2017.1419996

Bateman RM, Molnár AV, Sramkó G (2017) In situ morphometric survey elucidates the evolutionary systematics of the Eurasian *Himantoglossum* clade (Orchidaceae: Orchidinae). PeerJ 5: e2893. https://doi.org/10.7717/peerj.2893

Battaglia E (1957a) A new '5 minutes-fixation' using cold hydrolysis. Caryologia 9: 368–370. https://doi.org/10.1080/00087114.1957.10797602

Battaglia E (1957b) A simplified Feulgen method using cold hydrolysis. Caryologia 9: 372–373. https://doi.org/10.1080/00087114.1957.10797604

Baumann H, D'Emerico S, Lorenz R, Pulvirenti S (2012) Supernumerary chromosomes and speciation processes in *Dactylorhiza urvilleana* subsp. *phoenissa* (*Orchidaceae*) from Lebanon. Journal Europäischer Orchideen 44(4): 811–824.

Bellusci F, Aquaro G (2008) Contribution to the cytotaxonomical knowledge of four species of *Serapias* L. (Orchidaceae). Caryologia 61(3): 294–299. https://doi.org/10.1080/00087114.2008.10589641

Bernardos S, Amich F, Gallego F (2003) Karyological and taxonomic notes on *Ophrys* (*Orchidoideae*, *Orchidaceae*) from the Iberian Peninsula. Botanical Journal of the Linnean Society 142(4): 395–406. https://doi.org/10.1046/j.1095-8339.2003.00198.x

Bernardos S, Amich F, Gallego F, Crespí A L (2002) Contributions to the knowledge on the orchid flora of Northern Portugal. Journal Europäischer Orchideen 34: 35–50.

Bernardos S, García-Barriuso M, León-Arencibia MC, Reyes-Betancort A, González-González R, Padrón M, Amich F (2006) A cytotaxonomic study of three endemic orchids of the Canary Islands. Annales Botanici Fennici 43: 161–166.

Bernardos S, Tyteca D, Amich F (2004) Cytotaxonomic study of some taxa of the subtribe Orchidinae (Orchidoideae, Orchidaceae) from the Iberian Peninsula. Israel Journal of Plant Sciences 52: 161–170. https://doi.org/10.1560/YD43-0MFC-ANN9-PYN0

Bianco P, D'Emerico S, Medagli P, Ruggiero L (1989) Karyological studies of some taxa of the genus *Ophrys* (Orchidaceae) from Apulia (Italy). Caryologia 42: 57–63. https://doi.org/10.1080/00087114.1989.10796953

Bianco P, D'Emerico S, Medagli P, Ruggiero L (1991) Polyploidy and aneuploidy in *Ophrys*, *Orchis* and *Anacamptis* (Orchidaceae). Plant Systematics and Evolution 178: 235–245. https://doi.org/10.1007/BF00937966

Bianco P, Medagli P, D'Emerico S, Ruggiero L (1987) Numeri cromosomici per la flora italiana: 1154. Informatore Botanico Italiano 19: 322–332.

Bianco P, Medagli P, D'Emerico S, Ruggiero L (1988) Nuovo rinvenimento di *Ophrys* × *venusiana* Baumann & Künkele (*O. tarentina* Gölz & Reinhard × *O. tenthredinifera* Willd.) e

studio cariologico delle specie parentali. Webbia 42: 43–47. https://doi.org/10.1080/00837792.1988.10670426

Brullo C, D'Emerico S, Pulvirenti S (2014) A cytological study of four Sicilian *Serapias* (Orchidaceae). Caryologia 67(3): 260–264. https://doi.org/10.1080/0144235X.2014.974354

Capineri R, Rossi W (1987) Numeri cromosomici per la flora italiana: 1130–1131. Informatore Botanico Italiano 19: 314–318.

D'Emerico S (2001) Orchideae, Cytogenetics. In: Pridgeon AM, Cribb PJ, Chase MC, Rasmussen FN (Eds) Genera Orchidacearum 2: Orchidoideae. Oxford, Oxford University Press, Part 1: 335.

D'Emerico S (2005) Cytogenetic diversity in *Orchis* s.l. and allied genera (Orchidinae, Orchidaceae). In: Sharma AK and Sharma A (Eds) Plant genome, biodiversity and evolution, phanerogams (Higher groups). Enfield (NH), Science, Inc., 1(Part B): 61–87.

D'Emerico S, Bianco P, Medagli P (1992) Karyological studies on Orchidaceae. Tribe Ophrydeae, subtribe Serapiadinae. Caryologia 45: 301–311. https://doi.org/10.1080/00087114.1992.10797233

D'Emerico S, Bianco P, Medagli P (1993) Cytological and karyological studies on Orchidaceae. Caryologia 46: 309–319. https://doi.org/10.1080/00087114.1993.10797271

D'Emerico S, Cozzolino S, Pellegrino G, Pignone D, Scrugli A (2002a) Heterochromatin distribution in selected taxa of the 42-chromosome *Orchis* s.l. (Orchidaceae). Caryologia 55: 55–62. https://doi.org/10.1080/00087114.2002.10589258

D'Emerico S, Cozzolino S, Pellegrino G, Pignone D, Scrugli A (2002b) Karyotype structure, supernumerary chromosomes and heterochromatin distribution suggest a pathway of karyotype evolution in *Dactylorhiza* (Orchidaceae). Botanical Journal of the Linnean Society 138: 85–91. https://doi.org/10.1046/j.1095-8339.2002.00008.x

D'Emerico S, Galasso I, Pignone D, Scrugli A (2001) Localization of rDNA loci by Fluorescent *In Situ* Hybridization in some wild orchids from Italy (Orchidaceae). Caryologia 54(1): 31–36. https://doi.org/10.1080/00087114.2001.10589211

D'Emerico S, Grünanger P, Scrugli A, Pignone D (1999) Karyomorphological parameters and C-bands distribution suggest phyletic relationship within the subtribe Limodorinae Bentham (Orchidaceae). Plant Systematics and Evolution 217: 147–161. https://doi.org/10.1007/BF00984927

D'Emerico S, Pignone D, Bartolo G, Pulvirenti S, Terrasi C, Stuto S, Scrugli A (2005) Karyomorphology, heterochromatic patterns and evolution in the genus *Ophrys* (Orchidaceae). Botanical Journal of the Linnean Society 148: 87–99. https://doi.org/10.1111/j.1095-8339.2005.00393.x

D'Emerico S, Pignone D, Bianco P (1996) Karyomorphological analyses and heterochromatin characteristic disclose phyletic relationships among $2n = 32$ and $2n = 36$ species of *Orchis* (Orchidaceae). Plant Systematics and Evolution 200: 111–124. https://doi.org/10.1007/BF00984752

D'Emerico S, Pignone D, Scrugli A (2000) Giemsa C-banded karyotypes in *Serapias* L. (Orchidaceae). Botanical Journal of the Linnean Society 133: 485–492. https://doi.org/10.1111/j.1095-8339.2000.tb01591.x

Del Prete C (1977) Numeri cromosomici per la flora italiana: 358–365. Informatore Botanico Italiano 9: 135–140.

Delforge P (2005) Orchids of Europe, North Africa and the Middle East. A & C. Black Ltd, London. [ISBN 10: 071367525X ISBN 13: 9780713675252]

Deniz IG, Genç I, Yücel G, Sümbül H, Sezik E, Tuna M (2017) Karyomorphology and nuclear DNA content for sixteen *Ophrys* L. taxa from Turkey. Plant Biosystems 152: 711–719. https://doi.org/10.1080/11263504.2017.1327899

Doro D (2020) *Anacamptis berica* – Una nuova specie tetraploide del gruppo di *Anacamptis pyramidalis*. J. Eur. Orch. 52(2–4): 427–460.

Fuchs J, Strehl S, Brandes A, Scheizer D, Schubert I (1998) Molecular-cytogenetic characterization of the *Vicia faba* genome - Heterochromatin differentiation, replication and sequence localization. Chromosome Research 6: 219–230. https://doi.org/10.1023/A:1009215802737

Galasso I, Blanco A, Katsiotis A, Pignone D, Heslop-Harrison JS (1997) Genomic organization and phylogenetic relationships in the genus *Dasypyrum* analysed by Southern and in situ hybridization of total genomic and cloned DNA probes. Chromosoma 106: 53–61. https://doi.org/10.1007/s004120050224

Galasso I, Schmidt T, Pignone D, Heslop-Harrison JS (1995) The molecular cytogenetics of *Vigna unguiculata* (L.) Walp: the physical organization and characterization of 18s-5.8s-25s rRNA genes, 5s rRNA genes, telomere-like sequences, and a family of centromeric ripetitive DNA sequences. Theoretical and Applied Genetics 91: 928–935. https://doi.org/10.1007/BF00223902

Gerlach WL, Bedbrook JR (1979) Cloning and characterization of ribosomal RNA genes from wheat and barley. Nucleic Acids Research 7: 1869–1885. https://doi.org/10.1093/nar/7.7.1869

Gerlach WL, Dyer TA (1980) Sequence organization of the repeating units in the nucleus of wheat which contain 5s rRNA genes. Nucleic Acids Research 8: 4851–4855. https://doi.org/10.1093/nar/8.21.4851

GIROS, editor (2016) Orchidee d'Italia. Guida alle orchidee spontanee. Cornaredo (MI), Il Castello Ed., 303 pp.

Guerra M (2012) Cytotaxonomy: The end of childhood. Plant Biosystems 146(3): 703–710. https://doi.org/10.1080/11263504.2012.717973

Hennecke M, Galano C (2020) *Ophrys* subgen. *Bombyliflorae* sect. *Tenthrediniferae*, a synopsis. GIROS Orchidee Spontanee d'Europa 63(2): 358–419.

Heslop-Harrison JS, Schwarzacher T, Anamtawat Jonsoon K, Leitch AR, Sffl M, Leitch IJ (1991) In situ hybridization with automated chromosome denaturation. Technique 3: 109–116.

Heusser C (1938) Chromosomenverhältnisse bei schweizerischen basitonen Orchideen. Berichte der Schweizerischen Botanischen Gesellschaft 48: 562–599.

Ilnicki T (2014) Plant biosystematics with the help of cytology and cytogenetics. Caryologia 67(3): 199–208. https://doi.org/10.1080/00087114.2014.931642

Lacadena JR, Cermeno MC (1985) Nucleolus organizer competition in *Triticum aestivum–Aegilops umbellulata* chromosome addition lines. Theoretical and Applied Genetics 71: 278–285. https://doi.org/10.1007/BF00252067

Lan T and Albert VA (2011) Dynamic distribution patterns of ribosomal DNA and chromosomal evolution in *Paphiopedilum*, a lady's slipper orchid. BMC Plant Biology 11: 126. https://doi.org/10.1186/1471-2229-11-126

Levan A, Fredga K, Sandberg AA (1964) Nomenclature for centromeric position on chromosomes. Hereditas 52: 201–220. https://doi.org/10.1111/j.1601-5223.1964.tb01953.x

Levitsky GA (1931) The karyotype in systematics. Bull. Appl. Bot. Gen. Pl. Breed. 27: 220-240.

Maluszynska J, Heslop-Harrison JS (1993a) Physical mapping of rDNA in *Brassica* species. Genome 36: 774–781. https://doi.org/10.1139/g93-102

Maluszynska J, Heslop-Harrison JS (1993b) Molecular cytogenetics of the genus *Arabidopsis*: in situ localization of rDNA sites, chromosome numbers and diversity in centromeric heterochromatin. Annals of Botany 71: 479–484. https://doi.org/10.1006/anbo.1993.1063

Martellos S, Bartolucci F, Conti F, Galasso G, Moro A, Pennesi R, Peruzzi L, Elena Pittao E, Nimi PL (2020) FlorItaly – the portal to the Flora of Italy. PhytoKeys 156: 55–71. https://doi.org/10.3897/phytokeys.156.54023

Mazzola P, Crisafi F, Romano S (1981) Numeri cromosomici per la flora italiana: 850 Informatore Botanico Italiano 13: 182–188.

Moscone EA, Loidl J, Ehrendorfer F, Hunziker AT (1995) Analysis of active nucleolus organizing regions in *Capsicum* (Solanaceae) by silver staining. American Journal of Botany 82(2): 276–287. https://doi.org/10.1002/j.1537-2197.1995.tb11495.x

Moscone EA, Samuel R, Schwarzacher T, Schweizer D, Pedrosa-Harand A (2007) Complex rearrangements are involved in *Cephalanthera* (Orchidaceae) chromosome evolution. Chromosome Res 15: 931–943. https://doi.org/10.1007/s10577-007-1174-6

Paszko B (2006) A critical review and a new proposal of karyotype asymmetry indices. Plant Systematics and Evolution 258: 39–48. https://doi.org/10.1007/s00606-005-0389-2

Paun O, Bateman RM, Fay MF, Hedren M, Civeyrel L, MW Chase (2010) Stable epigenetic effects impact adaptation in allopolyploid orchids (*Dactylorhiza*: Orchidaceae) research article. Molecular Biology and Evolution 27: 2465–2473. https://doi.org/10.1093/molbev/msq150

Pavarese G, Tranchida-Lombardo V, Galesi R, D'Emerico S, Casotti R, Cristaudo A, and Cozzolino S (2013) When polyploidy and hybridization produce a fuzzy taxon: the complex origin of the insular neoendemic *Neotinea commutata* (Orchidaceae). Botanical Journal of the Linnean Society 173: 707–720. https://doi.org/10.1111/boj.12093

Pegoraro L, Cafasso D, Rinaldi R, Cozzolino S, Scopece G (2016) Habitat preference and flowering-time variation contribute to isolation between diploid and autotetraploid *Anacamptis pyramidalis*. Journal of Evolutionary Biology 29(10): 2070–2082. https://doi.org/10.1111/jeb.12930.

Pegoraro L, De Vos JM, Cozzolino S, Scopece G (2019) Shift in flowering time allows diploid and autotetraploid *Anacamptis pyramidalis* (Orchidaceae) to coexist by reducing competition for pollinators. Botanical Journal of the Linnean Society 191(2): 274–284. https://doi.org/10.1093/botlinnean/boz043

Pellegrino G, Cozzolino S, D'Emerico S, Grünanger P (2000) The taxonomic position of the controversial taxon *Orchis clandestina* (Orchidaceae): Karyomorphological and molecular analyses. Botanica Helvetica 110: 101–107. https://doi.org/10.5169/seals-73589

Peruzzi L, Eroğlu HE (2013) Karyotype asymmetry: again, how to measure and what to measure? Comparative Cytogenetics 7: 1–9. https://doi.org/10.3897/compcytogen.v7i1.4431

Pridgeon AM, Cribb PJ, Chase MW, Rasmussen FN (2001) Genera Orchidacearum, Orchidoideae (part 1), Vol. 2. Oxford, Oxford University Press, 464 pp.

Schwarzacher T, Schweizer D (1982) Karyotype analysis and heterochromatin differentiation with Giemsa C-banding and fluorescent counterstaining in *Cephalanthera* (Orchidaceae). Plant Syst Evol 141: 91–113. https://doi.org/10.1007/BF00986411

Scrugli A (1977) Numeri cromosomici per la flora italiana: 124–125 Informatore Botanico Italiano 9: 119–125.

Sharma SK, Mukai Y (2015) Chromosome research in orchids: current status and future prospects with special emphasis from molecular and epigenetic perspective. The Nucleus 58: 173–184. https://doi.org/10.1007/s13237-015-0152-1

Siljak-Yakovlev S, Peruzzi L (2012) Cytogenetic characterization of endemics: past and future. Plant Biosystems 146: 694–702.

Sramkó G, Molnár V, Hawkins JA, Bateman RM (2014) Molecular phylogeny and evolutionary history of the Eurasiatic orchid genus *Himantoglossum* s.l. (Orchidaceae). Annals of Botany 114: 1609–1626. https://doi.org/10.1093/aob/mcu179

Stace C A (2000) Cytology and cytogenetics as a fundamental taxonomic resource for the 20th and 21st centuries. Taxon 49: 451–477. https://doi.org/10.2307/1224344

Stebbins (1971). Chromosomal evolution in higher plants. London.

Ströhlein H, Sundermann H (1972) Chromosomenzählungen bei Erdorchideen. Jahresbericht naturwisschaften Vereins Wuppertal 25: 75–80.

Turco A, Albano A, Medagli P, D'Emerico S (2020) Contribution to the study of wild Orchidaceae, genus *Platanthera* L.C.M. Richard. Karyotype and C-banding analysis of two species from Italy. Caryologia 73 (4): 11–16. https://doi.org/10.13128/Caryologia-811

Turco A, Albano A, Medagli P, Pulvirenti S, D'Emerico S (2018) New cytological data in *Ophrys* sect. *Pseudophrys* Godfery and comparative karyomorphological studies in *Ophrys* L. (Orchidaceae). Plant Biosystems 152(5): 901–910. https://doi.org/10.1080/11263504.2017.1362058

Turco A, Medagli P, Wagensommer RP, D'Emerico S, Gennaio R, Albano A (2021) A morphometric study on *Ophrys* sect. *Pseudophrys* in Apulia (Italy) and discovery of *Ophrys japigiae* sp. nov. (Orchidaceae). Plant Biosystems, online first. https://doi.org/10.1080/11263504.2021.1897702

Wagensommer RP, Medagli P, Turco A, Perrino EV (2020) IUCN Red List evaluation of the orchidaceae endemic to Apulia (Italy) and considerations on the application of the IUCN protocol to rare species. Nature Conservation Research 5(suppl. 1): 90–101. https://doi.org/10.24189/ncr.2020.033

Wood J (2001) *Himantoglossum*. In: Pridgeon AM, Cribb PJ, Chase MW, Rasmussen FN (Eds) Genera Orchidacearum, Vol. 2, part 1: Orchidoideae. New York, Oxford University Press, 309 pp.

Zoldos V, Papes D, Cerbah M, Panaud O, Besendorfer V, Siljak-Yakovlev S (1999) Molecular-cytogenetic studies of ribosomal genes and heterochromatin reveal conserved genome organization among 11 *Quercus* species. Theoretical and Applied Genetics 99: 969–977. https://doi.org/10.1007/s001220051404

Zuo L, Yuan Q (2011) The difference between the heterogeneity of the centromeric index and intrachromosomal asymmetry. Plant Systematics and Evolution 297: 141–145. https://doi.org/10.1007/s00606-011-0528-x

ORCID

Antonella Albano https://orcid.org/0000-0002-0874-320X
Alessio Turco https://orcid.org/0000-0001-9071-344X
Robert P. Wagensommer https://orcid.org/0000-0002-1614-4821

CompCytogen 15(4): 527–541 (2021)
doi: 10.3897/compcytogen.v15.i4.76761
https://compcytogen.pensoft.net

RESEARCH ARTICLE

COMPARATIVE Cytogenetics
A peer-reviewed open-access journal
International Journal of Plant & Animal Cytogenetics, Karyosystematics, and Molecular Systematics

Revision of the banding sequence pool and new data on chromosomal polymorphism in natural populations of *Chironomus agilis* Shobanov et Djomin, 1988 (Diptera, Chironomidae)

Veronika V. Golygina[1,2], Oksana V. Ermolaeva[2]

1 *The Federal Research Center Institute of Cytology and Genetics of Siberian Branch of the Russian Academy of Science, Prospect academika Lavrentieva 10, Novosibirsk, 630090 Russia* **2** *Novosibirsk State University, ul. Pirogova, 2, Novosibirsk, 630090 Russia*

Corresponding author: Veronika V. Golygina (nika@bionet.nsc.ru)

Academic editor: Igor Sharakho | Received 19 October 2021 | Accepted 27 November 2021 | Published 17 December 2021

http://zoobank.org/399EE444-9268-4F3B-BC43-533EBEE8ABAF

Citation: Golygina VV, Ermolaeva OV (2021) Revision of the banding sequence pool and new data on chromosomal polymorphism in natural populations of *Chironomus agilis* Shobanov et Djomin, 1988 (Diptera, Chironomidae). CompCytogen 15(4): 527–541. https://doi.org/10.3897/compcytogen.v15.i4.76761

Abstract

Quantitative and qualitative analysis of chromosomal polymorphism in 19 natural populations of *Ch. agilis* had been performed. Most studied populations showed a medium level of chromosomal polymorphism: on average 45±3.0% of specimens are heterozygotes with 0.52±0.01 heterozygotic inversion per larvae. Besides inversions, B-chromosomes were found in two populations. The total number of banding sequences found in banding sequence pool of *Ch. agilis* is 16. Three banding sequences – p'agiB3, p'agiD3, p'agiF3 – are described for the first time.

Keywords

Banding sequence, *Ch. plumosus* group, inversion, karyotype, karyological analysis, polythene chromosome, sibling species

Introduction

Chironomus agilis Shobanov et Djomin, 1988 belongs to the *Ch. plumosus* group of sibling species. This group presents a good model for studies of the evolution of the

karyotype during speciation as well as chromosomal polymorphism in natural populations. Three species with the widest ranges – *Ch. plumosus* (Linnaeus 1758), *Ch. entis* Schobanov, 1989 and *Ch. balatonicus* Dévai, Wülker et Scholl, 1983 – have been studied most extensively. At the same time, only a few populations were studied karyologically for other species from the group. In case of *Ch. agilis* the data on chromosomal polymorphism were published only for two populations – one from Eastern Europe (Rybinskoe reservoir) and one from Siberia (Berdsky pond) – where only 9 banding sequences had been found in total (Schobanov and Djomin 1988; Kerkis et al. 1989). Two other studies where data on chromosomal polymorphism have been published cannot be taken into account as the karyotypes shown on photos designated as *Ch. agilis* actually belong to different species (Michailova et al. 2002; Krastanov and Michailova 2008). Thus, based on the known data the species could be considered as having a low level of polymorphism. In the book of Kiknadze and coauthors (2016) four new banding sequences were described, which brought the total number of banding sequences known for *Ch. agilis* to 13, but no new data on quantitative characteristics were published as it was not the purpose of that work.

In this paper we present data on chromosomal polymorphism in 19 natural populations of *Ch. agilis* from Eastern Europe, Siberia and the Far East.

Material and methods

The VI instar larvae from 19 natural populations of Eastern Europe, Siberia and the Far East were used for slide preparations of polytene chromosomes. The data on collection sites and larvae studied are presented in Table 1. In cases when larvae were obtained several times over years from the same collection site, data on all probes were combined as statistical analysis (Fisher criteria, Plokhinsky 1967) had shown that there were no significant differences in frequencies of banding sequences between probes.

The larvae were fixated with 3:1 *v/v* of 96% ethanol and glacial acetic acid and stored at –20 °C. Polytene chromosome squashes were prepared by a routine acetoorcein method (Keyl and Keyl 1959; Kiknadze et al. 1991). Chromosomal mapping of arms A, C, D, E and F was done using mapping system created by Keyl (1962) and Devai et al. (1989), with *Ch. piger* Strenzke, 1959 as the standard karyotype. Mapping of arm B was done according to Maximova mapping system (Maximova 1976) improved by Schobanov (1994), with *Ch. plumosus* chromosomes as the standard.

Each banding sequence is given a short designation as follows: three-letter abbreviation of the species name (agi for *Ch. agilis*) followed by the name of the arm and the serial number of banding sequence in this arm (according to the order of its discovery), and prefixed by a letter indicating its geographical distribution in the genus *Chironomus* (p' for Palearctic sequences or h' for Holarctic sequences). Thus, for example, h'agiE1 means that while Ch. agilis itself is a Palearctic species, this banding sequences is identical to banding sequences of some other species and was found in Nearctic populations of those species, thus have a Holarctic distribution

The statistical analysis and phylogenetic tree construction was done using programs PHYLIP (https://evolution.genetics.washington.edu/phylip.html) and MEGA11.0.8 (https://www.megasoftware.net). Genetic distances between populations were calculated using Nei criteria (Nei 1972). The neighbor-joining method was used for construction of the phylogenetic tree between populations.

The equipment of the Centre of Microscopical analysis of biological objects SB RAS in the Institute of Cytology and Genetics (Novosibirsk) was used for this work: microscope "Axioskop" 2 Plus, CCD-camera AxioCam HRc, software package AxioVision 4 (Zeiss, Germany).

Results and discussion

The species *Ch. agilis* belongs to "thummi" cytocomplex with haploid number of chromosomes n=4 and arm combination AB CD EF G. The chromosomes I (AB) and II (CD) are metacentric, III (EF) is submetacentric, and IV (G) is telocentric (Fig. 1). There are two nucleoli in *Ch. agilis* karyotype; both are situated on the arm G – one on the centromeric end of the arm, the other on the opposite end near the telomere. Such location of nucleoli is the distinctive feature of *Ch. agilis* karyotype that allows to easily differentiate it from karyotypes of other *Chironomus* species. The homologues of arm G are paired but often

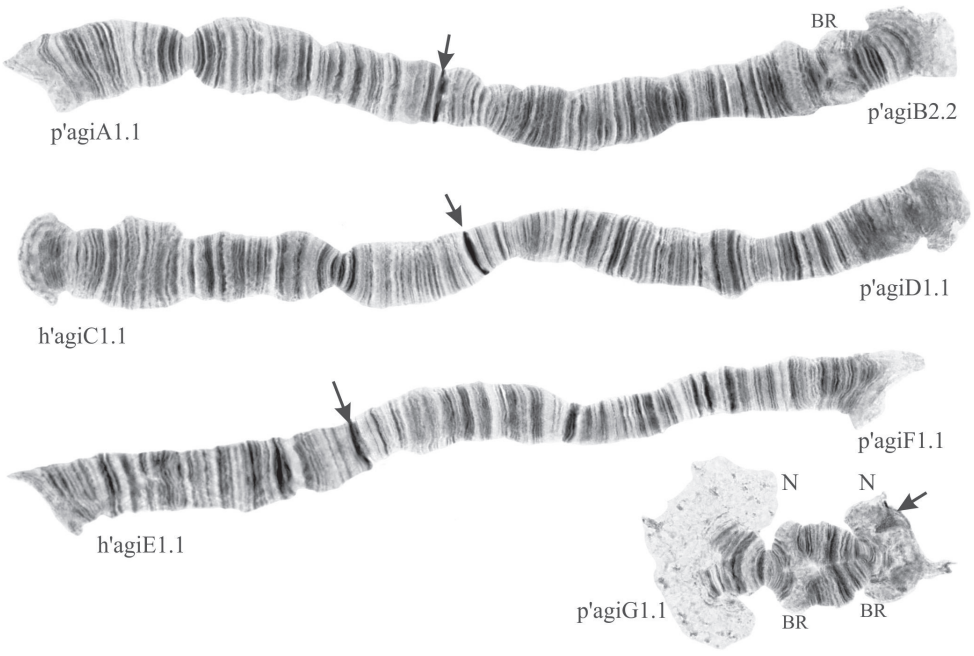

Figure 1. Karyotype of *Chironomus agilis*; p'agiA1.1, p'agiB2.2 etc. – genotypic combinations of banding sequences; BR – Balbiani ring, N – nucleolus. Arrows indicate centromeric regions.

Table 1. Collection sites.

Collection place	Abbreviation	Collection date	Geographic coordinates	Number of larvae
Yaroslavl region				
Rybinsk Reservoir	YAR-RY	13.05.1988 11.07.1988 01.08.1988	58°11'59.4"N, 38°24'59.5"E	4
Novosibirsk region				
Berdsky Pond, the Shadrikha Rivulet, Berdsk	NSK-BE	27.05.1985 18.06.1986 02.06.1987	54°43'60.0"N, 83°07'43.4"E	45
The Eltsovka River, Novosibirsk	NSK-EL	14.05.2001 16.05.2001	54°53'22.6"N, 83°05'27.5"E	4
Kainka Lake, Kainskaya Zaimka settlement	NSK-KA	20.09.1989 27.04.1991	54°52'13.7"N, 83°08'09.7"E	34
The Shadrikha River, mouth	NSK-SH	07.05.2008 12.05.2011 11.05.2012 05.05.2014 04.05.2016 05.05.2017	54°46'41.1"N, 83°10'14.0"E	259
Bol'shaya Protoka Lake, Rechport, Novosibirsk	NSK-2R	13.05.2005	54°56'06.5"N, 83°03'46.0"E	14
Pond on the Shipunikha River, Iskitim	NSK-SP	07.05.2015	54°34'13.6"N, 83°20'42.6"E	1
Pond on the Koynikha River, Linevo settlement	NSK-LI	18.05.2006	54°27'45.5"N, 83°20'49.5"E	32
Pond on the Chernodyrikha River, Ryabchinka village	NSK-CH	16.05.2006	54°35'59.9"N, 83°07'57.8"E	2
Pond on the Sarbayan River, Uchastok-Balta village	NSK-SA	16.05.2002	55°24'42.3"N, 83°56'20.1"E	5
Pond on the Ora River, Sokur settlement	NSK-OR	17.05.2002 12.05.2006	55°12'58.8"N, 83°18'06.9"E	52
Pond on the Tars'ma River, Yurti settlement	NSK-YU	14.05.2002 22.05.2004	54°51'04.7"N, 84°51'04.9"E	151
Pond on the Tars'ma River, Stepnogutovo settlement	NSK-ST	12.05.2011 12.05.2016	54°51'08.6"N, 84°57'31.6"E	54
Kemerovo region				
Tanaevo Lake, Zhuravlevo settlement	KEM-TA	14.05.2002	54°46'35.0"N, 85°02'52.4"E	1
Altai territory				
Gilovskoye Reservoir	ALT-GI	15.05.2003	51°04'14.3"N, 81°59'57.7"E	1
Travinayoe Lake, Oskolkovo settlement	ALT-TR	08.05.1994	52°19'11.9"N, 83°11'24.2"E	3
Khabarovsk territory				
The Amur River, Khabarovsk	KHA-AM	21.06.1987	48°24'56.5"N, 135°05'39.4"E	2
Evoron Lake	KHA-EV	17.07.2006	51°23'02.9"N, 136°27'55.8"E	36
Sakha Republic (Yakutiya)				
Solyonoe Lake, Yakutsk vicinity	YAK-SO	05.09.1987	61°57'51.3"N, 129°37'01.1"E	2

are unconjugated at the ends in nucleolus organiser regions. The centromeric regions are distinct and easily identifiable on all chromosomes with the exception of the arm G where the centromere sometime can be masked by the nucleolus. There are three Balbiani Rings (BR) in the karyotype of *Ch. agilis*: two are situated on the arm G (usually only the one in the center of the arm is visible as the other one is often masked by the nucleolus), and the third one – on the arm B. Unlike in many other species from the genus *Chironomus*, BR on the arm B is usually well developed and easily identifiable in *Ch. agilis*.

The revision of mapping of main banding sequences in arms A, B, C, D, E and F was presented by Golygina and Kiknadze previously (2008, 2012, 2018). Revised mapping of these banding sequences is shown on Fig. 2. For arm E two versions of mapping are presented (Fig. 2e). First is done according to how *Ch. agilis* banding sequence should be mapped if mapping of *Ch. plumosus* – reference species for mapping of all *Ch. plumosus* group sibling species – made by Keyl (1962) is considered to be

correct (marked as KV). The second one is done according to revised mapping of *Ch. plumosus* made by Golygina and Kiknadze (2018) (marked as GV).

Inversion polymorphisms were found in all chromosome arms except G, but only arms B and F show a noticeably high level of polymorphism throughout different populations. Only rare or unique inversion banding sequences were found in arms A, C, D, and E. In total, 16 banding sequences were present in the studied populations.

Arm A was monomorphic in all populations with the exception of the Siberian population from the pond on the Eltsovka river where banding sequence p'agiA2 was

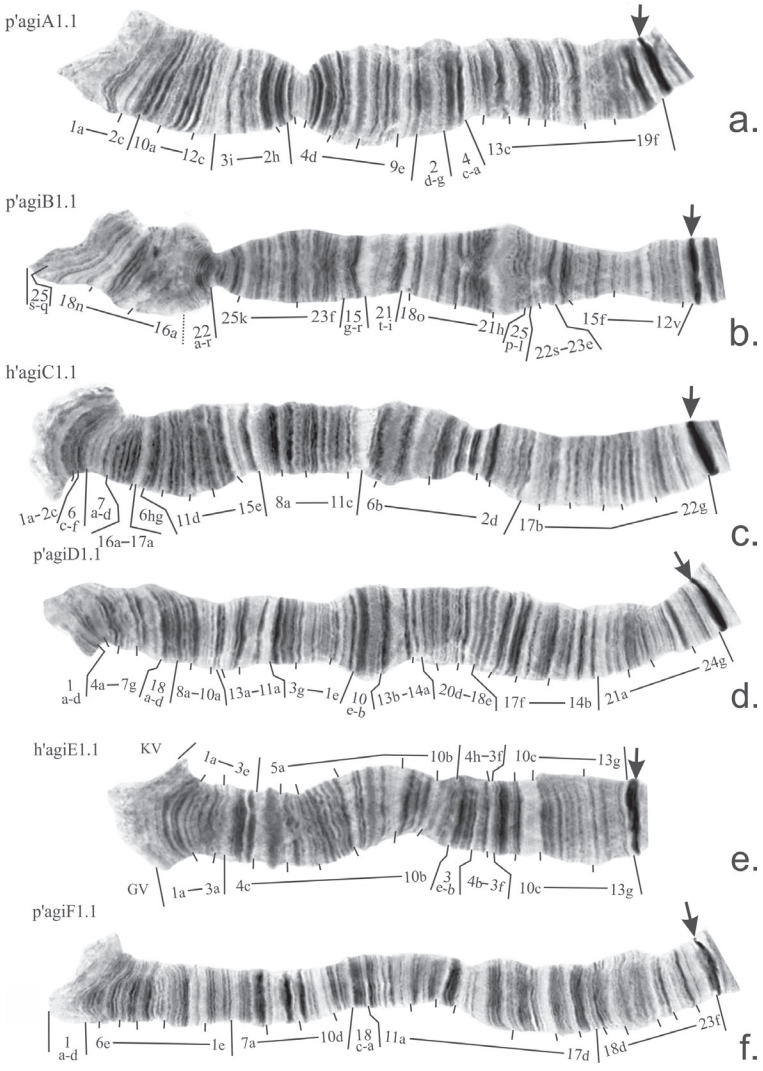

Figure 2. Mapping of main banding sequences in arms **a–f** of *Ch. agilis*. Arrows indicate centromeric regions. KV – version of mapping in arm E according to Keyl (1962), GV – version of mapping in arm E according to Golygina and Kiknadze (2018).

found in a heterozygous state in a single larvae (Table 2, 3). It differs from the main banding sequence p'agiA1 by the simple short paracentric inversion (Fig. 3a).

p'agiA1 1a-2c 10a-12c 3i-2h 4d-9e 2d-g 4c-a 13a-19f C
p'agiA2 1a-2c 10a-12c 3i 6a-4d 2h-3h 6b-9e 2d-g 4c-a 13a-19f C

Arm B is polymorphic. The standard banding sequence p'agiB1 was found in most populations, but shows high frequency of occurrence only in the western part of the species range – in the population from Rybinsk Reservoir (Table 2, 3).

p'agiB1 25s-q 18n-16a 22a-r 25k-23f 15g-r 21t-i 18o-21h 25p-l 22s-23e 15f-12v C

In all studied populations from Siberia and Far East the alternative banding sequence p'agiB2 was dominant, although only in one population – from Evoron lake – its frequency reached 100% (Table 2, 3). This banding sequence differs from p'agiB1 by the large simple inversion (Fig. 3b).

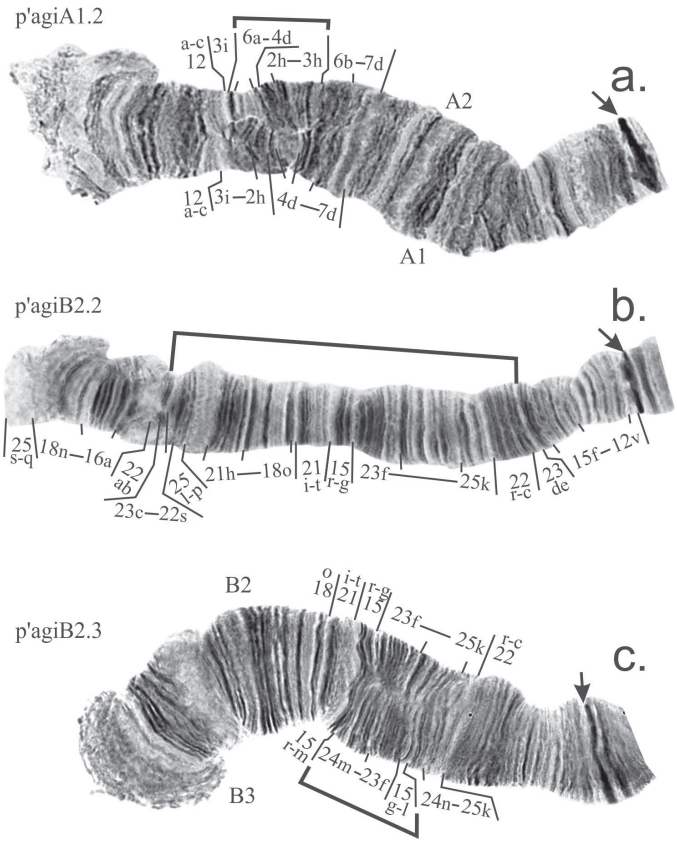

Figure 3. Inversions in arms A (**a**) and B (**b, c**) found in populations of *Ch. agilis*. Arrows indicate centromeric regions. Brackets show regions of inversions.

Table 2. Frequencies of genotypic combinations of banding sequences in populations of *Ch. agilis*.

Genotypic combination	Eastern Europe		Siberia															the Far East	
	YAR-RY†		NSK-BE	NSK-EL	NSK-KA	NSK-SH	NSK-2R	NSK-SP	NSK-LI	NSK-CH	NSK-SA	NSK-OR	NSK-YU	NSK-ST	KEM-TA	ALT-GI	ALT-TR	YAK-SO	KHA-EV	KHA-AM
	100‡§	**4**	**45**	**4**	**34**	**259**	**14**	**1**	**32**	**2**	**5**	**52**	**151**	**54**	**1**	**1**	**3**	**2**	**36**	**2**
p'agiA1.1	**1**	1	**1**	0.750	**1**	**1**	**1**	1	**1**	1	1	**1**	**1**	**1**	1	1	1	1	**1**	1
p'agiA1.2	**0**	0	**0**	0.250	**0**	**0**	**0**	0	**0**	0	0	**0**	**0**	**0**	0	0	0	0	**0**	0
p'agiB1.1	**1**	1	**0.044**	0	**0.029**	**0.042**	**0**	0	**0.031**	1	0	**0.019**	**0.007**	**0.056**	0	0	0	0.500	**0**	0.500
p'agiB2.2	**0**	0	**0.689**	1	**0.471**	**0.456**	**0.571**	1	**0.313**	0	1	**0.712**	**0.702**	**0.481**	1	1	0.667	0	**1**	0.500
p'agiB1.2	**0**	0	**0.267**	0	**0.500**	**0.498**	**0.429**	0	**0.656**	0	0	**0.269**	**0.291**	**0.463**	0	0	0.333	0.500	**0**	0
p'agiB2.3	**0**	0	**0**	0	**0**	**0.004**	**0**	0	**0**	0	0	**0**	**0**	**0**	0	0	0	0	**0**	0
h'agiC1.1	**1**	1	**1**	1	**1**	**1**	**1**	1	**1**	1	1	**1**	**1**	**1**	1	1	0.333	1	**1**	1
h'agiC1.p'agiC2	**0**	0	**0**	0	**0**	**0**	**0**	0	**0**	0	0	**0**	**0**	**0**	0	0	0.667	0	**0**	0
p'agiD1.1	**1**	1	**1**	1	**1**	**0.996**	**1**	1	**1**	1	1	**1**	**1**	**0.981**	1	1	1	1	**0.972**	1
p'agiD1.2	**0**	0	**0**	0	**0**	**0**	**0**	0	**0**	0	0	**0**	**0**	**0**	0	0	0	0	**0.028**	0
p'agiD1.3	**0**	0	**0**	0	**0**	**0.004**	**0**	0	**0**	0	0	**0**	**0**	**0.019**	0	0	0	0	**0**	0
h'agiE1.1	**1**	1	**1**	1	**1**	**0.996**	**1**	1	**1**	1	1	**1**	**1**	**1**	1	1	1	1	**1**	1
h'agiF1.p'agiE2	**0**	0	**0**	0	**0**	**0.004**	**0**	0	**0**	0	0	**0**	**0**	**0**	0	0	0	0	**0**	0
p'agiF1.1	**1**	1	**0.800**	0.750	**0.824**	**0.822**	**0.857**	1	**0.656**	1	1	**0.673**	**0.709**	**0.778**	0	0	0	0	**1**	1
p'agiF2.2	**0**	0	**0**	0	**0**	**0**	**0**	0	**0.063**	0	0	**0**	**0.007**	**0**	0	0	0	0	**0**	0
p'agiF1.2	**0**	0	**0.200**	0.250	**0.176**	**0.174**	**0.143**	0	**0.281**	0	0	**0.327**	**0.284**	**0.222**	1	1	1	1	**0**	0
p'agiF1.3	**0**	0	**0**	0	**0**	**0.004**	**0**	0	**0**	0	0	**0**	**0**	**0**	0	0	0	0	**0**	0
p'agiG1.1	**1**	1	**1**	1	**1**	**1**	**1**	1	**1**	1	1	**1**	**1**	**1**	1	1	1	1	**1**	1
B-chromosome	**0**	0	**0**	0	**0**	**0.050**	**0**	0	**0**	0	0	**0.038**	**0**	**0**	0	0	0	0	**0**	0
Number of banding sequences	**7**	7	**9**	9	**9**	**12**	**9**	7	**9**	7	7	**9**	**9**	**10**	7	7	9	8	**8**	8
Number of genotypic combinations of banding sequences	**7**	7	**10**	9	**10**	**14**	**9**	7	**11**	7	7	**10**	**11**	**11**	7	7	9	8	**8**	8
% of heterozygous larvae	**0**	0	**44.4**	50.0	**58.8**	**60.6**	**50.0**	0	**73.1**	0	0	**50.0**	**52.3**	**59.3**	0	0	66.7	50.0	**2.8**	0
Number of heterozygous inversions per larvae	**0**	0	**0.467**	0.500	**0.676**	**0.684**	**0.572**	0	**0.937**	0	0	**0.596**	**0.576**	**0.685**	0	0	1.0	0.500	**0.028**	0

† – populations highlighted with bold were used for quantitative analysis of chromosomal polymorphism; ‡ – number of larvae studied; § – the data were published by Shobanov and Djomin (1988).

p'agiB2 25s-q 18n-16a 22ab 23c-22s 25l-p 21h-18o 21i-t 15r-g 23f-25k 22r-c 23de 15f-12v C

The banding sequence p'agiB3 is a short simple inverstion in the middle of the arm that is originated from p'agiB2 and was found only once in the population from the pond on the Shadrikha river (Table 2, 3, Fig. 3c). The banding sequence p'agiB3 is new for the species and described for the first time.

p'agiB3 25s-q 18n-16a 22ab 23c-22s 25l-p 21h-18o 21i-t 15r-m 24m-23f 15g-l 24n-25k 22r-c 23de 15f-12v C

Arm C was monomorphic in all populations with the exception of the population from Travianoe Lake where the banding sequence p'agiC2 was found in a heterozygous state in a single larvae (Table 2, 3). It differs from the main banding sequence p'agiC1 by the large complex paracentric inversion. It was first described by Kiknadze and coauthors (2016), but it was not mapped in that study. We present its mapping for the first time. The banding sequence is identical to the main banding sequence of the sibling species *Ch.* sp. prope *agilis* (*Ch. agilis* 2) (Fig. 4a).

p'agiC1 1a-2c 6c-f 7a-d 16a-17a 6hg 11d-15e 8a-11c 6b-2d 17b-22g C
p'agiC2 1a-e 5b-4h 16h-a 7d-6c 2c-1f 5c-6b 11c-8a 15e-11d 6gh 17a 4g-2d 17b-22g C

Arm D was also monomorphic in most populations, but in total has three banding sequences. Both p'agiD2 and p'agiD3 banding sequences differ from p'agiD1 by simple paracentric inversions in the middle of the arm (Fig. 4b, c). The banding sequence p'agiD2 is mapped for the first time.

p'agiD1 1a-d 4a-7g 18a-d 8a-10a 13a-11a 3g-1e 10e-b 13b-14a 20d-18e 17f-14b 21a-24g C
p'agiD2 1a-d 4a-7g 18a-d 8a-10a 13a-11a 3g-1e 10e-b 13bc 16a-17f 18e-20d 14a-13d 15e-14b 21a-24g C
p'agiD3 1a-d 4a-7g 18a-d 8a-10a 13a-11a 3g-2h 19a-20d 14a-13b 10b-e 1e-2g 18g-e 17f-14b 21a-24g C

The banding sequence p'agiD2 can be classified as rare as it was found in two populations from Siberia, while p'agiD3 at present should be considered unique as it was found in a single larvae in one population from the Far East (Table, 2, 3). The banding sequence p'agiD3 is new for the species and described for the first time.

Arm E was monomorphic in all populations with the exception of the population from the pond on the Shadrikha river where the banding sequence p'agiE2 was found in a heterozygous state in a single larvae (Table 2, 3). It differs from the main banding sequence h'agiE1 by the simple short paracentric inversion located close to the centromeric region (Fig. 5a).

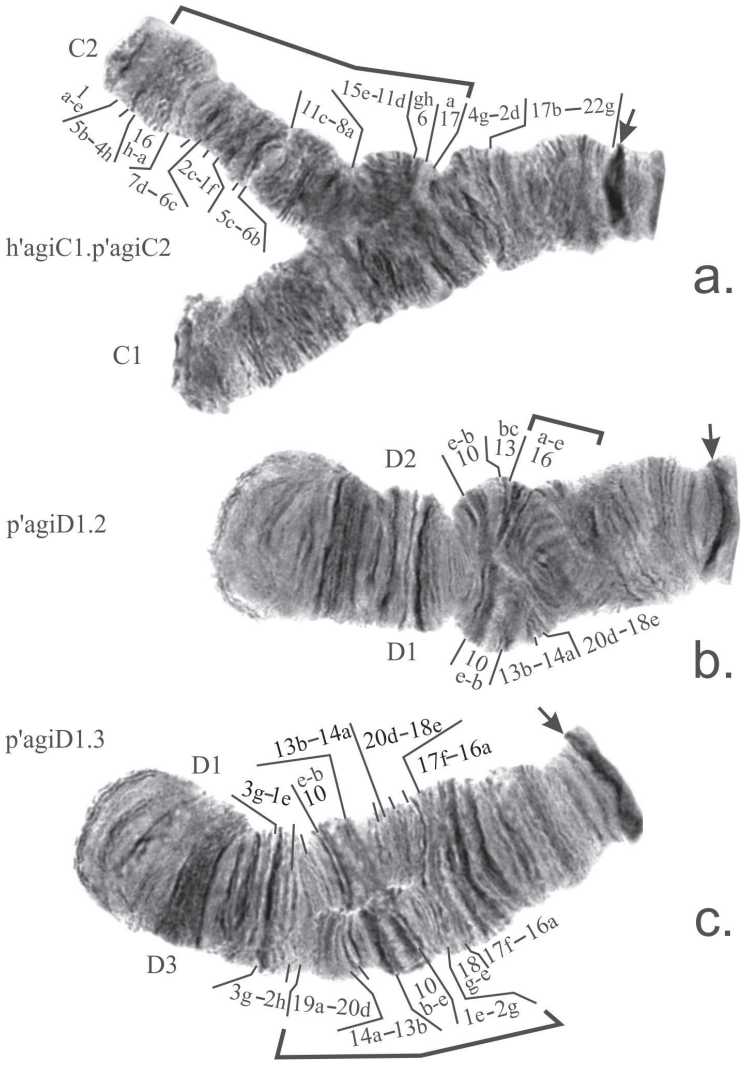

Figure 4. Inversions in arms C (**a**) and D (**b, c**) found in populations of *Ch. agilis.* Designations as on Fig. 3.

h'agiE1 1a-3e 5a-10b 4h-3f 10c-13g C (KV)
h'agiE1 1a-3a 4c-10b 3e-b 4b-3f 10c-13g C (GV)
p'agiE2 1a-3a 4c-10b 3e-b 4b-3f 10c-e 12g-10f 13a-g C (GV)

Arm F has three banding sequences. The main banding sequence p'agiF1 occurred in 100% of larvae from European and Far Eastern populations, and was dominant in all studied populations from Siberia (Table 2, 3). The banding sequence p'agiF2 was present in most Siberian populations, mostly in the heterozygous state, but homozygote p'agiF2.2 was also found (Table 3). It differs from p'agiF1 by the complex para-

Table 3. Frequencies of banding sequences in populations of *Ch. agilis*.|

Banding sequnce	Europe	Siberia								the Far East
	YAR-RY	NSK-BE	NSK-KA	NSK-SH	NSK-2R	NSK-LI	NSK-OR	NSK-YU	NSK-ST	KHA-EV
	100¶	45	34	259	14	32	52	151	54	36
p'agiA1	1	1	1	1	1	1	1	1	1	1
p'agiA2	0	0	0	0	0	0	0	0	0	0
p'agiB1	1	0.178	0.279	0.291	0.214	0.359	0.154	0.152	0.288	0
p'agiB2	0	0.822	0.721	0.707	0.786	0.641	0.846	0.848	0.712	1
p'agiB3	0	0	0	0.002	0	0	0	0	0	0
h'agiC1	1	1	1	1	1	1	1	1	1	1
p'agiC2	0	0	0	0	0	0	0	0	0	0
p'agiD1	1	1	1	0.998	1	1	1	1	0.991	0.986
p'agiD2	0	0	0	0	0	0	0	0	0	0.014
p'agiD3	0	0	0	0.002	0	0	0	0	0.009	0
h'agiE1	1	1	1	0.996	1	1	1	1	1	1
p'agiE2	0	0	0	0.004	0	0	0	0	0	0
p'agiF1	1	0.900	0.912	0.911	0.929	0.797	0.837	0.851	0.889	1
p'agiF2	0	0.100	0.088	0.087	0.071	0.203	0.163	0.149	0.111	0
p'agiF3	0	0	0	0.002	0	0	0	0	0	0
p'agiG1	1	1	1	1	1	1	1	1	1	1

| – only populations with enough larva for quantitative analysis (more than 10 specimens) are included into this table. ¶ – number of larvae studied.

centric inversion on the distal part of the arm (Fig. 5b). The banding sequence p'agiF3 was found once in the pond on the Shadrikha river and differs from p'agiF1 by the very short paracentric inversion near the centromere (Fig. 5c). This sequence p'agiF3 is new for the species and described for the first time.

p'agiF1 1a-d 6e-1e 7a-10d 18c-a 11a-17d 18d-23f C
p'agiF2 1a-d 6e-b 4c-6a 2a-4b 1i-e 7a-10d 18c-a 11a-17d 18d-23f C
p'agiF3 1a-d 6e-1e 7a-10d 18c-a 11a-17d 18d-21d 22e-a 23a-f C

Arm G was monomorphic in all studied populations. It was not mapped as several active regions such as two nucleoli and two Balbiani Rings significantly increase the difficulty of comparison of banding patterns.

As was mentioned above, *Ch. agilis* was earlier considered as low polymorphic species, but our study of populations from Siberia had shown that at least in this region it has considerable level of chromosomal polymorphism, albeit not diverse with only couple inversions widespread in populations. Among studied populations of *Ch. agilis* the highest level of chromosomal polymorphism was found in Siberia (Novosibirsk and Altai regions) with 44.4–73.1% of heterozygotic larvae and 0.467–0.937 heterozygotic inversion per larvae, while European and Far Eastern populations were almost monomorphic (Table 2). The highest number of banding sequences – 12 – was found in the population from the pond on the Shadrikha river, while 9–10 banding sequences were present in most other populations.

All populations suitable for quantitative analysis (with number of specimens more than 10) were checked for deviations from Hardy-Weinberg equation. Only two populations – from ponds on the Shadrikha river (NSK-SH) and the Koynikha river (NSK-

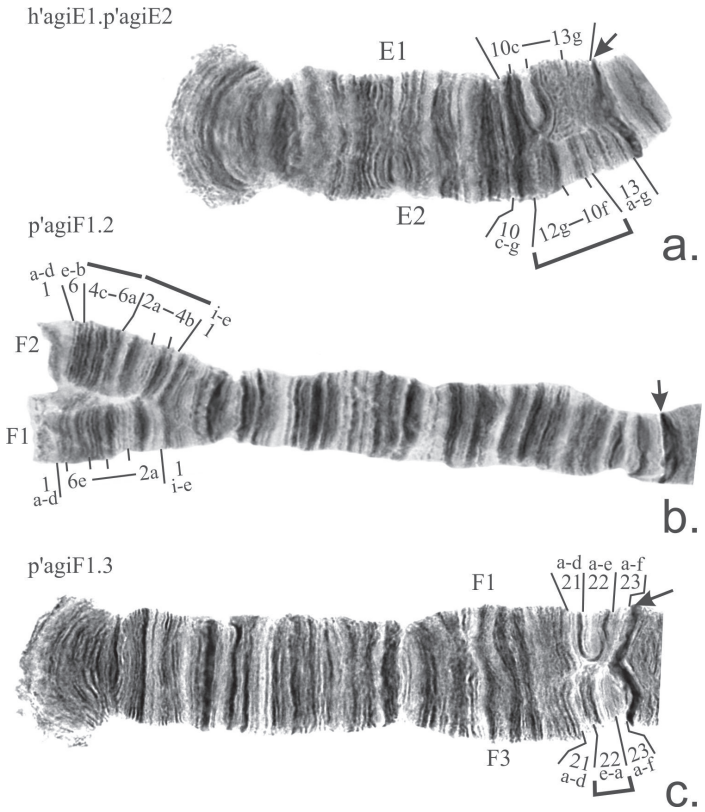

Figure 5. Inversions in arms E (**a**) and F (**b, c**) found in populations of *Ch. agilis*. Designations as on Fig. 3.

Table 4. Cytogenetic distances between populations of *Ch. agilis*, calculated based on the Nei criteria (Nei 1972).

	YAR-RY	NSK-BE	NSK-KA	NSK-SH	NSK-2R	NSK-LI	NSK-OR	NSK-YU	NSK-ST
NSK-BE	0.106								
NSK-KA	0.081	0.002							
NSK-SH	0.078	0.002	0.000						
NSK-2R	0.096	0.000	0.001	0.001					
NSK-LI	0.116	0.001	0.003	0.004	0.002				
NSK-OR	0.069	0.007	0.003	0.003	0.006	0.007			
NSK-YU	0.116	0.001	0.003	0.004	0.002	0.000	0.007		
NSK-ST	0.080	0.002	0.000	0.000	0.001	0.003	0.002	0.003	
KHA-EV	0.155	0.006	0.012	0.013	0.007	0.007	0.025	0.006	0.013

KO) – had shown a deviation from expected equation. In both populations number of heterozygotes in arm B exceeded expected values (P>0.99 and P>0.95, respectively): observed and expected frequencies of p'agiB1.2 were 49.8% and 41.1%, respectively, in NSK-SH, and 65.6% and 46.0% in NSK-KO. Unfortunately, the date on water quality in studied populations are not available so it is impossible to speculate about the cause of these deviations.

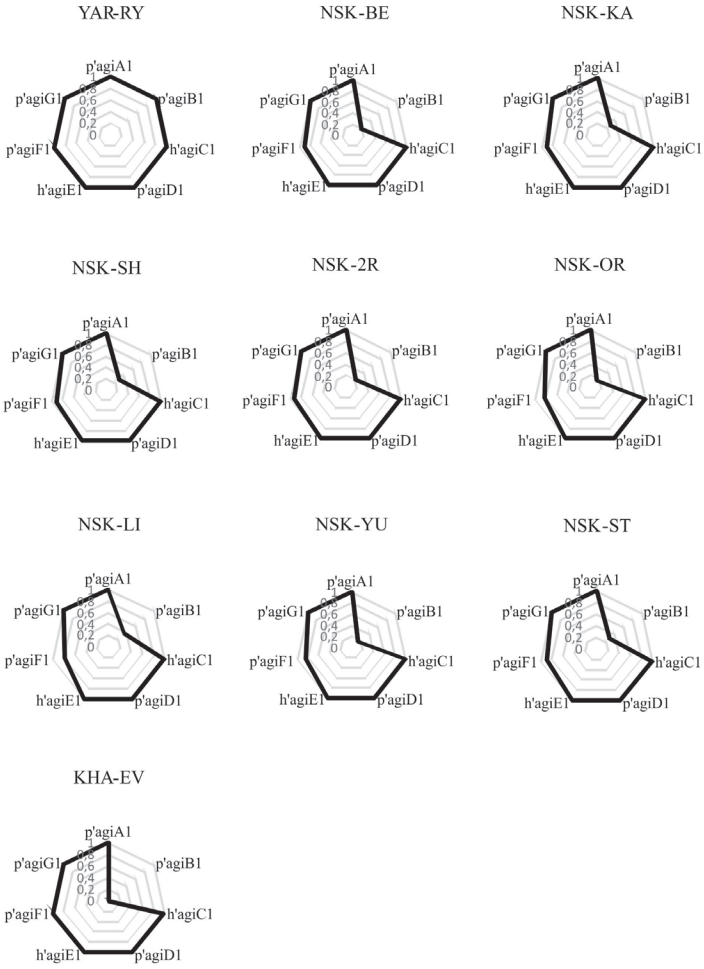

Figure 6. Cytogenetic structure (frequency polygons) of studied populations of *Ch. agilis*; YAR-RY, NSK-BE etc. – collections sites (see Table 1), p'agiA1, p'agiB1 etc. – main banding sequences of the species, 0.2, 0.4 etc. – frequencies of main banding sequences.

The cytogenetic structure of studied populations is shown on Fig. 6. The designation of types of population's cytogenetic structure is done according to the work of Gunderina et al. (1999). As can be seen, population from Rybinskoe Reservoir belongs to cytogenetic type 0 (all main banding sequences are dominant), while all populations from Siberia and the Far East belong to type B (an alternative banding sequence is dominant in the arm B, in this case it is p'agiB2).

The cytogenetic distances between populations varied from 0 to 0.155 (Table 4). They are well below the threshold of interspecies values, which for chironomids is considered to be around 1 for clearly differentiated species (Gunderina 2001). As expected, the minimal distances were observed between populations from Western Siberia, and the largest distance was seen between border populations – from Rybinskoe Reservoir and Evoron Lake. Phylogenetic tree calculated based on the neighbor-joining method is presented on Fig. 7.

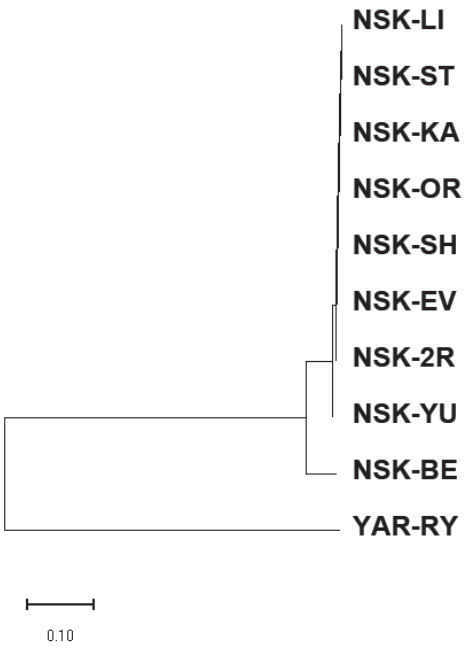

Figure 7. Phylogenetic tree of studied populations of *Ch. agilis*, calculated based on the neighbor-joining method.

Besides inversion polymorphism, genomic polymorphism in a form of additional B-chromosomes was also observed in two populations from Siberia – in ponds on the Ora and the Shadrikha rivers (Table 2).

The species *Ch. agilis* shows moderate level of chromosomal polymorphism in comparison with other well-studied species from plumosus group – *Ch. balatonicus*, *Ch. plumosus* and *Ch. entis*. For example, an average percent of heterozygotes found in Palearctic populations of *Ch. plumosus* is 63.2% with 0.95 inversion per larvae (Golygina and Kiknadze 2001), while these values for *Ch. agilis* are 45.1% and 0.52. The number of banding sequences found in populations of *Ch. agilis* is also lower – 9.2 on average vs 12.5 for Palearctic *Ch. plumosus* (Golygina and Kiknadze 2001), 15.3 for Palearctic *Ch. entis* (Kiknadze ert al. 2000) and 14.3 for *Ch. balatonicus* (Golygina et al. 1996). Although it is possible that this characteristic will change if more populations of *Ch. agilis* from different regions will be studied.

If we consider the distribution of chromosomal polymorphism between chromosome arms, *Ch. agilis* shows pattern similar to *Ch. balatonicus* where only two arms show high level of polymorphism in most populations, while other arms are almost completely monomorphic. At the same time, chromosome arms most heavily affected by inversion polymorphism are different in these two species: A and D in *Ch. balatonicus*, but B and F in *Ch. agilis*. In other two species – *Ch. plumosus* and *Ch. entis* – inversions are found with high frequencies in most or all chromosome arms.

At present, it is too early to draw a final conclusion about the characteristics of chromosomal polymorphism of *Ch. agilis*, as still not enough karyological data are

available, especially for Europe, Eastern Siberia and the Far East. However, it is possible to assume that Western Siberia is the center of the species range of *Ch. agilis* and populations here have higher level of chromosomal polymorphism, which is also more diverse than in populations from the borders of the species range.

Acknowledgements

The work was supported by the federal funding project 0259-2021-0011 "Structural and functional organization and role of chromosomes of humans and animals in evolution and ontogenesis".

References

Dévai Gy, Miskolczi M, Wülker W (1989) Standartization of chromosome arms B, C and D in *Chironomus* (Diptera: Chironomidae). Acta Biologica Debrecina. Supplementum Oecologica Hungarica Fasc 2(1): 79–92.

Golygina VV, Istomina AG, Rakisheva AZh, Kiknadze II (1996) New banding sequences in the *Chironomus balatonicus* karyofund (banding sequence pool). Tsitologiya 38(8): 869–883. [In Russian].

Golygina VV, Kiknadze II (2001) Karyofund (banding species pool) of *Chironomus plumosus* (Diptera, Chironomidae) in Palearctic. Tsitologiya 43(5): 507–519. [In Russian]

Golygina VV, Kiknadze II (2008) The revision of chromosome I (AB) mapping in *Chironomus plumosus* group (Diptera: Chironomidae). Comparative Cytogenetics 2(1): 37–55.

Golygina VV, Kiknadze II (2012) A revision of chromosome II (CD) mapping in *Chironomus plumosus* (Linnaeus, 1758) group (Diptera, Chironomidae). Comparative Cytogenetics 6(3): 249–266. https://doi.org/10.3897/compcytogen.v6i3.2831

Golygina VV, Kiknadze II (2018) A revision of chromosome III (EF) mapping in *Chironomus plumosus* (Linnaeus, 1758) group (Diptera, Chironomidae). Comparative Cytogenetics 12(2): 201–222. https://doi.org/10.3897/compcytogen.v12i2.23327

Gunderina LI, Kiknadze II, Golygina VV (1999) Intraspecific differentiation of the cytogenetic structure in natural populations of *Chironomus plumosus* L., the central species in the group of sibling species (Chironomidae: Diptera). Russian Journal of Genetics 35 (2): 142–150.

Gunderina LI (2001) Genetic variation in evolution of chironomids (Diptera, Chironomidae). Dissertation of Doctor of Science, Novosibirsk, Russian Federation: Institute of Cytology and Genetics SB RAS, 360 pp. [In Russian]

Keyl H-G (1962) Chromosomenevolution bei *Chironomus*. II. Chromosomenumbauten und phylogenetische Beziehungen der Arten. Chromosoma 13(4): 464–514. https://doi.org/10.1007/BF00327342

Keyl H-G, Keyl I (1959) Die cytologische Diagnostik der Chironomiden. I. Bestimmungstabelle für die Gattung *Chironomus* auf Grund der Speicheldrüsen-Chromosomen. Archiv für Hydrobiologie 56(1/2): 43–57.

Kerkis IE, Kiknadze II, Istomina AG (1989) Comparative analysis of karyotypes of three sibling-species in plumosus group (Diptera. Chironomidae). Tsitologiya 31: 713–720. [In Russian]

Kiknadze II, Shilova AI, Kerkis IE, Shobanov NA, Zelentzov NI, Grebenjuk LP, Istomina AG, Prasolov VA (1991) Karyotypes and morphology of larvae in the tribe *Chironomini*. Novosibirsk, 113 pp. [In Russian]

Kiknadze II, Butler MG, Golygina VV, Martin J, Wülker WF, Sublette JE, Sublette MF (2000) Intercontinental karyotypic differentiation of *Chironomus entis* Shobanov, a Holarctic member of the *C. plumosus* group (Diptera, Chironomidae). Genome 43(5): 857–873. https://doi.org/10.1139/g00-052

Kiknadze II, Istomina AV, Golygina VV, Gunderina LI (2016) Karyotypes of Palearctic and Holarctic species of the genus *Chironomus* [Electronic resource]. Russian Academy of Sciences, Siberian Branch, Federal Research Center Institute of Cytology and Genetics. Novosibirsk: Academic Publishing House "GEO", 489 pp. http://elibrary.ru/item.asp?id=27246690

Krastanov BD, Michailova PV (2008) Cytotaxonomic Characteristic of Four Species of plumosus Group in Genus *Chironomus* Meigen 1803 (Diptera: Chironomidae) from Bulgaria and Poland. Acta Zoologica Bulgarica, Suppl. 2: 49–60.

Maximova FL (1976) The karyotype of *Chironomus plumosus* from Ust'-Izhora wild population of Leningrad region. Tsitologiya 18: 1264–1268. [In Russian]

Michailova P, Krastanov B, Kownacki A (2002) Cytotaxonomical characteristics of genus *Chironomus* Meigen (Diptera: Chironomidae) from different localities of Poland. Annales Zoologici 52(2): 215–225.

Nei M (1972) The genetic distance between populations. American Naturalist 106: 283–292. https://doi.org/10.1086/282771

Plokhinsky NA (1967) Algorithms of biometry. Moscow University Press, 82 pp.

Shobanov NA (1994) Karyofund of *Chironomus plumosus* (L.) (Diptera, Chironomidae). I. Standartization of bands according to the Maximova system. Tsitologiya 36(1): 117–122. [In Russian]

Shobanov NA, Djomin SYu (1988) *Chironomus agilis* – new species of group plumosus (Diptera, Chironomidae). Zoologicheskiy Zhurnal 67(10): 1489–1497. [In Russian]